Arthritis & Rheumatology

An Official Journal of the American College of Rheumatology
www.athritisrheum.org and wileyonlinelibrary.com

Arthritis & Rheumatology

An Official Journal of the American College of Rheumatology
www.athritisrheum.org and wileyonlinelibrary.com

VOLUME 71 • February 2019 • NO. 2

Cover image: The figure on the cover (from Wang et al, page 244) shows a reconstructed 3-dimensional ultrasound image of knee synovium from a mouse with posttraumatic osteoarthritis that was treated with the proteasome inhibitor bortezomib. Decreased volume of the synovium suggests that bortezomib treatment reduced the severity of synovitis and osteoarthritis.

In this **Issue**

Highlights from this issue of *A&R* | **By Lara C. Pullen, PhD**

Treatment With Bortezomib Improves Mouse Posttraumatic Osteoarthritis

Although rheumatologists know that osteoarthritis (OA) is associated with high levels of catabolic factors and inflamma-

p. 244

tory cells in the joint space and the soft tissues surrounding the joint, the mechanism behind this presentation is not known. In this issue, Wang et al (p. 244) report that experimental posttraumatic knee OA is associated with several features, including decreased synovial lymphatic drainage, increased number of M1 macrophages, and enhanced inflammatory gene expression by lymphatic endothelial cells (LECs).

> BTZ may represent a new therapy for the restoration of synovial lymphatic function in subjects with posttraumatic knee OA.

The investigators began their study by injecting a vascular endothelial growth factor receptor 3 (VEGFR-3) neutralizing antibody into the joints of mice with posttraumatic knee OA. They found that anti-VEGFR-3 reduced synovial lymphatic drainage and accelerated joint tissue damage. When they looked more closely at the synovial LECs from the mouse OA joints, they saw that the LECs had dysregulated inflammatory pathways and expressed high levels of inflammatory genes. They also found that the number of M1 macrophages was increased in the knee joints of mice with posttraumatic OA and noted that these
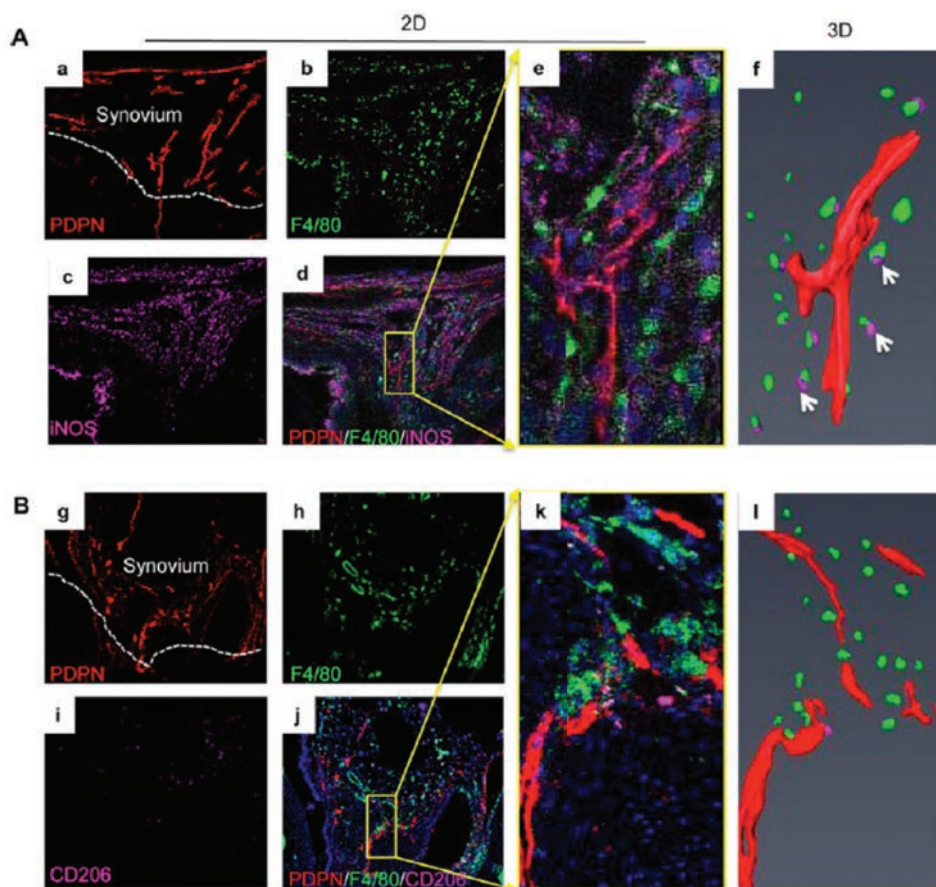
Figure 1. M1 macrophages accumulate adjacent to lymphatic vessels in the synovium of mice with posttraumatic osteoarthritis (OA). Frozen sections of OA mouse knees (30 μm thick) at 5 weeks post–meniscal ligamentous injury were immunostained with antibodies against podoplanin (PDPN) (red) for lymphatic vessels (a), F4/80 (green) for pan-macrophages (b), or inducible nitric oxide synthase (iNOS) or CD206 (purple) for macrophage subsets (c). M1 macrophages (A) were defined as F4/80+iNOS+ cells (a–d), and M2 macrophages (B) were defined as F4/80+CD206+ cells (g–l). Confocal microscopy was used for z-section imaging to obtain 20–25 consecutive images (e and k) with a step-width of 1 μm. PDPN+ lymphatic vessels (red) and M1 or M2 macrophages (purple) were detected by Amira to generate 3-dimensional (3-D) images (f and l) in a SurfaceGen module. Arrows in f indicate M1 cells near lymphatic vessels in a 3-D image. Original magnification x 20 in a–d and g–j; x 60 in e, f, k, and l.

macrophages likely promoted the expression of inflammatory genes by LECs.

The researchers then treated the mice with intraarticular administration of bortezomib (BTZ) and found that BTZ was able to block the expression of inflammatory genes by LECs, increase synovial lymphatic drainage, and decrease the number of M1 macrophages. Treatment with BTZ also decreased cartilage loss. These results demonstrate that BTZ may represent a new therapy for the restoration of synovial lymphatic function in subjects with posttraumatic knee OA.

Long-Term Clinical Outcomes of Childhood-Onset Lupus

In this issue, Groot et al (p. 290) report data from a large cohort of adults with childhood-onset systemic lupus erythematosus (SLE).

p. 290 — Theirs is the first study to describe disease manifestations over time, as well as long-term damage and health-related quality of life (HRQoL). The investigators found that these patients developed significant damage at a young age and experienced impaired HRQoL (relative to the overall Dutch population) without achieving drug-free remission. These findings indicate that childhood-onset SLE has a substantial impact on future life.

The researchers evaluated 111 patients with childhood-onset SLE who had a median disease duration of 20 years. The majority of patients (91%) was female and most were white (72%). The patients tended to have low disease activity, and 71% of patients received prednisone,
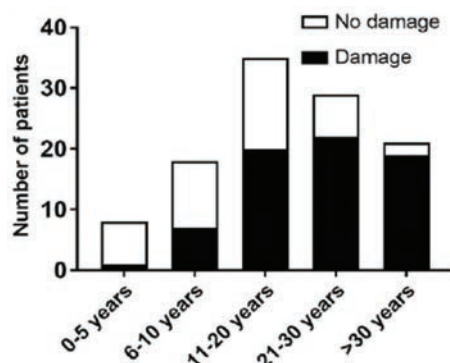
Figure 1. Childhood-onset systemic lupus erythematosus–related damage defined by a Systemic Lupus International Collaborating Clinics/American College of Rheumatology Damage Index score of ≥1. Number of patients with and without damage, by disease duration category.

hydroxychloroquine (HCQ), and/or other disease-modifying antirheumatic drugs.

When the investigators examined disease presentation over time, they found that most of the new childhood-onset, SLE-related

manifestations developed within 2 years of diagnosis. After approximately 5 years, manifestations such as myocardial infarctions began to occur. Over time, most patients (62%) experienced damage that occurred primarily in the musculoskeletal, neuropsychiatric, and renal systems. Patients often experienced significant medical events at a young median age as follows: cerebrovascular accidents (20 years), renal transplants (24 years), replacement arthroplasties (34 years), and myocardial infarctions (39 years). When the investigators performed a multivariate logistic regression analysis, they found that damage accrual was associated with disease duration, antiphospholipid antibody positivity, and hypertension. In contrast, current HCQ monotherapy was associated with a Systemic Lupus International Collaborating Clinics/American College of Rheumatology Damage Index (SDI) score of zero.

Sustained Minimal Disease Activity Protects Patients With PsA From Subclinical Atherosclerosis

In this issue, Cheng et al (p. 271) report the results of their prospective cohort study, designed to investigate the effects of

p. 271 — achieving minimal disease activity (MDA) on the progression of subclinical atherosclerosis and arterial stiffness in patients with psoriatic arthritis (PsA). This is the first longitudinal study to demonstrate that effective control of systemic inflammation in patients with PsA is associated with less progression of subclinical atherosclerosis as compared to individuals who did not achieve sustained MDA (sMDA). The study included 90 patients with PsA (mean ± SD age 50 ± 11 years) who completed 24 months of follow-up. More than half of the patients (63%) achieved MDA at 12 months, but fewer (46%) achieved sMDA. While subclinical atherosclerosis and arterial stiffness were similar between the MDA and non-MDA groups, achieving sMDA had a protective effect on plaque
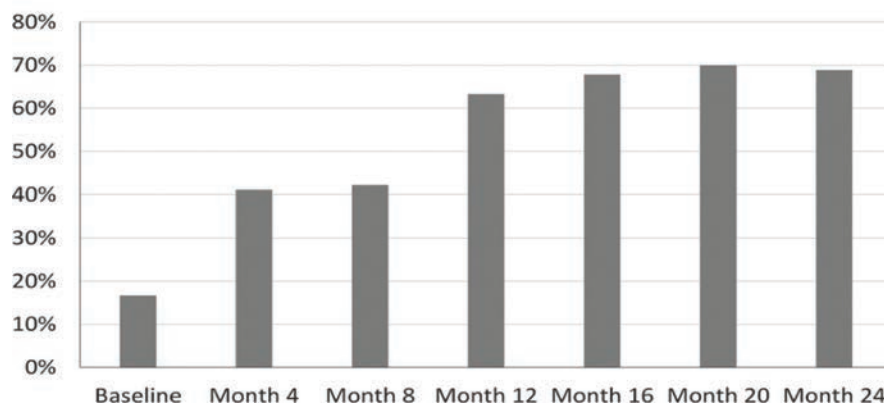
Figure 1. Proportion of subjects achieving minimum disease activity across the study period.

progression, mean intima-media thickness, and augmentation index values.

The results support the recommendation that once MDA is achieved in patients with PsA, it should be maintained for an

extended period. Such an approach prevents progression of carotid atherosclerosis and arterial stiffness and is essential even in patients who do not have traditional cardiovascular risk factors.

Clinical **Connections**

Suppressive Regulation of MFG-E8 of Latent Transforming Growth Factor β–Induced Fibrosis via Binding to αv Integrin: Significance in the Pathogenesis of Fibrosis in Systemic Sclerosis

CORRESPONDENCE
Sei-ichiro Motegi, MD, PhD: smotegi@gunma-u.ac.jp
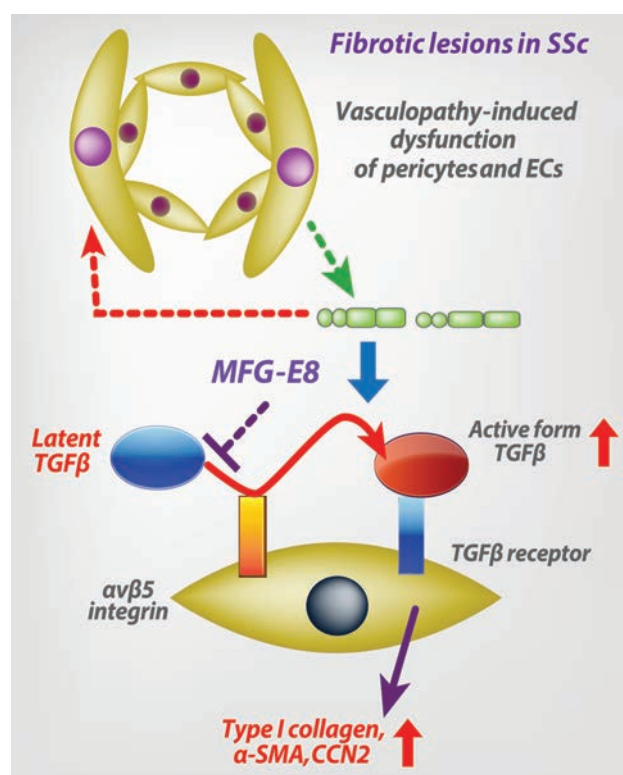
SUMMARY

Vasculopathy precedes the onset of fibrosis in systemic sclerosis (SSc) and may be a primary event in the pathogenesis of SSc. The serum and dermal expression of milk fat globule–associated protein with epidermal growth factor– and factor VIII–like domains (MFG-E8) is reduced in SSc patients. MFG-E8 inhibits latent transforming growth factor β (TGFβ)–induced expression of type I collagen, α-smooth muscle actin (α-SMA), and CCN2 by the interaction with the RGD domain of αv integrin in fibroblasts. Fujiwara et al found that in bleomycin-induced fibrosis and TSK mouse models of SSc, deficient expression of MFG-E8 enhanced both pulmonary and skin fibrosis, and administration of recombinant MFG-E8 (rMFG-E8) significantly inhibited dermal fibrosis. These results suggest that vasculopathy-induced dysfunction of pericytes and endothelial cells (ECs), the main secretory cells of MFG-E8, may be associated with the decreased expression of MFG-E8 in SSc and may contribute to the pathogenesis of SSc. Integrin-modulating therapy, such as the administration of rMFG-E8, could hold promise for the treatment of fibrosis in SSc.

KEY POINTS

- There is decreased expression of MFG-E8 in the serum as well as the ECs and pericytes of lesioned skin in SSc patients.

- Recombinant MFG-E8 inhibits TGFβ-induced and fibrosis-related gene/protein expression in SSc fibroblasts by binding to αv integrin.

- In bleomycin-induced fibrosis and TSK mouse models of SSc, deficient expression of MFG-E8 significantly enhances both pulmonary and skin fibrosis.

- Administration of rMFG-E8 significantly inhibits bleomycin-induced dermal fibrosis in mice.

Recognition of Amino Acid Motifs, Rather Than Specific Proteins, by Human Plasma Cell–Derived Monoclonal Antibodies to Posttranslationally Modified Proteins in Rheumatoid Arthritis

Steen et al, *Arthritis Rheumatol* 2019;71:196–209

CORRESPONDENCE
Vivianne Malmström, PhD: vivianne.malmstrom@ki.se
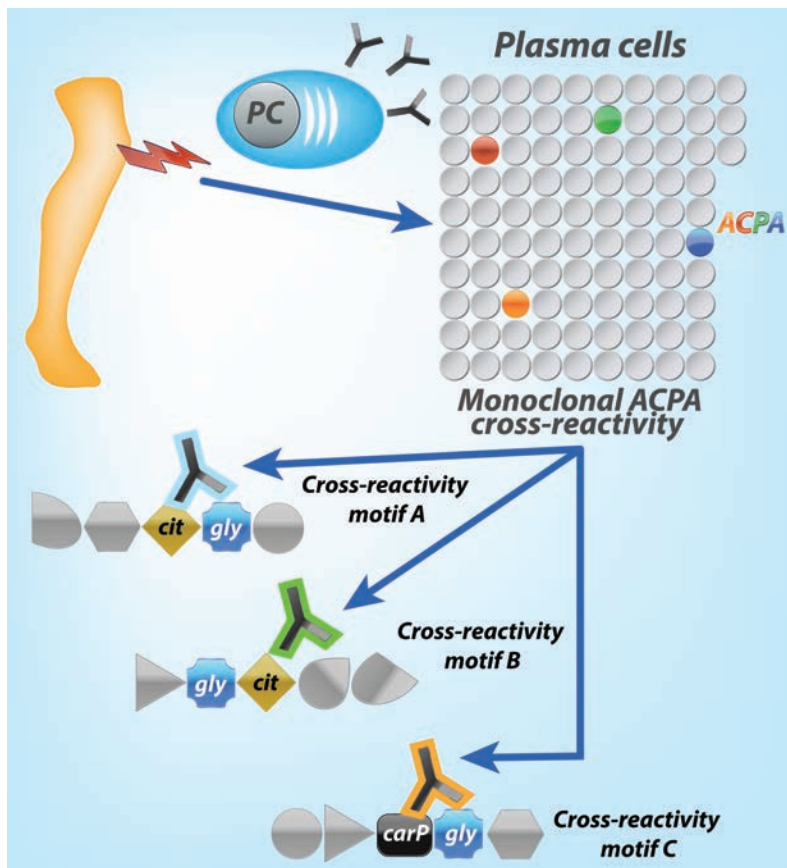
KEY POINTS

- Monoclonal antibodies were generated from individual plasma cells from RA synovial fluid; 4% (4 of 93) were ACPAs.

- All 4 ACPAs were found to be cross-reactive to several citrullinated (cit) proteins and large numbers of peptides by recognition of distinct amino acid motifs.

- Despite the observed cross-reactivity, only 1 of the ACPAs promoted osteoclastogenesis.

- Half of the ACPAs also cross-reacted with carbamylated peptides.

SUMMARY

Anti–citrullinated peptide antibodies (ACPAs) are a hallmark of rheumatoid arthritis (RA) and can preceed clinical diagnosis. Early bone loss has been linked to ACPA status even in the absence of joint inflammation. In order to investigate the precise reactivity of ACPAs, Steen et al used single-cell technology and expressed recombinant antibodies from RA-derived plasma cells (PCs). They identifed several highly mutated ACPAs that were not clonally related. In contrast to classical antibody responses, reactivity was observed toward linear citrulline-containing amino acid motifs, resulting in pronounced protein and peptide cross-reactivity. This cross-reactivity could also extend to lysine residues converted to homocitrulline (carP) by the process of carbamylation. One of the identified ACPAs promoted bone resorption in vitro. Overall, these data suggest that citrulline-reactive B cells do not share the same differentiation history, Ig reactivity, or pathologic functions.

AMERICAN COLLEGE
OF RHEUMATOLOGY
EDUCATION · TREATMENT · RESEARCH

EDITORIAL

To Eat the Elephant

Michael D. Lockshin

In this issue of *Arthritis & Rheumatology*, Hanly et al and the Systemic Lupus International Collaborating Clinics (SLICC) report that 1.5% of patients with systemic lupus erythematosus (SLE) experience an episode of psychosis within 3 years of diagnosis (1). Psychosis occurs early and is transient. Patients usually fully recover. They rarely relapse.

In presenting this information, the article shifts no paradigms about central nervous system (CNS) SLE, but it does provide answers to some common questions, and it offers lessons about clinical research that transcend the article's face message. This study answers the *what*, *who*, and *when* epidemiologic questions about psychosis in SLE but not the *who* or *why* questions about biologic mechanisms or treatment.

To answer *what*, the authors adopted the American College of Rheumatology (ACR) definition of psychosis, made more stringent by exclusion of patients whose psychosis is primary or reactive, due to depression or cognitive decline, or associated with prescribed or illicit drugs. Their data did not change, nor were meant to change, the definition. There are no objective criteria for psychosis, and other physicians may diagnose it differently. Nonetheless, the ACR definition reflects consensus within the rheumatology community; the SLICC physicians used standardized terms and procedures to assure the quality of their study.

The authors do provide data to answer the *who* question about psychosis in SLE. Patients with psychosis are more often young, male, and of African ancestry than are patients without. This finding is not surprising—experienced clinicians might have guessed the result—but it does, for the first time, provide strong documentation for a field that otherwise lacks good information. The authors' answer to the *when* question is that psychosis occurs early during the course of SLE, and not later, for reasons unknown. The authors do not offer an answer to the *where* question. However, having conducted their study in 31 centers in 10 countries, they imply that SLE psychosis, equally distributed throughout the world, is not driven by regional factors.

Answers to the epidemiologic questions help physicians determine whether psychosis occurs because of, or is coincidental to, SLE. Although the authors do not ask this question directly, they do provide data from which one can impute an answer. In their report, the incidence of acute psychosis during the first year after an SLE diagnosis is 383/100,000, almost 40-fold higher than the rate in a general population (2). The number is so large that psychosis in an SLE patient must be attributable to the illness.

SLE psychosis is rare, therefore challenging to study. The article nicely demonstrates how a collaborative group like SLICC overcomes the problem. The authors agreed, a priori, on consensus definitions and procedures; they committed a large amount of personal and administrative effort; and they followed up their patients for long periods of time. In doing so they were able to put an important new description of SLE psychosis into the public domain, as they have done before with other CNS and non-CNS SLE syndromes (3). Continuous collaboration, over long periods of time, is important. Descriptive studies have value.

The article illustrates the manner in which hypothesis generation and hypothesis testing complement each other. In hypothesis generation, investigators identify heterogeneity within a population, find elements that change simultaneously, then hypothesize reasons for the association of the changes. In hypothesis testing, investigators select homogeneous representatives from a population, introduce a variable that they hypothesize will alter a stable factor, and measure the induced change. Hypothesis generation determines the boundaries of SLE psychosis and creates a common vocabulary; hypothesis testing interrogates the mechanisms of psychosis to develop a go-forward plan that can change patient care.

Regarding hypothesis generation, in the mid–20th century Dubois posited that SLE neurologic syndromes share a common pathogenesis and treatment (4). Using descriptive data, Sergent et al showed that different CNS syndromes respond differently to the treatment Dubois' proposed and so, likely, have different pathogeneses (5). Kassan and Lockshin used newly available computed tomography scan evidence to propose a roadmap for distinguishing among CNS SLE syndromes (6). From that roadmap, Singer and Denburg proposed preliminary diagnostic criteria for CNS SLE (7). In 1999 an ACR

Michael D. Lockshin, MD: Barbara Volcker Center, Hospital for Special Surgery, New York, New York.

Address correspondence to Michael D. Lockshin, MD, Barbara Volcker Center, Hospital for Special Surgery, 535 East 70th Street, New York, NY 10021. E-mail: LockshinM@hss.edu.

committee led by Matthew Liang, building on that proposal and using a more formal process, developed the nomenclature and case definitions that we use today (8). In the ensuing decades many descriptive studies have shown that the many different syndromes of CNS SLE occur in different demographic groups and in different clinical circumstances, and that they have different imaging, anatomic pathologies, and prognoses.

With boundaries among CNS SLE syndromes now cleanly drawn, investigators use contemporary technology to ask the *how* and *why* questions of the hypothesis tester. New dynamic contrast-enhanced magnetic resonance imaging (MRI), functional MRI, positron emission tomography scanning, and analyses of brain anatomy and metabolism increase our ability to study normal and abnormal brain function (9,10). Improved technologies in the fields of molecular immunology, blood–brain barrier function, and cognitive function (11), and new concepts like microglial metabolism and pruning (12), are beginning to demystify the complexity of CNS SLE.

Today's studies are still mostly descriptive, but they generate hypotheses testable in mouse models. Admittedly, a confused mouse with a genetic or induced illness similar to but not precisely like human SLE is not a fully convincing proxy for a hallucinating, convulsing, demented, or hemiparetic human. Nonetheless, when hypotheses generated from well-described human syndromes are tested in mice, sometimes startlingly new findings or off-the-wall treatment suggestions appear—for instance, the idea of treating CNS SLE with angiotensin-converting enzyme inhibitors (13).

While it is hard to predict where the future will lead, major advances seem likely soon. CNS SLE research is still mostly phenomenology, but, when descriptive clinical science joins hypothesis testing in mice or men, paradigms are likely to shift. The epidemiologic description of SLE psychosis is a good start. CNS SLE is the huge elephant sitting upon our dinner plate. If the best way to eat that elephant is to take the first small bite, the tastiest bit might be the acute, transient psychosis that occurs in patients with new-onset SLE.

AUTHOR CONTRIBUTIONS

Dr. Lockshin drafted the article, revised it critically for important intellectual content, and approved the final version to be published.

REFERENCES

1. Hanly JG, Li Q, Su L, Urowitz MB, Gordon C, Bae SC, et al. Psychosis in systemic lupus erythematosus: results from an international inception cohort study. Arthritis Rheumatol 2019; 71:281–9.

2. Castagnini A, Bertelsen A, Berrios GE. Incidence and diagnostic stability of ICD-10 acute and transient psychotic disorders. Compr Psychiatry 2008;49:255–61.

3. Hanly JG, Urowitz MB, Sanchez-Guerrero J, Bae SC, Gordon C, Wallace DJ, et al. Neuropsychiatric events at the time of diagnosis of systemic lupus erythematosus: an international inception cohort study. Arthritis Rheum 2007;56:265–73.

4. Dubois EL. Lupus erythematosus. New York: McGraw-Hill; 1966. p. 389.

5. Sergent J, Lockshin M, Klempner M, Lipsky B. Central nervous system dysfunction in systemic lupus erythematosus: prognosis and therapy. Am J Med 1975;58:644–54.

6. Kassan S, Lockshin M. Central nervous system lupus erythematosus: the need for classification. Arthritis Rheum 1979;22:1382–5.

7. Singer J, Denburg JA. Diagnostic criteria for neuropsychiatric systemic lupus erythematosus: the results of a consensus meeting. The Ad Hoc Neuropsychiatric Lupus Workshop Group. J Rheumatol 1990;17:1397–402.

8. ACR Ad Hoc Committee on Neuropsychiatric Lupus Nomenclature. The American College of Rheumatology nomenclature and case definitions for neuropsychiatric lupus syndromes. Arthritis Rheum 1999;42:599–608.

9. Magro-Checa C, Ercan E, Wolterbeek R, Emmer B, van der Wee NJ, Middelkoop HA, et al. Changes in white matter microstructure suggest an inflammatory origin of neuropsychiatric systemic lupus erythematosus. Arthritis Rheumatol 2016;68:1945–54.

10. Mackay M, Chi JM, Hoang A, Cheng K, Ivanidze J, Volpe B, et al. Dynamic contrast enhanced MRI (DCE-MRI) demonstrates hippocampus permeability in SLE. Lupus Sci Med 2018;5 Suppl 2:A73.

11. Hanly JG, Kozora E, Beyea SD, Birnbaum J. Nervous system disease in systemic lupus erythematosus: current status and future directions. Arthritis Rheumatol doi: http://onlinelibrary.wiley.com/doi/10.1002/art.40591/abstract. E-pub ahead of print.

12. Acharjee S, Verbeek M, Gomez CD, Bisht K, Lee B, Benoit L, et al. Reduced microglial activity and enhanced glutamate transmission in the basolateral amygdala in early CNS autoimmunity. J Neurosci 2018;38:9019–33.

13. Nestor J, Arinuma Y, Huerta TS, Kowal C, Nasiri E, Kello N, et al. Lupus antibodies induce behavioral changes mediated by microglia and blocked by ACE inhibitors. J Exp Med 2018;215:2554–66.

AMERICAN COLLEGE
OF RHEUMATOLOGY
EDUCATION · TREATMENT · RESEARCH

EDITORIAL

Ustekinumab Fails to Show Efficacy in a Phase III Axial Spondyloarthritis Program: The Importance of Negative Results

Philip Mease

In this issue of *Arthritis & Rheumatology*, Deodhar et al report negative phase III study results for ustekinumab in axial spondyloarthritis (SpA) (1). Ustekinumab is an interleukin-12 (IL-12)/IL-23 inhibitor approved for the treatment of psoriasis, psoriatic arthritis (PsA), and Crohn's disease. PsA has close clinical and genetic associations with axial SpA, including genetic association with variants in the IL-23 receptor signaling pathway. In addition, ustekinumab demonstrated promising results in a phase II open-label proof-of-concept study among 20 patients with ankylosing spondylitis (AS). In this previous study, ustekinumab at 90 mg was given subcutaneously (SC) at baseline and at weeks 4 and 16, and 65% of patients met the Assessment of SpondyloArthritis international Society criteria for 40% improvement in disease activity (achieved an ASAS40 response) at 24 weeks (2). Many other outcomes also favored ustekinumab, including reduced evidence of inflammation on magnetic resonance imaging (MRI). These results suggested that ustekinumab's benefits may be comparable to those of tumor necrosis factor (TNF) and IL-17 antagonists, 2 classes of agents approved for use in AS. Thus, the negative results of the phase III trial came as a real surprise, notwithstanding that the earlier study was not placebo controlled.

The phase III program for ustekinumab was well designed and comprehensive. Three different studies were undertaken: one in patients with radiographic axial SpA (otherwise known as AS) who were naive to biologic therapy; a second in patients with radiographic axial SpA who were intolerant of (or whose disease was refractory to) a single TNF inhibitor (TNFi); and a third in patients with nonradiographic axial SpA who had an inadequate response to nonsteroidal antiinflammatory drugs and could have been exposed to a single TNFi. These are now standard populations for a phase III program in axial SpA. Patients were randomized to receive either 45 mg or 90 mg ustekinumab or placebo administered SC. Sample size estimates for all 3 studies were chosen to achieve 90% power to detect treatment differences between ustekinumab and placebo for the primary end point at a significance level of 0.05. Estimates of 40% achieving an ASAS40 response in the treatment group and 20% in the placebo group were used for power calculation.

What was demonstrated? At 24 weeks in study 1, the ASAS40 responses in the placebo, 45 mg ustekinumab, and 90 mg ustekinumab arms were 28.4%, 31.0%, and 28.1%, respectively, showing no separation between treatment arms and placebo. Other measures, including spine MRI, showed no significant separation between the treatment arms and placebo. Based on these negative results, the decision was made to stop the whole phase III study program; thus, studies 2 and 3 were not completed. Results for patients in those studies who did complete 24 weeks showed a similar lack of difference between placebo and treatment arms.

Did biomarker analysis shed any light on the results? In study 1, several analytes at baseline were either correlated with disease activity according to the Ankylosing Spondylitis Disease Activity Score (ASDAS) (3) or elevated compared with matched healthy controls. Critically, however, neither Th17 cytokines (IL-17A, IL-17F, IL-22, and IL-23) nor Th1 cytokines (interferon-γ [IFNγ] and IL-12p70) were dysregulated at baseline in AS patients compared with healthy controls. In study 2, with the TNFi-experienced population, there were greater elevations of inflammatory cytokines compared with study 1, including statistically significant elevations of IL-17A, matrix metalloproteinase 3 (MMP-3), and MMP-9, but not of IL-17F, IFNγ, or IL-12p70. In study 1, MMP-3, serum amyloid A, and IL-8 declined with ustekinumab treatment, but these changes were not correlated with any clinical change. The negative results raise many questions. How could the apparently positive results from the open-label trial be so different from those of the controlled phase III trials? Why would a drug that has a modulating role in both the

Philip Mease, MD, MACR: Swedish Medical Center and University of Washington Medical School, Seattle.

Address correspondence to Philip Mease, MD, MACR, 601 Broadway, Suite 600, Seattle, WA 98122. E-mail: pmease@philipmease.com.

Th1 and Th17 pathways have no apparent effect on disease activity in axial SpA, while having a good effect in psoriasis and PsA? Why is a drug that inhibits IL-23, which acts upstream from IL-17, not effective in axial SpA when IL-17 inhibition is? Could there be a biologic explanation? Or is it a problem with the patient population or trial conduct?

There are 2 initial points to comment upon. The first is the importance of obtaining placebo-controlled trial data in rheumatic diseases in which there are many subjective components (e.g., pain, global disease activity, and fatigue) that can influence the results of outcome measures, especially in an open-label trial. This lesson is well understood by rheumatic disease trialists, including those who performed the open-label study of ustekinumab simply to get some signal about efficacy, as well as those in the phase III program. In hindsight, it might have been prudent to perform a phase II, placebo-controlled, dose-ranging study to gain further confidence before proceeding into phase III, but the findings in the open-label study were robust enough that I suspect the drug manufacturer and its advisors were reasonably confident to proceed directly into phase III. The possibility that the doses and dose frequency used were not high enough could have been addressed in such a study, a point acknowledged by the authors.

The second point is the high placebo response rate in study 1, which contributed to the inability to separate treatment from placebo statistically. If we look at the ASAS40 response in placebo arms of other trials, instead of 28%, we see 16% and 15%, respectively, in the certolizumab and golimumab 24-week data, the most recent TNFi trials, and we see 18% in the TNFi-naive secukinumab AS population at 16 weeks. Reasons for such a high placebo response rate would be speculative, but these could include considerations about the study population, and one should keep in mind that the elements that comprise the ASAS40 are all patient-reported. However, the fact that there was no separation from placebo in MRI score in the 45 mg group and minimal separation in the 90 mg group suggests that there was little signal even from more objective markers.

What about potential biologic explanations? An important cautionary tale about the potential effectiveness, or lack thereof, of an IL-23 inhibitor is the recently published negative trial of risankizumab in AS. Risankizumab inhibits IL-23, but not IL-12, by binding to the p19 subunit of the IL-23 molecule. It has shown effectiveness in psoriasis and PsA. At week 12, ASAS40 response rates were 25.5%, 20.5%, and 15.0% in the 18 mg, 90 mg, and 180 mg risankizumab groups, respectively, and 17.5% in the placebo group (4). Ustekinumab inhibits IL-23 via binding to its p40 subunit, also present on IL-12, thus blocking both cytokines. Although they have different mechanisms, both drugs block IL-23, which appears to be the prominent mechanism for their efficacy in psoriasis and PsA. A role of IL-23 is to stimulate the activity of Th17 cells, which have IL-23 receptors on their surface. These cells in turn produce a number of different cytokines, including IL-17A, which is targeted by IL-17A inhibitors such as secukinumab, which is approved for the treatment of AS. It stands to reason that by blocking IL-23 upstream from the production of IL-17, not only might there be some direct effect of IL-23 inhibition on axial SpA, but also there would be an indirect effect by at least partial inhibition of IL-17 downstream. Conversely, it is becoming apparent that IL-23 inhibition benefits patients with inflammatory bowel disease (IBD), while IL-17 inhibition is ineffective or may even worsen IBD, suggesting that treatment effect may depend on which tissue is being targeted.

A recent European League Against Rheumatism abstract is illustrative of this point (5). Stavre et al injected SKG mice, which are prone to an SpA phenotype, with curdlan, which stimulates production of TNF, IL-23, and IL-17. At the ankle, exuberant enthesophytes formed that were associated with increased expression of up-regulators of transforming growth factor β and Wnt-3a genes. In contrast, in the spine, vertebral erosion but not new bone formation occurred in association with increased expression of aryl hydrocarbon receptor upstream regulators. The point of citing this study is not that it directly relates to apparent lack of efficacy of IL-23 inhibition in the spine, but rather that there could be differing biologic mechanisms operating in spinal sites of inflammation as compared to peripheral joints and entheses, resulting in differential responses to IL-23 inhibition in the periphery and the spine.

Another potential explanation for the negative results is that in axial SpA there is production and proinflammatory activity of IL-17 independent of IL-23, perhaps derived from innate γδ T cells or other innate lymphocytes, which is driving disease pathogenesis independent of Th17 cell stimulation by IL-23. Translational studies suggest that mechanical load and stress response of ligament and tendon insertions through prostaglandin E_2 activation of group 3 innate lymphoid cells can generate IL-17A production independent of IL-23–activated Th17 cell production of IL-17A (6). Further illustrating this independence, Deodhar et al cite a study in which differential effects of IL-23 and IL-17 have been demonstrated in gut membrane integrity (7). An additional possibility is that IL-23 may play a role in a different stage of disease (e.g., during the initiation phase of the disease but not in established disease). Might a higher magnitude of IL-23 inhibition be necessary in the spine than in the periphery? Further dose-ranging investigation would be necessary to test this hypothesis. These and other hypotheses could explain lack of or diminished effectiveness of IL-23 inhibition while IL-17 inhibition continues to be effective. A further point is that baseline biomarkers of the Th1 and Th17 pathways were not elevated in study 1, although it is important to note that there may not be a correlation between serum levels of these cytokines and tissue-level expression of them.

Whatever the reason or reasons, whether biologic mechanisms, high placebo response rate, inadequate dose, or combination thereof, we now have 2 axial SpA studies of IL-23

inhibitory drugs which have shown negative results. There is currently an axial SpA trial underway with tildrakizumab, an IL-23p19 inhibitor. We await with interest the results of this trial to learn whether it too demonstrates a negative result, or, for reasons to be determined, shows otherwise. Publication of these negative studies is important to further our understanding of the complex immunologic mechanisms of diseases such as axial SpA and to help us appreciate their differences from related conditions such as PsA, psoriasis, and IBD, as well as to provide evidence for effective and ineffective treatment pathways.

AUTHOR CONTRIBUTIONS

Dr. Mease drafted the article, revised it critically for important intellectual content, and approved the final version to be published.

REFERENCES

1. Deodhar A, Gensler LS, Sieper J, Clark M, Calderon C, Wang Y, et al. Three multicenter, randomized, double-blind, placebo-controlled studies evaluating the efficacy and safety of ustekinumab in axial spondyloarthritis. Arthritis Rheumatol 2019;71:258–70.
2. Poddubnyy D, Hermann KG, Callhoff J, Listing J, Sieper J. Ustekinumab for the treatment of patients with active ankylosing spondylitis: results of a 28-week, prospective, open-label, proof-of-concept study (TOPAS). Ann Rheum Dis 2014;73:817–23.
3. Machado P, Landewe R, Lie E, Kvien TK, Braun J, Baker D, et al. Ankylosing Spondylitis Disease Activity Score (ASDAS): defining cut-off values for disease activity states and improvement scores. Ann Rheum Dis 2011;70:47–53.
4. Baeten D, Ostergaard M, Wei JC, Sieper J, Järvinen P, Tam LS, et al. Risankizumab, an IL-23 inhibitor, for ankylosing spondylitis: results of a randomised, double-blind, placebo-controlled, proof-of-concept, dose-finding phase 2 study. Ann Rheum Dis 2018;77:1295–302.
5. Stavre Z, Maeda Y, Huang T, Gravallese E. Genes regulating bone homeostasis are differentially expressed at peripheral versus axial enthesial sites in an animal model of spondyloarthritis. Ann Rheum Dis 2018;77 Suppl:A621.
6. Schett G, Lories RJ, D'Agostino MA, Elewaut D, Kirkham B, Soriano ER, et al. Enthesitis: from pathophysiology to treatment. Nat Rev Rheumatol 2017;13:731–41.
7. Lee JS, Tato CM, Joyce-Shaikh B, Gulen MF, Cayatte C, Chen Y, et al. Interleukin-23-independent IL-17 production regulates intestinal epithelial permeability. Immunity 2015;43:727–38.

SPECIAL ARTICLE

Proceedings of the American College of Rheumatology/Association of Physicians of Great Britain and Ireland Connective Tissue Disease–Associated Interstitial Lung Disease Summit: A Multidisciplinary Approach to Address Challenges and Opportunities

Aryeh Fischer,[1] Mary E. Strek,[2] Vincent Cottin,[3] Paul F. Dellaripa,[4] Elana J. Bernstein,[5] Kevin K. Brown,[6] Sonye K. Danoff,[7] Oliver Distler,[8] Nik Hirani,[9] Kirk D. Jones,[10] Dinesh Khanna,[11] Joyce S. Lee,[1] David A. Lynch,[6] Toby M. Maher,[12] Ann B. Millar,[13] Ganesh Raghu,[14] Richard M. Silver,[15] Virginia D. Steen,[16] Elizabeth R. Volkmann,[17] Ronan H. Mullan,[18] David N. O'Dwyer,[11] and Seamas C. Donnelly[18]

INTRODUCTION

Interstitial lung disease (ILD), a group of diffuse parenchymal lung disorders classified together based on specific clinical, radiologic, and histopathologic features, is often associated with significant morbidity and mortality and is a common manifestation in connective tissue disease (CTD) (1). ILD often arises within the context of a specific exposure or is associated with an underlying CTD. The CTDs are a spectrum of systemic autoimmune disorders with significant clinical heterogeneity characterized by immune-mediated organ dysfunction, and the lung is a frequent target. All CTD patients are at risk of developing ILD, and those with systemic sclerosis (SSc), polymyositis/dermatomyositis (PM/DM), and rheumatoid arthritis (RA) are at particularly high risk (1,2). ILD may develop at any point in the natural history of CTD, is most frequently identified in the setting of an established CTD, and may also be the first clinically apparent manifestation of occult CTD. Determining whether a patient has a diagnosis of CTD-associated ILD is important, as this knowledge may impact treatment decisions, guide surveillance for other concomitant clinical features, and help with assessment of prognosis (3).

[1]Aryeh Fischer, MD, Joyce S. Lee, MD: University of Colorado, Denver; [2]Mary E. Strek, MD: University of Chicago, Chicago, Illinois; [3]Vincent Cottin, MD: University of Lyon, UMR754, Reference Center for Rare Pulmonary Diseases, Hospices Civils de Lyon, Lyon, France; [4]Paul F. Dellaripa, MD: Brigham and Women's Hospital, Boston, Massachusetts; [5]Elana J. Bernstein, MD, MSc: Columbia University Medical Center, New York, New York; [6]Kevin K. Brown, MD, David A. Lynch, MB, BCh: National Jewish Health, Denver, Colorado; [7]Sonye K. Danoff, MD, PhD: Johns Hopkins Medicine, Baltimore, Maryland; [8]Oliver Distler, MD: University of Zurich, Zurich, Switzerland; [9]Nik Hirani, PhD, MRCP: Edinburgh Lung Fibrosis Clinic, NHS Lothian and Centre for Inflammation Research, University of Edinburgh, Edinburgh, UK; [10]Kirk D. Jones, MD: University of California, San Francisco; [11]Dinesh Khanna, MD, MS, David N. O'Dwyer, MB, BCh, BAO, PhD: University of Michigan, Ann Arbor; [12]Toby M. Maher, MD, PhD: National Heart and Lung Institute, Imperial College London and NIHR Respiratory Clinical Research Facility, Royal Brompton Hospital, London, UK; [13]Ann B. Millar, MD: University of Bristol, Bristol, UK; [14]Ganesh Raghu, MD: University of Washington, Seattle; [15]Richard M. Silver, MD: Medical University of South Carolina, Charleston; [16]Virginia D. Steen, MD: Georgetown University, Washington, DC; [17]Elizabeth R. Volkmann, MD, MS: University of California, Los Angeles; [18]Ronan H. Mullan, MBChB, Seamas C. Donnelly, MD: Trinity College, Dublin, Ireland.

The intersection of CTD with ILD is complex and fraught with areas of controversy and uncertainty. There are numerous gaps in our understanding of why certain CTD populations are more likely to develop ILD, but certain phenotypic risk factors have been identified. In RA, these include older age, cigarette smoking, male sex, rheumatoid factor positivity, anti–citrullinated protein antibody (ACPA) positivity, and more severe articular disease (4–6). In SSc, autoantibodies are the most reliable predictor of ILD, with anti–Scl-70 being one of the strongest (7). In PM/DM, autoantibody profiles also are useful predictors of ILD, especially antisynthetase antibodies (e.g., Jo-1, PL-7, PL-12), anti-PM/Scl antibody, and anti–melanoma differentiation–associated protein 5 antibody (8–10). Knowledge of reliable risk factors for ILD development in other CTDs is lacking. Since the advent of computed tomography (CT), it has been possible to characterize ILD with greater precision than previously (11,12), yet significant gaps remain with respect to reliable determinants of the prevalence of ILD among patients with CTD, and there is controversy surrounding whether to implement early detection strategies in these patients.

Perhaps the greatest unmet needs for ILD in CTD are in the realm of therapeutics. Few effective therapies exist, most decisions about management are based on experience rather than evidence, and there remains a desperate need for well-designed multicenter clinical trials of both existing and novel agents (13).

With a desire to highlight key areas needing scientific and therapeutic focus in CTD-associated ILD, in 2017 the Association of Physicians of Great Britain and Ireland and the American College of Rheumatology supported a multidisciplinary panel of international clinician-scientists from pulmonology, rheumatology, thoracic radiology, and lung pathology specialties with interests and expertise in ILD to convene a 1-day summit on CTD-associated ILD. The goals of the summit were to highlight key clinical and research aspects of CTD-associated ILD, identify unmet needs, and outline future research goals in this complex intersection of diseases. In this report we detail the proceedings of this summit, which were anchored around 5 domains: 1) clinical, 2) biomarkers, 3) diagnostic imaging and histopathology, 4) treatment and clinical trials design and outcome measures, and 5) translational research.

Clinical domain

Statement of the problem and current understanding. ILD is among the leading causes of morbidity and mortality in patients with CTD (1,2). Our understanding of ILD in the setting of CTD is challenged by a combination of factors including the systemic nature of the patients' rheumatologic disease. Patients with CTD-associated ILD, compared to those with idiopathic pulmonary fibrosis (IPF), present with a greater degree of heterogeneity and marked variability in natural history. IPF is a devastating progressive fibrosing ILD associated with a high burden of morbidity and mortality (14). A clinical diagnosis of IPF is made only after careful interpretation of integrated clinical, radiologic, and often lung histopathologic data. Classification of IPF is restricted to those individuals with a lung injury pattern of usual interstitial pneumonia (UIP) based on high-resolution CT (HRCT) scanning or surgical lung biopsy, after all known etiologies for UIP—such as underlying CTD—have been evaluated and excluded (14). Patients with CTD may have a mix of inflammatory and fibrotic ILD along with multicompartment lung involvement including airways, pleural, and pulmonary vascular disease, which may confound determination of the etiology of their respiratory impairment and potential responses to therapy. Furthermore, the ability to predict progression of ILD in CTD is challenging as some patients develop ILD that is mild and nonprogressive, while others have a more progressive course with unrelenting decline in function as seen in IPF.

Optimal care of patients with CTD-associated ILD requires collaboration and close interaction by the rheumatology and pulmonology communities. Rheumatologists have begun to improve their surveillance for lung involvement in patients with CTD, though clear guidelines (and training) have been lacking. Pulmonologists evaluating patients with ILD have become more attuned to the demographic, historical, and phenotypic features that may suggest an underlying CTD, though their level of expertise with that evaluation varies widely. Our understanding of natural history has been limited mostly to prospective observational studies and retrospective analyses, but clinical, pulmonary physiologic, and radiologic data emerging from prospective trials may identify those patients at highest risk for developing ILD and those who are candidates for treatment and participation in clinical trials (15). While there has been greater emphasis on a multidisciplinary approach to patient care and education of physicians, effective collaboration between pulmonologists and rheumatologists still falls short due to practical reasons including interest, limited expertise in this area, and availability of and access to ancillary resources. Collective experience and a recent study demonstrate that collaborative efforts can be effective in enhancing patient care (16,17).

Challenges and unmet needs. One of the challenges in CTD-associated ILD is that the prevalence of ILD among different groups of patients with CTD varies so widely (Table 1), with the highest estimated prevalence rates noted among patients with SSc and those with PM/DM (1,2,18). Severity of disease is most notable in patients in whom ILD is predominantly fibrotic such as patients with UIP as is seen in RA, with mortality rates comparable to those of IPF (6,19,20). While prevalence may define the frequency of ILD in any given CTD, focusing on the severity of disease based on features identified by chest imaging, with pathologic correlation when histologic data are available, may offer greater insight into prognosis compared to a focus on any specific CTD, and may thus guide decision-making with regard to treatment and inclusion in clinical trials.

Table 1. Connective tissue disease–associated interstitial lung disease: estimated prevalence rates, lung injury patterns, and clinical presentation*

CTD	Estimated prevalence of ILD†	ILD pattern	Frequency CTD is occult
Polymyositis, dermatomyositis, antisynthetase syndrome	40%	NSIP with OP, NSIP, OP, UIP	Often
Rheumatoid arthritis	10% clinical, 30% subclinical	UIP, NSIP, OP	Less often
Sjögren's syndrome	40%	NSIP, UIP, LIP	Less often
Systemic sclerosis	30–40% clinical, 80% subclinical	NSIP, UIP	Less often
Systemic lupus erythematosus	8–12%	DAH, NSIP	ILD is infrequent
Interstitial pneumonia with autoimmune features	100%	NSIP, OP, NSIP with OP, UIP, LIP	Always

* CTD = connective tissue disease; ILD = interstitial lung disease; NSIP = nonspecific interstitial pneumonia; OP = organizing pneumonia; UIP = usual interstitial pneumonia; LIP = lymphocytic interstitial pneumonia; DAH = diffuse alveolar hemorrhage.
† From refs. 1, 2, 6, 18, 45, 76, and 77.

Efforts to identify CTD patients with ILD or those who are at risk of developing ILD require an approach to screening that has the dual objectives of identifying early-stage disease and more specifically identifying those at greatest risk for progression and functional decline. Our present approaches do not allow us to fulfill either of those screening goals effectively, though emerging evidence suggests a framework for screening. In RA for example, as highlighted in a recent high-level review (6), the pattern of UIP predominates in most series (6,20,21), and certain phenotypic features (older age, male sex, history of smoking, and ACPA positivity) that may predict a higher risk for ILD have been identified in retrospectively studied cohorts. However, prospective data are only now being gathered to test and validate predictive models that may allow selective and targeted screening efforts (22–26). In RA there is a suggestion that pulmonary physiologic data can predict decline, though it is unclear whether this can serve as the sole screening strategy (27). In SSc and PM/DM, retrospective studies have identified phenotypic, autoantibody, radiologic, and pulmonary physiologic data that identify patients at increased risk for ILD and for mortality (28–30). Such understanding has led to the development of algorithms utilizing a combination of HRCT and pulmonary physiologic data to assess severity of disease and offers insights into assessment of prognosis (28–30). Screening strategies that identify ILD are important in view of evidence indicating that immunosuppressive treatment produces modest benefits. Data on utilization of antifibrotic drugs approved for use in IPF are not available, but these agents are being investigated in ongoing prospective trials.

Proposed future directions. A clearer understanding of long-term historical data will require multicenter cooperation using prospective databases that encompass phenotypic, pulmonary physiologic, radiologic, genomic, and proteomic data that may help elucidate factors that can best predict which patients are at risk for ILD and for progressive disease. Heightened awareness and recognition that lung disease is common among patients with CTD should lead to creative and sustained efforts to improve education of rheumatologists regarding clinical features of lung disease and utilization of pulmonary physiologic data to facilitate prompt and appropriate referral, and to forge closer collaborations with pulmonology colleagues. For the pulmonologist, dedicated education and training is needed to aid in recognizing important clinical and historical features that indicate a diagnosis of a CTD and to gain better understanding of autoimmune serologies in the evaluation in patients with ILD. Much of this can be accomplished by greater cooperation between the academic societies of the two disciplines, utilizing existing educational opportunities but also creating additional learning modalities such as case-based online educational modules. Finally, enhanced fellowship training in both disciplines with elective rotations in one another's specialty during fellowship, and encouragement of collaborative pulmonary and rheumatology fellowship opportunities, will also enhance recognition of these disorders and will hopefully improve the care of patients with CTD-associated ILD.

Biomarker domain

Current understanding and unmet needs. Biomarkers refer to a category of objective medical signs that correlate with certain aspects of normality or abnormality and may be defined as "a characteristic that is objectively measured and evaluated as an indicator of normal biologic processes, pathogenic processes, or pharmacologic responses to a therapeutic intervention" (31). Given the heterogeneity of ILD complicating CTD, the identification of biomarkers is an important endeavor. However, to date there are no validated biomarkers for CTD-associated ILD.

Diagnosis of CTD-associated ILD is currently limited to the use of clinical data including history, physical examination, pulmonary function testing, and data from lung imaging and histopathologic studies. In order for biomarkers to become important tools for clinical practice, the specific measures should be accessible, reproducible, accurate, and clinically useful. Obtaining samples must be feasible, and the risk acceptable. While

biomarkers in ILD studies may be obtained from lung tissue and bronchoalveolar lavage (BAL) fluid, biomarkers obtained from peripheral blood would be far better given ease of access, convenience, and cost factors. At the same time, analysis of tissue or BAL fluid from the site of pathophysiologic activity in the lungs is a potentially more promising route for discovering ILD-relevant biomarkers than analysis of the blood. This is especially the case when other organ involvement in a systemic disease contributes to the overall heterogeneity of measured signals in the blood, thereby potentially confounding or limiting interpretation of a serologic finding (e.g., rheumatoid factor, antinuclear antibody, erythrocyte sedimentation rate).

Several challenges need to be met before the acquisition of valid biomarkers for CTD-associated ILD can become a reality. A systematic review using an NCBI search strategy with the terms "interstitial lung disease," "connective tissue disease," and "biomarker" was used in preparation for this summit. Case reports, case series, studies with inappropriate design or patient populations, pediatric studies, and studies with <20 cases were excluded from the analysis. The Outcome Measures in Rheumatology (OMERACT) filter was applied to evaluate articles for truthfulness, feasibility, and discriminatory ability (32,33). Articles were also subjected to analysis of whether the proposed biomarker measured an appropriate target domain (34). There were only 23 articles that passed these initial stages.

Candidate biomarkers have been identified in a number of the studies fulfilling the search criteria and passing the OMERACT filter. Chen and colleagues reported a strong association between the presence of ILD in RA patients and elevated peripheral blood levels of matrix metalloproteinase 7 (MMP-7) and interferon-γ–inducible protein 10 (CXCL10) as measured by multiplex enzyme-linked immunosorbent assay (ELISA). This association was confirmed in 2 independent Chinese RA cohorts. The authors subsequently validated their findings using a different quantitative platform (sandwich ELISA) in a separate cohort of RA patients from the US (22). Further work by Doyle and colleagues demonstrated that a regression model composed of several clinical variables could be used to identify both clinically evident ILD and subclinical ILD in 2 independent RA cohorts (25). This association was significantly improved with the addition of the peripheral blood biomarkers MMP-7, surfactant protein D (SP-D), and activation regulated chemokine/CCL18. In the Scleroderma Lung Study (SLS I), analysis of serum Krebs von den Lungen 6 and SP-D in peripheral blood demonstrated significant associations with parenchymal lung disease in SSc patients with ILD (35).

BAL also has proven utility in the assessment of alveolitis in SSc. Schmidt et al compared the levels of alveolar cytokines in 32 SSc patients, by multiplex ELISA (36). They found higher levels of interleukin-7 (IL-7), IL-4, IL-6, IL-8, and CCL2 in BAL fluid from patients who had ILD. However, their observations were limited by the small sample size of the cohort. Though potential biomarkers for CTD-associated ILD from different sources including peripheral blood and BAL have been studied in patient cohorts, to date the use of these biomarkers has not been adopted in everyday practice. Further prospective studies are clearly needed.

Overall, the current evidence in support of specific candidate biomarkers consists predominantly of results obtained from relatively small retrospective or cross-sectional studies with limited power. Most published studies have been conducted at single-center academic institutions and results may not be broadly applicable. Furthermore, given the clinical heterogeneity of CTD-associated ILD, it is likely that no single biomarker will have utility in diagnosis and prognosis, or act as a measure of disease progression and response to therapy.

Proposed future directions. A number of future directions are proposed to address these unmet needs and challenges in CTD-associated ILD biomarker development (Figure 1). Ideally, biomarkers will be used to achieve a number of specific aims in CTD-associated ILD. They may facilitate screening or diagnosis to identify individuals at high risk of developing ILD, or alternatively to identify those with early, preclinical disease. In addition, biomarkers may be used to risk-stratify patients at baseline and assess prognosis. They may provide data on disease progression and/or response to therapy. Furthermore, they may serve as surrogate markers for use as clinical trial end points or as tools to provide mechanistic pathophysiologic insight. Biomarker studies in other forms of ILD, namely IPF, have led to significant ongoing improvements in our understanding of the pathophysiology of pulmonary fibrosis (37–39), and these data exemplify the types of studies that may be considered in future investigations addressing CTD-associated ILD.

In conclusion, the development of accurate and practical biomarkers for diagnosis, prognosis assessment, analysis of disease progression, and evaluation of treatment response in CTD-associated ILD is an important research endeavor with considerable implications related to clinical trials and clinical practice. Further deliberations by multidisciplinary stakeholders are needed to determine the best course for the future development of CTD-associated ILD biomarkers.

Diagnostic imaging/histopathology domain

Imaging. *Current understanding*. CT imaging of the chest plays a critical role in identifying and characterizing CTD-associated ILD and in longitudinal follow-up when ILD is present. Its use must also be balanced against longer-term risk associated with radiation exposure. In addition to ILD, clinically important findings that may be identified on CT include features that indicate airways, pulmonary vascular, or pleural disease. Any pattern of ILD may occur in any of the CTDs, and the estimated prevalence of specific patterns varies by disease (40–42) (Table 1). CT
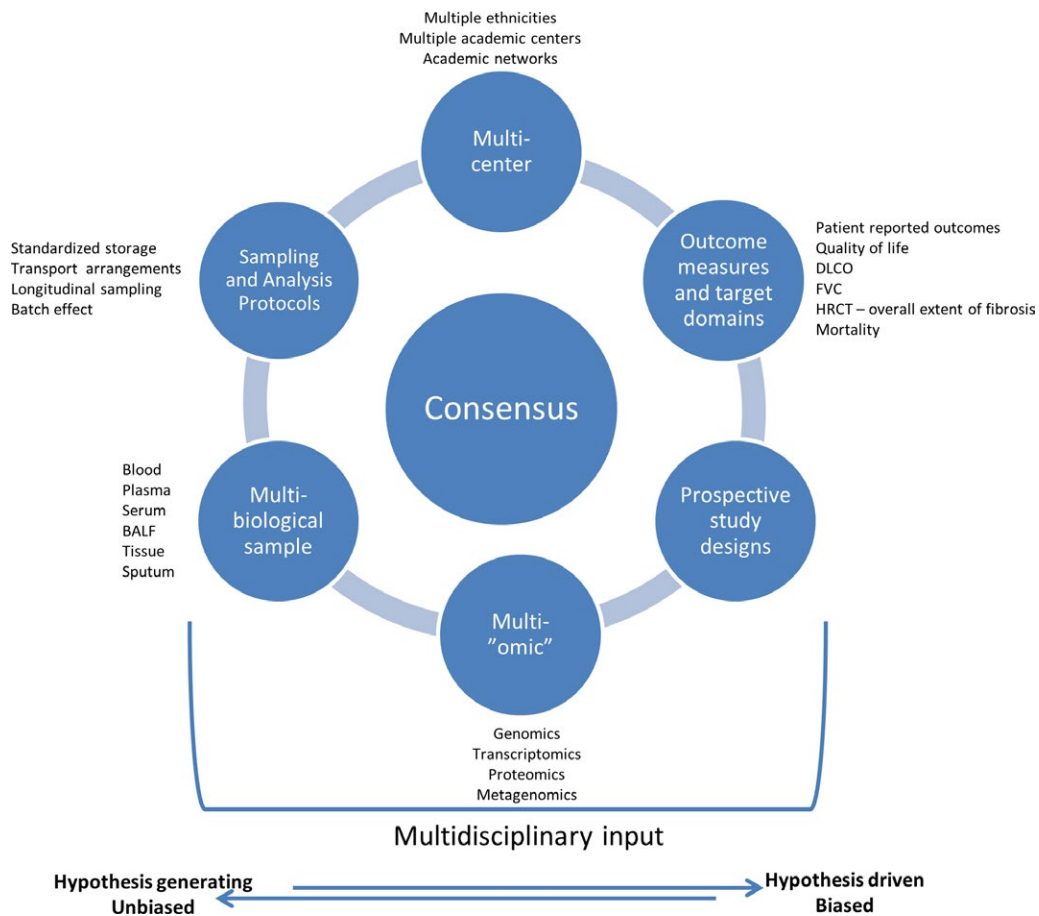
Figure 1. Proposed future investigative directions for the development of connective tissue disease–associated interstitial lung disease biomarkers. DLco = diffusing capacity for carbon monoxide; FVC = forced vital capacity; HRCT = high-resolution computed tomography; BALF = bronchoalveolar lavage fluid.

can reveal asymptomatic lung disease in a substantial proportion of patients with CTD, and these changes may progress slowly over time (Figure 2).

Unmet needs. The utility of CT in screening for early CTD–associated ILD is unknown. If ILD is present, we do not know how to identify patients in whom it is likely to progress, and optimal follow-up and treatment of patients with early changes remains unclear. Quantitative methods are increasingly being used for determining the extent of disease evidenced on CT, and have been used to document decreases in the extent of CTD-associated ILD in clinical trials (43,44). However, a standardized quantitative approach has not yet been developed, and the sensitivity of these techniques in identifying short-term longitudinal change is unknown.
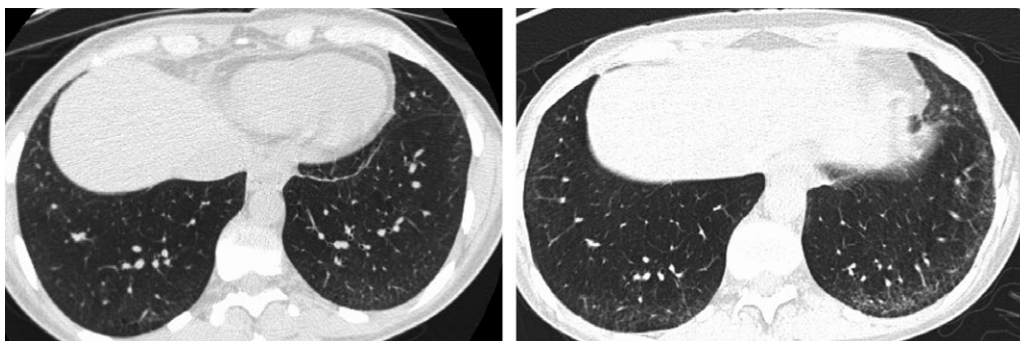
Figure 2. Progression of interstitial lung abnormalities in a patient with systemic sclerosis, as demonstrated by computed tomography. The image on the right was obtained 3 years after the image on the left.

Proposed future directions. There is a critical need for assembly of prospective cohorts of well-characterized patients with SSc, RA, and PM/DM/antisynthetase syndrome who would undergo CT at enrollment, with follow-up scanning at specific intervals. This could be achieved through a multi-institutional network, and perhaps by collaboration with industry to share CT scans performed in the context of clinical trials. Specifically, achievement of the following could yield valuable insights: 1) elucidation of the relationship between CT-determined phenotype (UIP, nonspecific interstitial pneumonia [NSIP], organizing pneumonia, lymphocytic interstitial pneumonia) and progression of CTD-associated ILD or response to treatment, 2) elucidation of the relationship between baseline extent of abnormality on quantitative CT and both short-term and medium-term outcome (death, progression, improvement), and 3) development and validation of techniques for phenotyping and quantifying CTD-associated ILD.

Histopathology. *Current understanding*. The decision on whether histologic examination of the lung would be useful in cases of CTD requires an analysis of potential benefit versus risk of an invasive procedure. Microscopic examination of surgical lung biopsy specimens from patients with CTDs often shows histologic clues indicating that the etiology is of an autoimmune nature (Table 2) as opposed to the findings being idiopathic or the result of other disease (45–47). Some of these histologic features (e.g., fibrosis) have been shown to be related to prognosis, but none have been influential in determining treatment decisions (48–50). These cases often do not fit into a single histologic category when using the criteria for idiopathic interstitial pneumonia (IIP), and instead show overlapping features of 2 or more entities (51). The risk of mortality from surgical lung biopsy was recently evaluated. In 2 large series in the US and the UK (52,53), the 30-day mortality rate with elective surgical lung biopsies was 1.5% and 1.0%, respectively. However, in the US series, the risk of death was 6.0% in patients with CTDs. The odds ratio for 90-day mortality in patients with CTD was similar to that in the overall cohort in the UK study. The risk of mortality was increased in patients who were being treated with glucocorticoids.

Table 2. Histologic features associated with underlying connective tissue disease

Prominent lymphoid aggregates with germinal center formation
Increased lymphocytic inflammation with plasma cell infiltrates
Overlapping features of peripheral honeycombing with central fibrosis
Involvement of multiple pulmonary compartments (interstitial disease with additional small airway, vascular, or pleural disease)
Nonspecific interstitial pneumonia pattern with additional organizing pneumonia
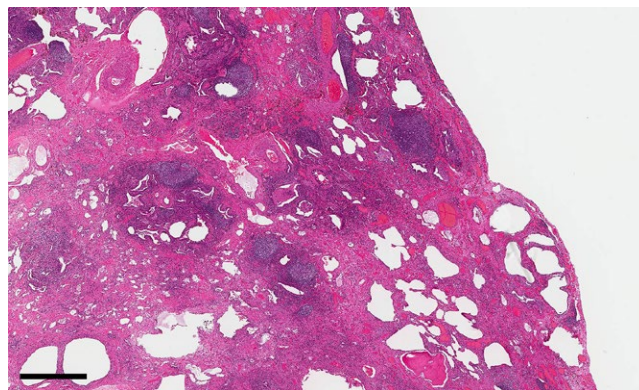
Figure 3. Surgical lung biopsy specimen from a patient with known connective tissue disease–associated interstitial lung disease (ILD) in whom the ILD was progressing typically, showing a mixed pattern of subpleural and centrilobular fibrosis with prominent lymphoid aggregates. Bar = 1 mm.

Whether to obtain a surgical lung biopsy depends on the clinical situation, and several frequently encountered scenarios were considered, and consensus reached, by the summit participants: 1) A patient has known CTD, has been shown clinically and/or radiologically to have ILD, and the ILD is progressing typically (Figure 3). In this case, the participants recommended not obtaining a biopsy because the results would not alter the treatment strategy. 2) A patient has certain clinical or serologic features suggesting possible CTD-associated ILD but does not meet established criteria for a CTD. In this case, the consensus was that a biopsy may be performed to assess whether specific histologic features support the presence of an autoimmune ILD (e.g., "interstitial pneumonia with autoimmune features") that might impact treatment strategies. 3) A patient has a known CTD but has an atypical clinical picture suggesting hypersensitivity pneumonitis, has drug-induced lung toxicity, or has an atypical radiologic pattern. In this case, the participants agreed that biopsy may be indicated
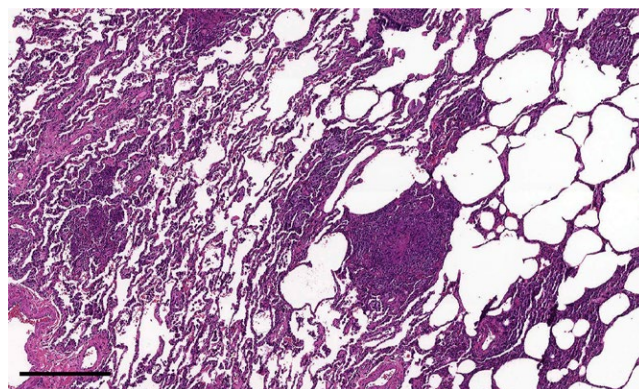
Figure 4. Surgical lung biopsy specimen from a patient with rheumatoid arthritis treated with biologic agents who developed nodular ground-glass opacities seen on computed tomography. The biopsy demonstrates granulomatous *Pneumocystis pneumonia*. Bar = 400 μm.

in order to differentiate between hypersensitivity pneumonitis, drug toxicity, or an infectious etiology (Figure 4) rather than CTD-associated ILD.

The availability of antifibrotic therapies raises the question of whether a biopsy may reveal certain histologic features that would guide therapy (e.g., whether a CTD patient with a UIP pattern of fibrosis should be offered antifibrotic therapy). However, there are currently no available data to answer this question.

Proposed future directions. The recent advances with the technique of cryobiopsy (54)—and wider application of this innovative procedure—may provide valuable insights into lung histopathology in CTD-associated ILD. However, as recently emphasized by an international cryobiopsy working group (55), the technique has not yet been standardized, and its place in the diagnostic algorithm of ILD remains to be defined. In part, this reflects concerns over the diagnostic yield and safety of the procedure, along with the rapid spread of the technique without safety or competency standards (55). Another limitation and concern regarding cryobiopsy is the substantial procedural variability among centers and interventional pulmonologists (55). Usual practice is not to perform a surgical lung biopsy in "typical" scenarios as discussed above, but the advent of cryobiopsy may change this paradigm by providing a safer and easier approach to obtaining parenchymal lung tissue. It remains to be seen whether cryobiopsy will become a common procedure in the evaluation of ILD, but if it does, we would anticipate that access to far greater numbers of histopathologic samples in CTD-associated ILD will allow for a greater understanding of the correlations between lung injury patterns on HRCT and histopathology. Cryobiopsy might also lead to insights into whether specific autoimmune histopathology features are more predictive of underlying CTD and could help with refining of the histopathologic criteria for interstitial pneumonia with autoimmune features (45). We anticipate a need for approaches based on imaging or histopathology to optimize treatment strategies, i.e., antiinflammatory versus antifibrotic therapies—and having more access to lung tissue should enhance such approaches as histopathologic findings remain the gold standard to define presence of fibrosis.

Treatment/clinical trials domain

Statement of the problem and current understanding. The clinical management of CTD-associated ILD is challenging, as 1) the natural history remains poorly understood though with significant recognized disease and individual patient heterogeneity, 2) there are no approved therapies, and 3) with the exception of recent clinical trials in SSc-associated ILD (44,56,57), there has been a paucity of interventional clinical trials. A similar dilemma existed in IPF, but over the last decade the performance of multiple large multicenter clinical trials in IPF led to a much better understanding of the disease trajectory, and to the availability of approved antifibrotic therapy. There are significant challenges to embarking on large clinical trials in CTD-associated ILD, but the substantial unmet need, especially in RA-associated and SSc-associated ILD, is a powerful incentive for overcoming these obstacles.

Phenotypic heterogeneity and natural history diversity. In clinical trials the goal is to recruit subjects with diseases of uniform pathobiology and natural history (i.e., homogeneity). However, the CTD-associated ILDs have complex systemic manifestations, multicompartment pulmonary disease, and a highly variable natural history. Their interstitial component can be classified according to the recognized pathologic patterns of the IIPs (58). The most common histologic patterns associated with CTD are NSIP and UIP, but any of the pathologic patterns can occur. Given that the systemic disease in CTD is immune driven, there is a rationale to believe that humoral and T cell–directed inflammatory processes contribute to the lung injury. However, many patients with CTD-associated ILD develop progressive ILD despite treatment with a variety of immunomodulatory agents that control the underlying disease.

Some CTD patients have clear symptoms of lung disease at the time of ILD diagnosis. Others have "subclinical" disease, i.e., radiologic findings suggestive of ILD in the absence of symptoms, and some have no evidence of lung disease at the time of the CTD diagnosis, but are at risk of developing ILD. There are no consensus guidelines that define either subclinical or clinically overt ILD in this context. Any potential definition would have to include subjective reports (symptom scores), chest imaging with qualitative and quantitative HRCT scoring, and pulmonary physiology assessment. For instance, subclinical CTD-associated ILD could be defined according to a threshold in extent and pattern of abnormality on HRCT in the setting of normal pulmonary physiology and the absence of respiratory symptoms. Clinically overt CTD-associated ILD could be defined as HRCT-detected abnormality plus lung function impairment or decline and/or respiratory symptoms. This potentially offers a unique opportunity to initiate clinical trials for all "stages" of disease and therein generate much-needed natural history data.

Proposed future directions. One option to improve study subject homogeneity is to pool subjects based on the underlying pathologic pattern of the ILD rather than the specific CTD (e.g., grouping patients with a UIP pattern of disease regardless of the underlying CTD). A limitation to this approach is that biopsy is infrequently performed in CTD-associated ILD, so the pathologic pattern cannot always be confirmed. Even when a biopsy is performed, a "classic" UIP histologic pattern is relatively uncommon, and "mixed" patterns are frequent. The radiologic pattern seen on HRCT of the chest is often used as a surrogate for lung biopsy, and thereby to classify the type of CTD-associated ILD. This is common practice in the IIPs based on consensus criteria, and it seems intuitively attractive to extrapolate this HRCT classification

to CTD-associated ILD. However, HRCT patterns have not been as robustly correlated with pathology in CTD-associated ILD. The relationship between HRCT patterns and disease progression is reasonably well established in idiopathic disease (e.g., a UIP pattern is associated with a worse outcome than a non-UIP pattern), but comparative studies in CTD-associated ILD are scarce. There is a pressing need for longitudinal HRCT-based studies in CTD-associated ILD. Presently, it may be more practical to perform trials according to the underlying CTD and subsequently stratify according to HRCT pattern.

With regard to natural history diversity, an attractive investigational model would be to enroll unselected patients with CTD into a multicenter longitudinal observational cohort, in which both incident and prevalent cases at all stages could be studied (Figure 5). In isolation, unbiased observational cohort studies, though informative, can be difficult to perform and fund. A therapeutic intervention study is more likely to be attractive and is easy to justify in clinically overt CTD-associated ILD, but in patients who have subclinical ILD or are at risk for ILD the justification is more nuanced. A number of these at-risk patients will develop ILD, but the proportion and time scale are uncertain. Moreover, some of these patients are likely to already be receiving treatment for extrapulmonary features of their CTD. Such a trial design was, however, recently applied in a phase III study of anti–IL-6 antagonist treatment of patients with early SSc and elevated acute-phase reactant levels (59). Treatment, in the context of a trial, could only be justified if the intervention is known to have low risk of harm. Mycophenolate mofetil (MMF) is a commonly used immunosuppressant in various CTD-associated ILDs. In early diffuse SSc, it is used for management of skin fibrosis, although there are differences among practices. Consideration can be given to case–control or longitudinal observational cohorts to assess the incident cases of ILD in patients who have been treated with MMF versus those who have not, accounting for covariates such as duration of disease, ethnicity, autoantibody status, and geographic distribution. The safety profile is good, and a randomized controlled trial of MMF for primary prevention of ILD in at-risk patents with CTD may be ethically justifiable.

Addressing systemic manifestations. Well-executed clinical trials demand a defined standard of care. For subjects at risk for developing CTD-associated ILD and those with subclinical ILD, this would be "no-treatment" for the underlying ILD. While there are currently no approved drugs for CTD-associated ILD, there are ongoing late-phase trials with pirfenidone and nintedanib, drugs currently approved for IPF, that include patients with clinically significant CTD-associated ILD. Many clinicians prescribe glucocorticoids and/or other immunomodulatory drugs, commonly cyclophosphamide (CYC), MMF, or azathioprine, for CTD-associated ILD. In rapidly progressing CTD-associated ILD, which can occur in DM, for example, these and other agents are accepted as appropriate therapy. A similar case may be made for SSc-associated ILD, in which there is some prospective trial evidence of efficacy of CYC and MMF (44,57), especially in specific subgroups. Thus, while placebo-controlled studies may still be ethically viable for patients with CTD-associated ILD, the fact that routine care often includes immunomodulatory therapies makes such trial design more difficult to successfully recruit patients for and implement. Trial stratification methodology could be utilized to ensure the veracity of results.

End points for clinical trials in CTD-associated ILD. Trial end points are often dependent on the phase of study and study aims. For subjects recruited into a trial for CTD patients at risk for ILD, the end point would be the development of subclinical or clinically overt ILD, as defined a priori. There have been few efficacy trials in the setting of clinically overt CTD-associated ILD, and primary end points are not well established. In IPF, mortality, while clinically relevant, does not appear to be a feasible primary end point (60). Because the association between decline in forced vital capacity (FVC) and subsequent death is high, change in FVC is now the established primary end point in IPF efficacy trials and has been recognized by regulatory agencies as a surrogate for mortality. In contrast to IPF, our understanding of the behavior of CTD-associated ILD within a trial setting, in terms of change in lung function, hospitalization, and mortality, is very limited. It is unlikely that studies in CTD-associated ILD powered on a mortality end point could be practically performed. There are data to confirm that change in FVC correlates with mortality in CTD-associated ILD as it does in IPF (27,61), but hospitalization rates are unknown. Tools, such as blood biomarkers and/or risk scores to improve the ability to determine "predicted events" during the period of observation, would be invaluable.

Trial population	Primary Outcome
No ILD	Presence or absence of ILD
Subclinical ILD	Resolution/ stability or progression
Clinically significant disease	Stability or progression
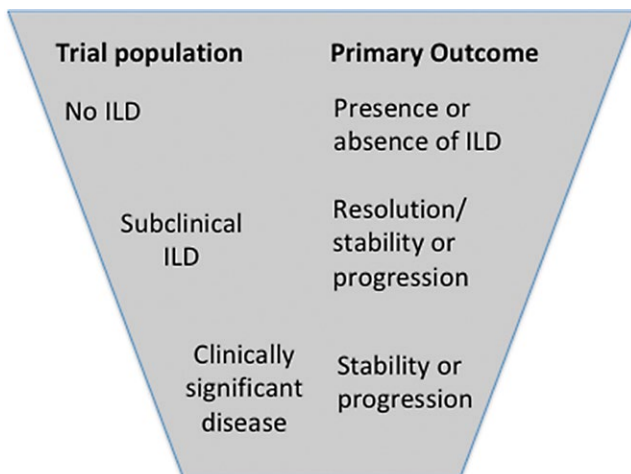
Figure 5. Suggested disease population stratification, and corresponding primary trial outcome, for interstitial lung disease (ILD) clinical trials in patients with connective tissue disease.

In the absence of an established relevant single end point, a composite "event-driven" end point may be a tempting solution, comprising, for example, ≥10% decline in FVC, ≥15% decline in diffusing capacity for carbon monoxide, hospitalization, and/or death (62,63). However, the use of composite end points presents its own difficulties that may limit interpretation of the data (64). Finally, patient-reported outcomes (PROs), including dyspnea, cough, or quality of life, should be considered in all efficacy trials. The OMERACT group recently provided consensus-based domains and PROs for use in clinical trials. Although some PRO-related instruments, such as the Mahler dyspnea index and St. George's Respiratory Questionnaire, have been validated via clinical trials (SLS-I and II) (65) and observational cohort studies, many have not. Therefore, ongoing and future trials should proactively validate outcome measures. Table 3 summarizes ongoing clinical studies in CTD-associated ILD that have been submitted to ClinicalTrials.gov.

In conclusion, the unmet need for therapy in CTD-associated ILD, combined with a plethora of potential antifibrotic drugs in industry pipelines, demands a new age of clinical trials. Lessons learned from studies in IPF suggest that recruitment of patients into well-designed studies can both increase understanding of the natural history of disease and lead to the discovery of effective treatments. Recruitment of CTD patients from the full spectrum of disease, i.e., from those at risk for ILD to those with clinically overt CTD-associated ILD, is ambitious and would require multicenter cooperation, but offers the potential for dramatically increasing our knowledge in these understudied disorders.

Translational research domain

The purview of translational research in CTD-associated ILD is exceptionally broad. In this section we focus on several themes identified by summit participants as being of particular relevance due to high levels of future promise, as well as addressable barriers to progress. The discussion will be divided into 1) databases and bioregistries, 2) technology for precision medicine, 3) quality of life outcome measures, and 4) animal models.

Databases and bioregistries. *Statement of the problem*. While randomized controlled trials remain the gold standard for hypothesis-driven clinical research questions on treatment efficacy, the information contained in clinical registries and biorepositories offers unique opportunities for advancing our understanding of CTD-associated ILD. Particularly in the context of rare diseases such as CTD-associated ILD, maximizing the use of existing registries and biorepositories will be necessary to form the groundwork for targeted clinical trials.

Current understanding. The accumulation of real-world registry data over time provides a more dynamic and evolving picture of disease course, which is more generalizable and relevant to the real-world patient population (66). Targeted biologic sample repositories, particularly when aligned to clinical registry information, may be used with maximal effect both to specifically inquire into the connected contributions of genetic susceptibility, environmental, and lifestyle factors in influencing disease pathogenesis and to develop a future individualized precision medicine approach.

Challenges and unmet needs. There are significant barriers to data sharing when clinical and biologic registries are designed within disconnected, institutional "silos of information" or when there is no available technological platform for data sharing between institutions at a national or international level. Differences in defining the terms of reference of diseases for inclusion into disease registries, or in the precise domains of clinical information stored, prevent clinical equivalence between registry data sets, which in turn prevents the merging of information between research groups. For biologic samples, variations in sample collection and processing can lead to variations in the quality of available biobanked material and may affect their suitability for sample collaboration between groups. This is of particular importance with rare diseases, for which larger populations are needed to enable sufficient collection of relevant material.

Proposed future directions. A more collaborative approach from the research community is needed to maximize scientific output, with an emphasis on improved sharing of available data and on the standardization of future data collection through the formation of national and/or international disease registries. One such effort has been recently launched by the Pulmonary Fibrosis Foundation (PFF) with the creation of a large network of PFF Care Centers around the US. Within the PFF Care Network a collaborative PFF Registry was established, which now includes >2,000 patients with diverse forms of ILD. High-quality clinical data are being collected, there is an accompanying biorepository, and a potentially valuable research database will be available for access by independent investigators (https://www.pulmonaryfibrosis.org/medical-community/pff-patient-registry).

Technology for precision medicine. *Statement of the problem and current understanding*. In the pursuit of truly personalized medicine, the capacity to monitor individuals in their unique environments should be paramount. While a number of technologies have emerged to assess physiology (e.g., heart rate, blood pressure), mobility (accelerometry), and even to measure PROs on a daily basis, this technology has not adequately evolved to include outcomes relevant in CTD-associated ILD, nor has it been adopted in CTD-associated ILD research. The thoughtful proactive development and implementation of technology will provide a powerful new tool for research, including the assessment of therapy and potentially direct therapeutic interventions for CTD-associated ILD.

Table 3. Pending or currently recruiting clinical trials in CTD-associated ILD (as of September 2018)*

Trial name	ClinicalTrials.gov identifier	Study type	Disease entity	Participants (target or estimated)	End point
Abatacept in RA-ILD (APRIL)	NCT03084419	Interventional (phase II open label)	RA-ILD	30	No. of participants without significant decrease (≥10%) in FVC following abatacept treatment
Phase II Study of Pirfenidone in Patients With RA-ILD	NCT02808871	Interventional (phase II)	RA-ILD	270	Incidence of the composite end point of decline in FVC (% of predicted) of ≥10% or death
BI 1199.247: Efficacy and Safety of Nintedanib in Patients With Progressive Fibrosing Interstitial Lung Disease	NCT02999178	Interventional (phase III)	Progressive fibrosing ILD including CTD-ILD	600	Annual rate of decline in FVC (in ml) over 52 weeks
BI 1199.214: A Trial to Compare Nintedanib With Placebo for Patients With Scleroderma Related Lung Fibrosis	NCT02597933	Interventional (phase III)	SSc-ILD	520	Annual rate of decline in FVC (in ml)
Scleroderma Lung Study III: Combining Pirfenidone With Mycophenolate	NCT03221257	Interventional (phase II)	SSc-ILD	150	Change from baseline, measured at 3-month intervals, in the mean FVC
Study to Compare the Efficacy of Mycophenolate Mofetil in Systemic Sclerosis Related Early Interstitial Lung Disease	NCT02896205	Interventional (phase III)	SSc-ILD	60	Change from baseline in FVC at 6 months, after treatment with oral mycophenolate mofetil or placebo
Abituzumab in SSc-ILD	NCT02745145	Interventional (phase II)	SSc-ILD	22	Annual rate of absolute FVC change in volume (in ml)
Abatacept for Myositis-ILD	NCT03215927	Interventional/ pilot study	Antisynthetase syndrome–ILD	20	Primary outcome criterion for efficacy will be the % change in FVC from baseline visit to week 24 between the 2 treatment arms (standard of care/ placebo vs. standard of care/abatacept)
Rituximab Versus Cyclophosphamide in Connective Tissue Disease–ILD (RECITAL)	NCT01862926	Interventional	CTD-ILD	116	Absolute change in FVC (time frame 48 weeks)

* CTD-associated ILD = connective tissue disease–associated interstitial lung disease; RA-ILD = rheumatoid arthritis–associated ILD; FVC = forced vital capacity; SSc-ILD = systemic sclerosis–associated ILD.

Challenges and unmet needs. There are technological barriers to progress. The pace of technological advancement in information systems, including mobile technologies, has outstripped the rate of progress seen in health care information sharing. The academic health care community runs the risk of losing opportunities to improve and shape the quality and quantity of data

platforms that may be used to further enrich the information available for research.

Proposed future directions. Significant opportunities exist for the research community to influence the development of research technology, including mobile technologies, to enhance the type and quality of data collection. This could be achieved through partnership with biotechnology and engineering research communities, and through engagement with patient-centered organizations to ensure that both the research community and the patients themselves benefit from future partnerships.

Quality of life outcome measures. *Statement of the problem and current understanding.* Little is understood about the impact of CTD-associated ILD on daily living, including quality of life (QoL). Challenges to studying and understanding the effects of CTD-associated ILD on health-related QoL include the differing organ manifestations and effects of specific CTDs and elucidation of the pulmonary and extrapulmonary contributions to QoL. Nonetheless, it is critical to understand how patients experience disease as we assess the impact of treatments and other interventions. PRO questionnaires are designed to assess the influence of disease on patient function and individual subjective life experience. They remain an important outcome measure, due to both their reproducibility in quantifying the impact of disease severity and their sensitivity to change.

Challenges and unmet needs. The evaluation of how a specific disease impacts QoL for patients with simultaneously overlapping symptoms of ILD and systemic disease manifestations presents clear challenges. While some rheumatic disease–specific QoL instruments, including the Systemic Sclerosis QOL questionnaire (67), contain domains that are specific for respiratory manifestations of disease, others, including the Rheumatoid Arthritis Quality of Life questionnaire (68), which was validated using RA patients without ILD, have not been designed to determine the specific impact of RA-associated ILD on health-related QoL. Although efforts have been made to validate lung-specific QoL measures such as the King's brief ILD questionnaire for ILD other than IPF, other measures, including the St. George's Respiratory Questionnaire, which was initially designed for patients with chronic obstructive pulmonary disease, have been subsequently validated for patients with IPF but not those with CTD-associated ILD (69,70).

Proposed future directions. Future work is needed to determine whether a new QoL tool should be designed, tested, and validated in collaboration with CTD-associated ILD patients to fully reflect all disease-specific impacts on QoL. Alternatively, consideration should be given to whether an existing generic, and/or symptom-specific tool that has previously been validated in IPF or a CTD can be tested and validated in the CTD-associated ILD population. The establishment of a QoL outcome measure working group is needed in order to obtain

Table 4. Summary of proposed future directions in connective tissue disease–associated interstitial lung disease (CTD-associated ILD)

Standardized international criteria for the classification of CTD-ILD
Deliver international guidelines that standardize clinical, radiologic, histopathologic, and biologic parameters for the diagnosis and classification of CTD-ILD
Defining the natural history of CTD-ILD
Deliver multicenter global clinical networks of well-defined disease groups, encompassing longitudinal integrated collections of phenotypic, physiologic, radiologic, genomic, and biologic data
Clinical care
Deliver multidisciplinary clinics for rheumatology, pulmonology, and allied health care professionals to enhance patient care
Cross-disciplinary clinical training
Deliver cross-disciplinary fellowship clinical training opportunities for medical graduates
Biomarker development
Deliver precision medicine–based biomarker platforms to guide the optimal therapies to the individual patient
Early screening strategies for ILD
Develop and utilize early detection strategies that identify ILD earlier and ultimately predict those at highest risk for disease progression
Integration of imaging and histopathology
Generate ILD imaging repositories across the spectrum of CTD-associated ILD that correlate with histopathologic specimens
Refine cryobiopsy techniques to enrich the availability of parenchymal lung tissue specimens
Clinical trials of future interventions in CTD-ILD
Validate CTD-specific trial end points
Incorporate novel technologies to validate quality of life end points and patient-reported outcome measures
Develop and incorporate composite end points specific to CTD-ILD
Develop an integrated clinical, radiologic, laboratory, and biologic database solution that aligns large data sets and allows maximum interrogation
Translational research
Form shared national/international registries with biologic repositories
Create new, and optimize existing, quality of life measures in CTD-ILD
Develop animal models of CTD-ILD

consensus on whether such instruments should be symptom specific, disease specific, or generic (such as the Short Form 36 QoL questionnaire) (71). Validation testing of candidate QoL outcome measures, with engagement of patient-centered organizations, should be performed to assess their accuracy in determining association with disease severity and sensitivity to change.

Animal models. *Statement of the problem, current understanding, and unmet needs*. Animal models provide a critical tool in identifying relevant biologic pathways in disease as well as providing a model to test therapeutic agents. To better understand the pathogenesis of fibrotic lung diseases, a number of animal models have been developed. Recent advances have allowed for the development of models to study targeted injuries of type II alveolar epithelial cells, fibroblastic autonomous effects, and targeted genetic defects (72). However, there are few models of CTD-associated ILD. Although a model of RA-associated ILD in SKG mice has been described (73), other animal models for CTD, including in tight-skinned mice, either have not been characterized for lung disease or do not manifest lung disease (74). It remains uncertain whether murine models of fibrotic lung disease, which include bleomycin-induced, radiation-induced, or adoptive cell transfer models of lung fibrosis (72), are sufficiently similar to human CTD-associated ILD to be of use in identifying molecular targets for drug development (75).

Proposed future directions. An inventory of currently existing animal models of ILD, documenting their disease equivalence to specific manifestations of human CTD-associated ILD as well as any known overlap of the recognized molecular mechanisms of human and murine disease, is needed. Where adequate animal models do not currently exist, funding and research efforts will be needed to develop better animal models of CTD-associated ILD that more closely reflect the human condition and are therefore relevant for disease pathway evaluation and drug development in preclinical studies.

Summary

This document summarizes the proceedings of a recent summit on CTD-associated ILD attended by a multidisciplinary panel of international clinician-scientists with expertise in CTD-associated ILD. Key clinical aspects are outlined, and a variety of research initiatives are proposed (Table 4) with the aim of addressing the many unmet needs and challenges within the complex intersection between CTD and ILD. Our hope is that further multidisciplinary collaboration around the research into and care of patients with CTD-associated ILD will lead to greater disease awareness, earlier disease detection and diagnosis, implementation of interdisciplinary treatment approaches with novel therapeutic agents, and, ultimately, improved quality of life and outcomes for those who are affected by these diseases.

AUTHOR CONTRIBUTIONS

All authors were involved in drafting the article or revising it critically for important intellectual content, and all authors approved the final version to be published. Dr. Fischer had full access to all of the data in the study and takes responsibility for the integrity of the data and the accuracy of the data analysis.

Study conception and design. Fischer, Strek, Cottin, Dellaripa, Bernstein, Brown, Danoff, Distler, Hirani, Jones, Khanna, Lee, Lynch, Maher, Millar, Raghu, Silver, Steen, Volkmann, Mullan, O'Dwyer, Donnelly.

Acquisition of data. Fischer, Strek, Cottin, Dellaripa, Bernstein, Brown, Danoff, Distler, Hirani, Jones, Khanna, Lee, Lynch, Maher, Millar, Raghu, Silver, Steen, Volkmann, Mullan, O'Dwyer, Donnelly.

Analysis and interpretation of data. Fischer, Strek, Cottin, Dellaripa, Bernstein, Brown, Danoff, Distler, Hirani, Jones, Khanna, Lee, Lynch, Maher, Millar, Raghu, Silver, Steen, Volkmann, Mullan, O'Dwyer, Donnelly.

REFERENCES

1. Fischer A, du Bois R. Interstitial lung disease in connective tissue disorders. Lancet 2012;380:689–98.

2. Castelino FV, Varga J. Interstitial lung disease in connective tissue diseases: evolving concepts of pathogenesis and management. Arthritis Res Ther 2010;12:213.

3. Park JH, Kim DS, Park IN, Jang SJ, Kitaichi M, Nicholson AG, et al. Prognosis of fibrotic interstitial pneumonia: idiopathic versus collagen vascular disease-related subtypes. Am J Respir Crit Care Med 2007;175:705–11.

4. Assayag D, Lubin M, Lee JS, King TE, Collard HR, Ryerson CJ. Predictors of mortality in rheumatoid arthritis-related interstitial lung disease. Respirology 2014;19:493–500.

5. O'Dwyer DN, Armstrong ME, Cooke G, Dodd JD, Veale DJ, Donnelly SC. Rheumatoid arthritis (RA) associated interstitial lung disease (ILD). Eur J Intern Med 2013;24:597–603.

6. Spagnolo P, Lee JS, Sverzellati N, Rossi G, Cottin V. The lung in rheumatoid arthritis: focus on interstitial lung disease [review]. Arthritis Rheumatol 2018;70:1544–54.

7. Steen VD. Autoantibodies in systemic sclerosis. Semin Arthritis Rheum 2005;35:35–42.

8. Sato S, Hirakata M, Kuwana M, Suwa A, Inada S, Mimori T, et al. Autoantibodies to a 140-kd polypeptide, CADM-140, in Japanese patients with clinically amyopathic dermatomyositis. Arthritis Rheum 2005;52:1571–6.

9. Sato S, Masui K, Nishina N, Kawaguchi Y, Kawakami A, Tamura M, et al. Initial predictors of poor survival in myositis-associated interstitial lung disease: a multicentre cohort of 497 patients. Rheumatology (Oxford) 2018;57:1212–21.

10. Hirakata M, Suwa A, Takada T, Sato S, Nagai S, Genth E, et al. Clinical and immunogenetic features of patients with autoantibodies to asparaginyl–transfer RNA synthetase. Arthritis Rheum 2007;56:1295–303.

11. Lynch DA. Quantitative CT of fibrotic interstitial lung disease. Chest 2007;131:643–4.

12. Lynch DA, Travis WD, Muller NL, Galvin JR, Hansell DM, Grenier PA, et al. Idiopathic interstitial pneumonias: CT features. Radiology 2005;236:10–21.

13. Fischer A, Donnelly SC. Pulmonary fibrosis in connective tissue disease (CTD): urgent challenges and opportunities. QJM 2017;110:475–6.

14. American Thoracic Society, European Respiratory Society. American Thoracic Society/European Respiratory Society international multidisciplinary consensus classification of the idiopathic interstitial pneumonias. Am J Respir Crit Care Med 2002;165:277–304.

15. Khanna D, Nagaraja V, Tseng CH, Abtin F, Suh R, Kim G, et al. Predictors of lung function decline in scleroderma-related interstitial lung disease based on high-resolution computed tomography: implications for cohort enrichment in systemic sclerosis-associated interstitial lung disease trials. Arthritis Res Ther 2015;17:372.

16. Fischer A, Richeldi L. Cross-disciplinary collaboration in connective tissue disease-related lung disease. Semin Respir Crit Care Med 2014;35:159–65.

17. Castelino FV, Goldberg H, Dellaripa PF. The impact of rheumatological evaluation in the management of patients with interstitial lung disease. Rheumatology (Oxford) 2011;50:489–93.

18. Solomon JJ, Olson AL, Fischer A, Bull T, Brown KK, Raghu G. Scleroderma lung disease. Eur Respir Rev 2013;22:6–19.

19. Strand MJ, Sprunger D, Cosgrove GP, Fernandez-Perez ER, Frankel SK, Huie TJ, et al. Pulmonary function and survival in idiopathic vs secondary usual interstitial pneumonia. Chest 2014;146:775–85.

20. Kim EJ, Elicker BM, Maldonado F, Webb WR, Ryu JH, van Uden JH, et al. Usual interstitial pneumonia in rheumatoid arthritis-associated interstitial lung disease. Eur Respir J 2010;35:1322–8.

21. Kim EJ, Collard HR, King TE Jr. Rheumatoid arthritis-associated interstitial lung disease: the relevance of histopathologic and radiographic pattern. Chest 2009;136:1397–405.

22. Chen J, Doyle TJ, Liu Y, Aggarwal R, Wang X, Shi Y, et al. Biomarkers of rheumatoid arthritis–associated interstitial lung disease. Arthritis Rheumatol 2015;67:28–38.

23. Zamora-Legoff JA, Krause ML, Crowson CS, Ryu JH, Matteson EL. Risk of serious infection in patients with rheumatoid arthritis-associated interstitial lung disease. Clin Rheumatol 2016;35:2585–9.

24. Kelly CA, Saravanan V, Nisar M, Arthanari S, Woodhead FA, Price-Forbes AN, et al. Rheumatoid arthritis-related interstitial lung disease: associations, prognostic factors and physiological and radiological characteristics: a large multicentre UK study. Rheumatology (Oxford) 2014;53:1676–82.

25. Doyle TJ, Patel AS, Hatabu H, Nishino M, Wu G, Osorio JC, et al. Detection of rheumatoid arthritis-interstitial lung disease is enhanced by serum biomarkers. Am J Respir Crit Care Med 2015;191:1403–12.

26. Zhang Y, Li H, Wu N, Dong X, Zheng Y. Retrospective study of the clinical characteristics and risk factors of rheumatoid arthritis-associated interstitial lung disease. Clin Rheumatol 2017;36:817–23.

27. Solomon JJ, Chung JH, Cosgrove GP, Demoruelle MK, Fernandez-Perez ER, Fischer A, et al. Predictors of mortality in rheumatoid arthritis-associated interstitial lung disease. Eur Respir J 2016;47:588–96.

28. Fujisawa T, Hozumi H, Kono M, Enomoto N, Hashimoto D, Nakamura Y, et al. Prognostic factors for myositis-associated interstitial lung disease. PLoS One 2014;9:e98824.

29. Goh NS, Desai SR, Veeraraghavan S, Hansell DM, Copley SJ, Maher TM, et al. Interstitial lung disease in systemic sclerosis: a simple staging system. Am J Respir Crit Care Med 2008;177:1248–54.

30. Winstone TA, Assayag D, Wilcox PG, Dunne JV, Hague CJ, Leipsic J, et al. Predictors of mortality and progression in scleroderma-associated interstitial lung disease: a systematic review. Chest 2014;146:422–36.

31. Biomarkers Definitions Working Group. Biomarkers and surrogate endpoints: preferred definitions and conceptual framework. Clin Pharmacol Ther 2001;69:89–95.

32. Boers M, Brooks P, Strand CV, Tugwell P. The OMERACT filter for outcome measures in rheumatology. J Rheumatol 1998;25:198–9.

33. Kowal-Bielecka O, Avouac J, Pittrow D, Huscher D, Behrens F, Denton CP, et al. Analysis of the validation status of quality of life and functional disability measures in pulmonary arterial hypertension related to systemic sclerosis: results of a systematic literature analysis by the Expert Panel on Outcomes Measures in Pulmonary Arterial Hypertension related to Systemic Sclerosis (EPOSS). J Rheumatol 2011;38:2419–27.

34. Saketkoo LA, Mittoo S, Huscher D, Khanna D, Dellaripa PF, Distler O, et al. Connective tissue disease related interstitial lung diseases and idiopathic pulmonary fibrosis: provisional core sets of domains and instruments for use in clinical trials. Thorax 2014;69:428–36.

35. Hant FN, Ludwicka-Bradley A, Wang HJ, Li N, Elashoff R, Tashkin DP, et al. Surfactant protein D and KL-6 as serum biomarkers of interstitial lung disease in patients with scleroderma. J Rheumatol 2009;36:773–80.

36. Schmidt K, Martinez-Gamboa L, Meier S, Witt C, Meisel C, Hanitsch LG, et al. Bronchoalveolar lavage fluid cytokines and chemokines as markers and predictors for the outcome of interstitial lung disease in systemic sclerosis patients. Arthritis Res Ther 2009;11:R111.

37. Ashley SL, Xia M, Murray S, O'Dwyer DN, Grant E, White ES, et al. Six-SOMAmer index relating to immune, protease and angiogenic functions predicts progression in IPF. PLoS One 2016;11:e0159878.

38. Jenkins RG, Simpson JK, Saini G, Bentley JH, Russell AM, Braybrooke R, et al. Longitudinal change in collagen degradation biomarkers in idiopathic pulmonary fibrosis: an analysis from the prospective, multicentre PROFILE study. Lancet Respir Med 2015;3:462–72.

39. Noth I, Zhang Y, Ma SF, Flores C, Barber M, Huang Y, et al. Genetic variants associated with idiopathic pulmonary fibrosis susceptibility and mortality: a genome-wide association study. Lancet Respir Med 2013;1:309–17.

40. Kim DS, Yoo B, Lee JS, Kim EK, Lim CM, Lee SD, et al. The major histopathologic pattern of pulmonary fibrosis in scleroderma is nonspecific interstitial pneumonia. Sarcoidosis Vasc Diffuse Lung Dis 2002;19:121–7.

41. Tsuchiya Y, Fischer A, Solomon JJ, Lynch DA. Connective tissue disease-related thoracic disease. Clin Chest Med 2015;36:283–97.

42. Yunt ZX, Chung JH, Hobbs S, Fernandez-Perez ER, Olson AL, Huie TJ, et al. High resolution computed tomography pattern of usual interstitial pneumonia in rheumatoid arthritis-associated interstitial lung disease: relationship to survival. Respir Med 2017;126:100–4.

43. Kim HJ, Brown MS, Elashoff R, Li G, Gjertson DW, Lynch DA, et al. Quantitative texture-based assessment of one-year changes in fibrotic reticular patterns on HRCT in scleroderma lung disease treated with oral cyclophosphamide. Eur Radiol 2011;21:2455–65.

44. Tashkin DP, Elashoff R, Clements PJ, Goldin J, Roth MD, Furst DE, et al. Cyclophosphamide versus placebo in scleroderma lung disease. N Engl J Med 2006;354:2655–66.

45. Fischer A, Antoniou KM, Brown KK, Cadranel J, Corte TJ, du Bois RM, et al. An official European Respiratory Society/American Thoracic Society research statement: interstitial pneumonia with autoimmune features. Eur Respir J 2015;46:976–87.

46. Fischer A, West SG, Swigris JJ, Brown KK, du Bois RM. Connective tissue disease-associated interstitial lung disease: a call for clarification. Chest 2010;138:251–6.

47. Leslie KO, Trahan S, Gruden J. Pulmonary pathology of the rheumatic diseases. Semin Respir Crit Care Med 2007;28:369–78.

48. Nakamura Y, Suda T, Kaida Y, Kono M, Hozumi H, Hashimoto D, et al. Rheumatoid lung disease: prognostic analysis of 54 biopsy-proven cases. Respir Med 2012;106:1164–9.

49. Solomon JJ, Ryu JH, Tazelaar HD, Myers JL, Tuder R, Cool CD, et al. Fibrosing interstitial pneumonia predicts survival in patients with rheumatoid arthritis-associated interstitial lung disease (RA-ILD). Respir Med 2013;107:1247–52.

50. Tansey D, Wells AU, Colby TV, Ip S, Nikolakoupolou A, du Bois RM, et al. Variations in histological patterns of interstitial pneumonia between connective tissue disorders and their relationship to prognosis. Histopathology 2004;44:585–96.

51. Cipriani NA, Strek M, Noth I, Gordon IO, Charbeneau J, Krishnan JA, et al. Pathologic quantification of connective tissue disease-associated versus idiopathic usual interstitial pneumonia. Arch Pathol Lab Med 2012;136:1253–8.

52. Hutchinson JP, Fogarty AW, McKeever TM, Hubbard RB. In-hospital mortality after surgical lung biopsy for interstitial lung disease in the United States: 2000 to 2011. Am J Respir Crit Care Med 2016;193:1161–7.

53. Hutchinson JP, McKeever TM, Fogarty AW, Navaratnam V, Hubbard RB. Surgical lung biopsy for the diagnosis of interstitial lung disease in England: 1997-2008. Eur Respir J 2016;48:1453–61.

54. Lentz RJ, Argento AC, Colby TV, Rickman OB, Maldonado F. Transbronchial cryobiopsy for diffuse parenchymal lung disease: a state-of-the-art review of procedural techniques, current evidence, and future challenges. J Thorac Dis 2017;9:2186–203.

55. Hetzel J, Maldonado F, Ravaglia C, Wells AU, Colby TV, Tomassetti S, et al. Transbronchial cryobiopsies for the diagnosis of diffuse parenchymal lung diseases: expert statement from the Cryobiopsy Working Group on Safety and Utility and a call for standardization of the procedure. Respiration 2018;95:188–200.

56. Hoyles RK, Ellis RW, Wellsbury J, Lees B, Newlands P, Goh NS, et al. A multicenter, prospective, randomized, double-blind, placebo-controlled trial of corticosteroids and intravenous cyclophosphamide followed by oral azathioprine for the treatment of pulmonary fibrosis in scleroderma. Arthritis Rheum 2006;54:3962–70.

57. Tashkin DP, Roth MD, Clements PJ, Furst DE, Khanna D, Kleerup EC, et al. Mycophenolate mofetil versus oral cyclophosphamide in scleroderma-related interstitial lung disease (SLS II): a randomised controlled, double-blind, parallel group trial. Lancet Respir Med 2016;4:708–19.

58. Travis WD, Costabel U, Hansell DM, King TE Jr, Lynch DA, Nicholson AG, et al. An official American Thoracic Society/European Respiratory Society statement: update of the international multidisciplinary classification of the idiopathic interstitial pneumonias. Am J Respir Crit Care Med 2013;188:733–48.

59. Khanna D, Denton CP, Lin CJ, van Laar JM, Frech TM, Anderson ME, et al. Safety and efficacy of subcutaneous tocilizumab in systemic sclerosis: results from the open-label period of a phase II randomized controlled trial (faSScinate). Ann Rheum Dis 2018;77:212–20.

60. Wells AU, Behr J, Costabel U, Cottin V, Poletti V, Richeldi L, et al. Hot of the breath: mortality as a primary end-point in IPF treatment trials—the best is the enemy of the good. Thorax 2012;67:938–40.

61. Goh NS, Hoyles RK, Denton CP, Hansell DM, Renzoni EA, Maher TM, et al. Short-term pulmonary function trends are predictive of mortality in interstitial lung disease associated with systemic sclerosis. Arthritis Rheumatol 2017;69:1670–8.

62. Khanna D, Mittoo S, Aggarwal R, Proudman SM, Dalbeth N, Matteson EL, et al. Connective tissue disease-associated interstitial lung diseases (CTD-ILD): report from OMERACT CTD-ILD Working Group. J Rheumatol 2015;42:2168–71.

63. Le Gouellec N, Duhamel A, Perez T, Hachulla AL, Sobanski V, Faivre JB, et al. Predictors of lung function test severity and outcome in systemic sclerosis-associated interstitial lung disease. PLoS One 2017;12:e0181692.

64. Collard HR, Bradford WZ, Cottin V, Flaherty KR, King TE Jr, Koch GG, et al. A new era in idiopathic pulmonary fibrosis: considerations for future clinical trials. Eur Respir J 2015;46:243–9.

65. Kafaja S, Clements PJ, Wilhalme H, Tseng CH, Furst DE, Kim GH, et al. Reliability and minimal clinically important differences of forced vital capacity: results from the Scleroderma Lung Studies (SLS-I and SLS-II). Am J Respir Crit Care Med 2017;197.

66. Collen MF. Clinical research databases: a historical review. J Med Syst 1990;14:323–44.

67. Ruof J, Bruhlmann P, Michel BA, Stucki G. Development and validation of a self-administered systemic sclerosis questionnaire (SySQ). Rheumatology (Oxford) 1999;38:535–42.

68. Whalley D, McKenna SP, de Jong Z, van der Heijde D. Quality of life in rheumatoid arthritis. Br J Rheumatol 1997;36:884–8.

69. Patel AS, Siegert RJ, Brignall K, Gordon P, Steer S, Desai SR, et al. The development and validation of the King's Brief Interstitial Lung Disease (K-BILD) health status questionnaire. Thorax 2012;67:804–10.

70. Yorke J, Jones PW, Swigris JJ. Development and validity testing of an IPF-specific version of the St George's Respiratory Questionnaire. Thorax 2010;65:921–6.

71. Ware JE Jr, Snow KK, Kosinski M, Gandek B. SF-36 health survey: manual and interpretation guide. 2nd ed. Lincoln (RI): QualityMetric; 2000.

72. Moore BB, Lawson WE, Oury TD, Sisson TH, Raghavendran K, Hogaboam CM. Animal models of fibrotic lung disease. Am J Respir Cell Mol Biol 2013;49:167–79.

73. Keith RC, Powers JL, Redente EF, Sergew A, Martin RJ, Gizinski A, et al. A novel model of rheumatoid arthritis-associated interstitial lung disease in SKG mice. Exp Lung Res 2012;38:55–66.

74. Pablos JL, Everett ET, Norris JS. The tight skin mouse: an animal model of systemic sclerosis. Clin Exp Rheumatol 2004;22:S81–5.

75. Moore BB, Hogaboam CM. Murine models of pulmonary fibrosis. Am J Physiol Lung Cell Mol Physiol 2008;294:L152–60.

76. Schwarz MI, King TE. Interstitial lung disease. 4th ed. Hamilton, ON, Canada: BC Decker; 2003.

77. Olson AL, Brown KK, Fischer A. Connective tissue disease-associated lung disease. Immunol Allergy Clin North Am 2012;32:513–36.

Recognition of Amino Acid Motifs, Rather Than Specific Proteins, by Human Plasma Cell–Derived Monoclonal Antibodies to Posttranslationally Modified Proteins in Rheumatoid Arthritis

Johanna Steen,[1] Björn Forsström,[2] Peter Sahlström,[3] Victoria Odowd,[4] Lena Israelsson,[1] Akilan Krishnamurthy,[1] Sara Badreh,[1] Linda Mathsson Alm,[5] Joanne Compson,[4] Daniel Ramsköld,[1] Welcome Ndlovu,[4] Stephen Rapecki,[4] Monika Hansson,[1] Philip J. Titcombe,[6] Holger Bang,[7] Daniel L. Mueller,[8] Anca I. Catrina,[1] Caroline Grönwall,[1] Karl Skriner,[9] Peter Nilsson,[2] Daniel Lightwood,[4] Lars Klareskog,[1] and Vivianne Malmström[1]

Objective. Antibodies against posttranslationally modified proteins are a hallmark of rheumatoid arthritis (RA), but the emergence and pathogenicity of these autoantibodies are still incompletely understood. The aim of this study was to analyze the antigen specificities and mutation patterns of monoclonal antibodies (mAb) derived from RA synovial plasma cells and address the question of antigen cross-reactivity.

Methods. IgG-secreting cells were isolated from RA synovial fluid, and the variable regions of the immunoglobulins were sequenced (n = 182) and expressed in full-length mAb (n = 93) and also as germline-reverted versions. The patterns of reactivity with 53,019 citrullinated peptides and 49,211 carbamylated peptides and the potential of the mAb to promote osteoclastogenesis were investigated.

Results. Four unrelated anti–citrullinated protein autoantibodies (ACPAs), of which one was clonally expanded, were identified and found to be highly somatically mutated in the synovial fluid of a patient with RA. The ACPAs recognized >3,000 unique peptides modified by either citrullination or carbamylation. This highly multireactive autoantibody feature was replicated for Ig sequences derived from B cells from the peripheral blood of other RA patients. The plasma cell–derived mAb were found to target distinct amino acid motifs and partially overlapping protein targets. They also conveyed different effector functions as revealed in an osteoclast activation assay.

Conclusion. These findings suggest that the high level of cross-reactivity among RA autoreactive B cells is the result of different antigen encounters, possibly at different sites and at different time points. This is consistent with the notion that RA is initiated in one context, such as in the mucosal organs, and thereafter targets other sites, such as the joints.

INTRODUCTION

Antibodies against citrullinated antigens (anti–citrullinated protein/peptide antibodies [ACPAs]), which were first described

in 1998 (1,2), constitute a hallmark of the subset of patients with rheumatoid arthritis (RA) displaying associations with distinct major histocompatibility complex class II genes (3,4) and with predominantly erosive disease (5,6). The presence of such

antibodies is also part of the American College of Rheumatology/European League Against Rheumatism 2010 classification criteria for RA (7). These antibodies generally develop before the onset of joint inflammation (8) in RA patients. Importantly, in vitro and in vivo models have shown that ACPAs induce phenotypes consistent with symptoms associated with RA, such as bone loss and joint pain (9–11).

ACPAs also represent a class of autoantibodies to posttranslationally modified (PTM) antigens, for which the actual targets of the antibodies remain incompletely understood. Thus, a number of citrullinated (Cit) peptide antigens recognized by ACPAs have been identified, including citrullinated fibrinogen (12), vimentin (13), α-enolase peptide (CEP-1) (14), type II collagen (15), tenascin-C (16), and histones (17). In addition, over recent years, antibodies recognizing other protein modifications, such as carbamylation (referred to as CarP) and acetylation of amino acids, have been found to be associated with RA (18,19). These observations have raised a number of new questions concerning the generation, specificity, and function of this group of autoantibodies in their interactions with PTM antigens; this group is sometimes referred to as anti–modified protein antibodies, or AMPAs.

In the present study, we generated monoclonal ACPAs from single plasma cells obtained from an inflamed joint of an anti–cyclic citrullinated peptide (anti-CCP)–positive RA patient. These autoantibodies were characterized in detail to assess their genetic features, reactivity with large numbers of citrullinated and carbamylated peptides, and critical functional properties.

MATERIALS AND METHODS

Cell isolation, assays, and cultures. Plasma cells were obtained from the synovial fluid of a patient with anti-CCP–positive RA, and antibody-secreting cells were isolated from synovial fluid mononuclear cells using the fluorescent foci method. In addition, single citrulline-specific B cells were sorted by flow cytometry from the peripheral blood of other RA patients, using an antigen-tetramer system. Further details on the synovial fluid and serum samples obtained from RA patients and the methods used for plasma cell isolation, blood-derived memory B cell tetramer isolation, Ig gene sequence analysis, cloning of Ig genes, generation of germline-reverted antibodies, expression and purification of monoclonal antibodies (mAb), surface plasmon resonance (SPR) assay, ACPA peptide array, PTM peptide enzyme-linked immunosorbent assay (ELISA), in solution citrullination ELISA, immunoprecipitation and osteoclast cultures, and in vitro bone erosion assay are provided in Supplementary Materials and Methods (available on the *Arthritis & Rheumatology* web site at http://onlinelibrary.wiley.com/doi/10.1002/art.40699/abstract).

Peptide ELISA. Peptide ELISAs were performed as previously described (20), with some minor modifications. The

ELISAs assessed binding to both citrulline-containing and arginine (Arg)–containing peptides, including filaggrin, α-enolase, vimentin, fibrinogen, and histones H4$_{14-34}$, H4$_{31-50}$, and H3$_{1-30}$. All peptides assessed by ELISA are described in further detail in Supplementary Table 1, available on the *Arthritis & Rheumatology* web site at http://onlinelibrary.wiley.com/doi/10.1002/art.40699/abstract. The mAb were added to the wells at a concentration of 5 µg/ml, which was diluted by a factor of 2 down to 0.15 ng/ml. All reactive samples were analyzed in at least 3 independent experiments.

Full-length protein ELISA. For the full-length protein ELISA, 10 µg/ml of fibrinogen (isolated from human plasma [Sigma]), recombinant vimentin (InVent), and histone H4 (in-house produced) were diluted in phosphate buffered saline (PBS) and coated on Nunc Maxisorp 96-well plates. The plates were blocked with 5% milk powder in PBS and thereafter incubated for 3 hours at 37°C with citrullination buffer (50 m*M* Tris, 10 m*M* CaCl$_2$, 1 m*M* dithiothreitol, 150 mU/ml human peptidylarginine deiminase 2 [hPAD2; Modiquest]) or buffer control, followed by incubation with ACPAs at a concentration of 5 µg/ml, which was diluted by a factor of 2 down to 0.15 ng/ml. Sequential incubation was carried out with secondary Fc-specific, horseradish peroxidase (HRP)–conjugated anti-human IgG (Sigma) or biotin-conjugated human IgG1-Fc (Invitrogen) plus HRP-conjugated streptavidin (Dako). This was followed by development with SeramunBlau fast TMB (Seramun Diagnostica), and the results were read with Spectra Fluor (Tecan).

Extracellular matrix peptide microarray. Peptides (16 amino acids in length) that covered all arginine and lysine sites of 1,610 extracellular matrix proteins and RA-related proteins (21–23) were synthesized in situ (Roche NimbleGen) as previously described (24). Citrulline (arginine) and homocitrulline (lysine) variants were synthesized, resulting in 53,019 citrullinated peptides and 49,211 carbamylated peptides, along with cognate unmodified peptides (n = 70,535), yielding a total of 172,765 unique peptides. The mAb were diluted to a concentration of 1 µg/ml (except mAb 1325:07E07, which was diluted to 0.55 µg/ml), while synovial fluid and serum samples were diluted 1/100.

Scanning for citrulline and homocitrulline reactivity with each mAb was performed at a resolution of 2 µm, using a NimbleGen MS200 Scanner (Roche NimbleGen). The median fluorescence intensities were calculated based on a peptide signal intensity variation (spot size) of 25 pixels. The cutoff value for positive signals was determined as 5 times the fluorescence intensity of the 98th percentile of values for a set of non-ACPA mAb.

Western blotting. For Western blot analyses, full-length proteins (same as those assessed by the full-length
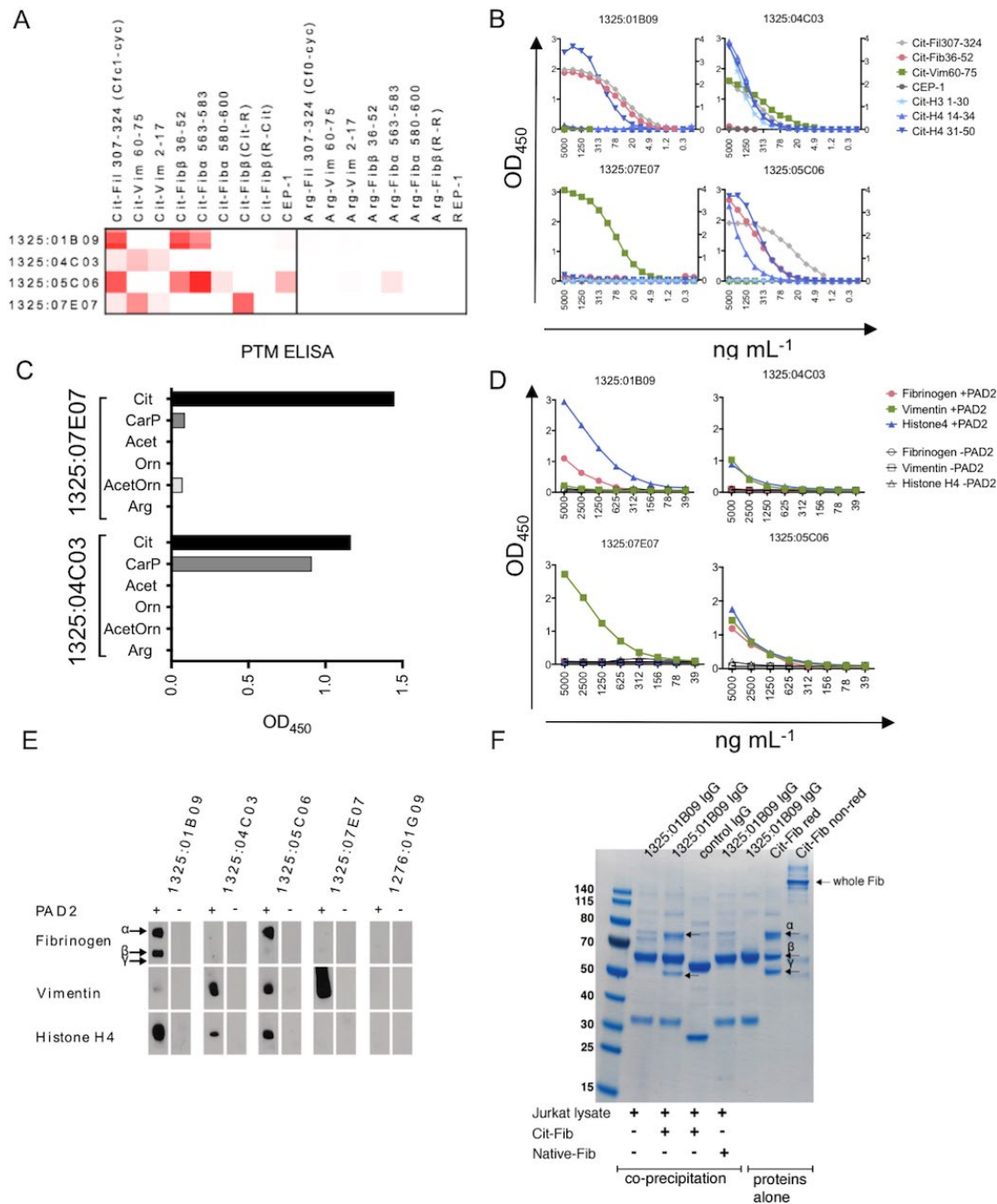
Figure 1. Reactivity pattern of monoclonal antibodies (mAb) against citrullinated proteins/peptides (ACPAs). **A,** Heatmaps depict ACPA mAb reactivity (at a concentration of 5 μg/ml) with rheumatoid arthritis–associated citrulline (Cit)– and arginine (Arg)–containing peptides. Shades of red indicate increased signal. **B,** Titration enzyme-linked immunosorbent assay (ELISA) curves show the dilution (1:2) in 4–14 steps of each mAb (starting at 5 μg/ml) to citrullinated peptides. **C,** Binding of mAb (at 5 μg/ml) to peptides with various posttranslational modifications (PTMs) was analyzed by ELISA, utilizing a vimentin (Vim)–derived peptide with modifications introduced in position 7 (sequence GRVYATXSSAVR-OH, with modification denoted by X). **D** and **E,** ELISA (**D**) and Western blotting (**E**) were used to assess mAb reactivity with full-length proteins. Antigens (fibrinogen [Fib], vimentin, and histone H4) were treated with or without human peptidylarginine deiminase 2 (PAD2) enzyme to generate citrullination. A concentration of 10 μg of protein was used for Western blots, and 10 μg/ml of antigen for ELISAs. Antibodies were added at 1 μg/ml to detect binding. **Arrows** in **E** indicate the size of the α-, β-, and γ-chains of fibrinogen. **F,** Immunoprecipitation of PAD4-citrullinated full-length fibrinogen (5 μg) from spiked Jurkat T cell line lysates with mAb 1325:01B09 (3 μg) was assessed. Stained sodium dodecyl sulfate–polyacrylamide electrophoresis gels of coprecipitated captured proteins or purified proteins alone are shown. Purified citrullinated fibrinogen is also shown as reduced (red) or nonreduced (non-red) to verify intact protein. **Arrows** indicate detected fibrinogen chains. Cit-Fil = citrullinated filaggrin; CEP-1 = citrulline-containing α-enolase peptide; REP = arginine-containing α-enolase peptide; CarP = homocitrulline/carbamylated; Acet = acetylated lysine; Orn = unmodified ornithine; AcetOrn = acetylated ornithine; Arg = unmodified arginine.

protein ELISA) were solubilized in 8M urea at 1 mg/ml, and 10 µg was electrophoresed on 12.5% sodium dodecyl sulfate–polyacrylamide electrophoresis gels, followed by blotting to a nitrocellulose membrane (GE Healthcare). Thereafter, the blots were incubated overnight at 37°C in citrullination buffer with 150 mU/ml hPAD2 (Modiquest) or with buffer control, followed by incubation with ACPAs at 5 µg/ml and sequential incubation with the same secondary antibody as that used for the full-length protein ELISA. Visualization was performed using Amersham Hyperfilm.

Sequence logo visualization of the consensus peptide sequences. The 4 flanking amino acids from each post-translational residue were analyzed using the WebLogo application (http://weblogo.threeplusone.com/), which allowed us to generate the consensus sequences of the surrounding amino acids.

Statistical analysis. Differences in the number of mutations and third complementarity-determining region (CDR3) characteristics between ACPAs and non-ACPAs were determined by Mann-Whitney nonparametric test. For in vitro experiments, statistically significant differences were calculated using one-way Kruskal-Wallis test followed by Dunn's test for multiple comparisons. P values less than or equal to 0.05 were consid-

ered significant. GraphPad Prism (version 7.0c) was utilized to calculate and visualize the statistical data.

RESULTS

Production by RA synovial fluid plasma cells of antibodies that recognize multiple PTM peptides and proteins. Plasma cells isolated from cryopreserved synovial fluid cells from a patient with RA exhibited spontaneous secretion of IgG, as identified by the fluorescent foci method (25). Sequences from paired IgG heavy- and light-chain variable regions from 182 plasma cells were generated, and of these, 93 were expressed as recombinant mAb at concentrations of >1 µg/ml; these 93 recombinant mAb were selected for further investigation.

Screening by peptide ELISA revealed that 4 of these mAb (1325:01B09, 1325:04C03, 1325:05C06, and 1325:07E07) showed citrulline reactivity (to peptides Cit-Vim$_{60-75}$, Cit-Fibβ$_{36-52}$, and CEP-1$_{5-21}$), whereas none of these antibodies reacted with the respective arginine-containing peptides. When these 4 mAb were further investigated utilizing an ACPA peptide microarray (26), the ACPAs all reacted against several citrulline-containing peptides, but each showed a different reactivity pattern (Figure 1A).

The results of the peptide microarray were verified and extended by ELISA for the RA candidate autoantigens Cit-Vim$_{60-75}$,

Table 1. Characteristics of the human anti–citrullinated protein mAb generated from synovial fluid plasma cells from a rheumatoid arthritis patient*

	mAb 1325:01B09	mAb 1325:04C03	mAb 1325:05C06	mAb 1325:07E07
Distribution, no. isolated cells/total	1/182	3/182	1/182	1/182
Genetic profile				
V_H	IGHV4–38	IGHV1–2	IGHV4–39	IGHV4–39
$V_{L/\kappa}$	IGLV1–44	IGKV1–5	IGLV1–51	IGLV3–21
Isotype	IgG1	IgG2	IgG1	NA
γ-chain CDR3	CATDGEGVLFDEW	CARTNFSPFRHW	CAKLGCSGGGCYFDFDYW	CARLDPFDYW
Light-chain CDR3	CAVWDDDLSGVVI	CQQYNGPSETF	CGTWDSSLSAGLF	CQVYDRKTDHQVF
Reactivity profile, µM affinity				
Cit-Fil$_{307-324}$	42	23	1.3	NA
Cit-Fibβ$_{36-52}$	20	NB	NB	NA
Cit-Vim$_{60-75}$	NA	25	NB	NA
CEP-1$_{5-21}$	NB	NB	50	NA
Arg-Fibβ$_{36-52}$	NB	NB	NB	NA
Arg-Vim$_{60-75}$	NA	NB	NB	NA
REP-1$_{5-21}$	NB	NB	NB	NA

* Genetic information on the variable (V) regions was generated from Immunogenetics V-Quest. Affinities were determined from surface plasmon resonance steady-state affinity measurements with biotinylated peptides immobilized and monoclonal antibodies (mAb) in solution at a maximum concentration of 100 µM (mAb 1325:01B09) or 50 µM (mAb 1325:04C03 and 1325:05C06). Lack of binding was defined as a sensogram showing such low affinity that no equilibrium constant could be determined. NA = not analyzed; CDR3 = third complementarity-determining region; Cit-Fil$_{307-324}$ = citrullinated filaggrin$_{307-324}$; Cit-Fibβ$_{36-52}$ = citrullinated fibrinogen β$_{36-52}$; NB = no binding; Cit-Vim$_{60-75}$ = citrullinated vimentin$_{60-75}$; CEP-1$_{5-21}$ = citrullinated α-enolase peptide$_{5-21}$; Arg-Fibβ$_{36-52}$ = arginine-containing fibrinogen β$_{36-52}$; Arg-Vim$_{60-75}$ = arginine-containing vimentin$_{60-75}$; REP-1$_{5-21}$ = arginine-containing α-enolase peptide$_{5-21}$.

Cit-Fibβ$_{36-52}$, Cit-Fil$_{307-324}$, Cit-H4$_{14-34}$, Cit-H4$_{31-50}$, Cit-H3$_{1-30}$, and CEP-1$_{5-21}$, demonstrating that some of the citrulline peptides were detected at an mAb concentration as low as 5–10 ng/ml (Figure 1B and Supplementary Figure 1, available on the *Arthritis & Rheumatology* web site at http://onlinelibrary.wiley.com/doi/10.1002/art.40699/abstract). The equilibrium constants (KDs) for binding to selected citrulline peptides were determined by SPR assay (of note, mAb 1325:07E07 was not analyzed by SPR assay because of the limited amounts obtained in our expression system). The steady-state affinities between the ACPAs and the peptide antigens were consistently low, with all KD values in the µ*M* range (Table 1 and Supplementary Figure 2, available on the *Arthritis & Rheumatology* web site at http://onlinelibrary.wiley.com/doi/10.1002/art.40699/abstract), even for antibody–peptide interactions that were positive by ELISA at antibody concentrations in the ng/ml range (Figure 1B).

Ability of monoclonal ACPAs to cross-react with other PTM antigens. As other PTM peptides, in addition to those modified by citrullination, have been proposed to generate epitopes recognized by autoantibodies in RA (18,19), the 4 plasma cell–derived ACPAs were also investigated for binding to synthetic peptides, which had additional PTMs based on a common backbone amino acid sequence derived from vimentin. In this analysis, only 1 of the Cit-Vim–reactive mAb, 1325:04C03, but not mAb 1325:07E07, cross-reacted with the CarP-Vim peptide (Figure 1C), whereas the 2 other mAb (1325:01B09 and 1325:05C06) were negative for both the Cit-Vim and CarP-Vim peptides (Supplementary Figure 3A, available on the *Arthritis & Rheumatology* web site at http://onlinelibrary.wiley.com/doi/10.1002/art.40699/abstract). No reactivity toward acetylated peptides or peptides with other modifications was seen.

Cross-reactivity of monoclonal ACPAs with various citrullinated and carbamylated peptides. To investigate the cross-reactivity of the monoclonal ACPAs in greater detail, and also to detect reactivity with additional target peptides, a multipeptide array was designed. This custom-made array consisted of peptides from 1,610 different extracellular matrix and RA-related proteins (21–23), i.e., potential targets for autoantibodies. Arginine- and lysine-containing peptides were duplicated with a citrulline respective homocitrulline (the PTM amino acid generated by carbamylation) version, which thus generated an array of 53,019 citrullinated, 49,211 carbamylated, and 70,535 unmodified peptides.

The reactivity patterns of the 4 RA synovial fluid plasma cell–derived monoclonal ACPAs were investigated, and all showed extensive reactivity to citrullinated peptides (Figures 2A–D and Supplementary Table 2, available on the *Arthritis & Rheumatology* web site at http://onlinelibrary.wiley.com/doi/10.1002/art.40699/abstract). Two of these

mAb (1325:01B09 and 1325:05C06) also showed robust signals for carbamylated peptides. The reactivity toward native, unmodified target peptides was consistently low, at <0.06% (Figures 2A–D and Supplementary Table 2). Thus, it may be concluded that the cross-reactivity of these mAb was exclusively confined to PTM peptides. Overall, only 0.14% of all detected citrulline peptides were shared by all 4 mAb (Figure 2E, left panel). The mAb 1325:04C03 had the most distinct repertoire, with 32% of its reactivity being with uniquely detected citrullinated peptides. The homocitrulline-reactive mAb 1325:01B09 and 1325:05C06 demonstrated 2.7% shared carbamylated target peptides (Figure 2E, right panel).

The monoclonal ACPAs together covered 28% of the citrullinated targets and 30% of the carbamylated targets that were recognized by the RA synovial fluid (polyclonal IgG [pAb]) from the same patient (Supplementary Figure 4C, available on the *Arthritis & Rheumatology* web site at http://onlinelibrary.wiley.com/doi/10.1002/art.40699/abstract).

We next analyzed synovial fluid and serum samples obtained 10 years later from the same RA patient. The patient had untreated chronic RA at both time points. A stable reactivity pattern was seen for PTM peptide reactivities (especially for citrullinated peptides) at both time points, with only a moderate number of new peptides (range 7.1–9.8%) being recognized at the second time point (Supplementary Figures 4D and E). In contrast, a large fraction of carbamylated peptides that were detected at the first time point were not detected at the 10-year follow-up (44% in synovial fluid and 58% in sera), implying that these reactivities were not as stable as those toward citrullinated peptides (for which 22% of the citrulline peptides in synovial fluid and 30% of the citrulline peptides in sera were detected at the first time point only). The 200 highest-binding PTM peptides for each mAb, as well as for the pAb in synovial fluid and sera of the same patient, all contained never before–described peptide targets for the ACPAs (Supplementary Tables 3–8, available on the *Arthritis & Rheumatology* web site at http://onlinelibrary.wiley.com/doi/10.1002/art.40699/abstract) as well as reactivity against previously known RA targets such as vimentin and fibrinogen.

To confirm our finding that the high multireactivity of the ACPAs was not restricted to a single patient, we next tested 2 mAb that were generated from citrulline-selected memory B cells isolated from the peripheral blood of 2 other RA patients (27) (Supplementary Figure 5 and Supplementary Table 2, available on the *Arthritis & Rheumatology* web site at http://onlinelibrary.wiley.com/doi/10.1002/art.40699/abstract). These independently generated ACPAs displayed extensive citrulline multireactivity. The ACPAs from 1 of the patients also detected multiple carbamylated peptides at levels of reactivity comparable to those observed for the synovial plasma cell–derived ACPAs described above.
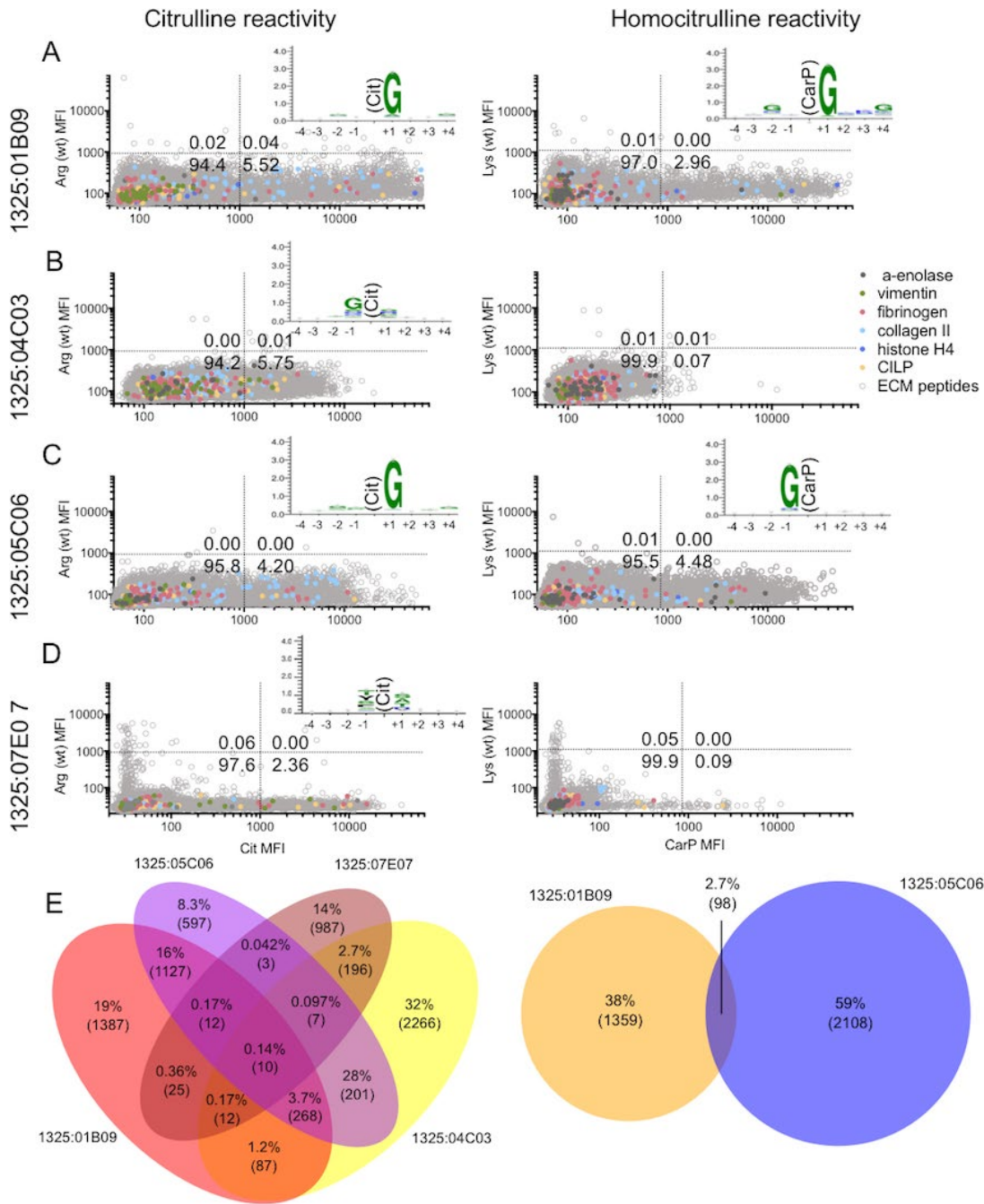
Figure 2. A broad repertoire of posttranslationally modified peptides are detected by mAb against ACPAs, and the mAb have distinct consensus sequence recognition. The mAb 1325:01B09, 1325:04C03, 1325:05C06, and 1325:07E07 were analyzed on an array of 53,019 citrullinated, 49,211 carbamylated, and 70,535 cognate unmodified (wild-type [wt]) peptides. Peptides (16 amino acids in length) were synthesized on the array, and reactivity with 1 μg/ml antibody (0.55 μg/ml for mAb 1325:07E07) was analyzed. **A–D,** The mean fluorescence intensity (MFI) of the modified (citrullinated or carbamylated) peptide is shown relative to the MFI of the cognate unmodified peptide. Various colors indicate peptides derived from some previously described rheumatoid arthritis–related antigens. Dotted lines show the cutoff for reactivity based on values for non-ACPA controls. Numbers in the quadrants are the percentage of detected peptides. **Insets,** Citrulline (Cit) and homocitrulline (CarP) amino acid positions in the consensus sequence motif are shown, as determined using WebLogo versions 3.5.0. and 3.6.0. **E,** Overlapping peptides with citrulline recognition by mAb 1325:01B09, 1325:04C03, 1325:05C06, and 1325:07E07 are shown (left), and the Venn diagram shows overlapping carbamylated peptides detected by mAb 1325:01B09 and 1325:05C06 (right). Numbers in parentheses indicate the number of overlapping peptides, and percentages are the fraction of all detected peptides in that section. Arg = arginine; Lys = lysine; CILP = cartilage intermediate layer protein; ECM = extracellular matrix (see Figure 1 for other definitions).

Overrepresentation of glycine residues in consensus epitopes of monoclonal ACPAs, but with distinct features for each mAb. The consensus sequences recognized by the mAb (Figures 2A–D and Supplementary Figure 5) and the pAb in the sera and synovial fluid samples from the same patient (Supplementary Figures 4A and B) were assessed using a WebLogo analysis. Among the mAb, a clear and shared motif was apparent for mAb 1325:01B09, mAb 1325:05C06, and the comparator ACPAs generated from the peripheral blood of 2 other RA patients, with a dominant glycine residue in position +1 (Figures 2A and C and Supplementary Figure 5). A glycine residue in position +1 was also the dominant consensus sequence for citrulline recognition of pAb in synovial fluid and sera from the same patient (Supplementary Figures 4A and B), suggesting that this is a dominant specificity. The mAb 1325:01B09 also had a similar consensus epitope for CarP recognition (Figure 2A). In contrast, the mAb 1325:05C06 CarP consensus epitope was different, in that it preferred a glycine in the −1 position (Figure 2C), and mAb 37CEPT2C04 had a lysine in the +4 position (Supplementary Figure 5). The mAb 1325:04C03, which only recognized the citrullinated and not the carbamylated peptides, displayed a consensus epitope with glycine being overrepresented in position −1. Lastly, the mAb 1325:07E07, which also only recognized citrullinated peptides, had a different preference, with small amino acids (serine, alanine, and threonine) flanking at the +1 position (Figure 2D).

Recognition by monoclonal ACPAs of multiple citrullinated full-length protein antigens. Next, in vitro citrullinated candidate full-length proteins were studied to validate the capacity of the mAb to bind epitopes of the intact autoantigens. Binding of full-length proteins correlated well with the peptide binding of the ACPAs, according to the results of both ELISA (Figure 1D and Supplementary Figure 6, available on the *Arthritis & Rheumatology* web site at http://onlinelibrary.wiley.com/doi/10.1002/art.40699/abstract) and Western blotting (Figure 1E). An interesting feature was that mAb 1325:01B09 bound to both the citrullinated α-chain and citrullinated β-chain of fibrinogen, whereas mAb 1325:05C06 displayed reactivity restricted to the α-chain (Figure 1E).

We could also show that the ACPAs had the potential to detect citrullinated protein targets in complex cell lysates (Figure 1F). Consistently, no reactivity toward unmodified proteins was detected.

Synovial ACPAs carrying more mutations, but shorter CDR3 regions in their B cell receptor heavy chain, compared to non-ACPAs. The 4 RA synovial fluid–derived monoclonal ACPAs, as well as the non-ACPAs isolated from the same donor (n = 78; 11 non-ACPA sequences were excluded from the analysis because either the heavy- and/or light-chain sequences were of poor quality), were investigated for mu-

tation frequencies, gene usage, and CDR3 characteristics. The ACPAs consistently displayed a large number of mutations, with a median frequency of nonconservative replacement mutations in the heavy-chain variable region of 19.5, as compared to 7.0 in the non-ACPAs ($P = 0.0008$). Heavy-chain silent mutations were also more numerous in the ACPAs compared to the non-ACPAs (median frequency 11 versus 1.5; $P < 0.0001$) (Figure 3A). To summarize, the total frequency of mutations in the heavy chain was more than 3 times higher in ACPAs as compared to non-ACPAs.

The same pattern was observed for the light-chain variable region, with ACPAs being almost 4 times more mutated as compared to non-ACPAs. In the light-chain variable region, the median frequency of replacement mutations was 16.0 in the ACPAs as compared to 4.0 in the non-ACPAs ($P = 0.0010$), and the median frequency of light-chain silent mutations was 12.5 in ACPAs and 1.0 in non-ACPAs ($P < 0.0001$) (Figure 3A).

Compared to non-ACPAs, the mutations in the ACPAs were distributed within the variable region, with enrichment of replacement mutations in the CDRs. However, ACPAs also carried enriched mutations in the framework regions (FWRs), especially in heavy-chain FWR3 (Figure 3B).

We next assessed the features of the CDR3 in ACPAs compared to non-ACPAs (Supplementary Table 9, available on the *Arthritis & Rheumatology* web site at http://onlinelibrary.wiley.com/doi/10.1002/art.40699/abstract). The synovial fluid–derived monoclonal ACPAs consistently had a short heavy-chain CDR3, consisting of a median of 10 amino acids, while the heavy-chain CDR3 of non-ACPAs had a median of 15 amino acids ($P = 0.0011$). In contrast, the length of the light-chain CDR3 displayed no differences, with a median of 9.7 amino acids in the non-ACPAs as compared to 10 amino acids in the ACPAs ($P = 0.5615$). Negatively charged amino acids were overrepresented in ACPAs as compared to non-ACPAs in the light-chain CDR3 ($P = 0.0002$). No difference between ACPAs and non-ACPAs could be detected with regard to the number of positive or hydrophobic amino acids.

Presence of both citrulline-reactive and citrulline-nonreactive clonal expansions in RA synovial fluid plasma cells. Next, the phylogenetic relationships of the heavy-chain and light-chain variable regions were investigated. Three of the ACPAs were found to belong to the V_H4 gene family, whereas 1 of the ACPAs was of V_H1 origin (mAb 1325:04C03) (Table 1). The variable-region gene usage was never ancestral for any of the 4 ACPAs (Figure 3C).

The clonality of all 182 isolated Ig clones was investigated using a definition of clonality in which 2 or more single cells generated a clonotype characterized by identical V–(D)–J gene usages and identical CDR3 nucleotide sequences. One of the 4 ACPAs was clonally expanded, i.e., the sequence coding for mAb 1325:04C03 was detected in 3 isolated
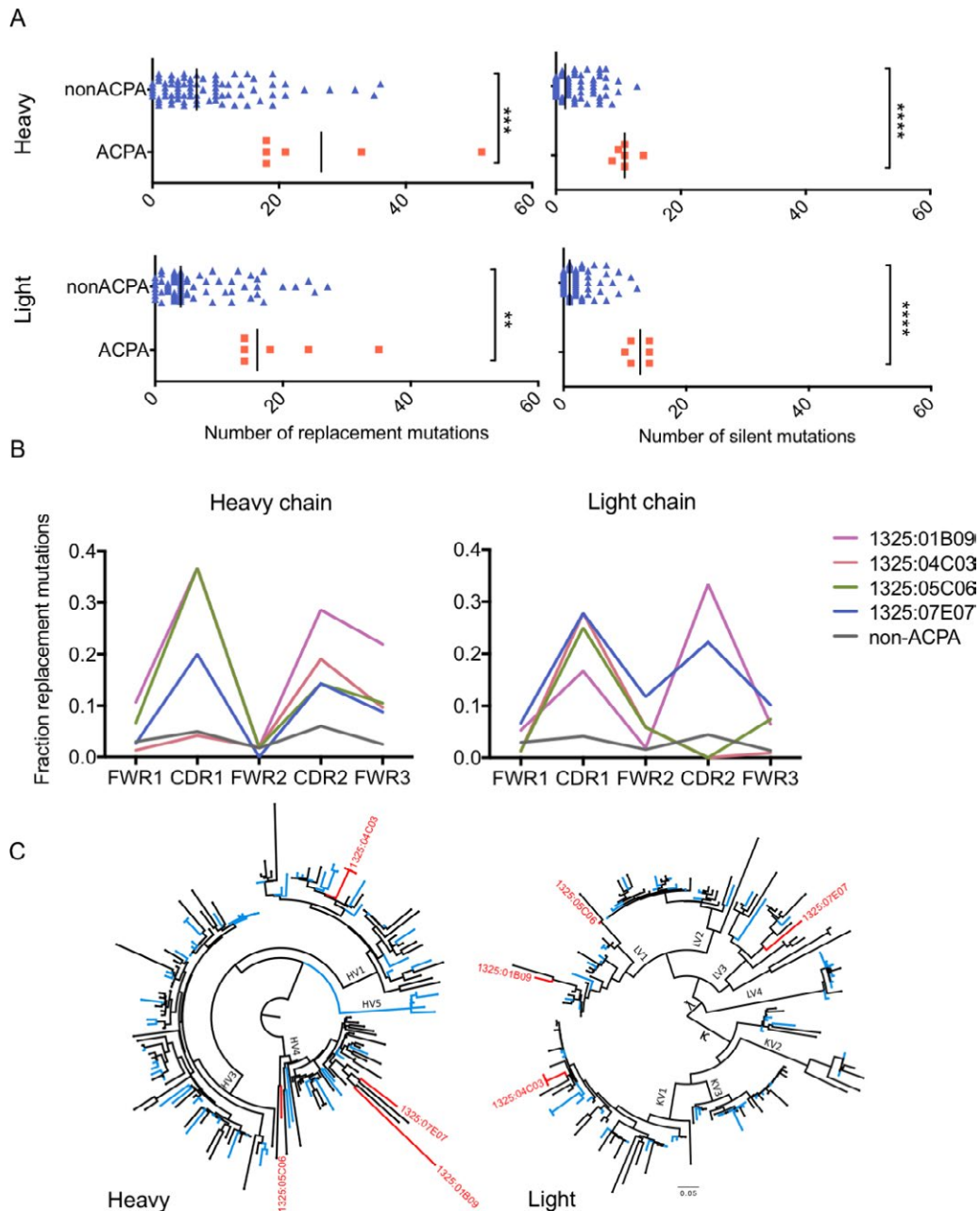
Figure 3. Mutation characteristics and phylogenetic relationship of Ig variable regions coding for ACPAs compared to non-ACPAs. **A,** The number of replacement and silent mutations in the heavy- and light-chain variable (V) regions are depicted for ACPAs (n = 6) and non-ACPAs (n = 78). **B,** Distributions of mutations within the heavy- and light-chain variable regions are shown for the individual ACPAs compared to non-ACPAs. All data was extracted from the Immunogenetics V-Quest database. Differences in the fraction of replacement mutations in the framework regions (FWRs) and complementarity-determining regions (CDRs) were calculated by Mann-Whitney nonparametric test. **C,** Phylogenetic relationships for heavy-chain and light-chain sequences are shown. Antibodies binding to citrullinated antigens (ACPAs) are indicated in red, whereas non-ACPAs are indicated in blue. Antibody sequences with unknown reactivity are labeled in black. The phylogenetic trees were generated utilizing Phylogeny.fr with MUSCLE alignment and visualized by FigTree. ** = $P < 0.01$; *** = $P < 0.001$; **** = $P < 0.0001$. See Figure 1 for other definitions.

antibody-secreting cells, which corresponded to 1.6% (3 of 182) of the isolated plasma cells. The variable regions of the other 3 ACPAs could only be detected in single cells (0.5%) (Table 1). Five additional clonalities were identified within the plasma cells in the non-ACPA group, and 1 additional clone

was found within the unexpressed sequences, i.e., with unknown reactivity. Intriguingly, 1 of the non-ACPA expanded clones was found in 8 individual cells (4.4% of all isolated cells). In total, 11.4% of the generated IgG sequences were expanded.

Reduced or lost citrulline reactivity in germline-reverted ACPAs. New sets of recombinant antibodies were constructed from the RA synovial fluid–derived plasma cells, in which the heavy and light chains of the monoclonal ACPAs were reverted to their predicted germline sequences. Two of the antibodies (mAb 1325:01B09 and 1325:05C06) completely lost their reactivity when converted back to germline (G + G in Figures 4A and B). However, the germline mAb 1325:07E07
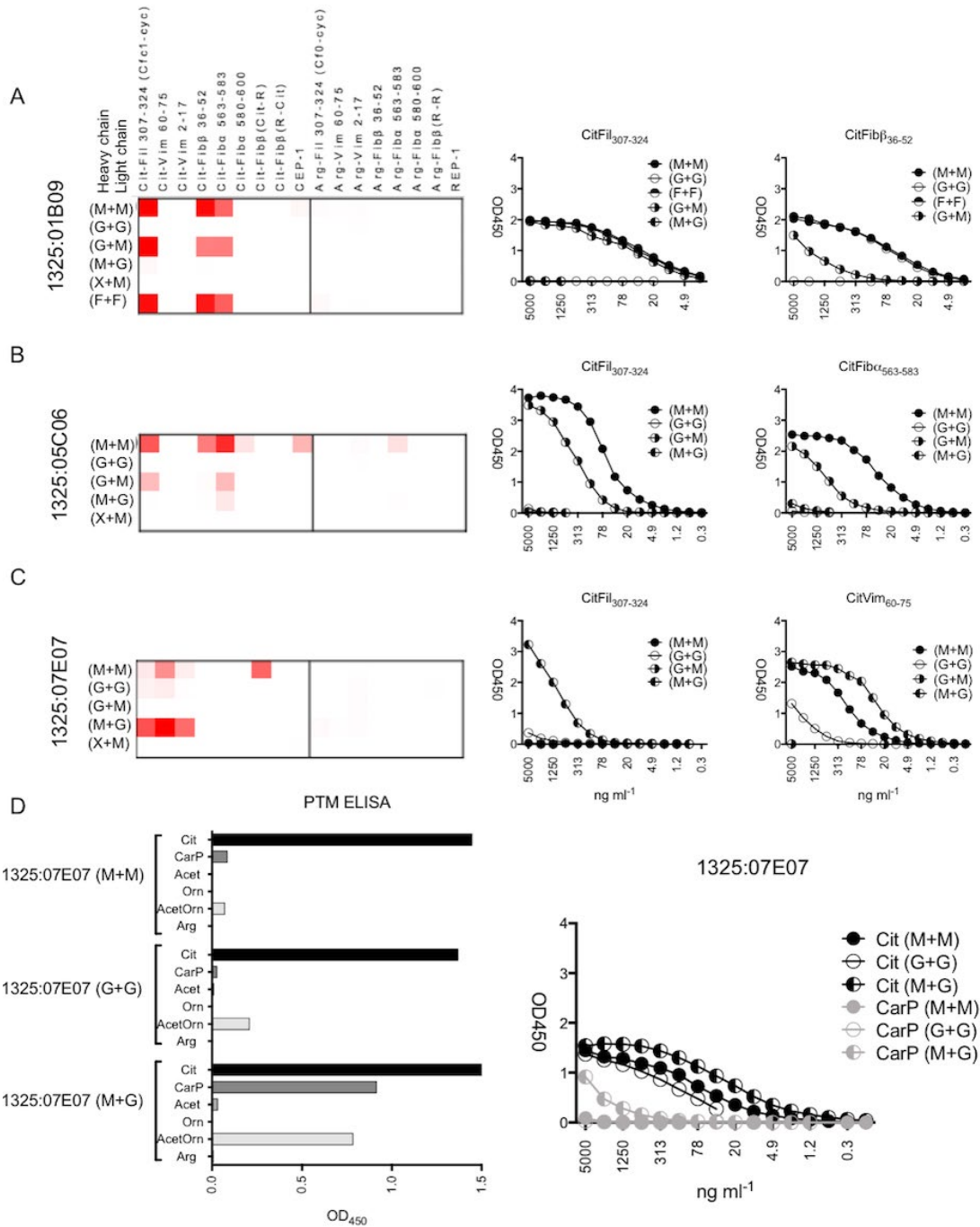
Figure 4. Binding pattern of the mAb with variable regions reverted to germline. **A–D,** Left, Heatmap summaries show ACPA peptide array antibody binding to the different citrullinated peptides (**A–C**) or PTMs (**D**). Right, Titration ELISA dilution curves show mAb (at different dilutions) binding to selected peptides. M + M = fully mutated antibody; G + G = fully germline antibody; M + G = heavy-chain mutated and light-chain germline; G + M = heavy-chain germline and light-chain mutated; X + M = heavy-chain unrelated (different V_H gene, third complementarity-determining region length, and other ACPAs) and light-chain mutated; F + F = framework regions converted to germline in heavy and light chains. In the ACPA peptide array, the mAb were analyzed at 5 μg/ml, and the ELISA titration curves start at an mAb concentration of 5 μg/ml and were diluted one-half in 12 steps. See Figure 1 for other definitions.

maintained citrulline reactivity, although at a reduced level, as compared to the fully mutated antibody (Figure 4C). Germline mAb 1325:04C03 did not express functional antibodies in our system, and thus could not be investigated.

Variations between ACPAs in the contributions of heavy- versus light-chain mutations to antigen recognition. As a further investigation of the molecular basis for citrulline recognition, we produced converted and chain-exchanged recombinant antibodies with germline-reverted (G) sequences in either only the heavy chains or only the light chains.

For mAb 1325:01B09, there was a strong dependency on the light-chain mutations for citrulline recognition. The citrulline

reactivity was thus sustained in the variant, where only the heavy chain was converted back to germline, while the mutations were retained in the light chain (G + M in Figure 4A). In contrast, all reactivity diminished in the opposite chain–exchanged version (heavy chain mutated and light chain germline) (M + G in Figure 4A).

Since this mAb displayed many mutations in the FWRs (Figure 3B), an additional construct was produced in which only the FWRs were reverted to germline, with mutations in the CDRs remaining. This construct displayed citrulline reactivity without any loss in sensitivity (F + F in Figure 4A).

A similar pattern of reactivity was found for the chain-exchanged variant mAb 1325:05C06, with a strong dependence
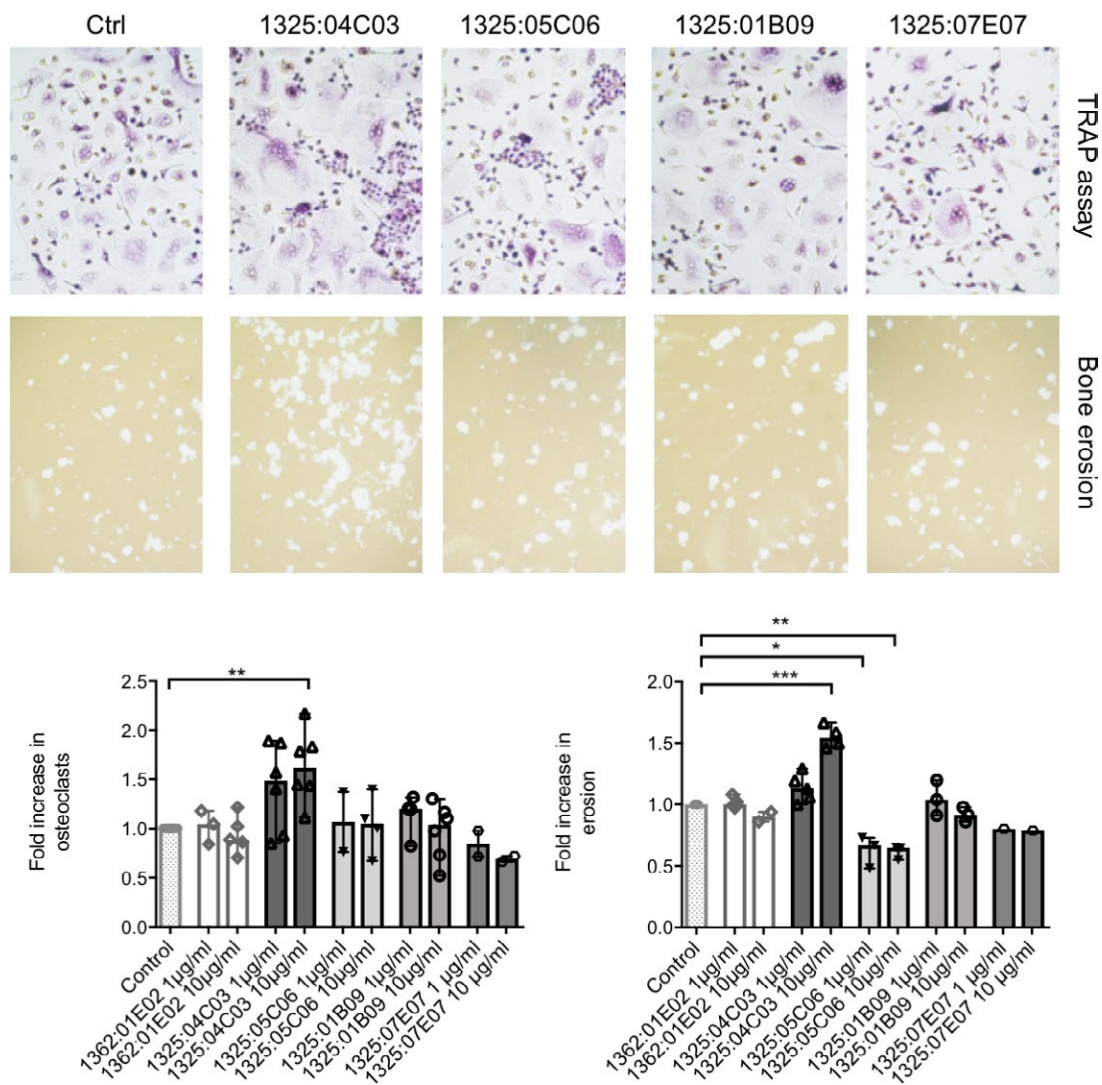
Figure 5. Effects of the 4 ACPA mAb on osteoclast differentiation and bone erosion. Top, Osteoclast differentiation in the presence of the 4 mAb (or control antibody [Ctrl]) was measured using a combination of tartrate-resistant acid phosphatase (TRAP) staining and >3 nuclei per cell (representative examples shown in upper panels). Effects of the 4 mAb on artificial bone erosion were investigated using a previously described in vitro assay (10) (representative examples shown in lower panels). Bottom, The effects of the 4 ACPA mAb (at 2 different concentrations) on osteoclast numbers and bone erosion in peripheral blood samples from several rheumatoid arthritis donors are summarized, showing the fold increase in osteoclast numbers and bone resorption. Results are the mean ± SEM of 1–6 samples per group. * = $P < 0.05$; ** = $P < 0.01$; *** = $P < 0.001$, by Kruskal-Wallis test followed by Dunn's test for multiple comparisons. See Figure 1 for other definitions.

of the light-chain mutations for its peptide reactivity. The citrulline binding was more profoundly reduced in this variant construct (Figure 4B), implying that the dependency was less absolute.

To further understand the function of the heavy chain of the 2 mAb in which only the mutations in the light chain contributed to citrulline binding, we next exchanged the original heavy chain to unrelated heavy-chain sequences, and thus addressed the contributions of various V_H genes, CDR3 lengths, or other investigated ACPA heavy chains. Interestingly, none of these combinations generated any citrulline binding, indicating that the original heavy-chain V–D–J rearrangement (even if germline) is essential for the citrulline binding for mAb 1325:01B09 and mAb 1325:05C06 (X + M in Figures 4A and B).

The mAb 1325:07E07 had the interesting feature of retaining some citrulline binding for the germline-converted mAb. Notably, the heavy chain of germline-converted mAb 1325:07E07 was more important than the light chain for binding (Figure 3C). The variant with germline light chain, as compared to the fully mutated 1325:07E07, demonstrated stronger citrulline binding for the chain-exchanged antibody (mAb 1325:07E07 [M + G] versus mAb 1325:07E07 [M + M] in Figure 4C), and also obtained reactivity with the peptides with PTMs CarP and acetylated ornithine (Figure 4D).

For mAb1325:04C03, only the germline heavy-chain construct, and not constructs with germline light chain, was productive. Based on the reactivity of the expressed mAb, we conclude that hypermutations of the light chain may not contribute significantly to the citrulline binding for this antibody (Supplementary Figure 7, available on the *Arthritis & Rheumatology* web site at http://onlinelibrary.wiley.com/doi/10.1002/art.40699/abstract).

Differential functional effects of monoclonal ACPAs on osteoclasts. The investigated monoclonal ACPAs had several features in common, such as high mutation frequencies and overlap in reactivities, and yet they also displayed essentially unique patterns of citrulline and homocitrulline reactivity with peptides and/or full-length proteins. To further understand whether these differences could result in different functions, we tested the 4 antibodies in an in vitro assay for antibody-dependent effects on osteoclastogenesis and in vitro bone destruction (10).

Of the 4 tested antibodies, mAb 1325:04C03 promoted osteoclastogenesis ($P = 0.0049$ at a concentration of 10 μg/ml) and increased erosion of an artificial bone surface ($P = 0.0005$ at a concentration of 10 μg/ml), whereas no such stimulatory effects were seen for the other 3 monoclonal ACPAs (Figure 5). Instead, mAb 1325:05C06 displayed an inhibitory effect on osteoclast-mediated bone erosion in vitro ($P = 0.0221$ at a concentration of 1 μg/ml, $P = 0.0067$ at a concentration of 10 μg/ml), but without a concomitant effect on osteoclast numbers ($P = 0.9$ at a concentration of 10 μg/ml) (Figure 5). Notably, polyclonal IgG ACPAs from RA patients have been shown to exert effects on osteoclast activation that were similar to those of mAb 1325:04C03 (10).

DISCUSSION

A major finding from our study of spontaneous production of antibody-secreting cells from the active RA joint was that the ACPAs are both highly specific and refined for recognition of PTMs, mainly citrullination, while at the same time they display extensive, but still partly unique, cross-reactivity patterns that are dependent on linear consensus sequences rather than distinct proteins. We also demonstrated that these features are confined neither to cells from inflamed joints nor to disease-modifying antirheumatic drug–naive disease, as we could replicate the extensive cross-reactivity also for citrulline-reactive B cells from the peripheral blood of additional RA patients.

We are intrigued by our finding that the combination of high numbers of somatic mutations and broad cross-reactivity against thousands of PTM peptides, and at least several PTM proteins, differed from what has been described for most previously investigated autoantibodies associated with organ-specific and systemic autoimmune diseases (28–31). For the presently investigated ACPAs, we hypothesize that multiple T cell–dependent selection processes with somatic Ig mutations may happen sequentially, for example, in germinal center–like structures located in mucosal tissues, in lymphoid organs, and in joints. Such germinal center–like structures have previously been described in these sites in RA patients (32–36). In addition, there are indications that immune responses toward citrullinated antigens may be initiated in mucosal tissues, for example, in the lungs. It will thus be very interesting to further analyze the emergence of somatic mutations at these different sites in order to better understand the mechanisms behind the development of the somatically hypermutated ACPAs described in the inflamed joints of patients with established RA.

Concerning the T cells that may have provided help to the generation of the B cells/plasma cells in this study, we note that some of the ACPA targets (α-enolase, vimentin, and fibrinogen, as well as cartilage intermediate layer protein) overlap with well-defined HLA–DRB1*04:01–associated T cell epitopes studied in ACPA+ RA (37,38). The difference in the underlying germinal center reactions, as compared to classic autoimmune reactions, would be that different PTM proteins in different organs may contribute to a consecutive selection of B cells that ultimately mature into plasma cells in the inflamed joint.

Another striking feature of ACPAs, both on a serologic and monoclonal level, is the recently discovered accumulation of mutations that introduces *N*-linked Fab glycosylation sites (39,40). Indeed, ACPAs (including the ones described herein) have been verified to carry Fab glycosylations in both their heavy- and light-chain variable regions (39), and it is possible that this confers an advantage in the B cell selection process that partly compensates for the relatively low affinities observed.

Although the affinities of our ACPAs were found to be in the μ*M* range, the ELISAs were also effective in mAb concentra-

tions down to the ng/ml range, thus ensuring that we detected antigen recognition and not classic polyreactivity. We also acknowledge that the measured affinities may not properly reflect the binding strength for targeted modified intact proteins in vivo. Furthermore, consistent with this notion, not all peptides in the extracellular matrix array should be regarded as physiologic target antigens for ACPAs, until further validated. Importantly, the autoantigenic peptides/proteins we used in our ELISAs and Western blots all originated from in situ identification of citrullination in serum and synovial fluid samples from RA patients.

The presently described monoclonal ACPAs all showed consistent and clear specific reactivity with citrullinated peptides and intact proteins in several assays in which we used low concentrations of the respective antibodies. This is true also for another set of recently published monoclonal ACPAs (27), from which 2 were also used in the validation experiment of our large peptide array (see Supplementary Figure 5 [http://onlinelibrary.wiley.com/doi/10.1002/art.40699/abstract]). Previously, studies utilizing human monoclonal ACPAs (41–43)*, including those from our own laboratory, have used single and more limited detection systems and often high concentrations of the antibodies, which may yield false-positive responses. Such false-positive signals may stem from specific types of polyreactive antibodies, which are common in systemic lupus erythematosus (44). These may very well be overrepresented in RA as well, and such reactivities, although potentially pathogenetically relevant, are very different from those described in the present report. In the current study, we therefore decided to use several different approaches, including detection of binding to intact proteins as complement to the peptide-based assays. We thus recommend that optimization of assays for reactivity against PTM peptides/proteins will be necessary for all future studies of ACPAs, and that some previously described antibodies with reported citrulline reactivity may not fulfill the more stringent criteria used in the present investigation. We consider such differences to be a main explanation for the differences in frequency of synovial B cells with citrulline reactivity in our present study as compared to that in our previous report (41).

Concerning the potential pathogenic role of ACPAs, it is interesting to note that 1 of them (mAb 1325:04C03), but not the other 3 multireactive ACPAs, was able to induce osteoclast activation and in vitro bone resorption. In addition, 1 ACPA described by Titcombe et al (27) (which was also 1 of the validation ACPAs [37CEPT2C04] used in our extracellular matrix peptide array) has been demonstrated to enhance joint inflammation in mice receiving a lipopolysaccharide challenge (27). At this point, it is not possible to identify the precise features of these 2 ACPAs that result in these effector functions. Instead, these observations further emphasize the importance of analyzing ACPAs at the monoclonal level, both concerning triggering events and

concerning disease-causing mechanisms. The growing list of reported monoclonal ACPAs (27,41–43,45–48) represents an important resource for such studies.

The observation that 2 of the predicted germline ACPAs did not recognize the investigated citrulline targets is consistent with the findings in other studies in different disease settings (41,49–51), and is consistent with the expected low affinity in germline-encoded, naive, IgM-positive B cells before antigen selection. Still, one of the constructs using the germline sequence of the investigated antibodies (germline-reverted mAb 1325:07E07) recognized some of the citrullinated autoantigens.

Interestingly, some of the ACPA mAb displayed a higher light-chain somatic hypermutation dependency than heavy-chain somatic hypermutation dependency. While the antigen-binding surface of immunoglobulins is predominantly built up by the interface of the light-chain and heavy-chain CDR loops, the heavy-chain CDRs, especially HCDR3, are generally thought to be most critical for the binding in a majority of antibodies. Notably, the results of our chain-swapping experiments showed that the ancestral heavy-chain V–D–J rearrangement was essential, even though the binding was independent of heavy-chain somatic hypermutations in these particular ACPA mAb.

In summary, we have demonstrated how plasma cells from an RA inflamed joint, as well as B cells from the circulation of RA patients, can produce antibodies that, on the one hand, have undergone extensive hypermutation and, on the other hand, react with a massive number of different PTM peptides and proteins with similar, but distinct, recognition amino acid patterns for each of the investigated mAb. We envision that such scenarios may also be valid for other autoimmune diseases in which potentially pathogenic antibodies, which develop over several years, may recognize different targets in different organs. Thus, studies on cross-reactivity patterns, in particular in the context of PTMs or other protein modifications, may provide us with new leads concerning both triggering and targeting of B cells involved in complex inflammatory diseases like RA.

ACKNOWLEDGMENTS

AUTHOR CONTRIBUTIONS

All authors were involved in drafting the article or revising it critically for important intellectual content, and all authors approved the final version to be published. Dr. Malmström had full access to all of the data

---

*Reference 41 has been retracted since the time of initial publication of this article.

in the study and takes responsibility for the integrity of the data and the accuracy of the data analysis.

Study conception and design. Steen, Forsström, Rapecki, Bang, Mueller, Catrina, Grönwall, Skriner, Nilsson, Lightwood, Klareskog, Malmström.

Acquisition of data. Steen, Forsström, Sahlström, Odowd, Israelsson, Krishnamurthy, Badreh, Mathsson Alm, Compson, Ndlovu, Hansson, Titcombe, Grönwall.

Analysis and interpretation of data. Steen, Forsström, Sahlström, Israelsson, Krishnamurthy, Mathsson Alm, Compson, Ramsköld, Hansson, Titcombe, Bang, Mueller, Catrina, Grönwall, Skriner, Lightwood, Klareskog, Malmström.

ADDITIONAL DISCLOSURES

REFERENCES

1. Schellekens GA, de Jong BA, van den Hoogen FH, van de Putte LB, van Venrooij WJ. Citrulline is an essential constituent of antigenic determinants recognized by rheumatoid arthritis-specific autoantibodies. J Clin Invest 1998;101:273–81.

2. Girbal-Neuhauser E, Durieux JJ, Arnaud M, Dalbon P, Sebbag M, Vincent C, et al. The epitopes targeted by the rheumatoid arthritis-associated antifilaggrin autoantibodies are posttranslationally generated on various sites of (pro)filaggrin by deimination of arginine residues. J Immunol 1999;162:585–94.

3. Eyre S, Bowes J, Diogo D, Lee A, Barton A, Martin P, et al. High-density genetic mapping identifies new susceptibility loci for rheumatoid arthritis. Nat Genet 2012;44:1336–40.

4. Padyukov L, Seielstad M, Ong RT, Ding B, Ronnelid J, Seddighzadeh M, et al. A genome-wide association study suggests contrasting associations in ACPA-positive versus ACPA-negative rheumatoid arthritis. Ann Rheum Dis 2011;70:259–65.

5. Van der Helm-van Mil AH, Verpoort KN, Breedveld FC, Toes RE, Huizinga TW. Antibodies to citrullinated proteins and differences in clinical progression of rheumatoid arthritis. Arthritis Res Ther 2005;7:R949–58.

6. Machold KP, Stamm TA, Nell VP, Pflugbeil S, Aletaha D, Steiner G, et al. Very recent onset rheumatoid arthritis: clinical and serological patient characteristics associated with radiographic progression over the first years of disease. Rheumatology (Oxford) 2007;46:342–9.

7. Aletaha D, Neogi T, Silman AJ, Funovits J, Felson DT, Bingham CO III, et al. 2010 rheumatoid arthritis classification criteria: an American College of Rheumatology/European League Against Rheumatism collaborative initiative. Arthritis Rheum 2010;62:2569–81.

8. Rantapaa-Dahlqvist S, de Jong BA, Berglin E, Hallmans G, Wadell G, Stenlund H, et al. Antibodies against cyclic citrullinated peptide and IgA rheumatoid factor predict the development of rheumatoid arthritis. Arthritis Rheum 2003;48:2741–9.

9. Harre U, Georgess D, Bang H, Bozec A, Axmann R, Ossipova E, et al. Induction of osteoclastogenesis and bone loss by human autoantibodies against citrullinated vimentin. J Clin Invest 2012;122:1791–802.

10. Krishnamurthy A, Joshua V, Haj Hensvold A, Jin T, Sun M, Vivar N, et al. Identification of a novel chemokine-dependent molecular mechanism underlying rheumatoid arthritis-associated autoantibody-mediated bone loss. Ann Rheum Dis 2016;75:721–9.

11. Wigerblad G, Bas DB, Fernades-Cerqueira C, Krishnamurthy A, Nandakumar KS, Rogoz K, et al. Autoantibodies to citrullinated proteins induce joint pain independent of inflammation via a chemokine-dependent mechanism. Ann Rheum Dis 2016;75:730–8.

12. Masson-Bessiere C, Sebbag M, Girbal-Neuhauser E, Nogueira L, Vincent C, Senshu T, et al. The major synovial targets of the rheumatoid arthritis-specific antifilaggrin autoantibodies are deiminated forms of the α- and β-chains of fibrin. J Immunol 2001;166:4177–84.

13. Vossenaar ER, Despres N, Lapointe E, van der Heijden A, Lora M, Senshu T, et al. Rheumatoid arthritis specific anti-Sa antibodies target citrullinated vimentin. Arthritis Res Ther 2004;6:R142–50.

14. Kinloch A, Tatzer V, Wait R, Peston D, Lundberg K, Donatien P, et al. Identification of citrullinated α-enolase as a candidate autoantigen in rheumatoid arthritis. Arthritis Res Ther 2005;7:R1421–9.

15. Burkhardt H, Sehnert B, Bockermann R, Engstrom A, Kalden JR, Holmdahl R. Humoral immune response to citrullinated collagen type II determinants in early rheumatoid arthritis. Eur J Immunol 2005;35:1643–52.

16. Schwenzer A, Jiang X, Mikuls TR, Payne JB, Sayles HR, Quirke AM, et al. Identification of an immunodominant peptide from citrullinated tenascin-C as a major target for autoantibodies in rheumatoid arthritis. Ann Rheum Dis 2016;75:1876–83.

17. Khandpur R, Carmona-Rivera C, Vivekanandan-Giri A, Gizinski A, Yalavarthi S, Knight JS, et al. NETs are a source of citrullinated autoantigens and stimulate inflammatory responses in rheumatoid arthritis. Sci Transl Med 2013;5:178ra40.

18. Shi J, Knevel R, Suwannalai P, van der Linden MP, Janssen GM, van Veelen PA, et al. Autoantibodies recognizing carbamylated proteins are present in sera of patients with rheumatoid arthritis and predict joint damage. Proc Natl Acad Sci U S A 2011;108:17372–7.

19. Juarez M, Bang H, Hammar F, Reimer U, Dyke B, Sahbudin I, et al. Identification of novel antiacetylated vimentin antibodies in patients with early inflammatory arthritis. Ann Rheum Dis 2016;75:1099–107.

20. Snir O, Widhe M, Hermansson M, von Spee C, Lindberg J, Hensen S, et al. Antibodies to several citrullinated antigens are enriched in the joints of rheumatoid arthritis patients. Arthritis Rheum 2010;62:44–52.

21. Bennike T, Lauridsen K, Olesen M, Andersen V, Birkelund S, Stensballe A. Optimizing the identification of citrullinated peptides by mass spectrometry: utilizing the inability of trypsin to cleave after citrullinated amino acids. J Proteomics Bioinform 2013;6:288–95.

22. Balakrishnan L, Bhattacharjee M, Ahmad S, Nirujogi RS, Renuse S, Subbannayya Y, et al. Differential proteomic analysis of synovial fluid from rheumatoid arthritis and osteoarthritis patients. Clin Proteomics 2014;11:1.

23. Naba A, Clauser KR, Ding H, Whittaker CA, Carr SA, Hynes RO. The extracellular matrix: tools and insights for the "omics" era. Matrix Biol 2016;49:10–24.

24. Forsstrom B, Axnas BB, Stengele KP, Buhler J, Albert TJ, Richmond TA, et al. Proteome-wide epitope mapping of antibodies using ultra-dense peptide arrays. Mol Cell Proteomics 2014;13:1585–97.

25. Clargo AM, Hudson AR, Ndlovu W, Wootton RJ, Cremin LA, O'Dowd VL, et al. The rapid generation of recombinant functional monoclonal antibodies from individual, antigen-specific bone marrow-derived plasma cells isolated using a novel fluorescence-based method. MAbs 2014;6:143–59.

26. Hansson M, Mathsson L, Schlederer T, Israelsson L, Matsson P, Nogueira L, et al. Validation of a multiplex chip-based assay for the detection of autoantibodies against citrullinated peptides. Arthritis Res Ther 2012;14:R201.

27. Titcombe PJ, Wigerblad G, Sippl N, Zhang N, Shmagel AK, Sahlstrom P, et al. Pathogenic citrulline-multispecific B cell receptor clades in rheumatoid arthritis. Arthritis Rheumatol 2018;70:1933–45.

28. Wang Y, Thomson CA, Allan LL, Jackson LM, Olson M, Hercus TR, et al. Characterization of pathogenic human monoclonal autoantibodies against GM–CSF. Proc Natl Acad Sci U S A 2013;110:7832–7.

29. Tipton CM, Fucile CF, Darce J, Chida A, Ichikawa T, Gregoretti I, et al. Diversity, cellular origin and autoreactivity of antibody-secreting cell population expansions in acute systemic lupus erythematosus. Nat Immunol 2015;16:755–65.

30. Chardes T, Chapal N, Bresson D, Bes C, Giudicelli V, Lefranc MP, et al. The human anti-thyroid peroxidase autoantibody repertoire in Graves' and Hashimoto's autoimmune thyroid diseases. Immunogenetics 2002;54:141–57.

31. Di Niro R, Mesin L, Zheng NY, Stamnaes J, Morrissey M, Lee JH, et al. High abundance of plasma cells secreting transglutaminase 2-specific IgA autoantibodies with limited somatic hypermutation in celiac disease intestinal lesions. Nat Med 2012;18:441–5.

32. Reynisdottir G, Olsen H, Joshua V, Engstrom M, Forsslund H, Karimi R, et al. Signs of immune activation and local inflammation are present in the bronchial tissue of patients with untreated early rheumatoid arthritis. Ann Rheum Dis 2016;75:1722–7.

33. Reynisdottir G, Karimi R, Joshua V, Olsen H, Hensvold AH, Harju A, et al. Structural changes and antibody enrichment in the lungs are early features of anti–citrullinated protein antibody–positive rheumatoid arthritis. Arthritis Rheumatol 2014;66:31–9.

34. Rangel-Moreno J, Hartson L, Navarro C, Gaxiola M, Selman M, Randall TD. Inducible bronchus-associated lymphoid tissue (iBALT) in patients with pulmonary complications of rheumatoid arthritis. J Clin Invest 2006;116:3183–94.

35. Ramwadhdoebe TH, Hahnlein J, Maijer KI, van Boven LJ, Gerlag DM, Tak PP, et al. Lymph node biopsy analysis reveals an altered immunoregulatory balance already during the at-risk phase of autoantibody positive rheumatoid arthritis. Eur J Immunol 2016;46:2812–21.

36. Dennis G Jr, Holweg CT, Kummerfeld SK, Choy DF, Setiadi AF, Hackney JA, et al. Synovial phenotypes in rheumatoid arthritis correlate with response to biologic therapeutics. Arthritis Res Ther 2014;16:R90.

37. James EA, Rieck M, Pieper J, Gebe JA, Yue BB, Tatum M, et al. Citrulline-specific Th1 cells are increased in rheumatoid arthritis and their frequency is influenced by disease duration and therapy. Arthritis Rheumatol 2014;66:1712–22.

38. Gerstner C, Dubnovitsky A, Sandin C, Kozhukh G, Uchtenhagen H, James EA, et al. Functional and structural characterization of a novel HLA-DRB1*04:01-restricted α-enolase T cell epitope in rheumatoid arthritis. Front Immunol 2016;7:494.

39. Lloyd KA, Steen J, Amara K, Titcombe PJ, Israelsson L, Lundstrom SL, et al. Variable domain N-linked glycosylation and negative surface charge are key features of monoclonal ACPA: implications for B-cell selection. Eur J Immunol 2018;48:1030–45.

40. Rombouts Y, Willemze A, van Beers JJ, Shi J, Kerkman PF, van Toorn L, et al. Extensive glycosylation of ACPA-IgG variable domains modulates binding to citrullinated antigens in rheumatoid arthritis. Ann Rheum Dis 2016;75:578–85.

41. Amara K, Steen J, Murray F, Morbach H, Fernandez-Rodriguez BM, Joshua V, et al. Monoclonal IgG antibodies generated from joint-derived B cells of RA patients have a strong bias toward citrullinated autoantigen recognition. J Exp Med 2013;210:445–55.

42. Li S, Yu Y, Yue Y, Liao H, Xie W, Thai J, et al. Autoantibodies from single circulating plasmablasts react with citrullinated antigens and porphyromonas gingivalis in rheumatoid arthritis. Arthritis Rheumatol 2016;68:614–26.

43. Corsiero E, Bombardieri M, Carlotti E, Pratesi F, Robinson W, Migliorini P, et al. Single cell cloning and recombinant monoclonal antibodies generation from RA synovial B cells reveal frequent targeting of citrullinated histones of NETs. Ann Rheum Dis 2016;75:1866–75.

44. Yurasov S, Wardemann H, Hammersen J, Tsuiji M, Meffre E, Pascual V, et al. Defective B cell tolerance checkpoints in systemic lupus erythematosus. J Exp Med 2005;201:703–11.

45. Raats JM, Wijnen EM, Pruijn GJ, van den Hoogen FH, van Venrooij WJ. Recombinant human monoclonal autoantibodies specific for citrulline-containing peptides from phage display libraries derived from patients with rheumatoid arthritis. J Rheumatol 2003;30:1696–711.

46. Van de Stadt LA, van Schouwenburg PA, Bryde S, Kruithof S, van Schaardenburg D, Hamann D, et al. Monoclonal anti-citrullinated protein antibodies selected on citrullinated fibrinogen have distinct targets with different cross-reactivity patterns. Rheumatology (Oxford) 2013;52:631–5.

47. Tan YC, Kongpachith S, Blum LK, Ju CH, Lahey LJ, Lu DR, et al. Barcode-enabled sequencing of plasmablast antibody repertoires in rheumatoid arthritis. Arthritis Rheumatol 2014;66:2706–15.

48. Tsuda R, Ozawa T, Kobayashi E, Hamana H, Taki H, Tobe K, et al. Monoclonal antibody against citrullinated peptides obtained from rheumatoid arthritis patients reacts with numerous citrullinated microbial and food proteins. Arthritis Rheumatol 2015;67:2020–31.

49. Zhou T, Georgiev I, Wu X, Yang ZY, Dai K, Finzi A, et al. Structural basis for broad and potent neutralization of HIV-1 by antibody VRC01. Science 2010;329:811–7.

50. Scheid JF, Mouquet H, Ueberheide B, Diskin R, Klein F, Oliveira TY, et al. Sequence and structural convergence of broad and potent HIV antibodies that mimic CD4 binding. Science 2011;333:1633–7.

51. Meyer S, Woodward M, Hertel C, Vlaicu P, Haque Y, Karner J, et al. AIRE-deficient patients harbor unique high-affinity disease-ameliorating autoantibodies. Cell 2016;166:582–95.

Structural Basis of Cross-Reactivity of Anti–Citrullinated Protein Antibodies

Changrong Ge,[1] Bingze Xu,[1] Bibo Liang,[2] Erik Lönnblom,[1] Susanna L. Lundström,[1] Roman A. Zubarev,[1] Burcu Ayoglu,[3] Peter Nilsson,[3] Thomas Skogh,[4] Alf Kastbom,[4] Vivianne Malmström,[5] Lars Klareskog,[5] René E. M. Toes,[6] Theo Rispens,[7] Doreen Dobritzsch,[8] and Rikard Holmdahl[2]

Objective. Anti–citrullinated protein antibodies (ACPAs) develop many years before the clinical onset of rheumatoid arthritis (RA). This study was undertaken to address the molecular basis of the specificity and cross-reactivity of ACPAs from patients with RA.

Methods. Antibodies isolated from RA patients were expressed as monoclonal chimeric antibodies with mouse Fc. These antibodies were characterized for glycosylation using mass spectrometry, and their cross-reactivity was assessed using Biacore and Luminex immunoassays. The crystal structures of the antigen-binding fragment (Fab) of the monoclonal ACPA E4 in complex with 3 different citrullinated peptides were determined using x-ray crystallography. The prevalence of autoantibodies reactive against 3 of the citrullinated peptides that also interacted with E4 was investigated by Luminex immunoassay in 2 Swedish cohorts of RA patients.

Results. Analysis of the crystal structures of a monoclonal ACPA from human RA serum in complex with citrullinated peptides revealed key residues of several complementarity-determining regions that recognized the citrulline as well as the neighboring peptide backbone, but with limited contact with the side chains of the peptides. The same citrullinated peptides were recognized by high titers of serum autoantibodies in 2 large cohorts of RA patients.

Conclusion. These data show, for the first time, how ACPAs derived from human RA serum recognize citrulline. The specific citrulline recognition and backbone-mediated interactions provide a structural explanation for the promiscuous recognition of citrullinated peptides by RA-specific ACPAs.

INTRODUCTION

A hallmark of autoimmune diseases is the production of autoantibodies. There has been a revival of interest in furthering understanding of their functional roles, since these autoantibodies precede the clinical onset in most autoimmune diseases. However, knowledge of their exact interactions with target epitopes is very limited. Rheumatoid arthritis (RA) is one of the most prevalent autoimmune diseases, affecting ~0.5% of the world population. The occurrence of rheumatoid factors (RFs), i.e., antibodies self-reactive with the Fc portion of IgG, and autoantibodies against citrullinated proteins (ACPAs) have been found to be specific for

RA, and both have been suggested to take part in disease development (1–4). RFs and ACPAs appear years before the clinical onset of RA (5,6), and both are included in the American College of Rheumatology (ACR)/European League Against Rheumatism 2010 classification criteria for RA (7).

ACPAs are typically detected by commercial enzyme-linked immunosorbent assay using a certain set of undisclosed cyclic citrullinated peptides (CCPs), specifically CCP-2. Up to 70% of RA patients are found to be anti–CCP-2 positive, and the occurrence of ACPAs is linked to poorer prognoses (8).

A variety of citrullinated autoantigens have been characterized and suggested to be potential ACPA targets, such as α-enolase,

fibrinogen, filaggrin, vimentin, and type II collagen (CII) (9–13). Some ACPAs may have a more antigen-specific reactivity to certain citrullinated proteins, but most seem to be widely cross-reactive (14).

It is believed that both RFs and ACPAs promote the formation of immune complexes, but their pathogenic roles in vivo remain unclear. Several lines of evidence have indicated that ACPAs may play a critical role in the pathogenesis of RA. ACPAs have been reported to activate osteoclasts, to trigger bone erosions via an interleukin-8 (IL-8)–dependent pathway, and to elicit joint pain when injected into mice (15–17). ACPAs are also capable of inducing the secretion of tumor necrosis factor from macrophages through Fcγ receptor engagement, and of mediating complement activation via both the classical and alternative pathways (18). However, it is still unclear whether the demonstrated pathogenic effects of ACPAs are specifically related to their citrulline specificity or whether they could be attributed to other intrinsic characteristics, such as Fc glycosylation (19,20).

So far, only a subtype of ACPAs cross-reactive with joint cartilage has been shown to be able to induce arthritis upon direct injection into mice (21,22). Interestingly, Fc glycan sialylation of these antibodies transforms them into protective antibodies (19). Most ACPA-positive sera from RA patients are cross-reactive with several different citrullinated peptides (14). However, the molecular interactions of ACPAs with their citrullinated epitopes, clarification of which could explain both their wide cross-reactivity and their specificity for citrulline, are poorly understood.

To address this question, we produced several human monoclonal ACPAs and characterized their binding properties. In this study, we characterized, for the first time, the crystal structures of the Fab fragment of 1 of these ACPAs in complex with 3 sequence-unrelated peptide epitopes. Our results showed that at least some ACPAs specifically recognize the citrulline residue in a manner largely independent of the peptide epitope sequences. This finding has general importance, since the autoantibody responses to 3 citrullinated antigens, which were bound by the monoclonal ACPA Fab fragment in the crystal complexes, reached high titers and were found to be present at a high frequency in the serum of patients in 2 well-characterized Swedish RA cohorts.

PATIENTS AND METHODS

Patient population. In the present study, serum samples from 2 cohorts of RA patients were used for assessment of antibody reactivity by Luminex immunoassay. First, a part of the cohort of the second Swedish Early Intervention in RA trial (TIRA-2) (23) was used (n = 504), and as controls, we used healthy subjects from the cohort of the Western Region Initiative to Gather Information on Atherosclerosis (n = 285). The study protocol was approved by the regional ethics review board in Linkköping, Sweden.

Second, a subset of RA patients in the previously described Swedish Epidemiological Investigation of RA (EIRA) cohort (24) was used (n = 575), and 191 healthy subjects were used as

controls. RA in the patients in the EIRA cohort was diagnosed according to the ACR 1987 classification criteria (25). The study was approved by the Karolinska Institutet ethics review board. For additional information on the study subjects and methods used, see Supplementary Patients and Methods (available on the *Arthritis & Rheumatology* web site at http://onlinelibrary.wiley.com/doi/10.1002/art.40698/abstract).

Suspension bead array. In the serum samples obtained from RA patients, autoantibody responses were analyzed by Luminex immunoassay, as described previously (26). The median fluorescence intensity (MFI) was used to quantify the interaction of serum antibody with the given peptides.

Expression and purification of chimeric antibodies. The corresponding DNA fragments for the given antibodies were cloned into the vector pCEP4 (Life Technologies), and then the plasmids were cotransfected into Expi293F cells (Life Technologies) with FectoPRO DNA transfection reagent (Polyplus transfection). The chimeric antibody was purified using a 5-ml HiTrap Protein G HP affinity column (GE Healthcare Life Sciences) according to the manufacturer's instructions.

Preparation and purification of the chimeric E4 Fab fragment. The E4 Fab fragment was prepared using an ImmunoPure Fab Preparation Kit (Pierce) in accordance with the manufacturer's instructions. The Fab fragments for D10 and B10 were produced as described previously (27).* The Fab fragments used for crystallization were further purified by size-exclusion chromatography using a HiLoad 16/600 Superdex 200 column.

Crystallization, data collection, and structure determination. For the complexes, the Fab fragments in 20 mM Tris (pH 7.4)–20 mM NaCl were mixed with the cognate peptides in 2–3 times molar excess, before crystallization. Diffraction data were collected at the beamlines (specific data are provided in Supplementary Table 3, available on the *Arthritis & Rheumatology* web site at http://onlinelibrary.wiley.com/doi/10.1002/art.40698/abstract). The images were processed using XIA2 (28–30), and scaled using the Aimless application (31) from the Collaborative Computational Project 4 (CCP4) program suite (32).

The structure of the E4$_{Fab}$–CII-C-13 complex was determined by molecular replacement using Phaser crystallographic software (33). Iterative cycles of the manual model building were carried out using the Coot crystallographic object-oriented molecular graphics toolkit (34) and translation-libration-screw crystallographic refinement, as well as restrained refinement with Phenix or REFMAC5 software (35), until R-factors converged. All final models were found to have good stereochemistry, with >96% of the res-

---

*Correction added 28 January 2019 after online publication: Reference 27 has been retracted since the time of initial publication of this article.

idues located in the most favored regions of the Ramachandran plot (see Supplementary Table 3, http://onlinelibrary.wiley.com/doi/10.1002/art.40698/abstract). The Protein Interfaces, Surfaces and Assemblies service (available from the European Bioinformatics Institute at http://www.ebi.ac.uk/pdbe/prot_int/pistart.html) (36) was used to analyze molecular surfaces. The Contact application in the CCP4 suite (32) was used to analyze peptide interactions, and Phenix (37) was used for calculation of elbow angles. Structure comparisons and root mean square deviation (RMSD) calculations were performed with the secondary-structure matching tool (38) as implemented in the Coot program. Figures were prepared with PyMOL (39). The crystallographic coordinates and structure factors have been deposited in the Protein Data Bank (PDB accession codes are listed in Supplementary Table 3, http://onlinelibrary.wiley.com/doi/10.1002/art.40698/abstract).

Statistical analysis. The nonparametric Wilcoxon's rank sum test was applied for analysis of differences in MFI ratio values between RA patients and healthy controls. Reactivity of a peptide was considered positive if the MFI ratio was above a predefined MFI ratio threshold, defined as the median plus 5 times the median absolute deviation of that obtained in healthy control serum. All calculations were done in R software using several packages (40).

RESULTS

Generation and characterization of monoclonal ACPAs. To characterize the binding profiles of ACPAs, we focused on several reported monoclonal ACPAs (21,22,27,41) (a complete list is provided in Supplementary Table 1, available on the *Arthritis & Rheumatology* web site at http://onlinelibrary.wiley.com/doi/10.1002/art.40698/abstract). Two of these autoantibodies (namely, E4 and F3) had *N*-linked glycans in the variable domains that could modulate their binding profiles to citrullinated antigens (41,42). Therefore, these antibodies were produced in 2 formats: as a chimeric, nonglycosylated (NG) antibody, and as a chimeric, glycosylated (wild-type [WT]) antibody, by genetically fusing the constant regions (C_L and C_H) of mouse IgG2b to the variable regions (V_L and V_H) of human E4 or F3. The Fc-glycosylation patterns were comparable between E4 and F3, as determined by mass spectrometry (results in Supplementary Figure 1, available on the *Arthritis & Rheumatology* web site at http://onlinelibrary.wiley.com/doi/10.1002/art.40698/abstract).

For comparison, we also analyzed 2 other previously reported monoclonal ACPAs, designated D10 and B2. They were originally generated from joint-derived B cells of RA patients and were reported to bind to citrullinated peptides derived from α-enolase (CEP-1), fibrinogen, and vimentin (27). They were produced in the same mouse IgG2b–based chimeric format. In addition, we analyzed 2 ACPAs (ACC1 and ACC4) that were generated from mouse serum. These have been shown to be arthritogenic, based on findings of their cross-reactivity with triple helical CII (ACC1) or with a citrullinated peptide derived from CII (ACC4) (21,22).

To comprehensively map the breadth of reactivity of chimeric E4 and F3, a large set of 17-mer cyclic CII–derived arginine-containing peptides and the corresponding citrulline-containing peptides were synthesized (see Supplementary Table 2, available on the *Arthritis & Rheumatology* web site at http://onlinelibrary.wiley.com/doi/10.1002/art.40698/abstract) and examined by Luminex immunoassay. Commonly used citrullinated peptides derived from α-enolase (CEP-1), fibrinogen, vimentin, and filaggrin (CCP-1) were also included (43). A remarkable difference in reactivity was observed between the citrullinated peptides and the respective arginine-containing peptides (Figure 1A). Neither E4 nor F3 showed reactivity toward any arginine-containing peptides. However, both E4 and F3 recognized several citrullinated CII peptides (CII–C-13, CII–C-23, CII–C-38, CII–C-39, and CII–C-48) and CEP-1. The CII peptides CII–C-17, CII–C-27, CII–C-29, CII–C-49, and CII–C-54 and the Vim_{58-77} peptide were only recognized by E4, while the peptides CCP-1, Vim_{1-20}, and CII–C-51 were solely recognized by F3, suggesting that there are qualitative differences in cross-reactivity between E4 and F3. Notably, all of the CII-derived peptides recognized by both ACPAs contained a conserved Cit-Gly motif in their sequences. In addition, both the WT and NG forms of E4 and F3 showed subtle differences of binding strength/affinity against the same peptide. This is consistent with our previous observation that variable-domain glycosylation was able to modify the binding avidity to citrullinated antigens (42). In contrast, we did not observe binding of the other 2 monoclonal ACPAs (D10 and B2) to any constituent of the present peptide library (data not shown).

Furthermore, we measured the affinity of both E4 and F3 for CEP-1 by surface plasma resonance (SPR) imaging, using the corresponding arginine control peptide as a reference. Our findings revealed that E4 had a stronger affinity/avidity for CEP-1 (measured by the dissociation constant [K_d]; $K_d = 2.5 \times 10^{-7}M$ for E4 IgG, and $K_d = 2.3 \times 10^{-6}M$ for $E4_{Fab}$) when compared to F3 ($K_d = 3.5 \times 10^{-6}M$ for F3 IgG) (Figures 1B–D). Both D10 and B2 showed weak binding to CEP-1 ($K_d = 2.0 \times 10^{-5}M$ for $D10_{Fab}$, and $K_d = 1.0 \times 10^{-5}M$ for $B2_{Fab}$) in our SPR assay in which an empty reference channel was used, but the specificity for CEP-1 was totally abrogated when the arginine-containing control peptide was used as the reference channel (results in Supplementary Figure 2, available on the *Arthritis & Rheumatology* web site at http://onlinelibrary.wiley.com/doi/10.1002/art.40698/abstract), thus showing that neither D10 nor B2 is a citrulline-specific antibody.

In summary, compared to F3, E4 showed a broader range of reactivity toward citrullinated CII peptides, but the *N*-glycan in the antibody combining site did not affect its specificity. Thus, the nonglycosylated forms of E4 (E4NG) and F3 (F3NG) were chosen for more detailed analyses in the present study.

Overall structure of the E4 Fab and complex forms. To identify the structural determinants of citrulline specificity and epitope cross-reactivity of the ACPAs, we determined the crystal structures of the E4 Fab fragment complexed with 3 distinct citrullinated peptides (CII–C-13, CII–C-48, and CEP-1) selected from
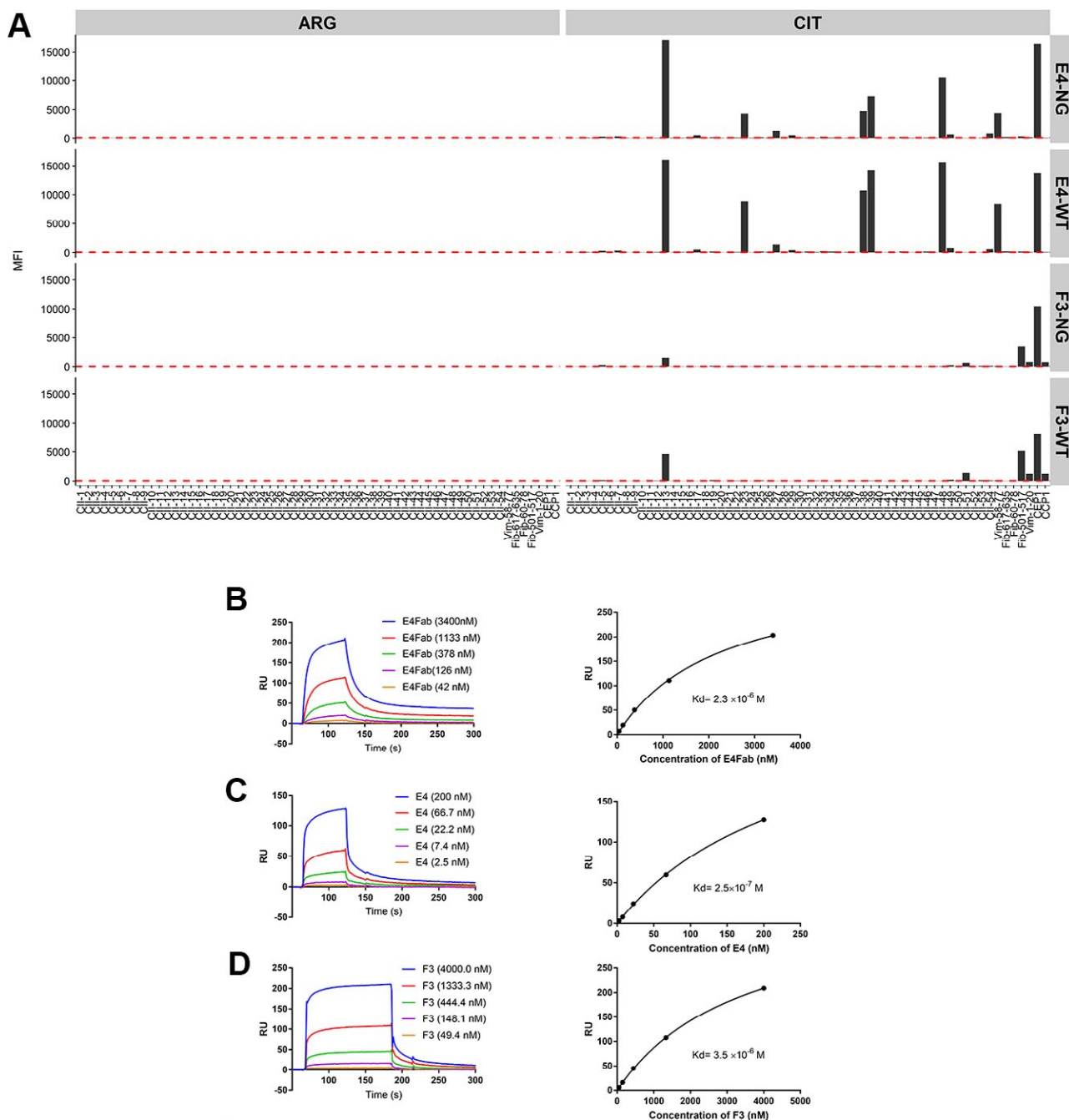
Figure 1. Reactivity of the E4 and F3 anti–citrullinated protein antibodies toward 17-mer cyclic citrullinated type II collagen (CII) peptides. **A,** Profiles of reactivity (measured as the mean fluorescence intensity [MFI]) of each peptide against 2 variants (glycosylated, wild-type [WT] or nonglycosylated [NG]) of E4 and F3 were analyzed in a Luminex immunoassay. A set of 108 cyclic 17-mer CII peptides (54 citrullinated and 54 corresponding unmodified peptides) covering the whole mature CII, with arginine (ARG) or citrulline (CIT) centered in the sequence, was designed and used in the assay. In addition, some other citrullinated peptides were also included. The broken red line indicates the threshold for positivity, defined as the mean plus 2 times the SD of MFI values obtained for all 54 unmodified peptides. **B–D,** The affinity of varying concentrations of the E4 Fab fragment (**B**), E4 IgG (**C**), or F3 IgG (**D**) for α-enolase peptide (CEP-1) (measured as the dissociation constant [K_d]) was determined by surface plasma resonance (SPR) analysis. The response units (RU) in the SPR sensorgrams represent the value obtained by subtraction of the CEP-1 channel from arginine analog channel results. Color figure can be viewed in the online issue, which is available at http://onlinelibrary.wiley.com/doi/10.1002/art.40698/abstract.

our peptide library, and for comparison, we also determined the crystal structures of E4$_{Fab}$ in an unbound state (Figure 2A). Peptides CII–C-13 ([1]CPAGEEGKXGARGEPGCA[18]) (X = the citrulline in these sequences) and CII–C-48 ([1]CEAGEPGEXGLKGHRGCA[18])

are derived from CII, whereas CEP-1 ([1]CKIHAXEIFDSXGNPT-VECK[20]) is a well-characterized peptide originating from α-enolase.

The crystallographic data collection and refinement parameters are summarized in Supplementary Table 3 (http://
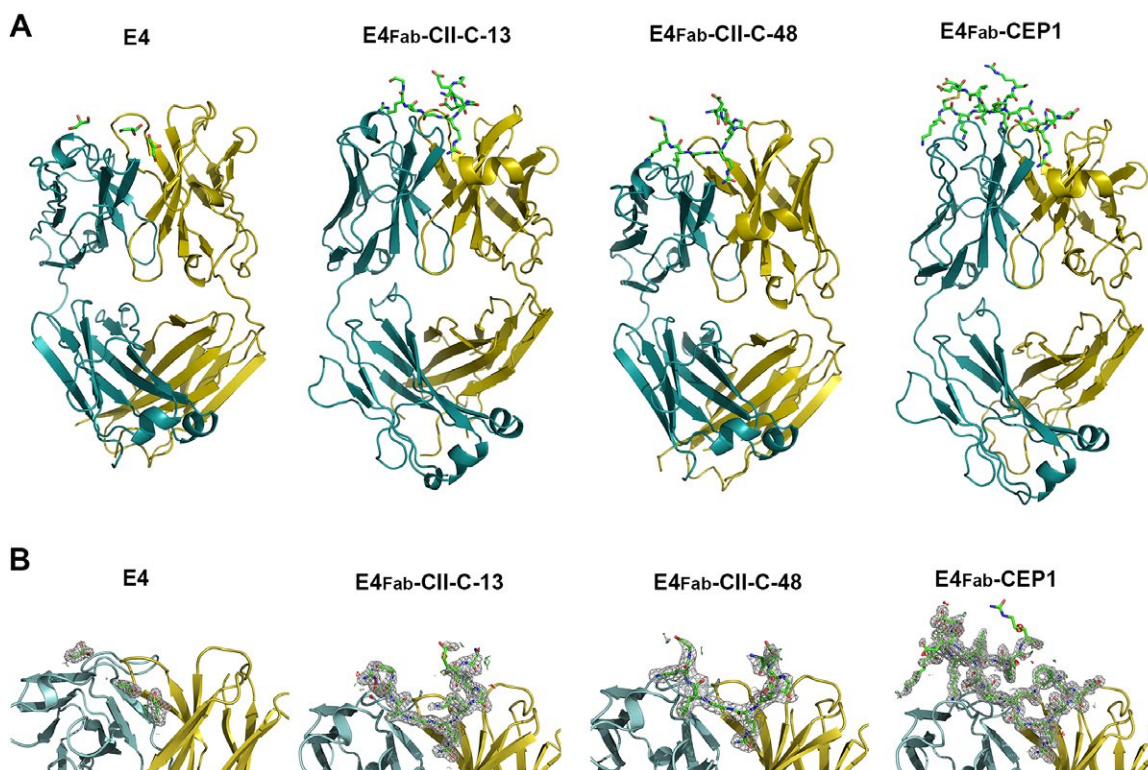
Figure 2. The crystal structures of E4$_{Fab}$ and its complexes. **A,** Overall structures of the E4$_{Fab}$, E4$_{Fab}$ in complex with type II collagen (CII) peptides (E4$_{Fab}$–CII-C-13 and E4$_{Fab}$–CII-C-48), and E4$_{Fab}$ in complex with α-enolase peptide (E4$_{Fab}$–CEP-1) are depicted, with light and heavy chains shown in blue and gold, respectively. The peptides bound to the E4$_{Fab}$ are shown as sticks with carbon, oxygen, nitrogen, and sulfur atoms colored green, red, blue, and yellow, respectively. **B,** The E4$_{Fab}$ paratope and electron density observed for the bound peptides and glycerol molecules are shown. The final 2F$_o$–F$_c$ electron density map (gray) is contoured at 1σ for a 2Å radius around the ligands. The F$_o$–F$_c$ map is contoured at 3σ (green) and −3σ (red). Color figure can be viewed in the online issue, which is available at http://onlinelibrary.wiley.com/doi/10.1002/art.40698/abstract.

onlinelibrary.wiley.com/doi/10.1002/art.40698/abstract). In 3 complex structures, the E4$_{Fab}$ adopted a characteristic Ig fold with clearly defined electron density. Peptides CII–C-13 and CII–C-48 were also well defined by electron density in the complexes, except for their terminal parts, which extended beyond the binding site. The entire CEP-1 peptide was clearly seen in the complex structure (Figure 2B). The Fab fragment in the complexes with CII–C-13 and CEP-1 contained the murine IgG2a constant region, whereas the E4 Fab fragment present in the crystals in the unbound state and in complex with CII–C-48 contained the murine IgG2b constant region.

Due to the differences in the constant region and/or the crystal lattice, the relative orientations of the variable and constant domains of the single E4$_{Fab}$ in these crystals (211° and 218° per asymmetric unit, respectively) deviated significantly from those observed for the E4$_{Fab}$ in the complexes with CII–C-13 and CEP-1 (149–150° per asymmetric unit) (results in Supplementary Figures 3A and B, available on the *Arthritis & Rheumatology* web site at http://onlinelibrary.wiley.com/doi/10.1002/art.40698/abstract). Pairwise superimposition of the individual (identical) constant and variable domains of all 4 structures resulted in RMSD values of 0.2–1.0Å (results in Supplementary Table 4, available on the *Arthritis & Rheumatology* web site at http://onlinelibrary.wiley.

com/doi/10.1002/art.40698/abstract). These findings indicate that the backbone conformational similarity was high.

Molecular determinants of citrulline recognition and cross-reactivity. The antigen-binding paratope was formed by the heavy (H)– and light (L)–chain variable domains involving all 6 complementarity-determining regions (CDRs), with the largest contributions coming from H3 and L1 (results in Supplementary Table 5, available on the *Arthritis & Rheumatology* web site at http://onlinelibrary.wiley.com/doi/10.1002/art.40698/abstract). It consisted of 2 narrow grooves that were connected at both ends, and in the middle it was separated by a ridge formed by H-G102 and H-S103 from CDR H3 and L-F33 of CDR L1, thus giving it an overall ring- or zero-like shape (Figure 3A). At one end of the "zero," the groove had a distinctly negative electrostatic potential, whereas the dominating features at the other end were an ~8Å deep pocket formed by H2 (H-W48, H-S51, H-Y59), H3 (H-I99, H-N105), and L3 (L-F99) residues, flanked by a hydrophobic patch and a patch of positive electrostatic potential (Figures 3A and B).

All 3 distinct peptide epitopes adopted a bent conformation to match the groove (Figure 2 and Supplementary Figure 3 [http://onlinelibrary.wiley.com/doi/10.1002/art.40698/abstract]). However, they showed identical conformations for the signature
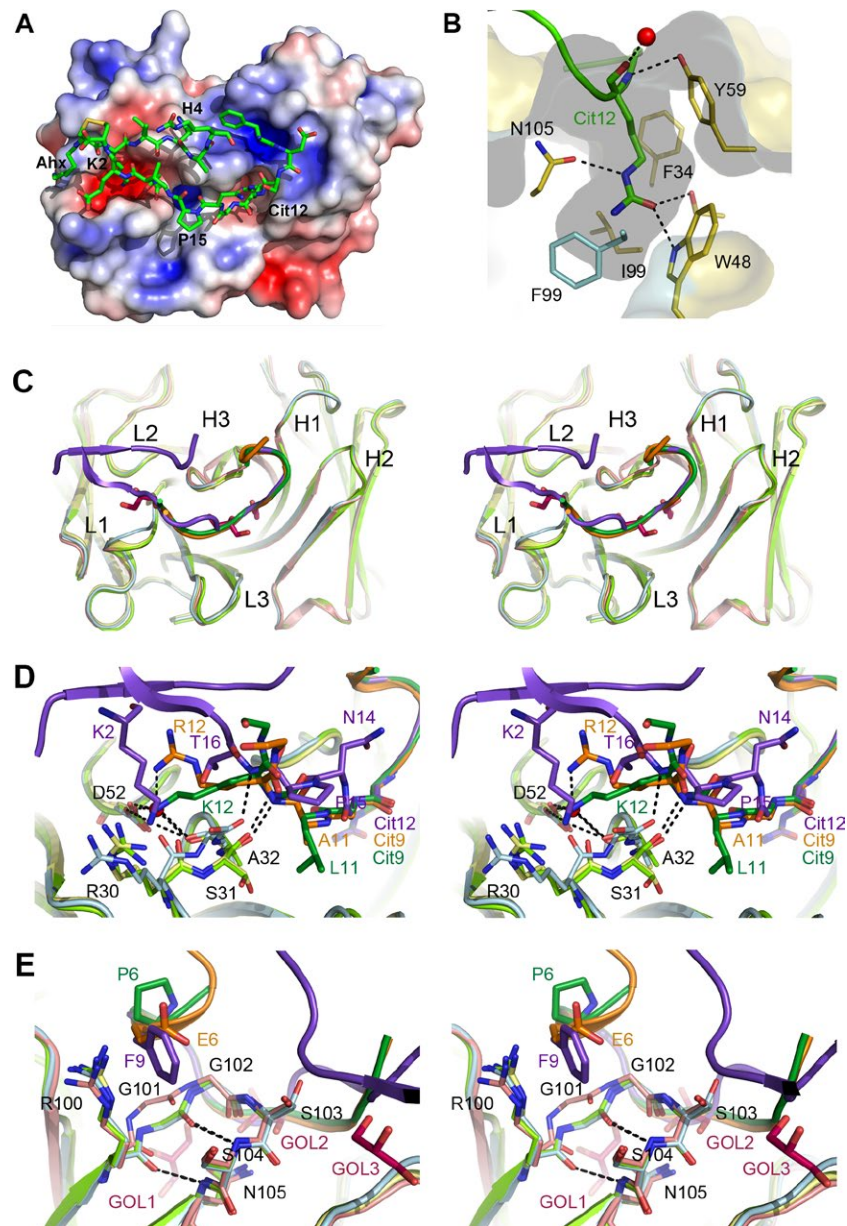
Figure 3. The E4$_{Fab}$ binding groove and superimposition of the crystal complexes. **A,** The shape and electrostatic surface potential of the E4$_{Fab}$ peptide-binding groove with the bound α-enolase peptide (CEP-1) are shown. Blue and red colors indicate areas of positive and negative surface potential, respectively. The peptide is shown as sticks. **B,** A magnified view of the citrulline binding pocket is shown. The heavy (H)–chain and light (L)–chain residues lining the pocket at a distance ≤3.8Å to the citrulline are shown as sticks with carbon atoms in blue and gold, respectively, according to heavy- or light-chain origin. The dimensions and shape of the pocket are outlined by the semitransparent molecular envelope of the E4$_{Fab}$. **C,** Stereochemistry views of the superimposed paratopes of the 4 E4$_{Fab}$ crystal structures are shown. The heavy and light chains of the E4$_{Fab}$ are shown in light blue (for the E4$_{Fab}$–CEP-1), yellow (for the type II collagen [CII] complex E4$_{Fab}$–CII–C-13), light green (for the E4$_{Fab}$–CII–C-48), and pink (for the E4$_{Fab}$-glycerol), whereas the bound ligands are depicted in purple (for CEP-1), orange (for CII–C-13), green (for CII–C-48), and darker magenta (for glycerol molecules). **D** and **E,** Magnified stereochemistry views of the L1 (**D**) and H3 (**E**) complementarity-determining region loops show larger structural deviations between the 4 E4$_{Fab}$ crystal structures. Hydrogen bonds are indicated by broken lines. GOL = glycerol. Color figure can be viewed in the online issue, which is available at http://onlinelibrary.wiley.com/doi/10.1002/art.40698/abstract.

Cit-Gly motif and the directly following residue, as well as the 3 preceding amino acids, with the long citrulline side chain being inserted into the deep pocket.

Superimposition of the variable domains of the E4$_{Fab}$–peptide complex revealed that the conformation of the CDR loops was almost identical, despite their binding to different peptide sequences (Figure 3C; see also Supplementary Table 5 and Supplementary Figure 3 [http://onlinelibrary.wiley.com/doi/10.1002/art.40698/abstract]). The only noteworthy exception was an adjustment of the L1 loop conformation at the L-S31 position in

the E4$_{Fab}$–CEP-1 complex (Figure 3D). Superimposition with the corresponding peptide-free structure revealed that the paratope was stably preformed in the absence of antigen, since peptide binding induced few and very modest changes in the CDR residue conformations (Figure 3E).

Citrulline recognition was largely mediated by formation of 3 hydrogen bonds to its side chain (Figure 3B), namely 1) between the oxygen atom of the ureido moiety and the hydroxyl group of

H-S51, as well as the amine nitrogen of H-W48, and 2) between 1 of the ureido group nitrogen atoms and the carboxamide oxygen of H-N105. Since this deep pocket is nonpolar, insertion of a charged side chain should be energetically disfavored, thereby explaining the strict selectivity for citrulline epitopes as compared to arginine-containing epitopes.

Furthermore, 3 direct and 2 water-mediated hydrogen bonds were found to be conserved in all 3 E4$_{Fab}$–peptide com-
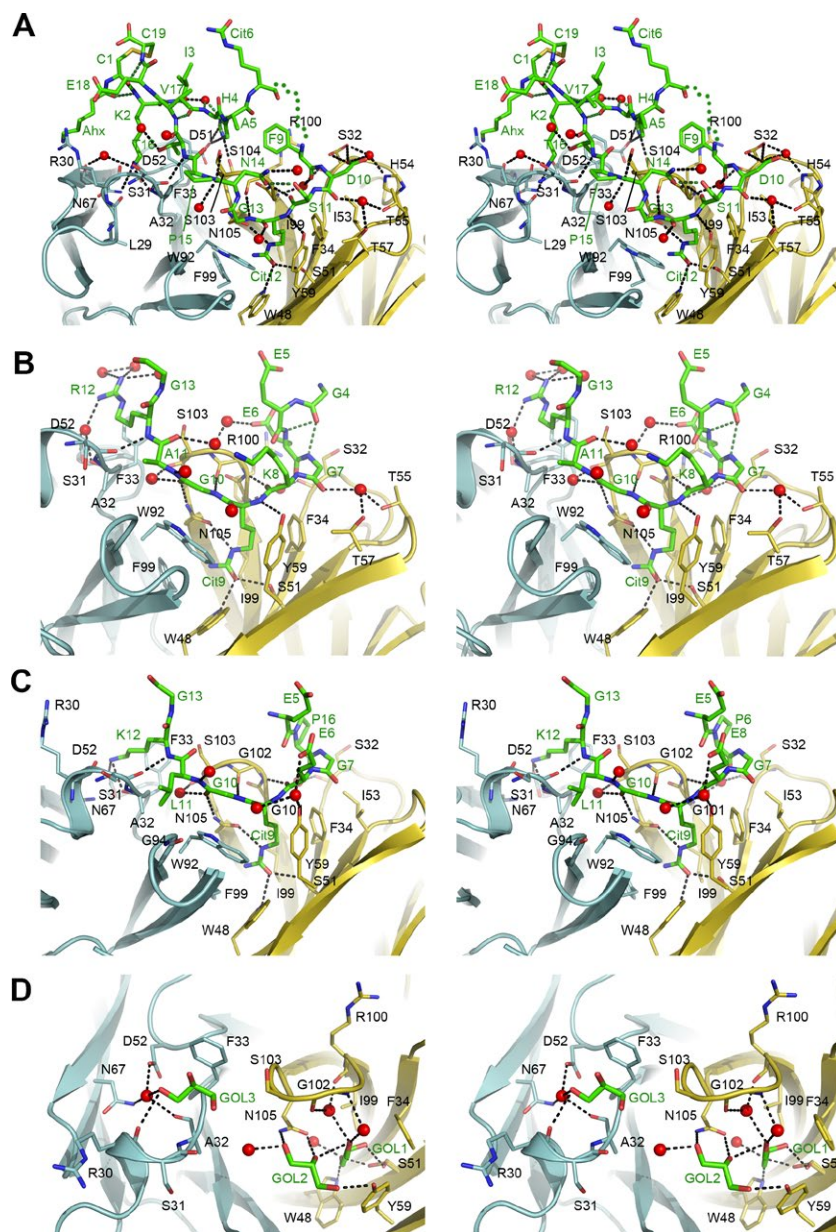
Figure 4. Stereochemistry views of the interactions of the E4$_{Fab}$ with bound ligands. The E4$_{Fab}$ heavy and light chains are shown in gold and blue, respectively. All residues within a 3.8Å radius to the bound ligands are represented as sticks with carbon atoms in the color of the chain they belong to and labels in black, whereas bound ligands are shown as sticks with carbon atoms and labels in green. Water molecules are depicted as red spheres, intrapeptide hydrogen bonds as broken lines in green, and other hydrogen bonds as broken lines in black. For the α-enolase peptide (CEP-1) complex E4$_{Fab}$–CEP-1, the approximate position of the 2 CEP-1 residues not resolved in electron density is indicated by a dotted line in green. **A–C,** The detailed polar interactions between E4$_{Fab}$ and bound ligands are shown for the E4$_{Fab}$–CEP-1 (**A**), and type II collagen (CII) complexes E4$_{Fab}$–CII-C-13 (**B**) and E4$_{Fab}$–CII-C-48 (**C**). **D,** Interactions of E4$_{Fab}$ with 3 glycerol (GOL) molecules bound to the paratope are shown. Color figure can be viewed in the online issue, which is available at http://onlinelibrary.wiley.com/doi/10.1002/art.40698/abstract.

plexes (Supplementary Table 5 [http://onlinelibrary.wiley.com/doi/10.1002/art.40698/abstract]). The citrulline interacted with the hydroxyl group of H-Y59, the Cit-Gly motif glycine, and the peptide residue preceding the citrulline, p(Cit-1). In addition, the citrulline interacted with both the backbone oxygen and nitrogen of H-G102, and the p(Cit-3) residue made water-mediated contacts to the backbone groups of both H-S32 and H-G101.

Several additional polar contacts were also observed, namely the hydrogen bonding of the Cit-Gly motif glycine to the carboxamide group of H-N105 (direct) and to the backbone oxygen of H-S103 (water-mediated) that was observed in the E4$_{Fab}$ complexes with CII–C-13 and CII–C-48, and the water-mediated hydrogen bonds between the p(Cit-2) and the hydroxyl groups of H-T55 and H-T57 that were observed in the CII–C-13 and CEP-1 complexes.

All of these polar interactions engaged peptide main-chain atoms. Therefore, they were not epitope sequence–specific, giving rise to the strong cross-reactivity of E4.

Based on our characterization of the 3 analyzed epitopes, CEP-1 binding showed several characteristic features not shared by the 2 CII-derived peptides. The entire CEP-1 sequence, except for pE7 and pI8, was well defined in electron density (Figure 2B). Both ends of the CEP-1 peptide were closely associated via 3 intrapeptide hydrogen bonds as well as a disulfide bridge (Figure 4A and Supplementary Figure 4, available on the *Arthritis & Rheumatology* web site at http://onlinelibrary.wiley.com/doi/10.1002/art.40698/abstract). Complex formation buried ~350Å^2, 265Å^2, and 690Å^2 of the E4 heavy chain, E4 light chain, and CEP-1 solvent-accessible surface areas, respectively (compared to the corresponding areas of 260Å^2, 180Å^2, and 510Å^2, respectively, for the complex with CII–C-13, and 265Å^2, 200Å^2, and 550Å^2, respectively, for the complex with CII–C-48). For CII–C-13 and CII–C-48, the electron density was observed only for residues 4-13 and 5-13, respectively (Figure 2B), with both N- and C-termini exiting the E4$_{Fab}$ paratope earlier than the corresponding CEP-1 residue. This could be attributed to differences in peptide-binding modes rather than to differences in crystal packing.

Both CII–C-13 and CII–C-48 contained a hydrophobic residue, a positively charged residue, and a glycine directly following the Cit-Gly motif (Figures 4B and C and Supplementary Figure 4 [http://onlinelibrary.wiley.com/doi/10.1002/art.40698/abstract]). The side chain of the hydrophobic residue (for CII–C-13, pA11; for CII–C-48, pL11) was inserted in a relatively nonpolar side extension of the main peptide-binding groove, whereas the long positively charged arginine (for CII–C-13) and lysine side chains (for CII–C-48) interacted with an area of negative electrostatic potential of the main groove, thus causing the exit of the p(Cit+4) glycine and all residues following from it. The positively charged p(Cit+3) side chains were hydrogen-bonded to the carboxyl group of L-D52 and the backbone oxygen of L-A32 in both the E4$_{Fab}$–CII–C-48 and E4$_{Fab}$–CII–C-13 complexes, although directly in the former and water-mediated in the latter.

The interactions between the E4 paratope and peptide antigen were dominated by the above-described polar contacts, as relatively few short-distance (<3.8Å) hydrophobic contacts were observed in all 3 complexes (Supplementary Table 5 [http://onlinelibrary.wiley.com/doi/10.1002/art.40698/abstract]). The primarily polar nature of the E4 paratope, providing numerous hydrogen bond donor and acceptor groups, was further highlighted by the observation of 3 glycerol molecules originating from the crystallization/cryoprotection solution in the peptide-binding groove of the antigen-free E4$_{Fab}$ crystal structure (Figure 4D and Supplementary Table 5).

Structural comparisons with other ACPAs. The crystal structures of 2 murine ACPAs, ACC1 (PDB accession code 5mu0) and ACC4 (PDB accession code 2w65) in complex with citrullinated peptides, have been reported previously (21,22). ACC1 is a highly arthritogenic antibody that targets the citrullinated C1 epitope on CII but also cross-reacts with several non-citrullinated epitopes on native CII, as well as with some classic citrullinated peptides such as CCP-2 and CCP-1. ACC4 is, on the other hand, specific for the citrullinated CII–C1 epitope in the non-native, single α-chain form. Interestingly, it enhanced arthritis severity when given concomitantly with another CII-specific antibody, M2139 (22). We also determined the crystal structures of the human antibodies B2 and D10, which were the first to be cloned from human RA serum and were reported to be specific for citrulline but cross-reactive with several citrullinated peptides (27). Both B2 and D10 were cocrystallized with full-length or truncated versions of CEP-1, but no electron density attributable to bound peptides was observed (Supplementary Figure 5). Furthermore, neither of them showed detectable affinity for a library of more than 150 citrullinated peptides in the binding assay. We could therefore conclude that these are not ACPAs.

Superimposition of the E4$_{Fab}$, ACC1$_{Fab}$, ACC4$_{Fab}$, B2$_{Fab}$, and D10$_{Fab}$ structures revealed significant differences in the size, shape, and properties of their paratopes. The ACC1 paratope is set apart from the others by being located in a deep, open-ended cleft between the heavy- and light-chain CDR that enables it to bind to a single α-chain of the CII epitope, most likely bulging out of a rigid triple-helical collagen structure (21) (Figures 5A–E). Citrulline-versus-arginine specificity is most likely imposed by the electrostatic properties of a nearby surface patch. In contrast, the ACC4 paratope is located in a smaller, enclosed groove, and the citrulline specificity is mediated by a network of hydrogen bonds to the ureido moiety.

Since the peptide specificities of B2$_{Fab}$ and D10$_{Fab}$ are unknown, the features of their peptide recognition could not be determined explicitly from the current forms of their unbound crystal structures. Notably, we did not observe a structurally similar binding pocket for an accommodating citrulline side chain in the paratopes of both B2$_{Fab}$ and D10$_{Fab}$ as that observed in the E4. This implies that they lack the structural determinants of specificity for citrulline.
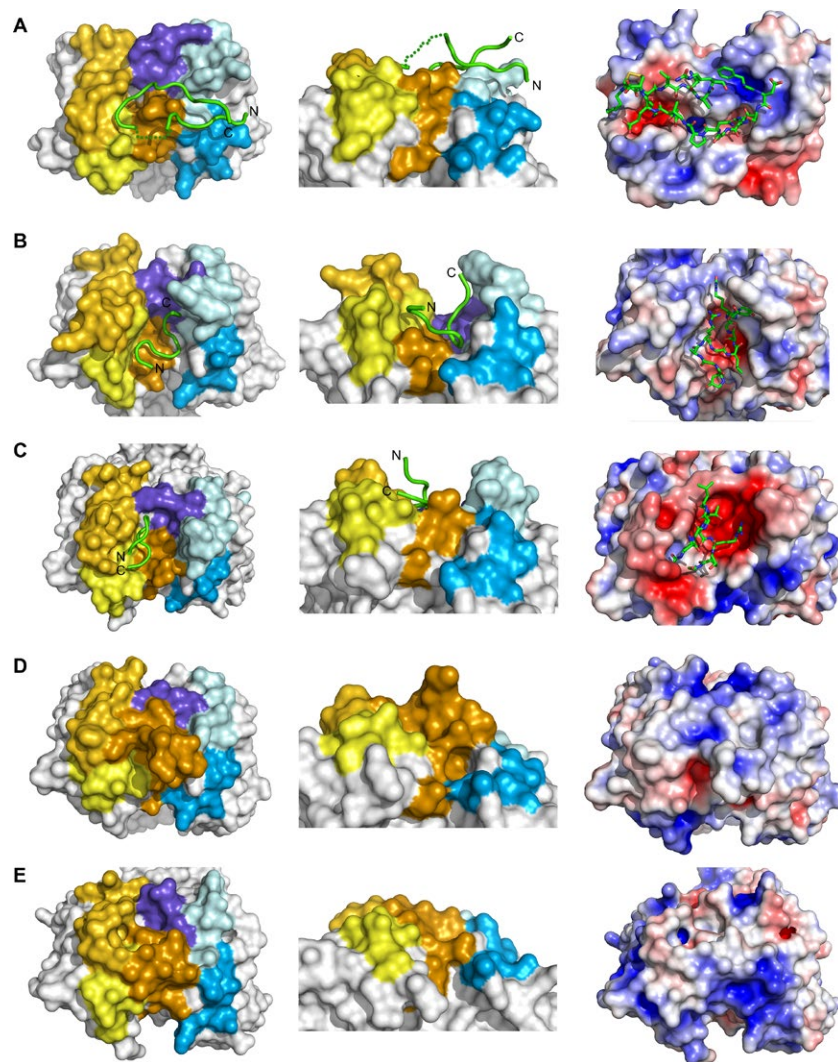
Figure 5. Comparison of the E4 paratope with the ACC1, ACC4, B2, and D10 paratopes. The molecular envelopes of the respective Fab fragments are shown. In the left panels (representing the top view) and middle panels (representing the side view), the H1, H2, and H3 complementarity-determining regions (CDRs) are shown in light blue, blue, and dark blue, respectively, and the L1, L2, and L3 CDRs are shown in yellow, bright orange, and dark orange, respectively. The remainder of the Fab fragment is shown in white. Bound peptides are shown in green; their N- and C-termini are indicated. The right panels show the molecular envelope, which is colored according to the electrostatic surface potential, and bound peptides are shown as sticks colored by atom, with carbon atoms in green. **A,** The α-enolase peptide (CEP-1) complex E4$_{Fab}$–CEP-1. The dotted green line indicates CEP-1 residues not resolved in electron density. **B,** ACC1$_{Fab}$–C1-Cit365-L (Protein Data Bank [PDB] accession code 5mu0). **C,** ACC4$_{Fab}$–C1-Cit1 (PDB accession code 2w65). **D,** B2$_{Fab}$. **E,** D10$_{Fab}$.

In summary, based on the crystal structures of the ACPAs in complex with citrullinated epitopes, we can conclude that citrulline specificity may be achieved in a manner that varies slightly, either by providing both a hydrogen-bonding partner group pattern selective for citrulline and electrostatic surface properties that bias against arginine, or by providing just the latter feature. However, no conserved feature regarding the shape of the citrulline-binding pocket can be expected.

Autoantibodies against E4-bound citrullinated peptides in RA. To evaluate the prevalence of the E4-bound citrullinated peptides in RA patients, we selected as potential targets the 3 representative citrullinated peptides that had been found

to cocrystallize with E4, and used a Luminex immunoassay to measure their autoantibody levels in 2 large cohorts of RA patients (the EIRA and TIRA-2 cohorts). In both cohorts, a statistically significant difference in antibody responses was clearly seen between healthy controls and RA patients, with regard to reactivity toward CEP-1, CII–C-13, and CII–C-48 (Figures 6A and B and Supplementary Table 6, available on the *Arthritis & Rheumatology* web site at http://onlinelibrary.wiley.com/doi/10.1002/art.40698/abstract). In ~46% of the RA patients in the EIRA cohort (and 51% of RA patients in TIRA-2), a response to citrullinated CII–C-13 was seen, which was comparable to the frequency of reactivity toward citrullinated CII–C-48 (40% of RA patients in EIRA, and 44% of RA patients in TIRA-2). The sen-
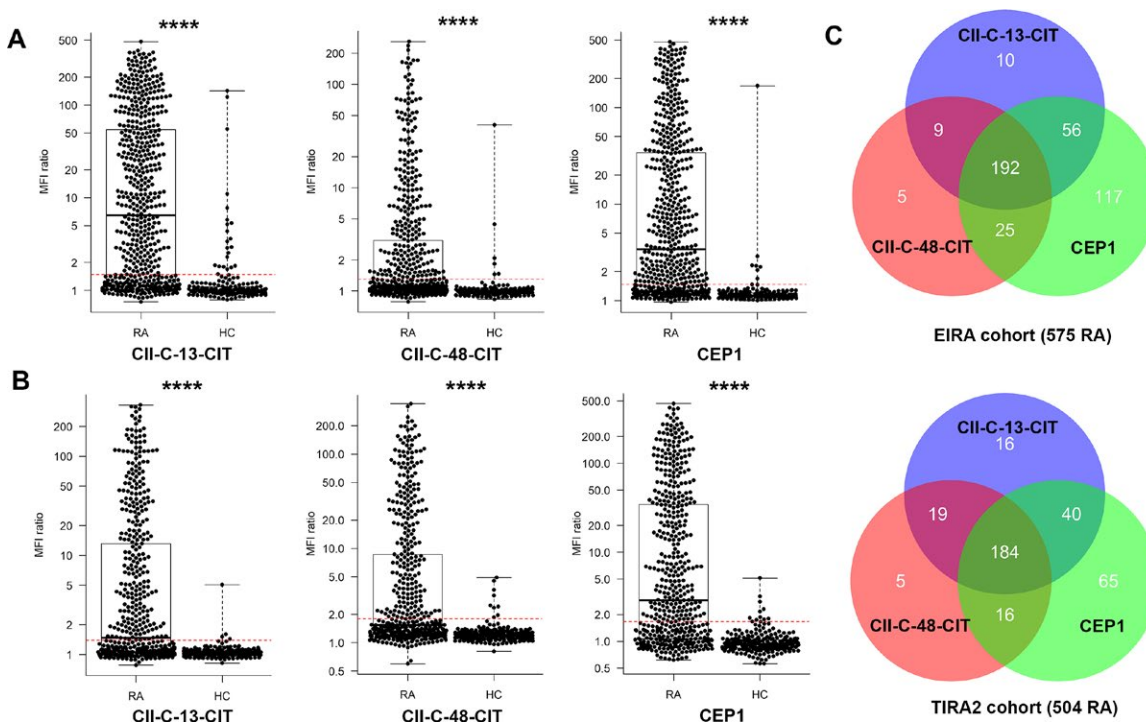
Figure 6. Autoantibody reactivity against type II collagen (CII) peptides CII-13 and CII-48, and α-enolase peptide (CEP-1). **A** and **B,** The antibody response to the given peptides in human serum samples from rheumatoid arthritis (RA) patients and healthy controls (HCs) in the Epidemiological Investigation of RA (EIRA) cohort (**A**) and the second Swedish Early Intervention in RA (TIRA2) cohort (**B**) was analyzed by Luminex immunoassay. The ratio (median fluorescence intensity [MFI] raw value divided by the MFI value for the 5 least-responsive cyclic arginine–containing peptides) was used to quantify the interaction of serum antibody with the given peptides. The red broken line indicates the cutoff for positivity (defined as the median + 5 times the median absolute deviation of that obtained in healthy control serum). Symbols represent individual subjects; horizontal lines with bars show the mean ± SD. **** = $P < 0.0001$ by Mann-Whitney U test. **C,** Venn diagrams show the overlapping autoantibody responses to CII–C–13, CII–C–48, and CEP-1 in RA patients in each cohort, as determined by Luminex immunoassay. Values in the diagrams represent the number of peptide-responsive patients. Color figure can be viewed in the online issue, which is available at http://onlinelibrary.wiley.com/doi/10.1002/art.40698/abstract.

sitivity for CEP-1 was higher than that for the 2 citrullinated CII peptides in both cohorts (68% of RA patients in EIRA, and 61% of RA patients in TIRA-2). In addition, in the serum from ~40% of RA patients in both cohorts, reactivity against all 3 citrullinated peptides was seen (Figure 6C), suggesting that a significant proportion of antibodies in patients with RA show a high degree of cross-reactivity.

DISCUSSION

We provide herein the first molecular characterization of the interactions between a human-derived ACPA and several citrullinated peptides, revealing the structural basis of the citrulline specificity and cross-reactivity of ACPAs, and explaining how both a promiscuous binding of citrullinated epitopes and a very high specificity of the citrulline side chain can be combined.

The crystal structures of the E4 ACPA bound to citrullinated peptides revealed conserved interactions with the citrulline residue. The citrulline is deeply inserted into a narrow pocket of the E4$_{Fab}$ paratope, where it is specifically recognized by the formation of 3 hydrogen bonds to its side chain. The nonpolar character of

this pocket biases against recognition of corresponding positively charged arginine. Almost all of the hydrogen-bonding interactions between the remaining epitope residues and the antibody CDR loops engaged peptide main-chain groups, allowing for extensive cross-reactivity.

Several studies showed that ACPA responses are highly cross-reactive toward citrullinated antigens, regardless of their origins (14,41,44,45). Consistent with these observations, the Luminex screening assay using a library of CCPs derived from CII and classic citrullinated peptides clearly showed that both E4 and F3 could recognize several peptides whose sequences were distinct except for the presence of a citrulline, strong preference for a glycine as the (Cit+1) residue, and the high frequency of Gly-X-Y repeats natively occurring in CII. Thus, the flanking residues of citrulline, in conjunction with specific recognition of the citrulline side chain, are most likely the determining factors in the reactivity of these ACPAs, rather than being attributable to a dependence on conserved amino acid sequence features.

The structures of E4$_{Fab}$ in both its antigen-free and peptide-bound forms provide valuable insights into the molecular mechanisms of antigen recognition. Peptide binding induced only minor

changes in the E4 paratope structure, which is largely preformed and relatively static. Thus, the significant cross-reactivity of E4 with epitopes that are very diverse in sequence appears not to be dependent on the flexibility/adjustability of the CDR loop conformation. By comparing the conformation of the 3 peptides bound to E4 in the crystals with their native forms (i.e., CII and α-enolase), we found that they indeed undergo substantial conformational rearrangements upon binding to E4. The fact that the peptide conformation is essential for autoantibody reactivity is a finding that has been observed previously (44,46,47).

E4 engages a key region (i.e., the 2–3 amino acids flanking the central citrulline residue on both sides) of the peptide that predominantly determines specificity but leaves the distal positions open to more diversity. Importantly, the primarily polar interactions involving peptide main-chain atoms could be identified as the major determinant of the cross-recognition of diverse citrullinated peptides by E4. Nevertheless, E4 or F3 still bound only to a subset of citrullinated peptides in our Luminex immunoassay. This indicates that the other physical characteristics of the peptide, such as neighboring residues flanking the citrulline, could influence the ACPA recognition that was previously investigated (48).

Characterization of the crystal structures of the E4$_{Fab}$–peptide complexes confirmed that the Cit-Gly motif is essential for recognition. It was reported that only the peptides containing the Cit-Gly motif showed significant antibody reactivity in the serum of RA patients, and that the substitution of glycine with residues harboring small side chains could reduce antibody reactivity (44,45,48). The preference for glycine at the (Cit+1) position is due to the steric hindrance imposed by the antibody residues at this position. In addition, the less spatial restriction due to the lack of a side chain allows glycine to occur frequently in the turn region of the polypeptide chain, which was seen for all 3 peptides in the crystal structures.

The same citrullinated peptides (CII–C-13, CII–C-48, and CEP-1) bound by monoclonal E4 in crystal complexes were also recognized by high titers of antibodies in 2 large well-characterized RA cohorts, thus confirming the clinical relevance of these peptides. As shown in Figure 6C, in the majority of RA patients, antibody reactivity to all 3 peptides was seen, suggesting that E4-like ACPAs are frequent in these patients. Notably, preferable binding to one particular peptide was seen in the RA serum, suggesting that nonoverlapping ACPAs are present. More importantly, the extensive intramolecular hydrogen bond formed by CEP-1, maintaining an overall favorable conformation for ACPA binding, leads to a higher sensitivity of CEP-1 compared to that of CII–C-13 and CII–C-48, both of which lack an intramolecular hydrogen bond. This corroborates the observation that the cyclic CEP-1 structure was fully visible in the crystal structures, while only one-half of the sequences from CII–C-13 and CII–C-48 were visualized.

In summary, we have provided a molecular explanation for the most significant antibody–antigen interactions associated with the development of RA. These findings may explain the promiscuous and specific recognition of citrullinated peptides by ACPAs.

AUTHOR CONTRIBUTIONS

All authors were involved in drafting the article or revising it critically for important intellectual content, and all authors approved the final version to be published. Dr. Holmdahl had full access to all of the data in the study and takes responsibility for the integrity of the data and the accuracy of the data analysis.

Study conception and design. Ge, Holmdahl.
Acquisition of data. Ge, Xu, Liang, Lönnblom, Lundström, Zubarev, Dobritzsch, Holmdahl.
Analysis and interpretation of data. Ge, Ayoglu, Nilsson, Skogh, Kastbom, Malmström, Klareskog, Toes, Rispens, Dobritzsch, Holmdahl.

REFERENCES

1. Steiner G, Smolen J. Autoantibodies in rheumatoid arthritis and their clinical significance. Arthritis Res 2002;4 Suppl 2:S1–5.

2. Schellekens GA, Visser H, de Jong BA, van den Hoogen FH, Hazes JM, Breedveld FC, et al. The diagnostic properties of rheumatoid arthritis antibodies recognizing a cyclic citrullinated peptide. Arthritis Rheum 2000;43:155–63.

3. Malmstrom V, Catrina AI, Klareskog L. The immunopathogenesis of seropositive rheumatoid arthritis: from triggering to targeting. Nat Rev Immunol 2017;17:60–75.

4. Waaler E. On the occurrence of a factor in human serum activating the specific agglutination of sheep blood corpuscles. APMIS 1940;17:172–88.

5. Aho K, Heliovaara M, Maatela J, Tuomi T, Palosuo T. Rheumatoid factors antedating clinical rheumatoid arthritis. J Rheumatol 1991;18:1282–4.

6. Aho K, Palosuo T, Heliovaara M, Knekt P, Alha P, von Essen R. Anti-filaggrin antibodies within "normal" range predict rheumatoid arthritis in a linear fashion. J Rheumatol 2000;27:2743–6.

7. Aletaha D, Neogi T, Silman AJ, Funovits J, Felson DT, Bingham CO III, et al. 2010 rheumatoid arthritis classification criteria: an American College of Rheumatology/European League Against Rheumatism collaborative initiative. Arthritis Rheum 2010;62:2569–81.

8. Van Gaalen FA, Linn-Rasker SP, van Venrooij WJ, de Jong BA, Breedveld FC, Verweij CL, et al. Autoantibodies to cyclic citrullinated peptides predict progression to rheumatoid arthritis in patients with undifferentiated arthritis: a prospective cohort study. Arthritis Rheum 2004;50:709–15.

9. Vossenaar ER, Despres N, Lapointe E, van der Heijden A, Lora M, Senshu T, et al. Rheumatoid arthritis specific anti-Sa antibodies target citrullinated vimentin. Arthritis Res Ther 2004;6:R142–50.

10. Lundberg K, Kinloch A, Fisher BA, Wegner N, Wait R, Charles P, et al. Antibodies to citrullinated α-enolase peptide 1 are specific for rheumatoid arthritis and cross-react with bacterial enolase. Arthritis Rheum 2008;58:3009–19.

11. Schellekens GA, de Jong BA, van den Hoogen FH, van de Putte LB, van Venrooij WJ. Citrulline is an essential constituent of antigenic determinants recognized by rheumatoid arthritis-specific autoantibodies. J Clin Invest 1998;101:273–81.

12. Takizawa Y, Suzuki A, Sawada T, Ohsaka M, Inoue T, Yamada R, et al. Citrullinated fibrinogen detected as a soluble citrullinated autoantigen in rheumatoid arthritis synovial fluids. Ann Rheum Dis 2006;65:1013–20.

13. Burkhardt H, Koller T, Engstrom A, Nandakumar KS, Turnay J, Kraetsch HG, et al. Epitope-specific recognition of type II collagen by rheumatoid arthritis antibodies is shared with recognition by antibodies that are arthritogenic in collagen-induced arthritis in the mouse. Arthritis Rheum 2002;46:2339–48.

14. Ioan-Facsinay A, el-Bannoudi H, Scherer HU, van der Woude D, Menard HA, Lora M, et al. Anti-cyclic citrullinated peptide antibodies are a collection of anti-citrullinated protein antibodies and contain overlapping and non-overlapping reactivities. Ann Rheum Dis 2011;70:188–93.

15. Wigerblad G, Bas DB, Fernades-Cerqueira C, Krishnamurthy A, Nandakumar KS, Rogoz K, et al. Autoantibodies to citrullinated proteins induce joint pain independent of inflammation via a chemokine-dependent mechanism. Ann Rheum Dis 2016;75:730–8.

16. Harre U, Georgess D, Bang H, Bozec A, Axmann R, Ossipova E, et al. Induction of osteoclastogenesis and bone loss by human autoantibodies against citrullinated vimentin. J Clin Invest 2012;122:1791–802.

17. Krishnamurthy A, Joshua V, Haj Hensvold A, Jin T, Sun M, Vivar N, et al. Identification of a novel chemokine-dependent molecular mechanism underlying rheumatoid arthritis-associated autoantibody-mediated bone loss. Ann Rheum Dis 2016;75:721–9.

18. Trouw LA, Haisma EM, Levarht EW, van der Woude D, Ioan-Facsinay A, Daha MR, et al. Anti–cyclic citrullinated peptide antibodies from rheumatoid arthritis patients activate complement via both the classical and alternative pathways. Arthritis Rheum 2009;60:1923–31.

19. Rombouts Y, Ewing E, van de Stadt LA, Selman MH, Trouw LA, Deelder AM, et al. Anti-citrullinated protein antibodies acquire a pro-inflammatory Fc glycosylation phenotype prior to the onset of rheumatoid arthritis. Ann Rheum Dis 2015;74:234–41.

20. Harre U, Lang SC, Pfeifle R, Rombouts Y, Fruhbeisser S, Amara K, et al. Glycosylation of immunoglobulin G determines osteoclast differentiation and bone loss. Nat Commun 2015;6:6651.

21. Ge C, Tong D, Liang B, Lonnblom E, Schneider N, Hagert C, et al. Anti-citrullinated protein antibodies cause arthritis by cross-reactivity to joint cartilage. JCI Insight 2017;2:e93688.

22. Uysal H, Bockermann R, Nandakumar KS, Sehnert B, Bajtner E, Engstrom A, et al. Structure and pathogenicity of antibodies specific for citrullinated collagen type II in experimental arthritis. J Exp Med 2009;206:449–62.

23. Svard A, Skogh T, Alfredsson L, Ilar A, Klareskog L, Bengtsson C, et al. Associations with smoking and shared epitope differ between IgA- and IgG-class antibodies to cyclic citrullinated peptides in early rheumatoid arthritis. Arthritis Rheumatol 2015;67:2032–7.

24. Stolt P, Bengtsson C, Nordmark B, Lindblad S, Lundberg I, Klareskog L, et al. Quantification of the influence of cigarette smoking on rheumatoid arthritis: results from a population based case-control study, using incident cases. Ann Rheum Dis 2003;62:835–41.

25. Arnett FC, Edworthy SM, Bloch DA, McShane DJ, Fries JF, Cooper NS, et al. The American Rheumatism Association 1987 revised criteria for the classification of rheumatoid arthritis. Arthritis Rheum 1988;31:315–24.

26. Ayoglu B, Szarka E, Huber K, Orosz A, Babos F, Magyar A, et al. Bead arrays for antibody and complement profiling reveal joint contribution of antibody isotypes to C3 deposition. PLoS One 2014;9:e96403.

27. Amara K, Steen J, Murray F, Morbach H, Fernandez-Rodriguez BM, Joshua V, et al. Monoclonal IgG antibodies generated from joint-derived B cells of RA patients have a strong bias toward citrullinated autoantigen recognition. J Exp Med 2013;210:445–55.

28. Winter G, Lobley CM, Prince SM. Decision making in xia2. Acta Crystallogr D Biol Crystallogr 2013;69:1260–73.

29. Sauter NK, Grosse-Kunstleve RW, Adams PD. Robust indexing for automatic data collection. J Appl Crystallogr 2004;37:399–409.

30. Evans P. Scaling and assessment of data quality. Acta Crystallogr D Biol Crystallogr 2006;62:72–82.

31. Evans PR, Murshudov GN. How good are my data and what is the resolution? Acta Crystallogr D Biol Crystallogr 2013;69:1204–14.

32. Collaborative Computational Project Number 4. The CCP4 suite: programs for protein crystallography. Acta Crystallogr D Biol Crystallogr 1994;50:760–3.

33. McCoy AJ, Grosse-Kunstleve RW, Adams PD, Winn MD, Storoni LC, Read RJ. Phaser crystallographic software. J Appl Crystallogr 2007;40:658–74.

34. Emsley P, Lohkamp B, Scott WG, Cowtan K. Features and development of Coot. Acta Crystallogr D Biol Crystallogr 2010;66:486–501.

35. Murshudov GN, Vagin AA, Dodson EJ. Refinement of macromolecular structures by the maximum-likelihood method. Acta Crystallogr D Biol Crystallogr 1997;53:240–55.

36. Krissinel E, Henrick K. Inference of macromolecular assemblies from crystalline state. J Mol Biol 2007;372:774–97.

37. Adams PD, Afonine PV, Bunkoczi G, Chen VB, Davis IW, Echols N, et al. PHENIX: a comprehensive Python-based system for macromolecular structure solution. Acta Crystallogr D Biol Crystallogr 2010;66:213–21.

38. Krissinel E, Henrick K. Secondary-structure matching (SSM), a new tool for fast protein structure alignment in three dimensions. Acta Crystallogr D Biol Crystallogr 2004;60:2256–68.

39. The PyMOL Molecular Graphics System, Version 1.8. New York: Schrodinger, LLC. 2015.

40. R Development Core Team. R: a language and environment for statistical computing. Vienna, Austria: R Foundation for Statistical Computing; 2017.

41. Van de Stadt LA, van Schouwenburg PA, Bryde S, Kruithof S, van Schaardenburg D, Hamann D, et al. Monoclonal anti-citrullinated protein antibodies selected on citrullinated fibrinogen have distinct targets with different cross-reactivity patterns. Rheumatology (Oxford) 2013;52:631–5.

42. Rombouts Y, Willemze A, van Beers JJ, Shi J, Kerkman PF, van Toorn L, et al. Extensive glycosylation of ACPA-IgG variable domains modulates binding to citrullinated antigens in rheumatoid arthritis. Ann Rheum Dis 2016;75:578–85.

43. Burska AN, Hunt L, Boissinot M, Strollo R, Ryan BJ, Vital E, et al. Autoantibodies to posttranslational modifications in rheumatoid arthritis. Mediat Inflamm 2014;2014:492873.

44. Trier NH, Leth ML, Hansen PR, Houen G. Cross-reactivity of a human IgG(1) anticitrullinated fibrinogen monoclonal antibody to a citrullinated profilaggrin peptide. Protein Sci 2012;21:1929–41.

45. Trier NH, Dam CE, Olsen DT, Hansen PR, Houen G. Contribution of peptide backbone to anti-citrullinated peptide antibody reactivity. PLoS One 2015;10:e0144707.

46. Trier NH, Holm BE, Slot O, Locht H, Lindegaard H, Svendsen A, et al. Physical characteristics of a citrullinated pro-filaggrin epitope recognized by anti-citrullinated protein antibodies in rheumatoid arthritis sera. PLoS One 2016;11:e0168542.

47. Nair DT, Singh K, Siddiqui Z, Nayak BP, Rao KV, Salunke DM. Epitope recognition by diverse antibodies suggests conformational convergence in an antibody response. J Immunol 2002;168:2371–82.

48. Dam CE, Houen G, Trier NH. The dependency on neighboring amino acids for reactivity of anti-citrullinated protein antibodies to citrullinated proteins. Scand J Clin Lab Invest 2016;76:417–25.

AMERICAN COLLEGE
OF RHEUMATOLOGY
EDUCATION · TREATMENT · RESEARCH

Role of Anti-Fractalkine Antibody in Suppression of Joint Destruction by Inhibiting Migration of Osteoclast Precursors to the Synovium in Experimental Arthritis

Kana Hoshino-Negishi,[1] Masayoshi Ohkuro,[2] Tomoya Nakatani,[1] Yoshikazu Kuboi,[1] Miyuki Nishimura,[1] Yoko Ida,[1] Jungo Kakuta,[1] Akiko Hamaguchi,[1] Minoru Kumai,[1] Tsutomu Kamisako,[1] Fumihiro Sugiyama,[3] Wataru Ikeda,[1] Naoto Ishii,[1] Nobuyuki Yasuda,[1] and Toshio Imai[1]

Objective. To elucidate the role of the fractalkine (FKN)/CX$_3$CR1 pathway in joint destruction in rheumatoid arthritis.

Methods. We examined the effect of treatment with anti–mouse FKN (anti-mFKN) monoclonal antibody (mAb) on joint destruction and the migration of osteoclast precursors (OCPs) into the joint, using the collagen-induced arthritis (CIA) model. DBA/1 mice were immunized with bovine type II collagen to induce arthritis, and then treated with anti-mFKN mAb. Disease severity was monitored by arthritis score, and joint destruction was evaluated by soft x-ray and histologic analyses. Plasma levels of joint destruction markers were assessed by enzyme-linked immunosorbent assay. FKN expression on endothelial cells was detected by immunohistochemistry. Bone marrow–derived OCPs were labeled with fluorescein and transferred to mice with CIA, and the migration of the OCPs to the joints was then analyzed.

Results. Both prophylactic and therapeutic treatment with anti-mFKN mAb significantly decreased the arthritis and soft x-ray scores. Plasma levels of cartilage oligomeric matrix protein and matrix metalloproteinase 3 decreased after treatment with anti-mFKN mAb. Histologic analysis revealed that anti-mFKN mAb inhibited synovitis, pannus formation, and cartilage destruction, as well as suppressed bone damage, with a marked reduction in the number of tartrate-resistant acid phosphatase–positive osteoclasts. Anti-mFKN mAb strongly inhibited the migration of bone marrow–derived OCPs into the affected synovium.

Conclusion. Anti-mFKN mAb notably ameliorates arthritis and joint destruction in the CIA model, as well as inhibits migration of OCPs into the synovium. These results suggest that inhibition of the FKN/CX$_3$CR1 pathway could be a novel strategy for treatment of both synovitis and joint destruction in rheumatoid arthritis.

INTRODUCTION

Rheumatoid arthritis (RA) is a chronic autoimmune disease that is characterized by synovitis, progressive bone erosion, and cartilage destruction. A hallmark of RA is the rapid recruitment of leukocytes to the site of inflammation. Additionally, patients with active RA exhibit elevated levels of activated peripheral leukocytes, especially monocyte/macrophages, which may contribute to the immunopathogenesis of RA (1). In addition, RA is exacerbated and perpetuated by proinflammatory cytokines, including tumor necrosis factor (TNF) and interleukin-6 (IL-6),

which are produced primarily by monocyte/macrophages and play a critical role in the pathogenesis of joint inflammation and destruction (2,3). Several biologic agents are widely used to relieve RA symptoms, and notable examples of these include anti-TNF agents. However, up to 30% of RA patients either do not respond to existing medications or must discontinue treatment, typically because of adverse effects or limited drug efficacy (4). Moreover, systemic suppression of TNF may be associated with the development of serious infections (5).

Chemokines and their receptors orchestrate tissue-specific and cell type–selective trafficking and retention of leukocytes (6).

[1]Kana Hoshino-Negishi, MS, Tomoya Nakatani, Yoshikazu Kuboi, MS, Miyuki Nishimura, AS, Yoko Ida, AS, Jungo Kakuta, MS, Akiko Hamaguchi, Minoru Kumai, Tsutomu Kamisako, BA, Wataru Ikeda, PhD, Naoto Ishii, PhD, Nobuyuki Yasuda, PhD, Toshio Imai, PhD: KAN Research Institute, Inc., Kobe, Japan; [2]Masayoshi Ohkuro, PhD: Tsukuba Research Laboratories, Eisai Company Ltd., Tsukuba, Japan; [3]Fumihiro Sugiyama, PhD: University of Tsukuba, Tsukuba, Japan.

Elevated levels of several chemokines have been detected in the synovial tissue and synovial fluid of RA patients (7). CX$_3$CL1/fractalkine (FKN) is a membrane-bound chemokine with a chemokine/mucin hybrid structure and a transmembrane domain (8). The unique structure of FKN allows it to work as an adhesion molecule when it is in the membrane-bound form, and as a chemoattractant when it is in the soluble form; transformation into the soluble form follows cleavage of FKN by ADAM-10 or ADAM-17 (9). FKN promotes extravasation of circulating leukocytes by binding to its receptor, CX$_3$CR1, through integrin-independent and -dependent mechanisms (10). Synovial fluid and serum FKN concentrations are increased in patients with RA, compared with osteoarthritis patients and healthy controls. In addition, serum FKN concentration correlates with disease severity in patients with RA (11).

Increased expression of FKN is exhibited in activated endothelial cells and fibroblasts in patients with RA, as well as in rat models of arthritis (12,13). CX$_3$CR1 is expressed on monocyte/macrophages, osteoclast precursors (OCPs), cultured RA fibroblast-like synoviocytes (FLS), effector CD4+ T cells and killer CD8+ T cells, and dendritic cells (DCs) (12–15). Multinucleated giant osteoclasts are bone-resorbing cells that differentiate from OCPs, which differentiate from the monocyte/macrophage lineage that is derived from bone marrow cells (16). RANKL, which is derived from osteoblasts and activated synovial fibroblasts, binds to RANK, its specific membrane-bound receptor, on OCPs/pre-osteoclasts, whereby OCPs/pre-osteoclasts begin differentiation into osteoclasts (17). FKN induces the migration of OCPs and monocyte/macrophages expressing CX$_3$CR1 positivity, as well as the differentiation of osteoclasts in vitro (15,18).

Therefore, the interaction between FKN and CX$_3$CR1 may play an important role in inflammation due to monocyte/macrophage infiltration and in the regulation of OCPs and their differentiation to osteoclasts. In a previous study, an anti-FKN–neutralizing monoclonal antibody (mAb) reduced the migration of inflammatory cells into the synovium in a bovine type II collagen–induced arthritis (CIA) mouse model in vivo (14). However, the precise mechanisms of the FKN/CX$_3$CR1 pathway in the pathology of RA, especially those of bone and cartilage destruction, have not yet been elucidated. In the present study, we investigated the role of the FKN/CX$_3$CR1 pathway in a mouse model of CIA using an anti–mouse FKN (anti-mFKN) mAb, with emphasis on the mechanism of joint destruction.

MATERIALS AND METHODS

Animals. All animal studies were approved by the Animal Ethics Committee at Eisai Company/KAN Research Institute and conducted in accordance with their Laboratory Animal Welfare guidelines. Male DBA/1 mice (5–6 weeks old) were obtained from Charles River Japan. Mice were reared within a Japan Health Sciences Foundation–accredited animal facility, and they were group-housed under controlled conditions with a constant temperature (23°C [± 3°C]) and humidity (55% [± 5%]), on a 12-hour light/dark cycle, with ad libitum access to water and standard pelleted food.

Antibodies and reagents. Monoclonal antibody against mFKN was generated from Armenian hamsters that were immunized with recombinant mFKN (R&D Systems) using a standard method at KAN Research Institute. The clone 5H8-4 was selected as an anti-mFKN–neutralizing mAb that was highly specific to mFKN, as determined by enzyme-linked immunosorbent assay (ELISA) with a panel of mouse chemokines, and by chemotaxis assay using mouse CX$_3$CR1 (mCX$_3$CR1)–expressing cells (14). Hamster IgG (used as a control) was generated from Armenian hamsters immunized with dinitrophenol (DNP). For flow cytometry, the clone L2D11 was selected as an anti-mCX$_3$CR1 mAb that was highly specific to mCX$_3$CR1 (Nishimura M, et al, unpublished observations). An isotype-matched control IgG was purchased from Jackson ImmunoResearch. For flow cytometry and immunohistochemical analysis, the following antibodies were used: Alexa Fluor 488–conjugated rat anti-mouse CD115 mAb (AFS98; BioLegend), allophycocyanin–Cy7–conjugated rat anti-mouse CD11b mAb (M1/70; eBioscience), rat anti-mouse RANK mAb (LOB14-8; Bio-Rad), goat anti-mFKN polyclonal antibody (pAb) (R&D Systems), rat anti-mouse CD31 mAb (390; BioLegend), and goat anti–cathepsin K pAb (Santa Cruz Biotechnology).

An Alexa Fluor 647 protein labeling kit was purchased from ThermoFisher Scientific for the labeling of goat anti–cathepsin K pAb. A Phycolink R-Phycoerythrin conjugation kit was purchased from ProZyme for the labeling of the anti-mCX$_3$CR1 mAb. To detect primary antibodies, secondary antibodies from Jackson ImmunoResearch were used. A mouse CD115 MicroBead kit was purchased from Miltenyi Biotec. A CellTrace 5,6-carboxyfluorescein succinimidyl ester (CFSE) cell proliferation kit (ThermoFisher Scientific) was used for cell labeling. For cell cultures, recombinant mouse macrophage colony-stimulating factor (M-CSF) and RANKL were purchased from R&D Systems; RPMI 1640 medium (ThermoFisher Scientific), fetal bovine serum (FBS; Nichirei Biosciences), 2-mercaptoethanol (2-ME), and sodium pyruvate (both from ThermoFisher Scientific) were also used for cell culture protocols.

Induction and assessment of CIA. Bovine type II collagen (Collagen Research Center) was dissolved in 0.05M acetic acid (3 mg/ml) and emulsified in an equal volume of Freund's complete adjuvant (Difco). Mice were immunized intracutaneously with 100 μl of the emulsion at the base of the tail. On day 21 postimmunization, the mice were boosted with the same amount of bovine type II collagen, emulsified in Freund's incomplete adjuvant (Difco). The progression of arthritis was

monitored continuously after the first immunization by assessing the arthritis score (defined as the sum of scores on a scale of 0–4 for all 4 limbs and based on the swelling of the limbs, for a total possible score of 16 for each mouse), using methods modified from those of Seeuws et al (19) and Huang et al (20). The arthritis score measured disease severity as follows: 0 = a normal joint, without inflammation or redness; 1 = redness and swelling in 1 digit; 2 = redness and swelling in 2 digits, or redness and mild swelling in the ankle and wrist joints; 3 = redness and swelling in >3 digits, or moderate swelling in the ankle and wrist joints and the paw; and 4 = severe swelling in the ankle and wrist joints and the paw. The arthritis score for each mouse was defined as the sum of the scores of all 4 feet.

Antibody treatment. In the prophylactic treatment study, 400 μg of hamster anti-mFKN mAb (clone 5H8-4) or control IgG (anti-DNP mAb) was administered intraperitoneally to 8–12 mice twice per week from the day of the first immunization. In the therapeutic treatment study, when the arthritis score had reached 1–3 (early arthritis) or 6–8 (severe arthritis), mice were randomly assigned to receive anti-mFKN mAb or control IgG (400 μg/mouse, 4–9 mice/group) intraperitoneally twice weekly.

Soft x-ray analysis. At the end point, mice were killed, and radiologic analysis of all 4 limbs was performed to determine the soft x-ray score for bones of the limb (scale 0–36 per mouse), which is the sum of 3 parameters (osteopenia, bone erosion, and new bone formation) on a scale of 0–3. This analysis was performed for all 4 limbs in a blinded manner using methods modified from a study by Inoue et al (21).

Measurement of plasma parameters. Plasma levels of cartilage oligomeric matrix protein (COMP; AnaMar AB) and matrix metalloproteinase 3 (MMP-3; R&D Systems) were assessed by ELISA, according to the instructions of the manufacturers.

Histologic analysis. At the end point of the animal study, mice were deeply anesthetized with isoflurane and perfused with phosphate buffered saline (PBS) and 1% paraformaldehyde in PBS. After perfusion, all 4 limbs were collected from each mouse and postfixed with 1% paraformaldehyde in PBS at 4°C for 24 hours. After the limbs were postfixed, they were washed with PBS and placed in 0.5*M* EDTA (Invitrogen) for 5 days to decalcify. The skin, muscles, and ligaments were peeled off the limbs, and the limb samples were cryoprotected in 10% and 20% sucrose in PBS, then embedded in Tissue-Tek OCT compound (Sakura Finetek). Cryosections were obtained by cutting OCT blocks of 10-μm thickness, using the method described by Kawamoto and Kawamoto (22) (type C9 film; Leica Microsystems). Frozen sections of the limb samples were then examined histologically. Samples were stained with 1 of the following: hematoxylin and eosin (H&E) solution; acid phosphatase, leukocyte (tartrate-

resistant acid phosphatase [TRAP]) kit (Sigma-Aldrich); or Alcian blue (AB)/alizarin red (AR). Using a BioRevo BZ-X710 microscope (Keyence), a constant view area of the joint, centered on the bone marrow cavity, was taken with a low-power field (10×, 20×). The number of TRAP+ cells per field was counted. TRAP+ cells were analyzed with NIS-Elements image analysis software (Nikon) in a blinded manner, using methods modified from those of Ono et al (23). The number of TRAP+ osteoclasts was averaged for all the joints in 1 limb of each animal. To evaluate cartilage and bone destruction, AB/AR staining was performed. The sections were incubated in 1% AB (AB staining kit, pH 2.5) (ScyTek). After the sections were rinsed with distilled water, they were incubated in 0.1% AR, pH 6.0 (Wako).

Histologic scoring. Histologic scores were obtained using H&E-stained sections (low-power field, 10×) and AB/AR-stained sections (low-power field, 20×) via NIS-Elements image analysis software. For histologic analysis of arthritis severity, scoring was performed in a blinded manner based on a previously described method (24). Sections were scored according to changes in synovitis (where 0 = no changes, 1 = >2 cell layers, 2 = >5 cell layers, and 3 = >5 cell layers, combined with pannus formation), changes in cartilage damage (where 0 = no changes, 1 = erosion in part of the cartilage surface, 2 = erosion of the cartilage surface and cartilage destruction, and 3 = cartilage erosion and destruction, combined with cartilage covered by connective tissue), and changes in bone destruction (where 0 = no changes, 1 = bone remodeling close to the joint capsule, 2 = bone remodeling in deeper locations, reaching the epiphyseal plate, and 3 = deep bone remodeling and bone degradation). In each category, joints were independently evaluated in a blinded manner. The synovitis score, cartilage score, and bone destruction score were averaged for all the joints in 1 limb of each animal.

Immunohistochemistry. For immunohistochemical analysis, sections were washed twice with 0.1% Triton X-100 in PBS and blocked in Block Ace (DS Pharma Biomedical) at room temperature for 1 hour. They were then incubated with primary antibodies at room temperature for 2 hours, followed by 3 washes with 0.1% Triton X-100 in PBS and incubation with the following secondary antibodies: fluorescein- or Cy3-conjugated anti-rabbit or anti-mouse IgG (Jackson ImmunoResearch). Sections were then incubated at room temperature for 1 hour, washed 3 times with 0.1% Triton X-100 in PBS, and mounted with Prolong Gold mounting medium (ThermoFisher Scientific). The prepared sections were analyzed by confocal laser microscopy (Nikon A1).

Preparation and characterization of OCPs for adoptive transfer. Bone marrow from normal DBA/1 mice was cultured in RPMI 1640 medium, containing 50 ng/ml M-CSF, 10% FBS, sodium pyruvate, and 2-ME for 2 days (25). CD11b, CD115, RANK, and

CX$_3$CR1 expression levels on adherent cells were analyzed by flow cytometry, based on a previously described method (26). Adherent cells were purified using a CD115 MicroBead Kit (Miltenyi Biotec). A CellTrace CFSE cell proliferation kit (10 μM; ThermoFisher Scientific) was used to label CD115+ cells according to the instructions of the manufacturer, thereby generating CFSE-labeled cells. These CFSE-labeled cells were cultured in RPMI 1640 medium containing 10 ng/ml M-CSF, 25 ng/ml RANKL, 10% FBS, sodium pyruvate, and 2-ME for 5–6 days; the cells were then stained using an acid phosphatase, leukocyte (TRAP) kit.

Analysis of the migration of adoptively transferred OCPs into the synovium in mice with CIA. Recipient mice with CIA were injected intraperitoneally with 400 μg of anti-mFKN mAb or control IgG 24 hours and 2 hours before cell transfer. CFSE-labeled OCPs (5 × 10^5) were injected intravenously into the mice. One hour or 24 hours after cell transfer, the limbs of the mice were collected. The number of CFSE+ cells in the synovium, or the positive area of CFSE+ cells in the cathepsin K+ area within the joint, was quantified with NIS-Elements image analysis software, and the number of CFSE+ cells and the ratio (CFSE+ area to cathepsin K+ area) were calculated, based on a modification of a previously described method (27). A total of 7–8 slides from each mouse (n = 7–8 mice) were independently evaluated in a blinded manner.

Statistical analysis. Data were expressed as the mean ± SEM. For statistical analysis, the nonparametric Kruskal-Wallis test was performed, followed by the Mann-Whitney U test. P values less than 0.05 were considered significant. Statistical analyses were performed using GraphPad Prism software, version 6.02 (see Supplementary Materials and Methods, available on the Arthritis & Rheumatology web site at http://onlinelibrary.wiley.com/doi/10.1002/art.40688/abstract).

RESULTS

Effects of prophylactic treatment with anti-mFKN mAb. Prophylactic treatment with anti-mFKN mAb significantly suppressed the progression of CIA, as demonstrated by decreases in the arthritis score and as compared with the joints of mice treated with control IgG (Figures 1A and E). Administration of anti-mFKN mAb significantly reduced bone destruction compared with control IgG, as determined by soft x-ray analysis (Figure 1B). Plasma levels of COMP, a marker of cartilage destruction, and MMP-3, a marker that reflects synovitis
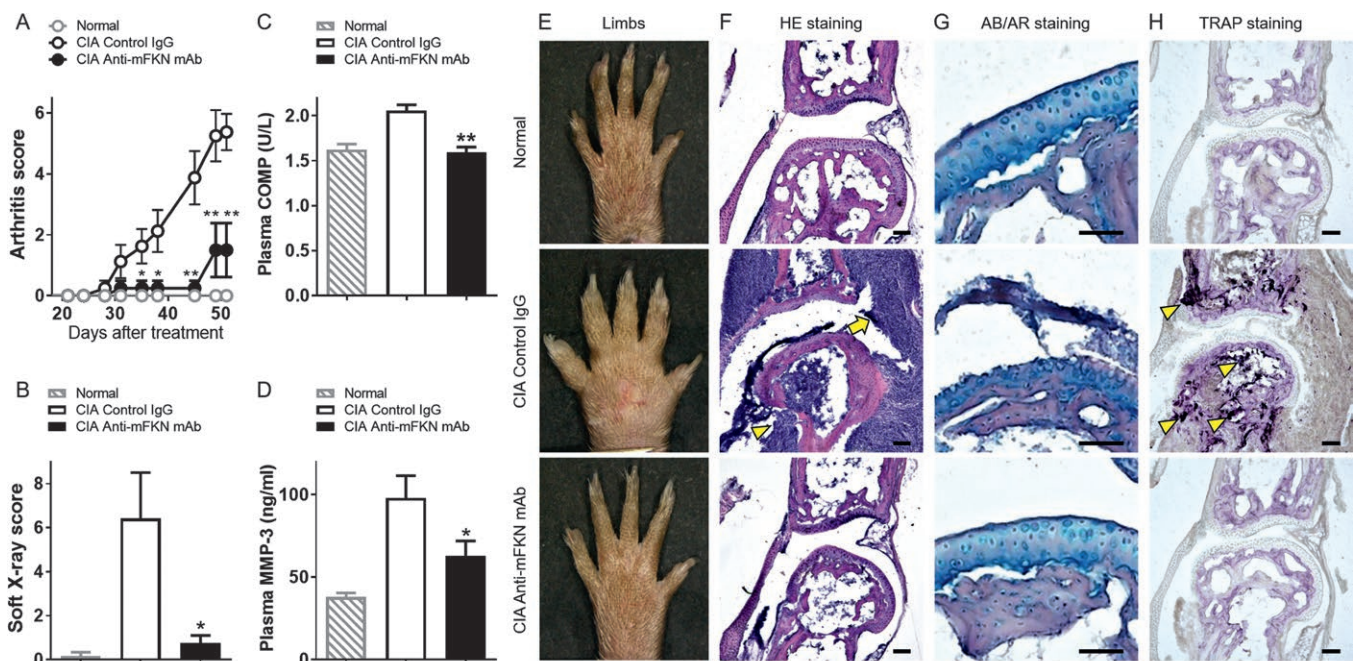
Figure 1. Results of prophylactic treatment with anti–mouse fractalkine (anti-mFKN) monoclonal antibody (mAb) in mice with collagen-induced arthritis (CIA). **A–D**, Arthritis score (**A**), soft x-ray score (**B**), plasma level of cartilage oligomeric matrix protein (COMP) (**C**), and plasma level of matrix metalloproteinase 3 (MMP-3) (**D**) in normal mice, control IgG–treated mice with CIA, or anti-mFKN mAb–treated mice with CIA (n = 6–12 mice in each group). Values are the mean ± SEM. * = $P < 0.05$; ** = $P < 0.01$ versus control IgG–treated mice with CIA. **E–H**, Stereomicroscopic images of mouse limbs (**E**), hematoxylin and eosin (H&E) staining of joints showing pannus (**arrowhead**) and synovitis (**arrow**) (**F**), Alcian blue (AB)/alizarin red (AR) staining of joints (**G**), and tartrate-resistant acid phosphatase (TRAP) staining of joints (**H**), with **arrowheads** indicating TRAP+ cells. Representative images of the joints of normal mice (top), control IgG–treated mice with CIA (middle), or anti-mFKN mAb–treated mice with CIA (bottom) are shown. Bars = 100 μm (**F** and **H)** or 50 μm (**G**).
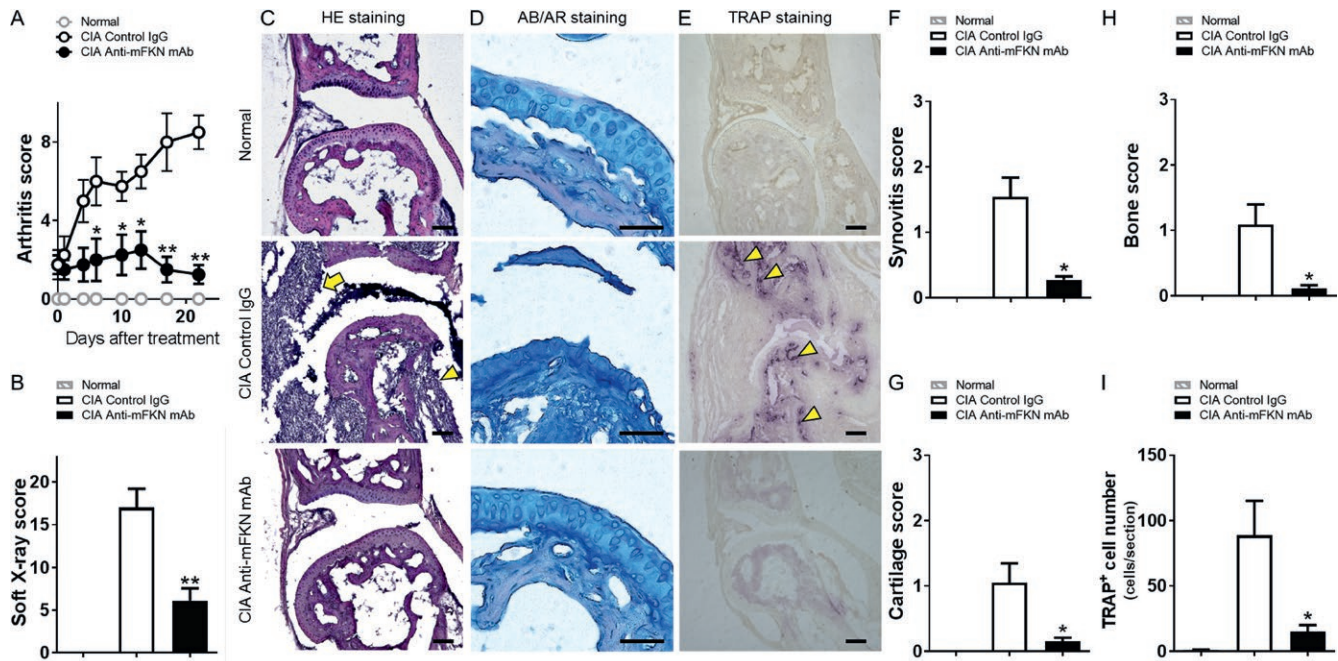
Figure 2. Results of therapeutic treatment with anti–mouse fractalkine (anti-mFKN) monoclonal antibody (mAb), starting after collagen-induced arthritis (CIA) onset. **A** and **B**, Arthritis score (**A**) and soft x-ray score (**B**) in normal mice, control IgG–treated mice with CIA, or anti-mFKN mAb–treated mice with CIA (n = 4–9 mice in each group). Values are the mean ± SEM. **C–E**, Representative images of the joints of normal mice (top), control IgG–treated mice with CIA (middle), or anti-mFKN mAb–treated mice with CIA (bottom). Hematoxylin and eosin (H&E) staining of joints (**C**) (**arrowhead** indicates pannus, **arrow** indicates synovitis), Alcian blue (AB)/alizarin red (AR) staining of joints (**D**), and tartrate-resistant acid phosphatase (TRAP) staining of joints (**E**) (**arrowheads** indicate TRAP+ cells) are shown. Bars = 100 μm (**C** and **E**) or 50 μm (**D**). **F–I**, Calculated scores for synovitis (**F**), cartilage destruction (**G**), bone damage (**H**), and number of TRAP+ cells in a section of joints (**I**) of normal mice, control IgG–treated mice with CIA, or anti-mFKN mAb–treated mice with CIA (n = 4 mice in each group). Values are the mean ± SEM. * = $P < 0.05$; ** = $P < 0.01$ versus control IgG–treated mice with CIA.

and cartilage destruction, were also significantly reduced in the anti-mFKN mAb–treated group compared with the control IgG–treated group (Figures 1C and D). At the joint, gene expression levels of TNF and IL-6, markers that reflect local inflammation, were significantly reduced in the anti-mFKN mAb–treated group compared with the control IgG–treated group (see Supplementary Figure 1, available on the *Arthritis & Rheumatology* web site at http://onlinelibrary.wiley.com/doi/10.1002/art.40688/abstract).

To more accurately evaluate the extent of joint destruction, pathologic analyses were performed. Histologic analysis by H&E staining revealed that synovitis and pannus formation, which were not seen in the normal mice, were present in control IgG–treated mice (Figure 1F). Conversely, these same symptoms were suppressed in anti-mFKN mAb–treated mice. Cartilage was also degraded in control IgG–treated mice compared with normal mice; however, mice that were treated with the anti-mFKN mAb retained cartilage and rarely exhibited destruction (Figure 1G). Furthermore, TRAP+ osteoclasts were rarely detected in the joints of normal mice, whereas a large number of TRAP+ osteoclasts were detected in the joints of control IgG–treated mice (Figure 1H). In contrast, TRAP+ osteoclasts were rarely detected in the joints of anti-mFKN mAb–treated mice.

Effects of therapeutic treatment with anti-mFKN mAb. To mimic therapeutic intervention in human patients with RA, anti-mFKN mAb was administered after the onset of arthritis. Therapeutic treatment with anti-mFKN mAb significantly decreased the arthritis score (Figure 2A) and soft x-ray score (Figure 2B) compared with treatment with control IgG. In affected joints, histologic analysis revealed that synovitis and pannus formation were inhibited in anti-mFKN mAb–treated mice compared with control IgG–treated mice (Figure 2C). Cartilage was also degraded in control IgG–treated mice compared with normal mice; however, mice that were treated with anti-mFKN mAb retained cartilage and rarely exhibited destruction (Figure 2D). TRAP+ osteoclasts were scarce in the joints of normal mice, whereas a large number of TRAP+ osteoclasts were detected in the joints of control IgG–treated mice. In contrast, TRAP+ osteoclasts were rarely detected in the joints of anti-mFKN mAb–treated mice (Figure 2E). Furthermore, synovitis, cartilage, and bone destruction scores were all significantly reduced in the anti-mFKN mAb–treated group compared with the control IgG–treated group (Figures 2F–H). Quantitative analysis showed that the reduction in the number of TRAP+ osteoclasts in the joints of mice in the anti-mFKN mAb–treated group compared with mice in the control IgG–treated group was statistically significant (Figure 2I).
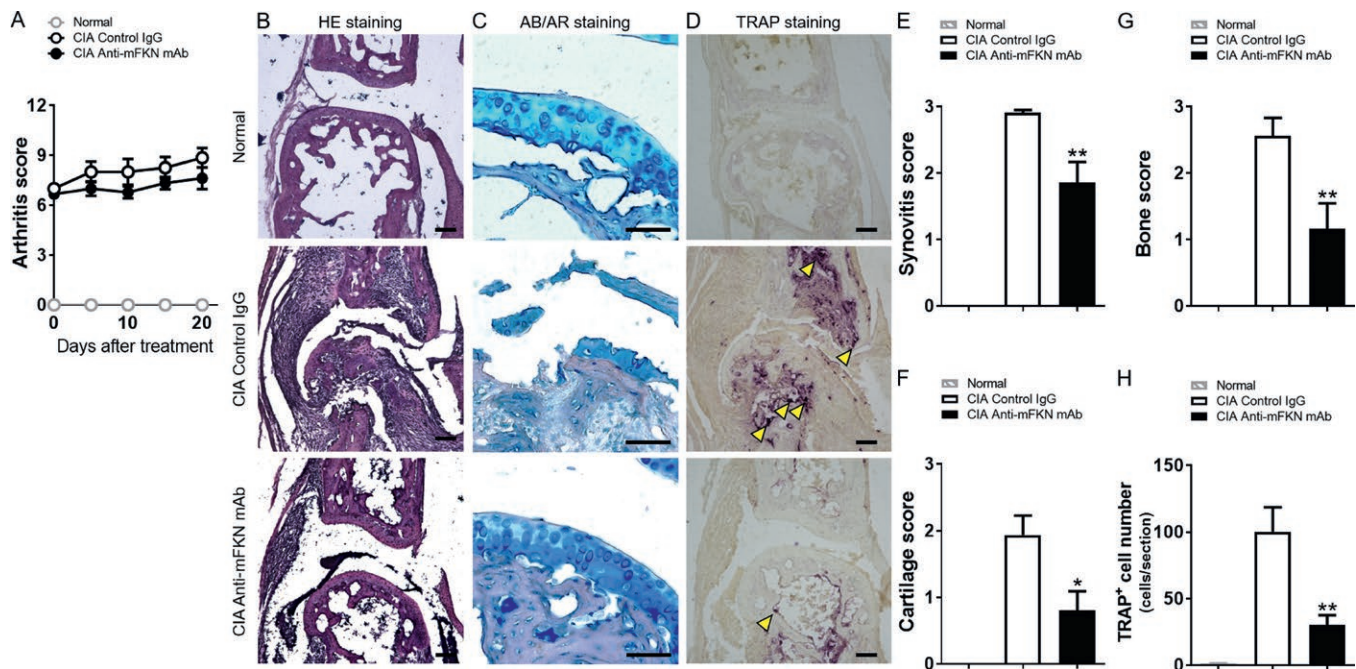
Figure 3. Results of therapeutic treatment with anti–mouse fractalkine (anti-mFKN) monoclonal antibody (mAb), starting after the arthritis score had reached 6–8. **A**, Arthritis score in normal mice, control IgG–treated mice with collagen-induced arthritis (CIA), or anti-mFKN mAb–treated mice with CIA (n = 8–9 mice in each group). Values are the mean ± SEM. **B–D**, Representative images of the joints of normal mice (top), control IgG–treated mice with CIA (middle), or anti-mFKN mAb–treated mice with CIA (bottom). Hematoxylin and eosin (H&E) staining of joints (**B**), Alcian blue (AB)/alizarin red (AR) staining of joints (**C**), and tartrate-resistant acid phosphatase (TRAP) staining of joints (**D**) (**arrowheads** indicate TRAP+ cells) are shown. Bars = 100 μm (**B** and **D**) or 50 μm (**C**). **E–H**, Calculated scores of synovitis (**E**), cartilage destruction (**F**), bone damage (**G**), and the number of TRAP+ cells in a section of joints (**H**) of normal mice, control IgG–treated mice with CIA, or anti-mFKN mAb–treated mice with CIA (n = 4–9 mice in each group). * = $P < 0.05$; ** = $P < 0.01$ versus control IgG–treated mice with CIA.

We next examined the effect of therapeutic treatment with anti-mFKN mAb on severe CIA. Anti-mFKN mAb did not decrease the arthritis score (Figure 3A). However, histologic analysis revealed that synovitis, cartilage destruction, and bone damage were clearly inhibited in anti-mFKN mAb–treated mice compared with control IgG–treated mice (Figures 3B–D). Additionally, the synovitis, cartilage, and bone destruction scores all decreased significantly in the anti-mFKN mAb–treated group compared with the control IgG–treated group (Figures 3E–G), and the number of TRAP+ osteoclasts was significantly reduced in the joints of mice in the anti-mFKN mAb–treated group compared with joints of mice in the control IgG–treated group (Figure 3H). Taken together, these results indicate that anti-mFKN mAb suppressed the destruction of the affected joints, irrespective of edema as evaluated by the arthritis score.

Effects of anti-mFKN mAb on OCP migration into the synovium of mice with CIA. Although FKN was scarcely detected on synovial vascular endothelial cells in normal mice (Figures 4A and B), it was expressed on a portion of synovial vascular endothelial cells in mice with CIA (Figures 4C and D). Bone marrow–derived cells were cultured with M-CSF, and flow cytometry revealed that these CD11b^{high}CD115+ cells co-

expressed RANK and CX$_3$CR1 (Figure 5A). Furthermore, after being purified with anti-CD115 mAb, CD115+ cells differentiated into TRAP+ multinucleated osteoclasts when cultured with M-CSF and RANKL in vitro (Figure 5B). Thus, we confirmed that bone marrow–derived CD11b^{high}CD115+RANK+CX$_3$CR1+ cells exhibit characteristics of OCPs. CFSE-labeled OCPs migrated into the synovium of control IgG–treated mice after 1 hour of transfer. In contrast, migration of these cells was strongly inhibited in anti-mFKN mAb–treated mice (Figures 5C and E). In addition, 24 hours after CFSE-labeled OCPs were transferred to control IgG–treated mice with CIA, these cells were positive for cathepsin K and became multinuclear osteoclasts in the joints. Conversely, cathepsin K+CFSE+ osteoclasts were rarely observed in joints of mice with CIA that were treated with anti-mFKN mAb (Figures 5D and F and Supplementary Figure 2, available on the *Arthritis & Rheumatology* web site at http://onlinelibrary. wiley.com/doi/10.1002/art.40688/abstract). In order to rule out other potential pathways involved in this mechanism of action, we tested whether OCPs derived from CX$_3$CR1–knockout (KO) mice migrate into the synovium. We found reduced migration of CX$_3$CR1–KO mice–derived OCPs into the synovium, compared with OCPs derived from wild-type mice (Supplementary Figure 3, http://onlinelibrary.wiley.com/doi/10.1002/art.40688/abstract).
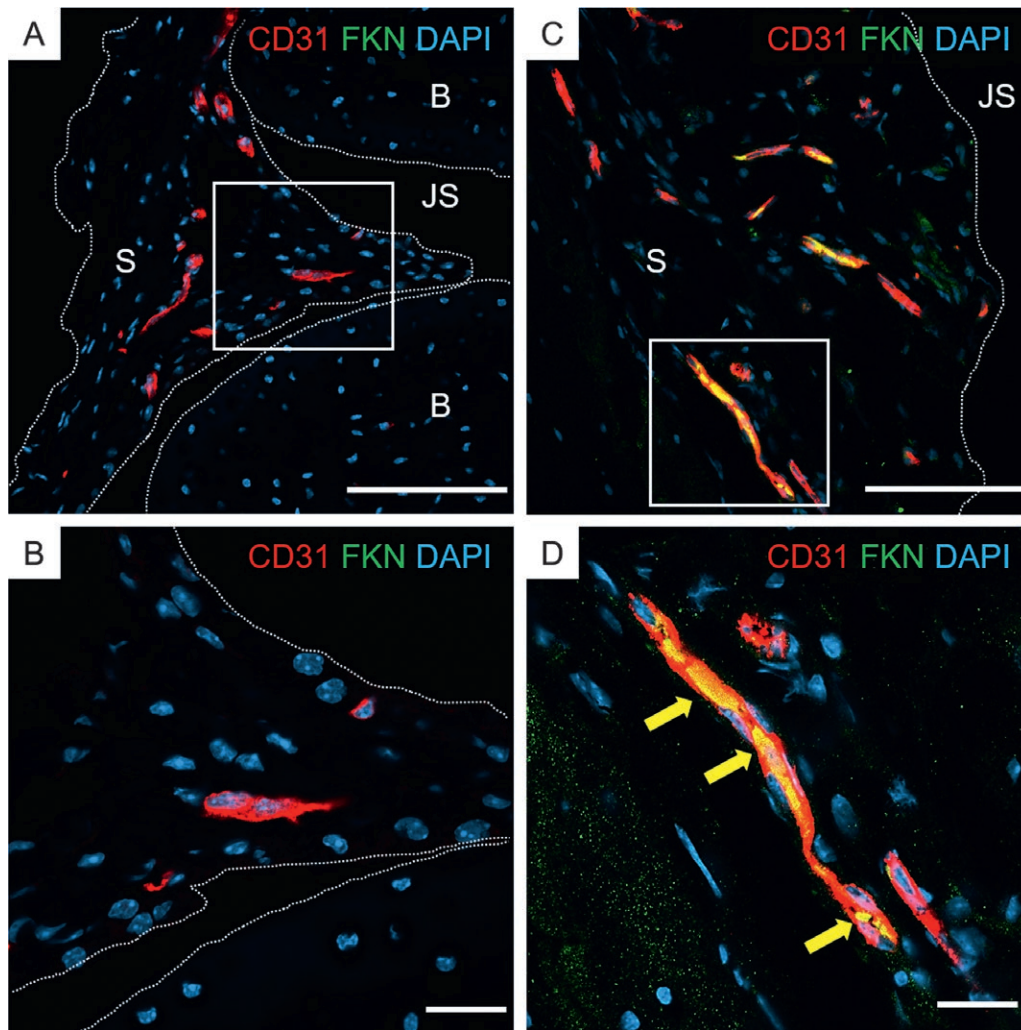
Figure 4. Expression of fractalkine (FKN) on vascular endothelial cells. **A**, Representative image from immunohistochemistry analysis of the digits of mice without collagen-induced arthritis (CIA). **B**, Enlarged view of the boxed area in **A**. **C**, Representative image from immunohistochemistry analysis of the digits of mice with CIA. **D**, Enlarged view of boxed area in **C**. **Arrows** indicate CD31+FKN+ endothelial cells. FKN expression was induced in a portion of vascular endothelial cells in the synovium of mice with CIA (**C** and **D**). Nuclear staining with DAPI appears in light blue. Original magnification × 40 in **A** and **C**; × 100 in **B** and **D**. Bars = 100 μm in **A** and **C**; bars = 50 μm in **B** and **D**. **B** = bone; **S** = synovium; **JS** = joint space.

DISCUSSION

In the present study, we showed that anti-mFKN mAb suppressed the migration of OCPs into the affected synovium and decreased the number of mature osteoclasts, leading to the inhibition of bone destruction. Furthermore, anti-FKN mAb also inhibited synovitis and cartilage destruction. These results indicate that the FKN/CX_3CR1 pathway plays a critical role in joint destruction via regulating the migration of OCPs.

OCPs express CX_3CR1 and initially emerge in the synovium, where they differentiate into osteoclasts at an early stage of disease in the arthritic rat model (28). In the present study, FKN was detected on a portion of synovial vascular endothelial cells in the affected synovium of mice with CIA; however, it was rarely detected on the synovial vascular endothelial cells of normal mice, suggesting that FKN+ vessels might serve as the migration gateway for OCPs to access the synovium in CIA pathology. Therefore, we examined whether anti-mFKN mAb could inhibit the migration of OCPs into the synovium. Transferred OCPs were detected in the vicinity of the FKN-expressing blood vessel in the synovium (results not shown). Importantly, the number of migrated OCPs was clearly reduced upon administration of anti-mFKN mAb, and a similar result was obtained when using OCPs of CX_3CR1–KO mice. In mice with CIA that were treated with anti-mFKN mAb, the number of OCPs that differentiated into cathepsin K+ multinuclear osteoblasts was also reduced. These results suggest that the inhibition of progressive bone destruction by anti-mFKN mAb was, at least partially, because of the inhibition of OCP migration into the synovium and the resulting reduction in the number of osteoclasts.
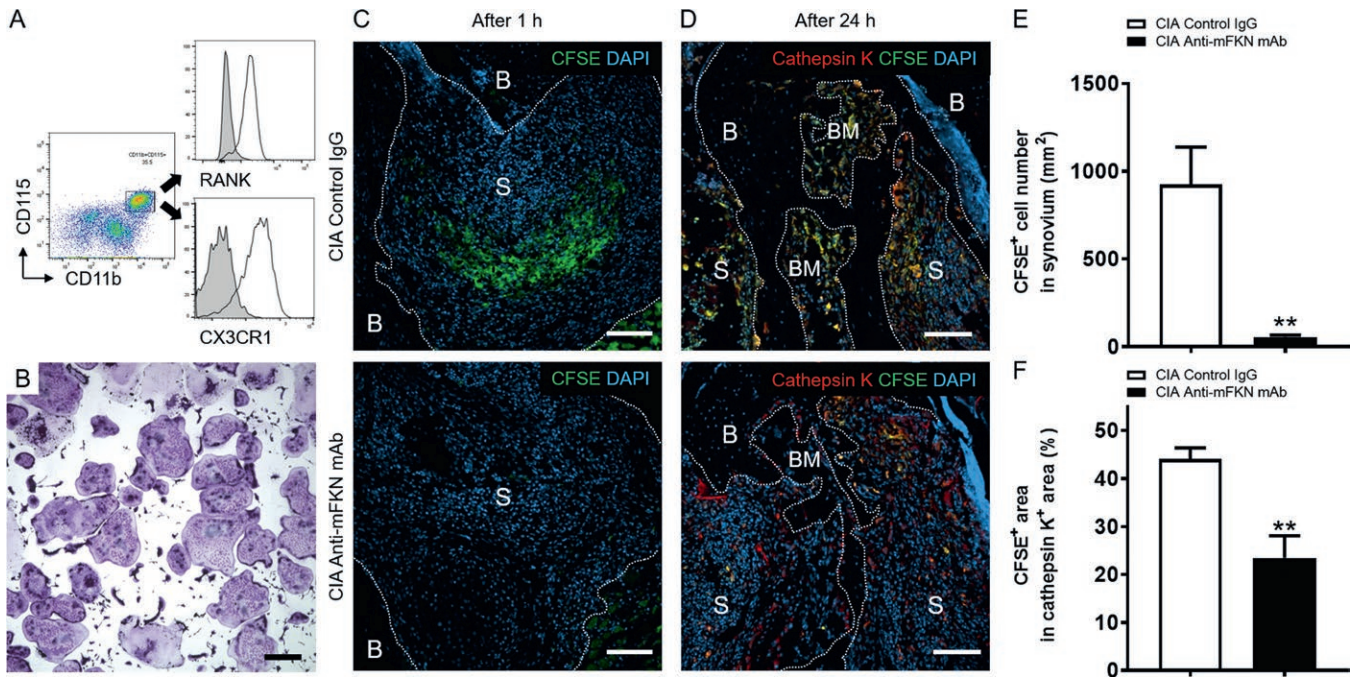
Figure 5. Effect of anti–mouse fractalkine (anti-mFKN) monoclonal antibody (mAb) on osteoclast precursor migration into the digits of mice with collagen-induced arthritis (CIA). **A**, RANK (top) or CX_3CR1 (bottom) expression on bone marrow–derived cultured $CD11b^{high}CD115+$ cells. **B**, Tartrate-resistant acid phosphatase (TRAP) staining of bone marrow–derived $CD115+CX_3CR1+$ cells cultured in mouse macrophage colony-stimulating factor and RANKL-containing medium. Bar = 300 µm. **C** and **D**, Representative images from immunohistochemistry analysis of the joints of mice with CIA. One hour (**C**) or 24 hours (**D**) after transfer of 5,6-carboxyfluorescein succinimidyl ester (CFSE)–labeled $CD115+CX_3CR1+$ cells, the synovial regions of mice with CIA were analyzed. Mice with CIA were treated with control IgG or with anti-mFKN mAb before cell transfer. Sections are stained with anti–cathepsin K polyclonal antibody (red). Nuclear staining with DAPI appears in light blue. CFSE staining appears in green. **B** = bone; **S** = synovium; **BM** = bone marrow. Bars = 100 µm. **E** and **F**, Number of CFSE+ cells in the synovium (**E**) and percent CFSE+ area in the cathepsin **K**+ area (**F**) in control IgG– and anti-mFKN mAb–treated mice with CIA. Values are the mean ± SEM (n = 5–8 mice in each group). ** = $P < 0.01$.

Anti-mFKN mAb has been shown to inhibit differentiation of bone marrow–derived OCPs into osteoclasts during coculture with osteoblasts (15). Hoshino et al reported that the FKN/CX_3CR1 pathway contributes to the maintenance of OCPs (26). Moreover, FKN provides essential survival signals to CX_3CR1-expressing monocytes, via activation of phosphatidylinositol 3-kinase (29). Therefore, the interaction of FKN and CX_3CR1 may also be involved in the differentiation of OCPs into osteoclasts, as well as in osteoclast survival after migration to the joints in mice with CIA. Furthermore, DCs have been reported to transdifferentiate into highly activated osteoclasts in inflammatory disorders such as RA (30). Myeloid DCs express CX_3CR1; thus, the role of these DC-derived osteoclasts in rheumatic disease and the expression of CX_3CR1 in osteoclasts are topics of great interest.

Prophylactic treatment with anti-mFKN mAb has been shown to inhibit the onset and progression of CIA (14), and migration of splenic F4/80+ macrophages into the synovium through the FKN/CX_3CR1 pathway has been demonstrated to play a crucial role in arthritis initiation (31). Synovium-infiltrating macrophages produce inflammatory cytokines and chemokines, thereby inducing the migration of immune cells; the com-

bination of these factors results in the development of synovitis (32,33). FLS comprise hyperplastic synovial pannus and actively invade cartilage and bone in RA. Stimulation of FLS by synovial fibroblast–derived FKN or inflammatory cytokines from infiltrating macrophages up-regulates the production of MMP, an important enzyme that contributes to matrix degradation (12,34). Therefore, as a driving force that initiates autoimmunity and inflammation, FLS have been recognized to play a central role in joint destruction in RA (12). In this study, anti-mFKN mAb also inhibited gene expression of inflammatory cytokines in joints and suppressed synovitis and pannus formation. Furthermore, anti-mFKN mAb inhibited COMP and MMP-3 production, as well as suppressed cartilage damage. Therefore, anti-mFKN mAb might also suppress cartilage destruction by reducing synovitis.

Although biologics are widely used to treat RA, some patients exhibit increased risk of complications (typically, severe infections) because of systemic administration (5,35). Several chemokine inhibitors have previously undergone clinical trials in RA patients; however, 2 inhibitors (SCH351125 and AZD5672), which target CCR5 expression on Th1 cells, did not suppress arthritis (36,37). Although CCL2 and CCR2 are representative

chemokines involved in the migration of monocyte/macrophages, no improvement in arthritis symptoms was observed in a clinical trial using the anti-CCL2 antibody (ABN 912 and MLN1202) (38,39). Presumably, these insufficiencies in efficacy occurred because of ligand receptor redundancy and/or compensation by other chemokines that may bind to CCR2 and CCR5 (40). In contrast, FKN is the sole high-affinity ligand for CX_3CR1; therefore, redundancy may be absent from the FKN/CX_3CR1 interaction.

Joint repair and erosion healing are suspected to be rare phenomena, despite effective treatment with TNF inhibitors (41). Moreover, because some patients do not respond to anticytokine therapy, RA treatment requires control of cartilage and bone destruction by novel approaches (4). Treatments with humanized anti-FKN mAb (E6011) have been investigated in a clinical trial in RA patients (NCT02196558); these therapies were safe and well-tolerated in patients with inadequate responses to methotrexate or to TNF inhibitors (42). In a clinical trial of RA treatment with humanized anti-FKN mAb (E6011), no serious adverse events (AEs) or deaths occurred; furthermore, no significant difference was observed in the incidence or severity of dose-dependent AEs (42). Therefore, FKN/CX_3CR1 pathway inhibition, by a humanized anti-FKN mAb (E6011), may be a safe and attractive strategy to treat both inflammatory synovitis and joint destruction in RA. Furthermore, FKN and/or CX_3CR1 exhibit increased expression in several inflammatory diseases, including atherosclerotic lesions (43), severe acute hepatitis (44), atopic dermatitis (45), asthma (46), and systemic sclerosis (47). Therefore, the FKN/CX_3CR1 pathway may contribute to the pathogenesis of additional chronic inflammatory diseases, providing an attractive therapeutic target for modulation of local inflammatory cell accumulation.

ACKNOWLEDGMENTS

We would like to thank Y. Arita and E. Nishioka for their assistance with preclinical experiments, H. Ogasawara for gene analysis, and H. Ishizaki and Y. Ono for the generation of CX_3CR1–KO mice. We are grateful to K. Matsuo and Y. Kuroda (Keio University) for their technical advice and expertise. We also thank Ryan Chastain-Gross (Edanz Group) for editing a draft of this manuscript. In addition, we thank all members of KAN Research Institute and Eisai Company for the helpful discussion and advice.

AUTHOR CONTRIBUTIONS

All authors were involved in drafting the article or revising it critically for important intellectual content, and all authors approved the final version to be submitted for publication. Dr. Imai had full access to all of the data in the study and takes responsibility for the integrity of the data and the accuracy of the data analysis.
Study conception and design. Hoshino-Negishi, Ohkuro, Imai.
Acquisition of data. Hoshino-Negishi, Ohkuro, Nakatani, Kuboi, Nishimura, Ida, Kakuta, Hamaguchi, Kumai, Kamisako, Sugiyama.
Analysis and interpretation of data. Hoshino-Negishi, Ohkuro, Nakatani, Kuboi, Ikeda, Ishii, Yasuda, Imai.

REFERENCES

1. Laria A, Lurati A, Marrazza M, Mazzocchi D, Re KA, Scarpellini M. The macrophages in rheumatic diseases. J Inflamm Res 2016;9:1–11.

2. Harris ED Jr. Rheumatoid arthritis: pathophysiology and implications for therapy. N Engl J Med 1990;322:1277–89.

3. Alam J, Jantan I, Bukhari SN. Rheumatoid arthritis: recent advances on its etiology, role of cytokines and pharmacotherapy. Biomed Pharmacother 2017;92:615–33.

4. Singh JA, Cameron DR. Summary of AHRQ's comparative effectiveness review of drug therapy for rheumatoid arthritis (RA) in adults: an update. J Manag Care Pharm 2012;18 Suppl C:S1–18.

5. Ellerin T, Rubin RH, Weinblatt ME. Infections and anti–tumor necrosis factor α therapy. Arthritis Rheum 2003;48:3013–22.

6. Nishimura M, Kuboi Y, Muramoto K, Kawano T, Imai T. Chemokines as novel therapeutic targets for inflammatory bowel disease. Ann N Y Acad Sci 2009;1173:350–6.

7. Szekanecz Z, Kim J, Koch AE. Chemokines and chemokine receptors in rheumatoid arthritis. Semin Immunol 2003;15:15–21.

8. Imai T, Hieshima K, Haskell C, Baba M, Nagira M, Nishimura M, et al. Identification and molecular characterization of fractalkine receptor CX3CR1, which mediates both leukocyte migration and adhesion. Cell 1997;91:521–30.

9. Hundhausen C, Misztela D, Berkhout TA, Broadway N, Saftig P, Reiss K, et al. The disintegrin-like metalloproteinase ADAM10 is involved in constitutive cleavage of CX3CL1 (fractalkine) and regulates CX3CL1-mediated cell-cell adhesion. Blood 2003;102:1186–95.

10. Goda S, Imai T, Yoshie O, Yoneda O, Inoue H, Nagano Y, et al. CX3C-chemokine, fractalkine-enhanced adhesion of THP-1 cells to endothelial cells through integrin-dependent and -independent mechanisms. J Immunol 2000;164:4313–20.

11. Matsunawa M, Isozaki T, Odai T, Yajima N, Takeuchi HT, Negishi M, et al. Increased serum levels of soluble fractalkine (CX_3CL1) correlate with disease activity in rheumatoid vasculitis. Arthritis Rheum 2006;54:3408–16.

12. Blaschke S, Koziolek M, Schwarz A, Benohr P, Middel P, Schwarz G, et al. Proinflammatory role of fractalkine (CX3CL1) in rheumatoid arthritis. J Rheumatol 2003;30:1918–27.

13. Ruth JH, Volin MV, Haines GK III, Woodruff DC, Katschke KJ Jr, Woods JM, et al. Fractalkine, a novel chemokine in rheumatoid arthritis and in rat adjuvant-induced arthritis. Arthritis Rheum 2001;44:1568–81.

14. Nanki T, Urasaki Y, Imai T, Nishimura M, Muramoto K, Kubota T, et al. Inhibition of fractalkine ameliorates murine collagen-induced arthritis. J Immunol 2004;173:7010–6.

15. Koizumi K, Saitoh Y, Minami T, Takeno N, Tsuneyama K, Miyahara T, et al. Role of CX3CL1/fractalkine in osteoclast differentiation and bone resorption. J Immunol 2009;183:7825–31.

16. Gravallese EM, Harada Y, Wang JT, Gorn AH, Thornhill TS, Goldring SR. Identification of cell types responsible for bone resorption in rheumatoid arthritis and juvenile rheumatoid arthritis. Am J Pathol 1998;152:943–51.

17. Boyle WJ, Simonet WS, Lacey DL. Osteoclast differentiation and activation. Nature 2003;423:337–42.

18. Matsuura T, Ichinose S, Akiyama M, Kasahara Y, Tachikawa N, Nakahama KI. Involvement of CX3CL1 in the migration of osteo-

clast precursors across osteoblast layer stimulated by interleukin-1β. J Cell Physiol 2017;232:1739–45.

19. Seeuws S, Jacques P, van Praet J, Drennan M, Coudenys J, Decruy T, et al. A multiparameter approach to monitor disease activity in collagen-induced arthritis. Arthritis Res Ther 2010;12:R160.

20. Huang G, Xu Z, Huang Y, Duan X, Gong W, Zhang Y, et al. Curcumin protects against collagen-induced arthritis via suppression of BAFF production. J Clin Immunol 2013;33:550–7.

21. Inoue K, Motonaga A, Suzuka H, Yoshifusa H, Fujisawa H, Nishimura T, et al. Effect of etodolac on type-II collagen-induced arthritis in mice. Agents Actions 1993;39:187–94.

22. Kawamoto T, Kawamoto K. Preparation of thin frozen sections from nonfixed and undecalcified hard tissues using Kawamot's film method (2012). Methods Mol Biol 2014;1130:149–64.

23. Ono Y, Inoue M, Mizukami H, Ogihara Y. Suppressive effect of Kanzo-bushi-to, a Kampo medicine, on collagen-induced arthritis. Biol Pharm Bull 2004;27:1406–13.

24. Beckmann J, Dittmann N, Schutz I, Klein J, Lips KS. Effect of M3 muscarinic acetylcholine receptor deficiency on collagen antibody-induced arthritis. Arthritis Res Ther 2016;18:17.

25. Marino S, Logan JG, Mellis D, Capulli M. Generation and culture of osteoclasts. Bonekey Rep 2014;3:570.

26. Hoshino A, Ueha S, Hanada S, Imai T, Ito M, Yamamoto K, et al. Roles of chemokine receptor CX3CR1 in maintaining murine bone homeostasis through the regulation of both osteoblasts and osteoclasts. J Cell Sci 2013;126:1032–45.

27. Andersen M, Ellegaard K, Hebsgaard JB, Christensen R, Torp-Pedersen S, Kvist PH, et al. Ultrasound colour Doppler is associated with synovial pathology in biopsies from hand joints in rheumatoid arthritis patients: a cross-sectional study. Ann Rheum Dis 2014;73:678–83.

28. Schett G, Stolina M, Bolon B, Middleton S, Adlam M, Brown H, et al. Analysis of the kinetics of osteoclastogenesis in arthritic rats. Arthritis Rheum 2005;52:3192–201.

29. Landsman L, Bar-On L, Zernecke A, Kim KW, Krauthgamer R, Shagdarsuren E, et al. CX3CR1 is required for monocyte homeostasis and atherogenesis by promoting cell survival. Blood 2009;113:963–72.

30. Rivollier A, Mazzorana M, Tebib J, Piperno M, Aitsiselmi T, Rabourdin-Combe C, et al. Immature dendritic cell transdifferentiation into osteoclasts: a novel pathway sustained by the rheumatoid arthritis microenvironment. Blood 2004;104:4029–37.

31. Nanki T, Imai T, Kawai S. Fractalkine/CX3CL1 in rheumatoid arthritis. Mod Rheumatol 2017;27:392–7.

32. Nanki T, Nagasaka K, Hayashida K, Saita Y, Miyasaka N. Chemokines regulate IL-6 and IL-8 production by fibroblast-like synoviocytes from patients with rheumatoid arthritis. J Immunol 2001;167:5381–5.

33. Kinne RW, Bräuer R, Stuhlmüller B, Palombo-Kinne E, Burmester GR. Macrophages in rheumatoid arthritis. Arthritis Res 2000;2:189–202.

34. Nagayoshi R, Nagai T, Matsushita K, Sato K, Sunahara N, Matsuda T, et al. Effectiveness of anti–folate receptor β antibody conjugated with truncated Pseudomonas exotoxin in the targeting

of rheumatoid arthritis synovial macrophages. Arthritis Rheum 2005;52:2666–75.

35. Burmester GR, Rubbert-Roth A, Cantagrel A, Hall S, Leszczynski P, Feldman D, et al. A randomised, double-blind, parallel-group study of the safety and efficacy of subcutaneous tocilizumab versus intravenous tocilizumab in combination with traditional disease-modifying antirheumatic drugs in patients with moderate to severe rheumatoid arthritis (SUMMACTA study). Ann Rheum Dis 2014;73:69–74.

36. Van Kuijk AW, Vergunst CE, Gerlag DM, Bresnihan B, Gomez-Reino JJ, Rouzier R, et al. CCR5 blockade in rheumatoid arthritis: a randomised, double-blind, placebo-controlled clinical trial. Ann Rheum Dis 2010;69:2013–6.

37. Gerlag DM, Hollis S, Layton M, Vencovsky J, Szekanecz Z, Braddock M, et al. Preclinical and clinical investigation of a CCR5 antagonist, AZD5672, in patients with rheumatoid arthritis receiving methotrexate. Arthritis Rheum 2010;62:3154–60.

38. Haringman JJ, Gerlag DM, Smeets TJ, Baeten D, van den Bosch F, Bresnihan B, et al. A randomized controlled trial with an anti-CCL2 (anti–monocyte chemotactic protein 1) monoclonal antibody in patients with rheumatoid arthritis. Arthritis Rheum 2006;54:2387–92.

39. Vergunst CE, Gerlag DM, Lopatinskaya L, Klareskog L, Smith MD, van den Bosch F, et al. Modulation of CCR2 in rheumatoid arthritis: a double-blind, randomized, placebo-controlled clinical trial. Arthritis Rheum 2008;58:1931–9.

40. Nanki T. Treatment for rheumatoid arthritis by chemokine blockade. Nihon Rinsho Meneki Gakkai Kaishi 2016;39:172–80.

41. Moller Døhn U, Boonen A, Hetland ML, Hansen MS, Knudsen LS, Hansen A, et al. Erosive progression is minimal, but erosion healing rare, in patients with rheumatoid arthritis treated with adalimumab: a 1 year investigator-initiated follow-up study using high-resolution computed tomography as the primary outcome measure. Ann Rheum Dis 2009;68:1585–90.

42. Tanaka Y, Takeuchi T, Umehara H, Nanki T, Yasuda N, Tago F, et al. Safety, pharmacokinetics, and efficacy of E6011, an antifractalkine monoclonal antibody, in a first-in-patient phase 1/2 study on rheumatoid arthritis. Mod Rheumatol 2018;28:58–65.

43. Greaves DR, Hakkinen T, Lucas AD, Liddiard K, Jones E, Quinn CM, et al. Linked chromosome 16q13 chemokines, macrophage-derived chemokine, fractalkine, and thymus- and activation-regulated chemokine, are expressed in human atherosclerotic lesions. Arterioscler Thromb Vasc Biol 2001;21:923–9.

44. Efsen E, Grappone C, DeFranco RM, Milani S, Romanelli RG, Bonacchi A, et al. Up-regulated expression of fractalkine and its receptor CX3CR1 during liver injury in humans. J Hepatol 2002;37:39–47.

45. Echigo T, Hasegawa M, Shimada Y, Takehara K, Sato S. Expression of fractalkine and its receptor, CX3CR1, in atopic dermatitis: possible contribution to skin inflammation. J Allergy Clin Immunol 2004;113:940–8.

46. Julia V, Staumont-Salle D, Dombrowicz D. Role of fractalkine/CX3CL1 and its receptor CX3CR1 in allergic diseases. Med Sci (Paris) 2016;32:260–6.

47. Hasegawa M, Sato S, Echigo T, Hamaguchi Y, Yasui M, Takehara K. Up regulated expression of fractalkine/CX3CL1 and CX3CR1 in patients with systemic sclerosis. Ann Rheum Dis 2005;64:21–8.

AMERICAN COLLEGE
OF RHEUMATOLOGY
EDUCATION · TREATMENT · RESEARCH

BRIEF REPORT

Risk of Knee Osteoarthritis With Obesity, Sarcopenic Obesity, and Sarcopenia

Devyani Misra,[1] Roger A. Fielding,[2] David T. Felson,[1] Jingbo Niu,[1] Carrie Brown,[1] Michael Nevitt,[3] Cora E. Lewis,[4] James Torner,[5] and Tuhina Neogi,[1] for the MOST study

Objective. Obesity, defined by anthropometric measures, is a well-known risk factor for knee osteoarthritis (OA), but there is a relative paucity of data regarding the association of body composition (fat and muscle mass) with risk of knee OA. We undertook this study to examine the longitudinal association of body composition categories based on fat and muscle mass with risk of incident knee OA.

Methods. We included participants from the Multicenter Osteoarthritis Study, a longitudinal cohort of individuals with or at risk of knee OA. Based on body composition (i.e., fat and muscle mass) from whole-body dual x-ray absorptiometry, subjects were categorized as obese nonsarcopenic (obese), sarcopenic obese, sarcopenic nonobese (sarcopenic), or nonsarcopenic nonobese (the referent category). We examined the relationship of baseline body composition categories with the risk of incident radiographic OA at 60 months using binomial regression with robust variance estimation, adjusting for potential confounders.

Results. Among 1,653 subjects without radiographic knee OA at baseline, significantly increased risk of incident radiographic knee OA was found among obese women (relative risk [RR] 2.29 [95% confidence interval {95% CI} 1.64–3.20]), obese men (RR 1.73 [95% CI 1.08–2.78]), and sarcopenic obese women (RR 2.09 [95% CI 1.17–3.73]), but not among sarcopenic obese men (RR 1.74 [95% CI 0.68–4.46]). Sarcopenia was not associated with risk of knee OA (for women, RR 0.96 [95% CI 0.62–1.49]; for men, RR 0.66 [95% CI 0.34–1.30]).

Conclusion. In this large longitudinal cohort, we found body composition–based obesity and sarcopenic obesity, but not sarcopenia, to be associated with risk of knee OA. Weight loss strategies for knee OA should focus on obesity and sarcopenic obesity.

INTRODUCTION

Obesity, a state of excess adiposity, is a major risk factor for knee osteoarthritis (OA) (1). Prior studies of obesity and knee OA have mostly defined obesity using anthropometric measures, such as body weight or body mass index (BMI) (1–3). However, anthropometric measurements are not exclusive measures of adiposity but instead reflect the composite of fat, muscle, and bone mass. Thus, it is not clear whether the effects of "BMI," typically interpreted as effects of obesity, are truly due to excess adiposity

rather than to overall loading due to the combined weight of body mass. The few studies that have examined body composition in relation to knee OA have mostly been cross-sectional in design, which limits one's ability to make an inference regarding directionality of the association (4–6). To better understand how total body mass as opposed to adiposity leads to knee OA, a longitudinal study of body composition and risk of knee OA is needed.

Further, studying body composition with knee OA lends an opportunity to examine another unique body composition state

that cannot be well studied by anthropometric measures alone (i.e., sarcopenic obesity). While fat and muscle mass grow in synchrony in young healthy adults, uncoupling of the 2 processes can occur with aging, leading to a state of high fat mass with relatively low muscle mass, referred to as sarcopenic obesity (7). A number of risk factors for development of sarcopenic obesity have been identified, such as low physical activity, inflammation, and malnutrition, among others (7). Thus, studying body composition allows evaluation of the additional risk posed by the state of high adiposity and low muscle mass over that of obesity without sarcopenia. Such insights would have novel clinical therapeutic implications in OA given the development and evaluation of treatments targeting sarcopenia. On the other hand, the absence of obesity may not necessarily be associated with reduced risk of developing knee OA, because those who are not obese can have either appropriate muscle mass or low muscle mass (i.e., sarcopenia). Sarcopenia itself is associated with several adverse outcomes, including functional limitations, but it is not known whether inappropriately low muscle mass as reflected by sarcopenia adversely impacts the risk of developing knee OA.

Thus, evaluating the effect of body composition on risk of knee OA may provide more insight into the relationship of obesity (versus that of body mass) to knee OA than traditional anthropometric measurements. Therefore, the aim of this study was to examine the longitudinal association of body composition defined by the relative presence of adiposity and sarcopenia with the risk of incident radiographic knee OA.

SUBJECTS AND METHODS

Study sample. We included participants from the Multicenter Osteoarthritis Study (MOST), a National Institutes of Health–funded longitudinal cohort of community-dwelling older adults with or at risk of knee OA, designed to study risk factors for knee OA. Details of the MOST study have been published elsewhere (8). Subjects included in this study sample were those who were free of radiographic knee OA (defined below) at baseline and who completed follow-up at the 60-month clinic visit.

Exposure. Fat and muscle mass were estimated from whole-body dual x-ray absorptiometry (DXA) (Horizon DXA System, software version 12.0; Hologic) obtained at baseline using a published protocol (9). Variables of fat and lean muscle mass (referred to hereafter as muscle mass) were recorded in kilograms from DXA. Sarcopenia was defined using the modified residual method used in geriatrics research as the lowest quintile of the residuals of appendicular skeletal muscle mass (sum of absolute muscle mass of upper and lower limbs), adjusting for age, height (in meters), and total body fat mass (in kilograms) (10). To maintain consistency with the definition of sarcopenia, we divided total body fat mass (in kilograms) into quintiles, and

the highest quintile was defined as obesity. Given the difference in body composition between men and women, obesity and sarcopenia were defined in a sex-specific manner. In a sensitivity analysis, obesity was defined by BMI ≥ 30 kg/m^2 instead of by DXA-derived fat mass. Subjects were then categorized into 4 sex-specific body composition categories: 1) obese nonsarcopenic, meeting the definition for obesity but not sarcopenia—these subjects will be referred to hereafter as obese; 2) sarcopenic obese, meeting the definitions for sarcopenia and obesity; 3) sarcopenic nonobese, meeting the definition for sarcopenia but not obesity—these subjects will be referred to hereafter as sarcopenic; and 4) nonsarcopenic nonobese, not meeting the definitions for obesity or sarcopenia (the referent category).

Outcome. Bilateral fixed-flexion posteroanterior knee radiographs were obtained at baseline and at the 60-month follow-up visit. Incident (new-onset) radiographic knee OA was defined as the presence of Kellgren/Lawrence (K/L) grade ≥ 2 in either or both knees at the 60-month follow-up visit, among those free of radiographic knee OA at baseline (i.e., K/L grade <2 in both knees at baseline) (11).

Confounders. The following covariates were selected as confounders based on literature review: age, height, race, physical activity measured by the Physical Activity Scale for the Elderly (PASE) (12), smoking status, Charlson comorbidity index (13), and history of knee injury.

Statistical analysis. We first assessed the longitudinal relationship of fat and muscle mass at baseline as continuous variables with the risk of incident radiographic knee OA over 60 months, using binomial regression with robust variance estimation to calculate risk ratios (RRs) with 95% confidence intervals (95% CIs). We then examined the longitudinal relationship of the body composition categories (obese, sarcopenic obese, sarcopenic, nonsarcopenic nonobese) defined at baseline with the risk of incident radiographic knee OA at the 60-month follow-up visit, using the same regression approach as described above. We adjusted for potential confounders as described above in the multivariable models.

In a sensitivity analysis, we defined obesity by BMI ≥ 30 kg/m^2 instead of by DXA-derived fat mass, and we recategorized subjects based on this BMI-based definition to enable comparison of the results defined by body composition with the results defined by the standard anthropometric measure of obesity used in previous studies of knee OA. All analyses were performed in the overall study population and then stratified by sex due to our a priori hypothesis of effect measure modification by sex.

SAS software, version 9.3 (SAS Institute) was used to perform the analyses. The protocol was approved by the Institutional Review Board at Boston University School of Medicine and by the MOST study review and executive committee.

RESULTS

A total of 3,026 subjects were enrolled in the MOST study, of whom 1,696 were included in the body composition categories (mean age 62 years, 61% women, and mean BMI 30 kg/m²). Our final analytic cohort was 1,653 subjects who were free of radiographic OA at baseline, after excluding those subjects not completing the 60-month visit. Among those included, 315 subjects developed incident radiographic knee OA by the 60-month follow-up visit (19%). The baseline characteristics of subjects by body composition categories (obese, sarcopenic obese, sarcopenic, nonsarcopenic nonobese) are outlined in Table 1. The differences in body weight, total body fat, and appendicular skeletal muscle mass among the groups were in the expected direction.

In the multivariable adjusted analysis of fat and muscle mass assessed as linear variables, we found greater fat mass to be numerically and statistically associated with increased risk of knee OA at 60 months in the overall population (RR 1.02 [95% CI 1.0–1.04]) and in women (RR 1.03 [95% CI 1.00–1.06]) when stratified by sex. In men, fat mass was neither numerically nor statistically associated with risk of knee OA (RR 1.00 [95% CI 0.95–1.13]). Increased muscle mass was associated with increased risk of knee OA at 60 months in the overall population (RR 1.03 [95% CI 1.0–1.06]). When stratified by sex, increased muscle mass was numerically but not statistically associated with increased risk of knee OA in women (RR 1.02 [95% CI 0.98–1.06]), while it was both numerically and statistically associated with increased risk in men (RR 1.07 [95% CI 1.01–1.13]).

In the evaluation of body composition based on fat and muscle mass in subjects categorized as obese, sarcopenic obese, or sarcopenic compared with the referent category of nonsarcopenic nonobese subjects, both obese subjects (RR 2.05 [95% CI 1.56–2.68]) and sarcopenic obese subjects (RR 1.91 [95% CI 1.17–3.10]) had increased risk of knee OA over 60 months (Table 2). When stratified by sex, the results in women and men were similar. In women, compared with nonsarcopenic nonobese subjects, a >2-fold increased risk of radiographic knee OA was found in obese subjects (RR 2.29 [95% CI 1.64–3.20]) and sarcopenic obese subjects (RR 2.09 [95% CI 1.17–3.73]) (Table 2). Similarly, in men, compared with nonsarcopenic nonobese subjects, a >70% increased risk of radiographic knee OA was noted among obese subjects (RR 1.73 [95% CI 1.08–2.78]) and sarcopenic obese subjects (RR 1.74 [95% CI 0.68–4.46]), although the results for sarcopenic obese men did not reach statistical significance. No significant association between sarcopenia without obesity and risk of radiographic knee OA was noted in either the overall analysis (RR 0.87 [95% CI 0.06–1.25]) or in sex-stratified analyses (for women, RR 0.96 [95% CI 0.62–1.49]; for men, RR 0.66 [95% CI 0.34–1.30]), as shown in Table 2.

In the sensitivity analyses in which obesity was defined by BMI ≥30 kg/m² instead of by DXA-derived fat mass, we found results similar to those in the body composition analysis, with an increase in risk of knee OA among obese subjects (RR 1.87 [95% CI 1.46–2.40]) and sarcopenic obese subjects (RR 1.99 [95% CI 1.32–3.02]) compared with nonsarcopenic nonobese subjects (Table 3). When stratified by sex, the risk of knee OA in women was 87% greater in obese subjects (RR 1.87 [95% CI 1.37–2.54]) and 60% greater in sarcopenic obese subjects (RR 1.60 [95% CI 0.93–2.77]) compared with nonsarcopenic nonobese subjects, although the latter comparison was not statistically significant (Table 3). In men, the risk of knee OA was almost 2-fold greater in obese subjects (RR 1.92 [95% CI 1.24–3.00])

Table 1. Characteristics of the participants at baseline*

	Obese (n = 244)	Sarcopenic obese (n = 62)	Sarcopenic (n = 283)	Normal (n = 1,107)
Age, years	63 ± 7.7	60 ± 7.8	65 ± 8.3	62 ± 8.0
Women, %	61	61	61	61
Caucasian, %	83	96	92	84
PASE score, 0–573	182 ± 93.4	160 ± 85.0	187 ± 95.0	185 ± 86.4
Charlson comorbidity index, 0–10	0.7 ± 1.2	0.8 ± 1.4	0.5 ± 0.9	0.6 ± 1.1
Never smoked, %	57	55	54	56
Knee injury, %	43	43	45	41
Body weight, kg	107 ± 13.2	104 ± 16.3	76 ± 11.5	80 ± 13.1
Height, m	1.7 ± 0.09	1.7 ± 0.10	1.7 ± 0.10	1.7 ± 0.09
Total body fat mass, mean (range) kg	45 (32–80)	46 (32–88)	27 (6–41)	26 (6–41)
Appendicular skeletal muscle mass, mean (range) kg	51 (39–74)	45 (35–63)	32 (21–46)	37 (20–56)

* Except where indicated otherwise, values are the mean ± SD. PASE = Physical Activity Scale for the Elderly.

Table 2. Relationship of obesity, sarcopenic obesity, and sarcopenia at baseline with risk of incident radiographic knee osteoarthritis over 5 years among community-dwelling older adults*

Sex-specific body composition category	No./total no.	Crude RR	Adjusted RR (95% CI)†
Overall			
Obese	79/244	1.95	2.05 (1.56–2.68)
Sarcopenic obese	18/62	1.75	1.91 (1.17–3.10)
Sarcopenic	35/246	0.86	0.87 (0.06–1.25)
Nonsarcopenic nonobese (referent)	183/1,101	1.0	1.00
Women			
Obese	54/137	2.11	2.29 (1.64–3.20)
Sarcopenic obese	13/36	1.94	2.09 (1.17–3.73)
Sarcopenic	25/139	1.00	0.96 (0.62–1.49)
Nonsarcopenic nonobese (referent)	121/650	1.00	1.00
Men			
Obese	25/107	1.70	1.73 (1.08–2.78)
Sarcopenic obese	5/26	1.40	1.74 (0.68–4.46)
Sarcopenic	10/107	0.70	0.66 (0.34–1.30)
Nonsarcopenic nonobese (referent)	62/451	1.00	1.00

* RR = risk ratio; 95% CI = 95% confidence interval.
† Adjusted for age, height, race, Physical Activity Scale for the Elderly score, smoking, Charlson comorbidity index, and knee injury.

and almost 3-fold greater in sarcopenic obese subjects (RR 2.89 [95% CI 1.49–5.59]) than in nonsarcopenic nonobese subjects. Similar to the body composition–based analyses, no significant association with risk of radiographic knee OA was noted in sar-copenic subjects in either the overall analysis (RR 1.03 [95% CI 0.68–1.54]) or in sex-stratified analyses (for women, RR 1.15 [95% CI 0.71–1.86]; for men, RR 0.80 [95% CI 0.38–1.67]), as shown in Table 3.

Table 3. Sensitivity analysis with body mass index–defined obesity categories to evaluate the relationship of obesity, sarcopenic obesity, and sarcopenia with risk of incident radiographic knee osteoarthritis over 5 years among community-dwelling older adults*

Sex-specific body composition category	No./total no.	Crude RR	Adjusted RR (95% CI)†
Overall			
Obese	151/585	1.81	1.87 (1.46–2.40)
Sarcopenic obese	29/110	1.77	1.99 (1.32–3.02)
Sarcopenic	31/212	1.00	1.03 (0.68–1.54)
Nonsarcopenic nonobese (referent)	111/760	1.00	1.00
Women			
Obese	98/326	1.80	1.87 (1.37–2.54)
Sarcopenic obese	16/64	1.50	1.60 (0.93–2.77)
Sarcopenic	22/114	1.16	1.15 (0.71–1.86)
Nonsarcopenic nonobese (referent)	77/461	1.00	1.00
Men			
Obese	53/259	1.80	1.92 (1.24–3.00)
Sarcopenic obese	13/46	2.49	2.89 (1.49–5.59)
Sarcopenic	9/98	0.80	0.80 (0.38–1.67)
Nonsarcopenic nonobese (referent)	34/299	1.00	1.00

* RR = risk ratio; 95% CI = 95% confidence interval.
† Adjusted for age, height, race, Physical Activity Scale for the Elderly score, smoking, Charlson comorbidity index, and knee injury.

DISCUSSION

In this large longitudinal study of the risk of knee OA in relation to DXA-derived body composition categories (obesity, sarcopenic obesity, and sarcopenia), we found increased risk of radiographic knee OA among obese women and men. Increased risk of knee OA was also found in sarcopenic obese women and men, although the results did not reach statistical significance in men. While the relationship of anthropometrically measured obesity with risk of knee OA is well known, this is the first longitudinal study to demonstrate an increased risk of knee OA with body composition–based obesity and also sarcopenic obesity. Our findings have implications for management of knee OA, such that weight loss interventions should target both high fat mass and low muscle mass. Similar results of increased risk with obesity and sarcopenic obesity were noted when obesity was defined by BMI instead of by DXA-derived fat mass and muscle mass.

The few previous studies that have examined the association of body composition with knee OA have found conflicting results (4–6,14). Issues with study design and lack of consistency in definition of obesity and sarcopenia from body composition assessment (i.e., fat and muscle mass) partly explain discordant results. For example, consistent with our results, a cross-sectional study by Lee et al found increased prevalence of radiographic knee OA among obese and sarcopenic obese subjects compared with nonsarcopenic nonobese individuals (4). Of note, sarcopenia was defined by low muscle mass, while obesity was defined by BMI, similar to our sensitivity analysis. In contrast, another cross-sectional study found anthropometric measures (BMI and body weight) more strongly associated with radiographic knee OA than fat or lean muscle mass from DXA assessed separately (5).

Yet another cross-sectional study found increasing odds of knee OA with increasing quartiles of BMI and fat mass, but no association was found with lower extremity muscle mass (6). In the same study, obese subjects with a low percentage of lower extremity muscle mass (comparable to sarcopenic obese subjects in our study) and nonobese subjects with a low percentage of lower extremity muscle mass (comparable to sarcopenic subjects in our study) were found to have greater odds of radiographic OA compared with nonobese subjects with normal lower extremity muscle mass. In contrast, obese subjects with normal lower extremity muscle mass (akin to obese subjects in our study) had no additional increased risk of knee OA (6). Further, yet another study using bioimpedance for assessment of body composition found increasing risk of severe radiographic OA and joint space narrowing with increase in fat and muscle mass (in separate analyses), although more variability was explained by muscle mass (14). To overcome some of the limitations of previous studies, we designed a longitudinal study using incident radiographic knee OA as the outcome and defined both obesity and sarcopenia based on fat and muscle

mass assessment from whole-body DXA, using definitions described in previous studies of body composition (7,10).

Knee OA is known to affect women disproportionately, but the reason for this gender disparity is not known. Despite the known difference in body composition between men and women, a similar increased risk of knee OA with adiposity for obese and sarcopenic obese categories was noted for both sexes, although this was not statistically significant in men. Of note, in additional analyses (see Supplementary Table 1, available on the *Arthritis & Rheumatology* web site at http://onlinelibrary.wiley.com/doi/10.1002/art.40692/abstract), upon additionally adjusting for body weight in the multivariable analysis of DXA-derived body composition categories and risk of knee OA, the association of obesity in women attenuated slightly, but in men the effect estimates attenuated considerably. These results might suggest a differential effect of loading on risk of knee OA by sex, although body weight may be problematic to use as a surrogate marker for loading effect. Sarcopenia was not significantly associated with risk of knee OA in men or women, although the effect estimates in men showed a trend toward a protective effect. Our results suggest that the risk of knee OA in both women and men is primarily conferred by adiposity, with perhaps a lesser independent effect of muscle mass.

Adiposity confers increased risk of many diseases primarily through a metabolic effect of adipose tissue products (adipokines). The role of adipokines has been demonstrated in knee OA (15). However, there is also evidence to suggest that increased loading across the joint in obesity leads to cartilage damage and knee OA (16). While the present study did not provide direct evidence for a metabolic or mechanical pathway for knee OA in obesity, it indicates the important role of adiposity (i.e., fat mass over muscle mass).

Although ours is the first longitudinal study that we are aware of to address this question, we acknowledge that it has limitations. First, the sample size of the sarcopenic obesity category was small, limiting our ability to precisely estimate the relationship of sarcopenic obesity with risk of knee OA in men, although all of the effect estimates were consistent in the direction and magnitude of effect. Second, the subjects in this study were primarily Caucasians; thus, these findings may not be generalizable to other racial groups, although we do not know of a biologic hypothesis to suggest that obesity and sarcopenia have effects that differ by race. Third, as physical activity levels can affect body composition, the use of the PASE instrument as a measure of physical activity level to control for its potential confounding effects is a limitation. Fourth, a quintile-based approach used to define obesity and sarcopenia may not be generalizable to other populations. However, these are approaches that have been developed to study body composition, particularly the combination of sarcopenia with obesity. Fifth, as with any observational study, there is a possibility of residual confounding.

Our study also has several strengths. The longitudinal design allows us to infer directionality. We assessed the relative

individual and combined effects of fat and muscle mass by combining the categories of obesity and sarcopenia. The comprehensive data with validated measurement of knee OA and whole-body DXA in large numbers of subjects constitute an additional strength of our study.

In conclusion, body composition assessment allows for new insights into the association of obesity with knee OA, especially the finding of increased risk conferred by sarcopenic obesity. Preventive efforts may need to focus not only on reducing obesity but also on ameliorating sarcopenic obesity to reduce the burgeoning incidence and prevalence of knee OA.

AUTHOR CONTRIBUTIONS

All authors were involved in drafting the article or revising it critically for important intellectual content, and all authors approved the final version to be published. Dr. Misra had full access to all of the data in the study and takes responsibility for the integrity of the data and the accuracy of the data analysis.

Study conception and design. Misra, Fielding, Felson, Niu, Brown, Nevitt, Lewis, Torner, Neogi.
Acquisition of data. Misra, Felson, Niu, Brown, Nevitt, Lewis, Torner, Neogi.
Analysis and interpretation of data. Misra, Felson, Niu, Brown, Neogi.

REFERENCES

1. Felson DT, Anderson JJ, Naimark A, Walker AM, Meenan RF. Obesity and knee osteoarthritis. The Framingham Study. Ann Intern Med 1988;109:18–24.

2. Hart DJ, Spector TD. The relationship of obesity, fat distribution and osteoarthritis in women in the general population: the Chingford Study. J Rheumatol 1993;20:331–5.

3. Grotle M, Hagen KB, Natvig B, Dahl FA, Kvien TK. Obesity and osteoarthritis in knee, hip and/or hand: an epidemiological study in the general population with 10 years follow-up. BMC Musculoskelet Disord 2008;9:132.

4. Lee S, Kim TN, Kim SH. Sarcopenic obesity is more closely associated with knee osteoarthritis than is nonsarcopenic obesity: a cross-sectional study. Arthritis Rheum 2012;64:3947–54.

5. Abbate LM, Stevens J, Schwartz TA, Renner JB, Helmick CG, Jordan JM. Anthropometric measures, body composition, body fat distribution, and knee osteoarthritis in women. Obesity (Silver Spring) 2006;14:1274–81.

6. Suh DH, Han KD, Hong JY, Park JH, Bae JH, Moon YW, et al. Body composition is more closely related to the development of knee osteoarthritis in women than men: a cross-sectional study using the Fifth Korea National Health and Nutrition Examination Survey (KNHANES V-1, 2). Osteoarthritis Cartilage 2016;24:605–11.

7. Stenholm S, Harris TB, Rantanen T, Visser M, Kritchevsky SB, Ferrucci L. Sarcopenic obesity: definition, cause and consequences. Curr Opin Clin Nutr Metab Care 2008;11:693–700.

8. Englund M, Guermazi A, Roemer FW, Aliabadi P, Yang M, Lewis CE, et al. Meniscal tear in knees without surgery and the development of radiographic osteoarthritis among middle-aged and elderly persons: the Multicenter Osteoarthritis Study. Arthritis Rheum 2009;60: 831–9.

9. Segal NA, Findlay C, Wang K, Torner JC, Nevitt MC. The longitudinal relationship between thigh muscle mass and the development of knee osteoarthritis. Osteoarthritis Cartilage 2012;20:1534–40.

10. Newman AB, Kupelian V, Visser M, Simonsick E, Goodpaster B, Nevitt M, et al. Sarcopenia: alternative definitions and associations with lower extremity function. J Am Geriatr Soc 2003;51:1602–9.

11. Kellgren JH, Lawrence JS. Radiological assessment of osteoarthrosis. Ann Rheum Dis 1957;16:494–502.

12. Washburn RA, McAuley E, Katula J, Mihalko SL, Boileau RA. The physical activity scale for the elderly (PASE): evidence for validity. J Clin Epidemiol 1999;52: 643–51.

13. Charlson ME, Pompei P, Ales KL, MacKenzie CR. A new method of classifying prognostic comorbidity in longitudinal studies: development and validation. J Chronic Dis 1987;40:373–83.

14. Sowers MF, Yosef M, Jamadar D, Jacobson J, Karvonen-Gutierrez C, Jaffe M. BMI vs. body composition and radiographically defined osteoarthritis of the knee in women: a 4-year follow-up study. Osteoarthritis Cartilage 2008;16:367–72.

15. Hu PF, Bao JP, Wu LD. The emerging role of adipokines in osteoarthritis: a narrative review. Mol Biol Rep 2011;38:873–8.

16. Bennell KL, Bowles KA, Wang Y, Cicuttini F, Davies-Tuck M, Hinman RS. Higher dynamic medial knee load predicts greater cartilage loss over 12 months in medial knee osteoarthritis. Ann Rheum Dis 2011;70:1770–4.

BRIEF REPORT

Molecular and Structural Biomarkers of Inflammation at Two Years After Acute Anterior Cruciate Ligament Injury Do Not Predict Structural Knee Osteoarthritis at Five Years

Frank W. Roemer,[1] [ID] Martin Englund,[2] [ID] Aleksandra Turkiewicz,[2] André Struglics,[2] Ali Guermazi,[3] L. Stefan Lohmander,[2] Staffan Larsson,[2] and Richard Frobell[2]

Objective. To determine the role of inflammatory biomarkers at 2 years post–anterior cruciate ligament (ACL) injury to predict radiographic knee osteoarthritis (OA) and magnetic resonance imaging (MRI)–defined knee OA at 5 years postinjury, with a secondary aim of estimating the concordance of inflammatory biomarkers assessed by MRI and synovial fluid (SF) analysis.

Methods. We studied 113 patients with acute ACL injury. Knee scans using 1.5T MRIs were read for Hoffa- and effusion-synovitis. Biomarkers of inflammation that we assessed included interleukin-6 (IL-6), IL-8, IL-10, tumor necrosis factor, and interferon-γ in serum and SF, and IL-12p70 in serum. We defined the outcome as radiographic knee OA (ROA) or MRI-defined OA (MROA) at 5 years. The area under the receiver operating characteristic curve (AUC), sensitivity, and specificity were evaluated in models that included MRI features only (model 1), inflammation biomarkers only (serum [model 2a] or SF [model 2b]), both MRI features and serum biomarkers (model 3a), or both MRI features and SF (model 3b) biomarkers. Linear regression analysis was used to evaluate the association between MRI features and SF biomarkers.

Results. At 5 years postinjury, ROA was present in 26% of the injured knees, and MROA was present in 32%. The AUCs for ROA in each model were 0.44 (95% confidence interval [95% CI] 0.42, 0.47) for model 1, 0.62 (95% CI 0.59, 0.65) for model 2a, 0.53 (95% CI 0.50, 0.56) for model 2b, 0.58 (95% CI 0.55, 0.61) for model 3a, and 0.50 (95% CI 0.46, 0.53) for model 3b. The AUCs for MROA in each model were 0.67 (95% CI 0.64, 0.70) for model 1, 0.49 (95% CI 0.47, 0.52) for model 2a, 0.56 (95% CI 0.52, 0.59) for model 2b, 0.65 (95% CI 0.61, 0.68) for model 3a, and 0.69 (95% CI 0.66, 0.72) for model 3b. The concordance between MRI and SF biomarkers was statistically significant only for effusion-synovitis and IL-8.

Conclusion. Neither MRI-detected inflammation nor selected SF/serum inflammation biomarkers at 2 years postinjury predicted ROA or MROA at 5 years postinjury. Concordance between MRI and SF inflammatory biomarkers was weak.

INTRODUCTION

Anterior cruciate ligament (ACL) injury is a common and serious joint injury leading to ~200,000 ACL reconstructions each year in the US alone (1). The purpose of ACL reconstruction is to improve joint stability and reduce the risk of subsequent development of knee osteoarthritis (OA) (1). However, long-term radiographic and epidemiologic studies suggest that ACL reconstruction may not protect against the development of posttraumatic OA, with reported OA rates varying between 10% and 90% of patients who experienced ACL injury (2–4).

Trauma-induced cytokine response and local inflammation after knee injury may be important in the development of posttraumatic OA (5). In the Knee ACL Nonsurgical versus Surgical Treatment (KANON) study, a randomized controlled trial, highly increased synovial fluid (SF) levels of inflammatory cytokines in the injured joint were observed early after trauma, and some levels remained increased up to 5 years after injury (5). In knees without radiographically evident OA (ROA), the risk of cartilage loss is markedly increased when magnetic resonance imaging (MRI)–defined joint effusion and synovitis are present (6). Based on these observations and given that ACL injury leads to severe local inflammation at the time of injury, one may argue that persistent inflammation following trauma or surgery can potentially increase the risk of subsequent OA development.

Thus, our primary aim in the present study was to determine the role of inflammation at 2 years post–ACL injury in predicting ROA and MRI-defined OA (MROA) in the knee at 5 years postinjury. As a secondary aim, we examined the concordance between inflammation as determined by MRI and biomarkers from SF.

PATIENTS AND METHODS

KANON study and subject inclusion. We used data from the KANON trial (International Standard Randomised Controlled Trial no. 84752559 [http://www.controlled-trials.com]), which compared a surgical treatment strategy to a nonsurgical treatment strategy for acute ACL injuries in 121 young, active individuals (4).

For the present analysis, we included patients with available data on inflammation biomarkers in serum or SF and MRI at 2 years postinjury, as well as ≥1 of our 2 outcome measures (ROA or MROA at 5 years), as described below. The decision to analyze the 2-year postinjury time point in regard to inflammatory activity based on MRI and SF biomarkers (as opposed to earlier time points) was due to the overarching goal of identifying patients that experience persistent or prolonged inflammation. All patients exhibited acute posttraumatic inflammation in their joints, as manifested by marked changes in imaging or laboratory results. As we recently reported, surgery imposed a

subsequent trauma to the knee joint, with secondary inflammatory peaks observed postsurgery (5).

For the prediction analysis, 113 individuals were included in the assessments using serum biomarkers, and 78 individuals were included in the assessments using SF; in the concordance analysis, 81 individuals were included in the assessments using only SF and MRI markers. The concordance analysis between MRI markers and SF markers was performed cross-sectionally only (i.e., at the 2-year time point). Three patients had 2-year data but not 5-year data. Our decision to focus the concordance analysis on SF markers and exclude serum biomarkers was based on the fact that MRI scans, radiographs, and SF markers all reflect local processes of the injured knee, whereas systemic fluids such as serum reflect processes of the entire body. This study was approved by the Regional Ethical Review Board at Lund University.

Radiographic acquisition and assessment. Fluoroscopically guided frontal posteroanterior radiographs with weight bearing, plus lateral radiographs of the tibiofemoral (TF) compartment and patella skyline view radiographs were obtained at baseline and at 5 years. For the injured (index) knee, an experienced musculoskeletal radiologist (FWR), who was blinded with regard to the treatment allocation and clinical data, graded baseline and 5-year radiographs for osteophytes (TF and patellofemoral [PF] compartments) and joint space narrowing (JSN) (TF compartment only), according to the Osteoarthritis Research Society International (OARSI) atlas (7). Kappa values for agreement between radiographic assessments of osteophyte formation and JSN obtained using Kellgren/Lawrence (K/L) grading (8) versus using OARSI atlas grading commonly range between 0.70 and 0.88 (9,10).

MRI acquisition. MRI was performed using a 1.5T system (Gyroscan Intera; Philips Medical Systems). The MRI pulse sequence protocol has been described in detail (11) and included a sagittal 3-dimensional (3-D) fast low-angle water excitation sequence, sagittal T2*-weighted 3-D gradient echo sequences, a sagittal and coronal dual-echo turbo spin–echo sequence, and sagittal and coronal short tau inversion recovery sequences.

MRI assessment. All available MRIs were read by a musculoskeletal radiologist (FWR) according to the Anterior Cruciate Ligament OsteoArthritis Scoring (ACLOAS) system (12). ACLOAS was determined by analyzing nonenhanced MRI scans and using an assessment of inflammation that includes whole-joint synovitis based on signal changes in Hoffa's fat pad (referred to as Hoffa-synovitis) and a composite measure of the amount of intraarticular joint fluid and synovial thickening on fluid-sensitive images (referred to as effusion-synovitis). Intraobserver reliability (kappa) for assessment of effusion-synovitis for all time points scored was 0.85 (95% confidence interval [95% CI] 0.78, 0.92),

and for Hoffa-synovitis it was 0.54 (95% CI 0.42, 0.66). Interobserver reliability was 0.75 (95% CI 0.66, 0.84) and 0.60 (95% CI 0.48, 0.72), respectively (12).

Inflammation biomarkers in serum and SF. Serum levels and SF levels of interleukin-1β (IL-1β), IL-6, IL-8, IL-10, IL-12p70, interferon-γ (IFNγ), and tumor necrosis factor (TNF) were previously assessed in the KANON samples using a Multiplex Human Pro-inflammatory 7-plex immunoassay (Meso Scale Discovery) (5). In a large proportion of the samples, cytokine concentrations were below their lower limits of quantification (LLOQ) and had high coefficients of variation (CVs) (5). For this reason, only the data on IL-6, IL-8, IL-10, IL-12p70, IFNγ, and TNF from serum and all of these except for IL-12p70 from SF were accepted for further analysis in the present study. Values below the LLOQ were imputed using the LLOQ value divided by 2. All biomarker values were log_{10}-transformed before analysis.

ROA and MROA outcome measures. To define patients in the KANON cohort as having developed ROA after 5 years, 1 of the following 3 criteria had to be fulfilled in either the medial or lateral TF compartment or in the PF compartment based on OARSI grading: JSN of grade 2 or higher (TF compartment only), sum of the 2 marginal osteophyte grades from the same compartment of ≥2, or JSN of grade 1 in combination with grade 1 osteophytes in the same compartment (TF compartment only) (13). MROA was defined based on the criteria described by Hunter et al (14).

Analytical approach. We used 4 definitions of structural knee OA: 1) whole-joint MROA (TF joint MROA and/or PF joint MROA), 2) whole-joint ROA (TF joint ROA and/or PF joint ROA), 3) TF joint OA (either TF joint ROA or TF joint MROA, or both), and 4) PF joint OA (either PF joint ROA or PF joint MROA, or both).

Three predictive models were evaluated for each outcome: model 1 that included Hoffa- and effusion-synovitis (MRI features only), model 2 that included all inflammatory biomarkers, and model 3 that included models 1 and 2. Age and sex were included as additional predictors in all models. Biomarkers with >70% of values below the LLOQ were included as categorical (below or above LLOQ) in the predictive models.

We used 2 approaches for developing predictive models: a logistic regression model with the lasso method to select predictors and, repeating the analyses using a more flexible model, classification and regression trees (CARTs) as implemented in the Classification and Regression Training package (15). We used repeated (10 times) 5-fold cross-validation for resampling, and the 1–standard deviation criterion was used to select the optimal model. The models were optimized to maximize either the area under the receiver operating characteristic curve (AUC) or sensitivity. The predictive accuracy of the model was assessed with AUC, sensitivity, and specificity, reported with 95% CIs. An additional analysis was performed including treatment (surgical or nonsurgical) as a predictor.

To evaluate concordance between MRI inflammatory features and SF inflammation biomarkers, we used regression models. The MRI scores (for Hoffa- or effusion-synovitis, categorized into values of 0, 1, or ≥2) were used as the independent variable, and SF inflammation biomarkers were used as the dependent variable. For the few values that were below the LLOQ for TNF and IL-8, linear regression with log_{10} values of

Table 1. Imaging (MROA and ROA)–defined osteoarthritis at 5 years postinjury*

MROA	ROA absent	ROA present	ROA missing	MRI total
Whole knee				
Absent	60	15	1	76
Present	22	14	1	37
Radiography total	82	29	2	113
TF joint†				
Absent	71	6	1	78
Present	27	7	1	35
Radiography total	98	13	2	113
PF joint‡				
Absent	86	16	1	103
Present	3	6	1	10
Radiography total	89	22	2	113

* MROA = magnetic resonance imaging (MRI)–defined osteoarthritis; ROA = radiographic OA.
† Tibiofemoral (TF) joint MROA was defined as described by Hunter et al (14), requiring presence of a definite osteophyte and full-thickness cartilage loss (or either of these 2 features), in addition to 2 or more of the following features: 1) subchondral bone marrow lesion or cyst not associated with meniscal or ligamentous attachments, 2) meniscal subluxation, maceration, or degenerative (horizontal) tear, 3) partial-thickness cartilage loss (where full-thickness loss is not present), or 4) bone attrition.
‡ Definition of patellofemoral (PF) joint MROA requires presence of a definite osteophyte and partial- or full-thickness cartilage loss in at least 1 of 4 patellofemoral subregions. ROA was defined as either TF joint OA, PF joint OA, or both TF joint OA and PF joint OA.

the biomarker was used. For IL-6, IL-10, and IFNγ (with a high proportion of values below the LLOQ), a 2-step approach was applied. First, a logistic regression model was used to estimate whether the MRI marker was associated with having biomarker values above the LLOQ. For values above the LLOQ, a negative binomial regression was applied, and intensity ratios were calculated. All statistical analyses were conducted using Stata release 14 (StataCorp).

RESULTS

Demographic and descriptive data. The 113 individuals included in the prediction analyses had a mean ± SD age of 26.1 ± 4.9 years, 28 patients (25%) were women, and the right knee was the injured knee in 61 cases (54%). The mean ± SD body mass index (BMI) was 24.4 ± 3.2 kg/m^2.

Five years postinjury, 29 patients (26%) had whole-joint ROA, 13 patients (12%) had TF joint ROA, and 22 patients (20%) had PF joint ROA. Whole-joint MROA was seen in 37 patients (33%). According to subtypes, 35 patients (31%) had TF joint MROA and 10 patients (9%) had PF joint MROA. While the MRI definition of whole-knee and TF joint OA categorized more knees as OA-positive compared to the radiography definition (37 versus 29 with whole-knee OA, respectively, and 35 versus 13 with TF joint OA), the opposite was the case for the PF joint definition of OA, with only 10 knees being MROA-positive and 22 having PF joint ROA (Table 1).

Two years postinjury, 22 patients (19%) had no signs of Hoffa-synovitis (i.e., grade 0), 58 patients (51%) had grade 1 Hoffa-synovitis, and 33 patients (29%) had grade 2 or 3 Hoffa-synovitis. Most patients (71%) did not show any signs of effusion-synovitis at 2 years, while 26 patients (23%) had grade 1 effusion-synovitis, and 7 patients (6%) had grade 2 or 3 effusion-synovitis.

At 2 years, there were 113 patients with serum samples and 81 with SF samples (see Supplementary Table 1, on the *Arthritis & Rheumatology* web site at http://onlinelibrary.wiley.com/doi/10.1002/art.40687/abstract). All patients with serum samples and 78 of those with SF samples had corresponding MRI-defined inflammation and at least 1 structural OA outcome at 5 years.

Prediction of OA. The overall discriminatory accuracy of biomarkers (models 1–3) in predicting knee OA at 5 years, according to the aforementioned 4 definitions, was weak. In the model maximizing AUC using logistic regression, values ranged between from 0.44 (model 1: MRI features only predicting ROA) to 0.69 (model 2b: SF biomarkers only predicting PF joint OA) (Table 2).

Results were comparable in models 1–3, maximizing sensitivity using logistic regression (Supplementary Table 2, http://onlinelibrary.wiley.com/doi/10.1002/art.40687/abstract). Calibration of all models was poor (data not shown). Similar results were obtained when using a more flexible CART model

Table 2. Discriminatory accuracy of imaging and serum/synovial fluid biomarkers at 2 years postinjury, with respect to knee OA development at 5 years*

Outcome at 5 years	MRI features only (model 1)	Serum biomarkers only (model 2a)	SF biomarkers only (model 2b)	MRI features and serum biomarkers (model 3a)	MRI features and SF biomarkers (model 3b)
MROA					
AUC	0.67 (0.64, 0.70)	0.49 (0.47, 0.52)	0.56 (0.52, 0.59)	0.65 (0.61, 0.68)	0.69 (0.66, 0.72)
Sensitivity	0.03 (0.01, 0.05)	0.00 (0.00, 0.00)	0.02 (0.00, 0.03)	0.00 (0.00, 0.00)	0.02 (0.00, 0.03)
Specificity	0.98 (0.97, 1.00)	1.00 (1.00, 1.00)	0.98 (0.96, 1.00)	1.00 (0.99, 1.00)	0.99 (0.98, 1.00)
ROA					
AUC	0.44 (0.42, 0.47)	0.62 (0.59, 0.65)	0.53 (0.50, 0.56)	0.58 (0.55, 0.61)	0.50 (0.46, 0.53)
Sensitivity	0.00 (0.00, 0.00)	0.01 (0.00, 0.03)	0.00 (0.00, 0.00)	0.01 (0.00, 0.02)	0.00 (0.00, 0.00)
Specificity	1.00 (1.00, 1.00)	1.00 (1.00, 1.00)	1.00 (1.00, 1.00)	1.00 (1.00, 1.00)	1.00 (1.00, 1.00)
TF joint					
AUC	0.68 (0.65, 0.71)	0.52 (0.50, 0.54)	0.53 (0.49, 0.56)	0.64 (0.62, 0.67)	0.64 (0.60, 0.68)
Sensitivity	0.22 (0.18, 0.26)	0.00 (0.00, 0.01)	0.02 (0.00, 0.04)	0.13 (0.10, 0.17)	0.14 (0.10, 0.19)
Specificity	0.89 (0.86, 0.93)	0.99 (0.98, 1.00)	0.95 (0.92, 0.98)	0.91 (0.88, 0.95)	0.87 (0.84, 0.91)
PF joint					
AUC	0.62 (0.59, 0.65)	0.64 (0.61, 0.67)	0.69 (0.65, 0.73)	0.65 (0.63, 0.68)	0.68 (0.64, 0.73)
Sensitivity	0.00 (0.00, 0.00)	0.22 (0.17, 0.26)	0.00 (0.00, 0.00)	0.03 (0.01, 0.06)	0.00 (0.00, 0.00)
Specificity	1.00 (1.00, 1.00)	0.93 (0.91, 0.94)	1.00 (1.00, 1.00)	0.99 (0.99, 1.00)	1.00 (1.00, 1.00)

* Data were recorded according to 4 definitions, using a logistic regression model maximizing the area under the receiver operating characteristic curve (AUC). Low sensitivity is a result of poor model performance. Values in parentheses are the 95% confidence interval. SF = synovial fluid (see Table 1 for other definitions).

Table 3. Linear regression model results for IL-8 and TNF in SF from patients with synovitis*

MRI-defined synovitis grade	Log_{10} SF TNF, pg/ml	Log_{10} SF IL-8, pg/ml
Hoffa-synovitis		
Grade 0 (reference)	0.00	0.00
Grade 1	−0.06 (−0.19, 0.07)	−0.11 (−0.40, 0.18)
Grade 2/3	−0.09 (−0.23, 0.04)	0.06 (−0.24, 0.37)
Effusion-synovitis		
Grade 0 (reference)	0.00	0.00
Grade 1	0.05 (−0.07, 0.17)	0.26 (0.01, 0.50)†
Grade 2/3	0.10 (−0.08, 0.28)	0.43 (0.05, 0.81)†

* The coefficients represent differences in the mean log_{10} value of the biomarker between subjects with different synovitis grades. Values in parentheses are the 95% confidence interval. IL-8 = interleukin-8; TNF = tumor necrosis factor; SF = synovial fluid; MRI = magnetic resonance imaging.
† $P < 0.05$.

maximizing the AUC (Supplementary Table 3) and maximizing sensitivity (Supplementary Table 4). Comparable results were observed when including a treatment variable as a predictor (Supplementary Table 5).

Concordance between MRI and SF inflammation biomarkers. With regard to markers assessed in SF, a statistically significant association was observed only between IL-8 level and effusion-synovitis. The results of the linear regression analysis for IL-8 and TNF are presented in Table 3. No statistically significant associations were observed between IL-6, IL-10 or IFNɣ and inflammatory MRI markers (Supplementary Table 6).

DISCUSSION

In this prospective cohort of patients with acute ACL injuries, selected local and systemic inflammation biomarkers derived from SF, serum, and MRI at 2 years did not predict structural knee OA at 5 years, regardless of treatment strategy. We used 4 outcome definitions of structural OA in 3 separate prediction models, including MRI results only, molecular biomarkers only, and a combination of the two.

In the same cohort, we reported a marked elevation of aggrecan ARGS neoepitope and inflammatory biomarker concentrations in SF shortly after injury, with decreasing concentrations over time (5). At 5 years, however, the TNF concentration in SF still remained higher than the reference level, indicative of extended local inflammation. A recent report from the KANON trial described higher inflammatory biomarker concentrations in SF from the injured knee at 4 months, 8 months, and 5 years, among subjects randomized to undergo early ACL reconstruc-

tion, suggesting that surgery constitutes a second trauma to the acutely injured joint (16).

Increasing evidence suggests that low-grade inflammation plays an important role in nontraumatic OA (6,17), though the role of inflammation in posttraumatic OA is less clear. Some authors have suggested that targeting inflammation posttrauma may have the potential to reduce the risk of OA (18).

While OA may be defined structurally, clinically, or by using both constructs, here we focused on structural OA as the outcome. ROA is classically defined as meeting the criterion of a K/L grade of ≥2. We used a simulated K/L grade based on readings according to the OARSI atlas (7) that included the PF joint. In addition, we applied an MRI definition of OA based on an exercise using the Delphi method (14).

As expected, the proportion of patients with whole-joint and TF joint MROA at 5 years was higher compared to patients with whole-joint and TF joint ROA. However, we observed an unexpectedly higher proportion of patients with PF joint ROA compared to those with PF joint MROA. The explanation for this may be multifold, but it is likely due to the fact that the radiography definition of PF joint OA required only a minimum sum of 2 from 4 possible marginal osteophytes, whereas the MRI definition required the simultaneous presence of a definite osteophyte and concomitant cartilage loss in the PF joint. Supplementary Figures 1 and 2 (http://onlinelibrary.wiley.com/doi/10.1002/art.40687/abstract) illustrate potential causes of the discrepancies between imaging methods, particularly for PF joint OA.

The concordance between MRI inflammation markers and SF cytokines, both considered to represent local inflammation, was surprisingly weak. The only statistically significant finding was that patients who had higher grades of effusion-synovitis showed, on average, higher SF levels of IL-8. One possible explanation may be our limited understanding of low-grade inflammation of the knee, resulting in a challenge to define and measure the inflammation using MRI and molecular biomarkers. The imaging measures used here are sensitive but nonspecific for inflammation, and the SF biomarkers, while considered to indicate inflammation, may not be the ones involved in this particular form or phase of OA. Another possible explanation could be that MRI markers change more slowly compared to SF cytokines.

Some limitations of our study should be noted. The KANON trial was conducted to find clinically relevant differences between 2 treatment strategies at 2 years postinjury, and our small sample size and relatively short follow-up limit the ability to draw firm conclusions. Inflammatory biomarker results were not available for all individuals, and some SF markers had a high proportion of concentrations below the LLOQ. Other important risk factors for OA, such as meniscus injury/surgery and osteochondral injury, were not analyzed. Despite the use of commonly reported inflammatory biomarkers and

well-described imaging features of inflammation and outcomes, it is possible that markers not assessed here may provide different results. SF samples were not available for all patients at 2 years, which may have introduced some bias. An explanation for unavailable samples was not recorded, but it may be due to a patient's refusal to undergo arthrocentesis or an unsuccessful attempt at fluid aspiration.

Another limitation is that only 25% of our cohort were female, despite the fact that females have a high risk of ACL injury. For this reason, we included sex as a predictor in our models. Although some of the observed associations and 95% CIs in the prediction analysis were >0.5, we do not interpret the range of values included in 95% CIs as representing any clinically useful discriminatory ability. This seemed even clearer when evaluating the sensitivity and specificity of the models. Finally, we did not include BMI in our models given that mean BMI in these young patients was normal and the standard deviation small. A particular strength of this study is the inclusion of patients treated both surgically and nonsurgically.

In our cohort of patients with acute ACL injury, inflammation at 2 years defined by MRI and selected local and systemic inflammatory biomarkers did not predict structural OA as defined by radiography and MRI at 5 years posttrauma. Additionally, the concordance of inflammatory biomarkers assessed by MRI and in SF was found to be surprisingly weak. Additional studies with longer follow-up will be needed to more firmly define the role of inflammation in OA development following acute ACL injury.

ACKNOWLEDGMENTS

AUTHOR CONTRIBUTIONS

All authors were involved in drafting the article or revising it critically for important intellectual content, and all authors approved the final version to be published. Dr. Roemer had full access to all of the data in the study and takes responsibility for the integrity of the data and the accuracy of the data analysis.
Study conception and design. Roemer, Englund, Lohmander, Frobell.
Acquisition of data. Roemer, Englund, Turkiewicz, Struglics, Guermazi, Lohmander, Larsson, Frobell.
Analysis and interpretation of data. Roemer, Englund, Turkiewicz, Struglics, Guermazi, Lohmander, Larsson, Frobell.

REFERENCES

1. Spindler KP, Wright RW. Clinical practice: anterior cruciate ligament tear. N Engl J Med 2008;359:2135–42.

2. Lohmander LS, Englund PM, Dahl LL, Roos EM. The long-term consequence of anterior cruciate ligament and meniscus injuries: osteoarthritis. Am J Sports Med 2007;35:1756–69.

3. Oiestad BE, Engebretsen L, Storheim K, Risberg MA. Knee osteoarthritis after anterior cruciate ligament injury: a systematic review. Am J Sports Med 2009;37:1434–43.

4. Frobell RB, Roos EM, Roos HP, Ranstam J, Lohmander LS. A randomized trial of treatment for acute anterior cruciate ligament tears. N Engl J Med 2010;363:331–42.

5. Struglics A, Larsson S, Kumahashi N, Frobell R, Lohmander LS. Changes in cytokines and aggrecan ARGS neoepitope in SF and serum and in C-terminal crosslinking telopeptide of type II collagen and N-terminal crosslinking telopeptide of type I collagen in urine over five years after anterior cruciate ligament rupture: an exploratory analysis in the Knee Anterior Cruciate Ligament, Nonsurgical versus Surgical Treatment trial. Arthritis Rheumatol 2015;67:1816–25.

6. Roemer FW, Guermazi A, Felson DT, Niu J, Nevitt MC, Crema MD, et al. Presence of MRI-detected joint effusion and synovitis increases the risk of cartilage loss in knees without osteoarthritis at 30-month follow-up: the MOST study. Ann Rheum Dis 2011;70:1804–9.

7. Altman RD, Gold GE. Atlas of individual radiographic features in osteoarthritis, revised. Osteoarthritis Cartilage 2007;15 Suppl A:A1–56.

8. Kellgren JH, Lawrence JS. Radiological assessment of osteoarthrosis. Ann Rheum Dis 1957;16:494–501.

9. Osteoarthritis Initative. Project 15 test-retest reliability of semiquantitative readings from knee radiographs. URL: https://oai.epi-ucsf.org/datarelease/SASDocs/kXR_SQ_Rel_BU_Descrip.pdf.

10. Guermazi A, Hunter DJ, Li L, Benichou O, Eckstein F, Kwoh CK, et al. Different thresholds for detecting osteophytes and joint space narrowing exist between the site investigators and the centralized reader in a multicenter knee osteoarthritis study–data from the Osteoarthritis Initiative. Skeletal Radiol 2012;41:179–86.

11. Frobell RB, Le Graverand MP, Buck R, Roos EM, Roos HP, Tamez-Pena J, et al. The acutely ACL injured knee assessed by MRI: changes in joint fluid, bone marrow lesions, and cartilage during the first year. Osteoarthritis Cartilage 2009;17:161–7.

12. Roemer FW, Frobell R, Lohmander LS, Niu J, Guermazi A. Anterior Cruciate Ligament OsteoArthritis Score (ACLOAS): longitudinal MRI-based whole joint assessment of anterior cruciate ligament injury. Osteoarthritis Cartilage 2014;22:668–82.

13. Englund M, Roos EM, Lohmander LS. Impact of type of meniscal tear on radiographic and symptomatic knee osteoarthritis: a sixteen-year followup of meniscectomy with matched controls. Arthritis Rheum 2003;48:2178–87.

14. Hunter DJ, Arden N, Conaghan PG, Eckstein F, Gold G, Grainger A, et al. Definition of osteoarthritis on MRI: results of a Delphi exercise. Osteoarthritis Cartilage 2011;19:963–9.

15. Kuhn M. Classification and regression training. 2018. URL: https://CRAN.R-project.org/package=caret.

16. Larsson S, Struglics A, Lohmander LS, Frobell R. Surgical reconstruction of ruptured anterior cruciate ligament prolongs trauma-induced increase of inflammatory cytokines in synovial fluid: an exploratory analysis in the KANON trial. Osteoarthritis Cartilage 2017;25:1443–51.

17. Roemer FW, Kwoh CK, Hannon MJ, Hunter DJ, Eckstein F, Fujii T, et al. What comes first? Multi-tissue involvement leading to radiographic osteoarthritis: MRI-based trajectory analysis over 4 years in the Osteoarthritis Initiative. Arthritis Rheumatol 2015;67:2085–96.

18. Lohmander LS, Atley LM, Pietka TA, Eyre DR. The release of crosslinked peptides from type II collagen into human synovial fluid is increased soon after joint injury and in osteoarthritis. Arthritis Rheum 2003;48:3130–9.

AMERICAN COLLEGE
OF RHEUMATOLOGY
EDUCATION · TREATMENT · RESEARCH

Attenuated Joint Tissue Damage Associated With Improved Synovial Lymphatic Function Following Treatment With Bortezomib in a Mouse Model of Experimental Posttraumatic Osteoarthritis

Wensheng Wang,[1] Xi Lin,[2] Hao Xu,[3] Wen Sun,[2] Echoe M. Bouta,[4] Michael J. Zuscik,[4] Di Chen,[5] Edward M. Schwarz,[4] and Lianping Xing[4]

Objective. To investigate the roles of the synovial lymphatic system in the severity and progression of joint tissue damage and functional responses of synovial lymphatic endothelial cells (LECs) to macrophage subsets, and to evaluate the therapeutic potential of the proteasome inhibitor bortezomib (BTZ) in a mouse model of experimental posttraumatic osteoarthritis (OA).

Methods. C57BL/6J wild-type mice received a meniscal ligamentous injury to induce posttraumatic knee OA. Lymphangiogenesis was blocked by a vascular endothelial growth factor receptor 3 (VEGFR-3) neutralizing antibody. Synovial lymphatic drainage was examined by near-infrared imaging. Joint damage was assessed by histology. RNA-sequencing and pathway analyses were applied to synovial LECs. Macrophage subsets in the mouse synovium were identified by flow cytometry and immunofluorescence staining. M1 and M2 macrophages were induced from mouse bone marrow cells, and their effects on LECs were examined in cocultures in the presence or absence of BTZ. The effects of BTZ on joint damage, LEC inflammation, and synovial lymphatic drainage were examined.

Results. Injection of a VEGFR-3 neutralizing antibody into the joints of mice with posttraumatic knee OA reduced synovial lymphatic drainage and accelerated joint tissue damage. Synovial LECs from the mouse OA joints had dysregulated inflammatory pathways and expressed high levels of inflammatory genes. The number of M1 macrophages was increased in the knee joints of mice with posttraumatic OA, thereby promoting the expression of inflammatory genes by LECs; this effect was blocked by BTZ. Treatment with BTZ decreased cartilage loss, reduced the expression of inflammatory genes by LECs, and improved lymphatic drainage in the knee joints of mice with posttraumatic OA.

Conclusion. Experimental posttraumatic knee OA is associated with decreased synovial lymphatic drainage, increased numbers of M1 macrophages, and enhanced inflammatory gene expression by LECs, all of which was improved by treatment with BTZ. Intraarticular administration of BTZ may represent a new therapy for the restoration of synovial lymphatic function in subjects with posttraumatic knee OA.

INTRODUCTION

Osteoarthritis (OA) is characterized by the degeneration of articular cartilage, subchondral bone sclerosis, angiogenesis, and synovitis. Increasing evidence indicates that not only carti-

lage, but also surrounding soft tissues (referred to as synovium in this study) contribute to the pathogenesis of OA. Catabolic factors, including proinflammatory cytokines, immune cells, and proteases, are detected in OA synovium and play a critical role in cartilage degeneration (1,2). Mechanisms or pathways by which

[1]Wensheng Wang, PhD: Henan Normal University, Xinxiang, China, and University of Rochester Medical Center, Rochester, New York; [2]Xi Lin, MS, Wen Sun, PhD: University of Rochester Medical Center, Rochester, New York; [3]Hao Xu, PhD: University of Rochester Medical Center, Rochester, New York, and Longhua Hospital, Shanghai University of Traditional Chinese Medicine,

Shanghai, China; [4]Echoe M. Bouta, PhD, Michael J. Zuscik, PhD, Edward M. Schwarz, PhD, Lianping Xing, PhD: Center for Musculoskeletal Research, University of Rochester Medical Center, Rochester, New York; [5]Di Chen, PhD: Rush Medical College, Chicago, Illinois.

Dr. Wang and Ms. Lin contributed equally to this work.

Address correspondence to Lianping Xing, PhD, Department of Pathology and Laboratory Medicine, 601 Elmwood Avenue, Box 626, Rochester, NY 14642. E-mail: Lianping_xing@urmc.rochester.edu.

these factors are removed from the OA synovium have not been well studied.

The lymphatic system plays an important role in maintaining metabolic and tissue fluid homoeostasis. Interstitial fluid, immune cells, proteins, and lipids are drained by lymphatic capillaries from the interstitial space. They are then transported to lymph nodes, to the thoracic duct, and finally to the bloodstream via collecting lymphatic vessels (3). Lymphatic capillaries are composed of a thin layer of lymphatic endothelial cells (LECs). The collecting lymphatic vessels are covered by 1 or more layers of lymphatic muscle cells that enable vessel contraction, moving the lymph against gravity (4). We previously reported that the mouse knee contains a synovial lymphatic system that drains into the iliac lymph nodes, as demonstrated using an intraarticular (IA)–injected near-infrared (NIR) dye. This synovial lymphatic drainage is reduced in joints with meniscal ligamentous injury (MLI)–induced posttraumatic OA, a mouse model of experimental OA (5). However, it is not known if reduced synovial lymphatic drainage is a consequence of posttraumatic knee OA or precedes the development of posttraumatic knee OA.

The function of lymphatic vessels is affected differently according to the duration of inflammation (6). Increased lymphangiogenesis, lymphatic vessel contraction, and lymph flow occur in areas with acute inflammation. In contrast, reduced lymphatic vessel contraction and lymph flow occur in areas with chronic inflammation. This may be related to the high levels of inducible nitric oxide synthase (iNOS) produced by macrophages and LECs. Inducible NOS directly affects lymphatic muscle cells via excess nitric oxide (7,8). We observed that in mice carrying the tumor necrosis factor transgene (TNF-Tg), a model of rheumatoid arthritis (RA), macrophages were attached to LECs in the collecting lymphatic vessel that drains the inflamed joints (9). However, whether macrophages affect LEC function directly remains to be determined. Effective lymphatic drainage promotes the resolution of inflammation.

Macrophages are plastic cells. Quiescent macrophages respond to different stimuli in vitro and will polarize to subsets of M1 (proinflammatory) and M2 (antiinflammatory) macrophages at opposite ends of the macrophage phenotype spectrum. M1 and M2 macrophages have distinct gene expression profiles (10). M2 macrophages promote tumor lymphangiogenesis by producing vascular endothelial growth factor C (VEGF-C), the growth factor for LECs (11). Synovium of OA patients contains both M1 and M2 macrophages (12), but the role of these distinct macrophage populations in the lymphatic system under non-tumor conditions, such as in knee OA, has not been studied.

Bortezomib (BTZ) is a proteasome inhibitor that is approved by the US Food and Drug Adminisration for the treatment of patients with multiple myeloma (13). BTZ inhibits proinflammatory cytokines in the T cells of RA patients (14), and inhibits joint inflammation and bone erosion in mice with adjuvant-induced RA (15). It suppresses TNF-induced type II collagen degradation and expression of matrix metalloproteinase 13 (MMP-13) in human chondrocytes (16). MG132, a proteasome inhibitor that is used in biologic research, was found to reduce cartilage loss when applied in a prevention protocol in experimental animal models of surgery-induced OA (17,18). However, whether proteasome inhibition has a therapeutic role in OA or whether it can be associated with improvement of synovial lymphatics is unknown.

In the present study, we hypothesized that the progression of posttraumatic knee OA is associated with lymphatic vessel inflammation that is induced by M1 macrophages. This leads to reduced synovial lymphatic drainage and facilitates joint tissue damage, which can be attenuated by intraarticular administration of BTZ. We predicted that 1) blocking lymphatic function will accelerate OA tissue damage, 2) OA synovial LECs will express high levels of inflammatory genes, 3) OA synovium will have increased numbers of M1 macrophages, and M1 macrophages will affect LEC function, and 4) treatment with BTZ will reduce tissue damage, attenuate LEC inflammation, and improve synovial lymphatic drainage. In this study, we used a mouse model of MLI-induced posttraumatic knee OA and demonstrated an association among M1 macrophage activity, LEC inflammation, and synovial lymphatic drainage in the OA joints. Our findings also demonstrated the therapeutic potential of BTZ in this posttraumatic knee OA model.

MATERIALS AND METHODS

Experimental mouse model of posttraumatic knee OA. Three-month-old male C57BL/6J mice were subjected to MLI surgery to induce posttraumatic knee OA, which was carried out in accordance with a standard operation procedure established by the Center for Musculoskeletal Research (CMSR) in Rochester, New York (5,19). Briefly, a 5-mm incision was made on the medial aspect of the right joint, and the medial collateral ligament was transected to open the joint space. The medial meniscus was detached from its anterior attachment to the tibia, and the anterior half of the detached medial meniscus was removed. In sham surgery, a 5-mm skin incision was made on the medial aspect of the left joint. Mice received sustained-release buprenorphine to control pain.

Two experiments were conducted. In the first experiment, a VEGFR-3 neutralizing antibody (mF4-31C1; ImClone) was used. Mice with MLI-induced posttraumatic knee OA were treated with the VEGFR-3 antibody (at 0.8 mg/kg by intraperitoneal [IP] injection) or with IgG, starting at day 3 postsurgery, 3 times per week for 6 weeks, based on a regimen previously used in TNF-Tg mice (20). In the second experiment, mice with MLI-induced posttraumatic knee OA were subjected to ultrasound imaging at 4 weeks postsurgery to obtain synovial volume (21,22). Based

on their synovial volume values, the mice were randomized into 1 of 2 treatment groups: BTZ (0.25 mg/ml in a 5-µl IA injection) or vehicle control (1% DMSO) weekly for 7 weeks. All animal experiments were approved by the Animal Care and Use Committee at the University of Rochester.

NIR–indocyanine green (ICG) lymphatic imaging. NIR-ICG imaging was performed by administering an IA injection of 5 µl (0.1 µg/µl) of ICG (Akorn) into the mouse knee joints, in accordance with the CMSR standard operating procedure (5,23,24). The dynamics of ICG fluorescence over the entire leg were visualized using an NIR imaging system. Briefly, the target area was excited with NIR illumination provided by a tungsten halogen nondichroic MR16 light bulb. A fluorescence emission filter was placed behind the lens and in front of a high-sensitivity 1.4-megapixel CCD camera sensor. The camera, NIR excitation, and background illumination were controlled using software developed in the LabView programming environment.

Synovial lymphatic drainage, as indicated by the percentage of ICG clearance, was assessed by calculating the percentage difference of ICG signal intensity between the 3- and 6-hour NIR scans from the regions of interest in the knee joint after ICG injection (24).

Histology and staining. Decalcified knee samples were used. For paraffin sectioning, 30 consecutive 4-µm–thick sections of the knee tissue were collected and evenly divided into 3 levels. One section from each of the 3 levels was stained with Alcian blue–hematoxylin–orange G. For frozen sectioning, 10 consecutive 7-µm–thick sections were collected. Sections 4 and 5 were stained with hematoxylin and eosin. An adjacent section was subjected to double immunofluorescence staining for lymphatic vessels and macrophage subsets using primary antibodies, including antibodies to podoplanin (PDPN) (1:200; Abcam) for LECs, F4/80 (1:50; BioLegend) for pan-macrophages, iNOS (1:50; Santa Cruz Biotechnology) for M1 macrophages, or CD206 (1:100; R&D Systems) for M2 macrophages. Stained sections were scanned with an Olympus VS120 whole-slide imager (5).

For 3-dimensional (3-D) reconstruction, one 30-µm–thick frozen section of the synovial tissue was stained with anti-F4/80, anti-iNOS, and anti-PDPN antibodies, while another 30-µm–thick frozen section was stained with anti-F4/80, anti-CD206, and anti-PDPN antibodies, followed by scanning with an Olympus FV1000 confocal microscope to collect a series of 20–25 images. Images were imported to Amira software (version 6.0) for 3-D reconstruction.

Histomorphometric analyses. Joint tissue damage was assessed on Alcian blue–orange G–stained sections using the CMSR standard operating procedure. Histomorphometric assessments of joint tissue damage included the modified Os-

teoarthritis Research International (OARSI) score for histopathologic assessment of murine cartilage (25), a score for the severity of synovitis (26), and determination of osteophyte numbers (5,19). Three sagittal joint sections from 3 levels were used for these assessments, carried out in a blinded manner by 4 independent observers. The mean score for the 3 levels from each observer was calculated, and the mean score from all 4 individual observers was then used. Interrater agreement for each score was evaluated by calculating the Fleiss kappa coefficient (27). The results indicated that there was no significant interobserver variation (data not shown).

For the OARSI score, measurements of histopathologic changes in the tibial and femoral surfaces were combined as 1 value (scale 0–6, where 0 = normal cartilage, 0.5 = loss of proteoglycan stain without cartilage damage, 1 = mild superficial fibrillation, 2 = fibrillation and/or clefting extending below the superficial zone, 3 = mild (<25%) loss of cartilage, 4 = moderate (25–50%) loss of cartilage, 5 = severe (50–75%) loss of noncalcified cartilage, and 6 = eburnation with >75% loss of cartilage). For the synovitis score, a subjective scoring system on a scale of 0–2 was used, in which 0 = synovial lining that has 2–3 cell layers or a thickness of <10 µm (normal), 1 = synovial thickening with 5–10 cell layers or a thickness of 10–20 µm, and 2 = severe thickening of the synovium with >10 cell layers or a thickness of >20 µm. For enumeration of osteophytes, the number of osteophytes protruding from the tibial or femoral surface to the joint space was counted.

Areas of the joint tissue that were F4/80+ (pan-macrophages), F4/80+iNOS+ (M1 macrophages), F4/80+CD206+ (M2 macrophages), or PDPN+ (lymphatic vessels) were analyzed with ImageProPlus software. The synovial area was segmented manually into regions of interest. The positive staining area was calculated as the ratio of positive staining pixels to total pixels (green pixels for pan-macrophages, and yellow pixels for M1 or M2 macrophages).

LECs. The mouse LEC line was provided by Dr. S. Ran (Southern Illinois University School of Medicine, Springfield, IL). This mouse LEC line was generated from benign lymphangiomas induced with Freund's complete adjuvant (28). Primary LECs were isolated from the synovium and surrounding soft tissues of mouse knee joints using a previously described method (illustrated in Supplementary Figure 1, available on the *Arthritis & Rheumatology* web site at http://onlinelibrary.wiley.com/doi/10.1002/art.40696/abstract) (29). In brief, knee joints comprising the whole tibia and femur were digested with 1 mg/ml type I collagenase. Cells isolated from the joints were incubated with phycoerythrin (PE)–conjugated anti-mouse PDPN antibodies (BioLegend), and then resuspended in anti-PE microbeads (Miltenyi Biotec) and loaded onto an MS Column. PDPN+ cells were eluted with 1 ml MACSQuant buffer.

For characterization, the cells were stained with PE-conjugated anti-mouse PDPN antibodies combined with biotin-

conjugated anti-mouse lymphatic vessel endothelial hyaluronan receptor 1 (LYVE-1; eBioscience) antibodies or goat anti-mouse VEGFR-3 antibodies (R&D Systems), followed by Texas Red–conjugated streptavidin (BD Biosciences) or Alexa Fluor 488–conjugated anti-goat antibodies. Cells were subjected to flow cytometry (LSRII 12-color; BD Biosciences). Results were analyzed using FlowJo software (version 7). We referred to these PDPN+ cells as synovial LECs.

RNA sequencing, pathway analysis, and real-time quantitative PCR (qPCR). Total RNA was extracted from the mouse knee joints using an RNeasy Mini kit, following the manufacturer's protocol (Qiagen). RNA-sequencing analysis was performed with an Illumina HiSeq2500 high-throughput DNA sequencer. More than 1,000 genes that were differentially expressed between posttraumatic OA mouse LECs and sham-operated mouse LECs (fold change ≥1.5 or ≤0.75) were identified. Data from the mice with posttraumatic knee OA and their counterpart controls were independently analyzed by Ingenuity Pathway Analysis (IPA) (Qiagen). IPA analyses focused on canonical pathways, biologic functions, and diseases. Real-time qPCR was performed using iQ SYBR Green Supermix and an iCycler PCR machine (a list of the sequence-specific primers used is shown in Supplementary Table 1, available on the *Arthritis & Rheumatology* web site at http://onlinelibrary.wiley.com/doi/10.1002/art.40696/abstract). The fold change in expression of genes of interest in mice with posttraumatic knee OA was calculated relative to the values in sham-operated control mice (set to a value of 1).

Cell cultures. *Generation of M1 and M2 macrophages*. Bone marrow (BM) cells were isolated from wild-type (WT) mouse tibiae and femora and cultured with macrophage colony-stimulating factor for 3 days, to generate BM-derived macrophages (BMMs). M1 macrophages were induced from the BMMs using 20 ng/ml interleukin-1 (IL-1), and M2 macrophages were induced using 20 ng/ml IL-4. The phenotypes of the M1 and M2 macrophages were confirmed by immunostaining for F4/80+iNOS+ M1 macrophages and F4/80+CD206+ M2 macrophages, as described previously (30) (results of immunostaining are shown in Supplementary Figure 2, available on the *Arthritis & Rheumatology* web site at http://onlinelibrary.wiley.com/doi/10.1002/art.40696/abstract).

Evaluation of the effect of macrophage-conditioned medium on LECs. Conditioned medium was collected from M1 or M2 macrophages. LECs from a murine LEC cell line were treated with 10%, 20%, or 40% macrophage-conditioned medium. Expression of inflammatory genes in the LECs was then examined by qPCR.

Evaluation of the effect of BTZ on M1 and M2 macrophages. M1 and M2 macrophages were treated with BTZ. The expression of effector genes by the M1 and M2 macrophages was determined by qPCR.

Evaluation of the effect of BTZ on M1 macrophage–mediated LEC inflammatory gene expression. BMMs on coverslips were induced to obtain the M1 macrophage subset. M1 macrophages were treated with BTZ or phosphate buffered saline (PBS) as a control. LECs were separately cultured on plastic dishes. Coverslips with BTZ- or PBS-pretreated M1 macrophages were transferred to the LEC culture dishes, and the cells were cocultured and then removed from the dishes. Expression of inflammatory genes by the LECs that were left on the plastic dishes was examined by qPCR.

Evaluation of the effect of BTZ on LECs. LECs were treated with BTZ or PBS. Expression of inflammatory genes by the treated LECs was assessed by qPCR.

Western blot analysis. BTZ was injected IA into the right knee joint of mice, while the left knee joint received vehicle control. The mice were killed 4 hours later. Synovial tissue and femoral cortical bone samples were harvested from the knee joints after removal of the BM. Proteins were extracted using ubiquitination lysis buffer. Total ubiquitinated proteins were determined by Western blotting using an anti-ubiquitin antibody (Santa Cruz Biotechnology), with β-actin used as a loading control.

Statistical analysis. All experiments were performed at least twice, with each yielding similar results. Data are presented as the mean ± SD. Student's unpaired *t*-test was used to compare 2 groups. One-way analysis of variance followed by Tukey's post hoc test was used to compare more than 2 groups. An X–Y linear regression test was used for determination of any correlation between ICG clearance and OARSI score. *P* values less than or equal to 0.05 were considered significant.

RESULTS

Worsening of experimental posttraumatic knee OA following neutralizing antibody blockade of lymphangiogenesis. To investigate the cause–effect relationship between the synovial lymphatic system and posttraumatic knee OA, we used a VEGFR-3 neutralizing antibody to block lymphangiogenesis (20) in the joints of mice with MLI-induced posttraumatic knee OA. Three groups of mice (n = 10 mice per group) were used, including IgG-treated sham-operated mice, IgG-treated mice with posttraumatic knee OA, and VEGFR-3 antibody–treated mice with posttraumatic knee OA. The treatment (administered IP) was started on day 3 postsurgery and given 3 times per week for 6 weeks. Synovial lymphatic drainage and joint tissue damage (5) were then assessed (Figure 1A).

Knees from IgG-treated mice with MLI-induced OA had a lower percentage of ICG clearance (indicative of the extent of synovial lymphatic drainage) compared to IgG-treated sham-operated mice, and the ICG clearance became significantly worse in VEGFR-3 antibody–treated mice (Figure 1B). Results of
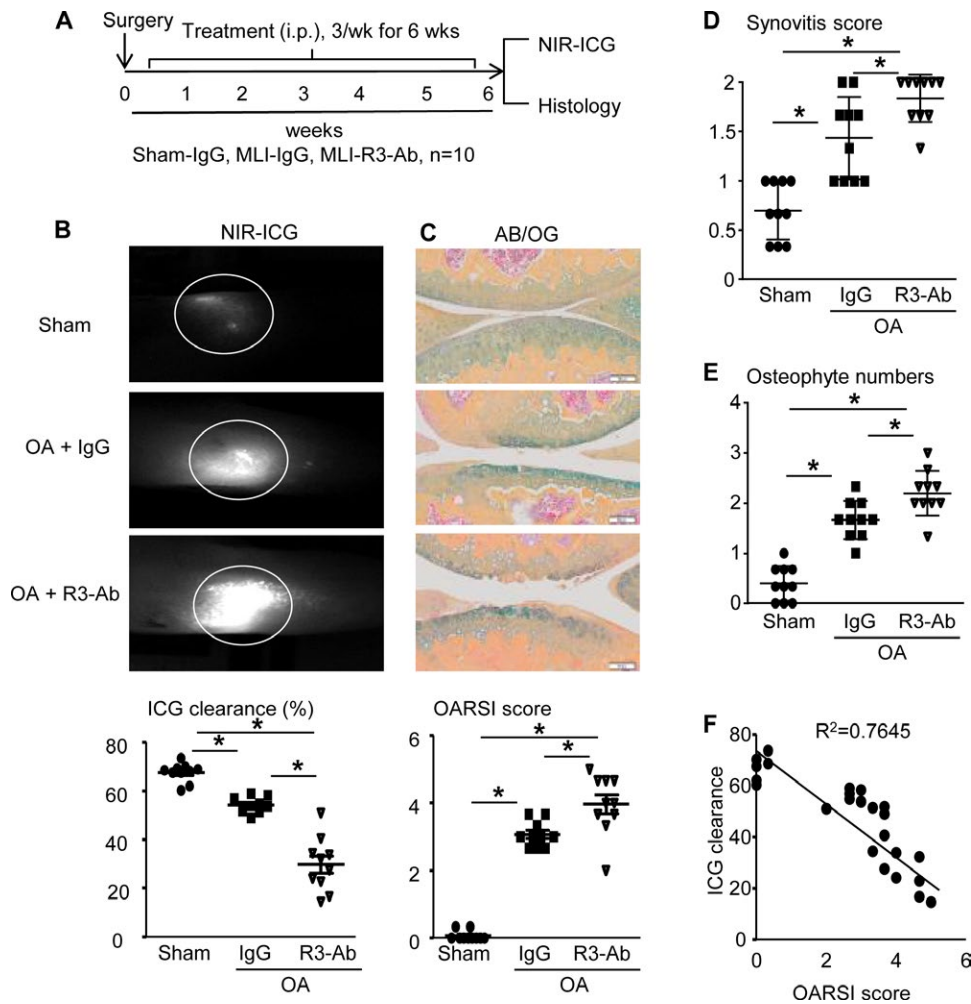
Figure 1. Inhibition of lymphangiogenesis by vascular endothelial growth factor receptor 3 (VEGFR-3) antibody blockade exacerbates cartilage destruction in the knee joints of mice with posttraumatic osteoarthritis (OA). **A,** Schematic illustration shows the experimental design, in which wild-type C57BL/6J mice received meniscal ligamentous injury (MLI) or sham surgery, and on day 3 postsurgery were randomized to receive treatment with anti–VEGFR-3 neutralizing antibody (R3-Ab; 0.8 mg/kg intraperitoneally [IP], 3 times/week) or IgG (placebo) for 6 weeks. **B,** Sham-operated knee joints and IgG- or R3-Ab–treated knee joints of mice with OA were subjected to near-infrared dye–indocyanine green (NIR-ICG) imaging to quantify synovial lymphatic drainage. Top, Representative images of the ICG remaining in the knee 24 hours postinjection are shown (circled regions) to illustrate the lack of lymphatic clearance in R3-Ab–treated mice. Bottom, ICG clearance was quantified. **C,** Paraffin-embedded sections of the knee joints were stained with Alcian blue–orange G (AB/OG) for histopathologic assessment. Top, Representative micrographs are shown (bars = 0.1 mm; original magnification × 10). Bottom, Sections were assessed for OA severity using Osteoarthritis Research Society International (OARSI) histopathologic scores. **D** and **E,** Synovitis scores (**D**) and osteophyte numbers (**E**) were compared (n = 10 mice per group). Symbols represent individual mice; results are presented as the mean ± SD. * = $P < 0.05$ by one-way analysis of variance followed by Tukey's post hoc test. **F,** The relationship between ICG clearance and OARSI score (n = 30 mice with posttraumatic knee OA) was determined by linear regression analysis ($P < 0.05$ for Pearson's correlation coefficient).

histology showed that the MLI procedure caused cartilage loss and fibrillation in the knee joints, both of which were more severe in VEGFR-3 antibody–treated mice.

Morphometric analysis revealed higher OARSI scores, synovitis scores, and osteophyte formation in IgG-treated MLI-operated mouse knee joints than in IgG-treated sham-operated mouse knee joints, and all 3 parameters were worse in the VEG-FR-3 antibody–treated knee joints of mice with MLI-induced OA (Figures 1C–E). There was a strong correlation between the percentage of ICG clearance and the OARSI score (R^2 = 0.7645;

$P < 0.001$) (Figure 1F). These data indicate that blocking lymphangiogenesis reduces lymphatic drainage and accelerates tissue damage in the knee joints of mice with posttraumatic OA, and that the synovial lymphatic system may play an active role in the progression of posttraumatic knee OA.

Inflammatory phenotype of primary LECs from the synovium of mice with posttraumatic knee OA. Lymphatic vessels are localized in the synovium and soft tissues, mainly around the joint capsule, ligaments, fat pads, and mus-

cles of a normal mouse knee (5). To determine whether LECs are changed in the posttraumatic OA microenvironment, we purified LECs from the synovium and soft tissues with an anti-PDPN antibody (29) (procedure outlined in Supplementary Figure 1, http://onlinelibrary.wiley.com/doi/10.1002/art.40696/abstract). The results of flow cytometric analysis (n = 6 mice) revealed that 80% of PDPN+ cells expressed VEGFR-3, a commonly used specific LEC marker (31), and 14% of them expressed LYVE-1, another LEC marker that is known to be expressed by a portion of LECs (32–34) (Figure 2A).

RNA sequencing of the synovial LECs from sham-operated mouse joints (n = 5) and posttraumatic knee OA mouse joints (n = 4) revealed ~1,000 differentially expressed genes. IPA analysis indicated that these differentially expressed genes are involved in 12 dysregulated pathways, 9 of which contain an NF-κB signaling signature (Figure 2B).

Since NF-κB regulates expression of a variety of proinflammatory genes, we examined expression levels of the genes for IL-1, TNF, endothelial nitric oxide synthase (eNOS), and iNOS in synovial LECs from a separate set of mice that received either MLI or sham surgery (n = 5 mice per group). We included the gene for MMP-13 in this panel because it plays a critical role in cartilage degeneration in posttraumatic knee OA. OA synovial LECs had markedly increased expression of inflammatory genes (mean ± SD fold change over sham, 10.58 ± 1.16 for Il1, 39.05 ± 10.35 for Tnf, 16.34 ± 0.78 for eNOS, and 13.78 ± 4.87 for iNOS), while the increase in Mmp13 gene expression was moderate (fold change over sham, 4.45 ± 0.44) (Figure 2C). These data suggest that LECs in the synovium of mice with experimental posttraumatic knee OA express high levels of inflammatory genes, a process we refer to herein as LEC inflammation.
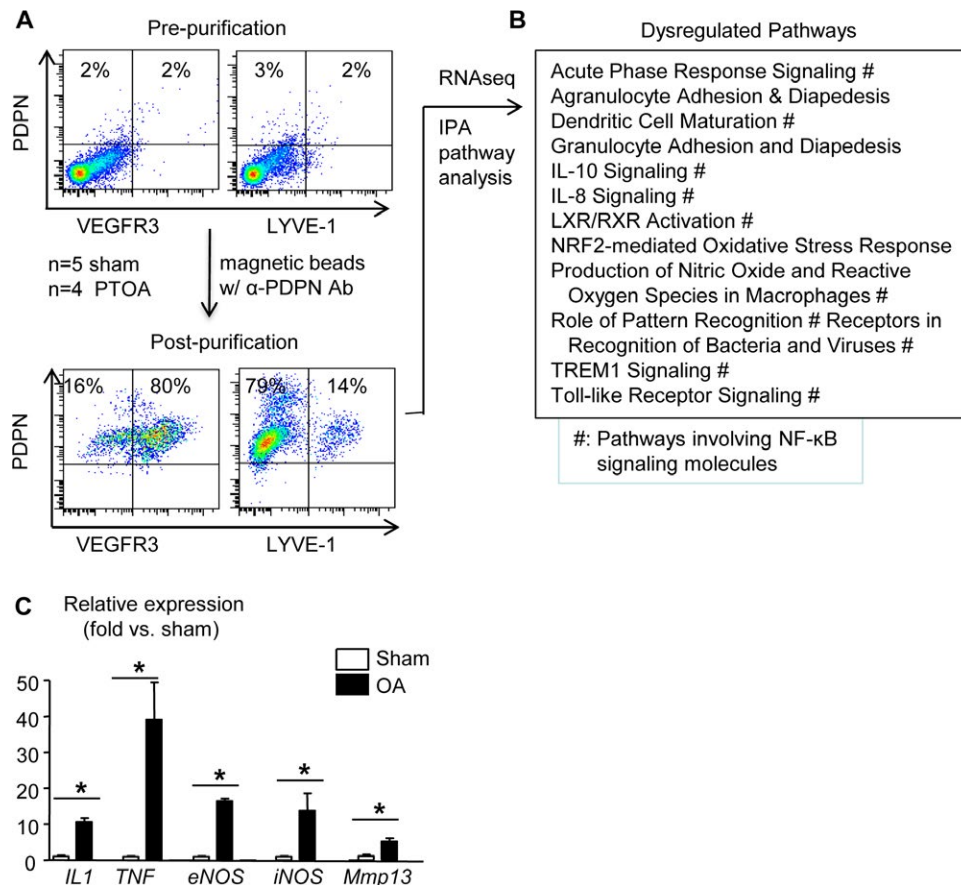
Figure 2. Lymphatic endothelial cells (LECs) in the synovium of mice with posttraumatic knee osteoarthritis (PTOA) have an inflammatory phenotype. Mice received meniscal ligamentous injury (to induce knee OA) or sham surgery. **A,** LECs were isolated from the synovium of mice (n = 6) with an anti-podoplanin antibody (α-PDPN Ab) at 6 weeks postsurgery. Enrichment of the PDPN+ cell population was confirmed by flow cytometry. **B,** RNA sequencing (RNAseq) of the PDPN+ cells was performed, revealing ~1,000 differentially expressed genes in synovial LECs from mice with posttraumatic knee OA versus sham-operated mice (n = 4–5 mice per group). Findings from Ingenuity Pathway Analysis (IPA) revealed 12 dysregulated pathways. **C,** Synovial LECs from a different cohort of mice with posttraumatic knee OA at 6 weeks postsurgery were subjected to quantitative polymerase chain reaction to assess gene expression levels. Results are the mean ± SD fold change relative to sham-operated joints (set as 1.0) (n = 5 mice per group). * = $P < 0.05$ by Student's unpaired t-test. LYVE-1 = lymphatic vessel endothelial hyaluronan receptor 1; IL-10 = interleukin-10; LXR = liver X receptor; RXR = retinoid X receptor; NRF2 = NF-κB–repressing factor 2; TREM1 = triggering receptor expressed on myeloid cells 1.

Association of experimental posttraumatic knee OA with increased numbers of M1 macrophages. We searched potential cellular mechanisms for the LEC inflammation in posttraumatic knee OA by examining cell populations by flow cytometry in the posttraumatic knee OA mouse joints compared to sham-operated mouse knee joints. The synovium of mice with posttraumatic knee OA had a significant increase in CD3+ T cells and F4/80+ macrophages (Figure 3A). In subsequent experiments, we focused on macrophages, since they are present in high numbers in knee OA and have a known role both in OA (12) and in chronic inflammation.

Macrophages are classified into inflammatory M1 or antiinflammatory M2 subsets (10). Using the F4/80+CD86+/CD36– phenotype to define the M1 macrophage subset, and F4/80+CD86–CD36+ to indicate the M2 macrophage subset, we found that synovial cells from mice with posttraumatic knee OA contained more M1 macrophages, but not M2 macrophages, compared to synovial cells from sham-operated mice (Figure 3B).
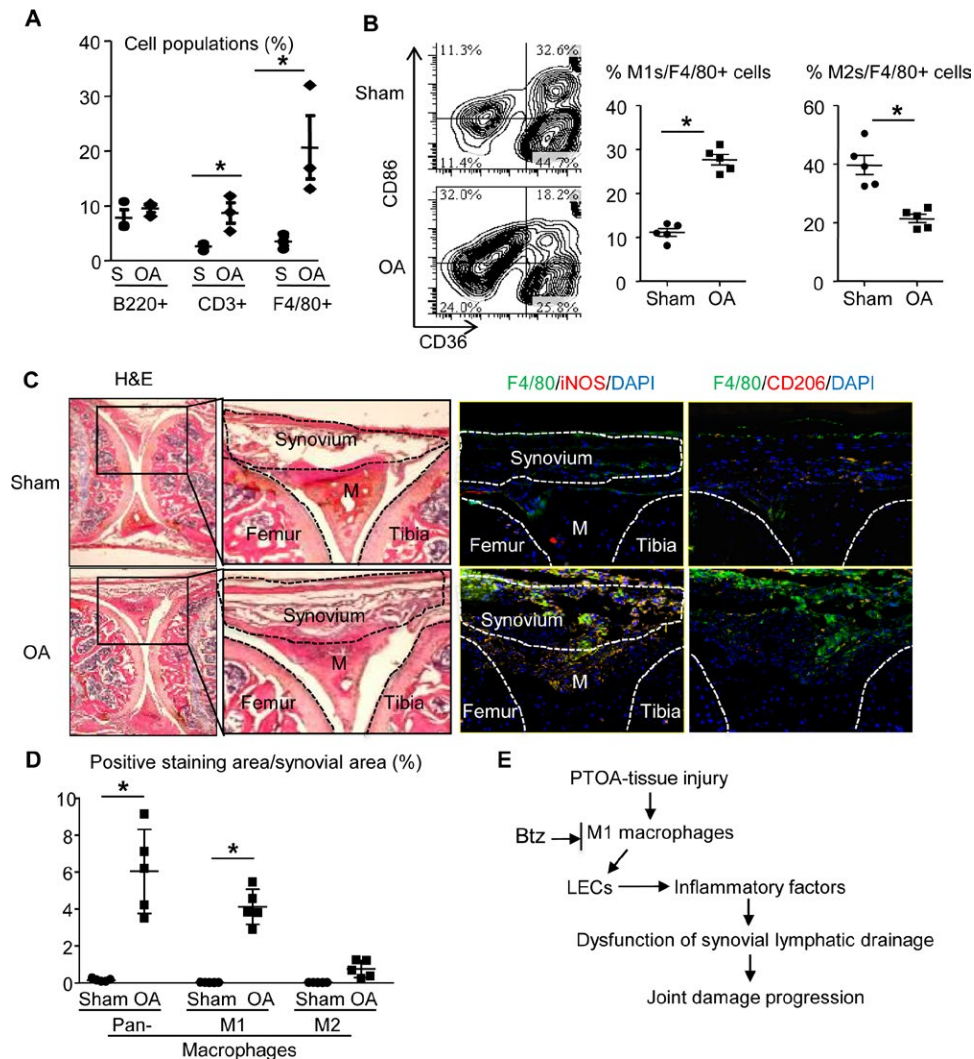
Figure 3. Numbers of M1 macrophages are increased in the synovium of mice with posttraumatic knee osteoarthritis (PTOA). Mice received meniscal ligamentous injury (MLI) or sham surgery, and knee joints were harvested at 6 weeks postsurgery for flow cytometry and histology. **A,** Total synovial cells from sham-operated knee joints (S) or knee joints from mice with MLI-induced OA (n = 3 mice per group) were subjected to flow cytometry to determine the percentage of B cells (B220+), T cells (CD3+), and macrophages (F4/80+). **B,** Percentages of M1 macrophages (CD86+CD36–) or M2 macrophages (CD86–CD36+) in total F4/80+ macrophages were compared (n = 5 mice per group). **C,** Left, Frozen sections were stained with hematoxylin and eosin (H&E). Low-magnification images show the regions of interest (original magnification × 2), while adjacent panels are higher-magnification images of the boxed areas (original magnification × 10), to illustrate the marked increase in F4/80+ inducible nitric oxide synthase–positive (iNOS+) M1 macrophages (yellow), but not M2 macrophages, in posttraumatic OA synovium. Middle and right, Frozen sections were stained with a marker for pan-macrophages (F4/80+; green) plus an M1 macrophage marker (iNOS+; red) or F4/80+ plus an M2 macrophage marker (CD206+; red). **M** = meniscus. Original magnification × 20. **D,** F4/80+ macrophages (Pan), F4/80+iNOS+ M1 macrophages, and F4/80+CD206+ M2 macrophages were quantified (n = 5 mice per group). **E,** The diagram illustrates the proposed model of the association between M1 macrophages and lymphatic endothelial cells (LECs) in posttraumatic knee OA. BTZ = bortezomib. In **A**, **B**, and **D**, symbols represent individual mice; bars show the mean ± SD. * = P < 0.05 by Student's unpaired t-test.

Immunostaining confirmed a markedly increased total of F4/80+ and F4/80+iNOS+ M1 macrophages, but not F4/80+CD206+ M2 macrophages, in OA mouse synovium compared to sham-operated mouse synovium (Figures 3C and D). Based on these data, we hypothesized that in synovium affected by posttraumatic knee OA, development of LEC inflammation can be attributed to the presence of M1 macrophages, which leads to reduced synovial lymphatic drainage and the progression of tissue damage. This process in the mouse posttraumatic OA model could be attenuated by IA administration of the proteasome inhibitor BTZ (Figure 3E).

M1 macrophage promotion of LEC inflammatory factors, and blockade by proteasome inhibitor BTZ. To test whether M1 macrophages affect LECs in posttraumatic knee OA synovium, as proposed in Figure 3E, the potential spatial relationship between lymphatic vessels and macrophage subsets was examined by immunostaining thick sections of the mouse synovial tissue with antibodies for M1 macrophages, M2 macrophages, and LECs. Analysis of 3-D images of the tissue (n = 4 mice) revealed numerous lymphatic vessels surrounded by M1 macrophages, but not M2 macrophages (Figures 4A and B).

LECs (a mouse LEC line) were treated with conditioned medium from BMMs, M1 macrophages, or M2 macrophages, and expression of inflammatory genes by LECs was examined. Compared to BMM–conditioned medium, M1 macrophage–conditioned medium increased Il1 and iNOS levels significantly, but the effect on Tnf and Mmp13 levels was minimal. In contrast, M2 macrophage–conditioned medium decreased the expression of all of these genes (Figure 5A).

BTZ, a proteasome inhibitor that has been used in clinical applications, inhibits inflammation by preventing proteasomal degradation of the negative regulators of NF-κB (14). We found that treatment with BTZ decreased M1 effector gene expression
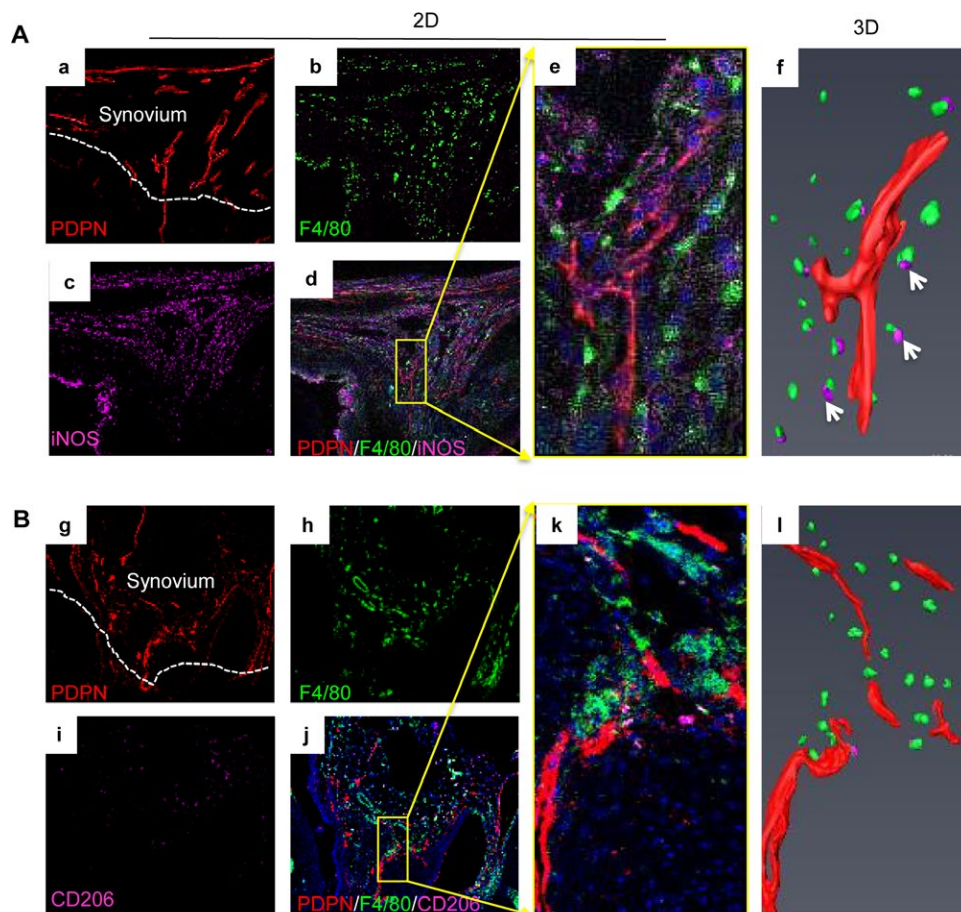
Figure 4. M1 macrophages accumulate adjacent to lymphatic vessels in the synovium of mice with posttraumatic osteoarthritis (OA). Frozen sections of OA mouse knees (30 μm thick) at 5 weeks post–meniscal ligamentous injury were immunostained with antibodies against podoplanin (PDPN) (red) for lymphatic vessels (**a**), F4/80 (green) for pan-macrophages (**b**), or inducible nitric oxide synthase (iNOS) or CD206 (purple) for macrophage subsets (**c**). M1 macrophages (**A**) were defined as F4/80+iNOS+ cells (**a–d**), and M2 macrophages (**B**) were defined as F4/80+CD206+ cells (**g–l**). Confocal microscopy was used for z-section imaging to obtain 20–25 consecutive images (**e** and **k**) with a step-width of 1 μm. PDPN+ lymphatic vessels (red) and M1 or M2 macrophages (purple) were detected by Amira to generate 3-dimensional (3-D) images (**f** and **l**) in a SurfaceGen module. Arrows in **f** indicate M1 cells near lymphatic vessels in a 3-D image. Original magnification × 20 in **a–d** and **g–j**; × 60 in **e**, **f**, **k**, and **l**.

in M1 macrophages, but had no effect on M2 effector gene expression in M2 macrophages (Figure 5B).

Similar to the effects of M1 macrophage–conditioned medium, M1 macrophages increased inflammatory gene expression by LECs when the M1 macrophages were cocultured with LECs together. This was abolished when M1 macrophages were pretreated with BTZ (Figure 5C). Impressively, BTZ did not inhibit IL-1–induced inflammatory gene expression if it was added directly to LECs alone (Figure 5D). These data suggest that BTZ inhibits the effects of M1 macrophages on LEC inflammation by mainly modulating M1 macrophage activity, without directly affecting LECs.

Effects of BTZ in reducing inflammatory gene expression by LECs, attenuating joint tissue damage, and improving synovial lymphatic function in experimental posttraumatic knee OA. BTZ is a drug for treating multiple myeloma. It is given to patients by intravenous or subcutaneous administration. We used IA injection of BTZ into the mouse knees because this route of administration could act mainly within the joints at a high local concentration. We demonstrated that BTZ, at a dose of 0.25 mg/kg, is optimal to inhibit proteasomal degradation of ubiquitinated proteins in mouse synovial tissue (Figure 6A).
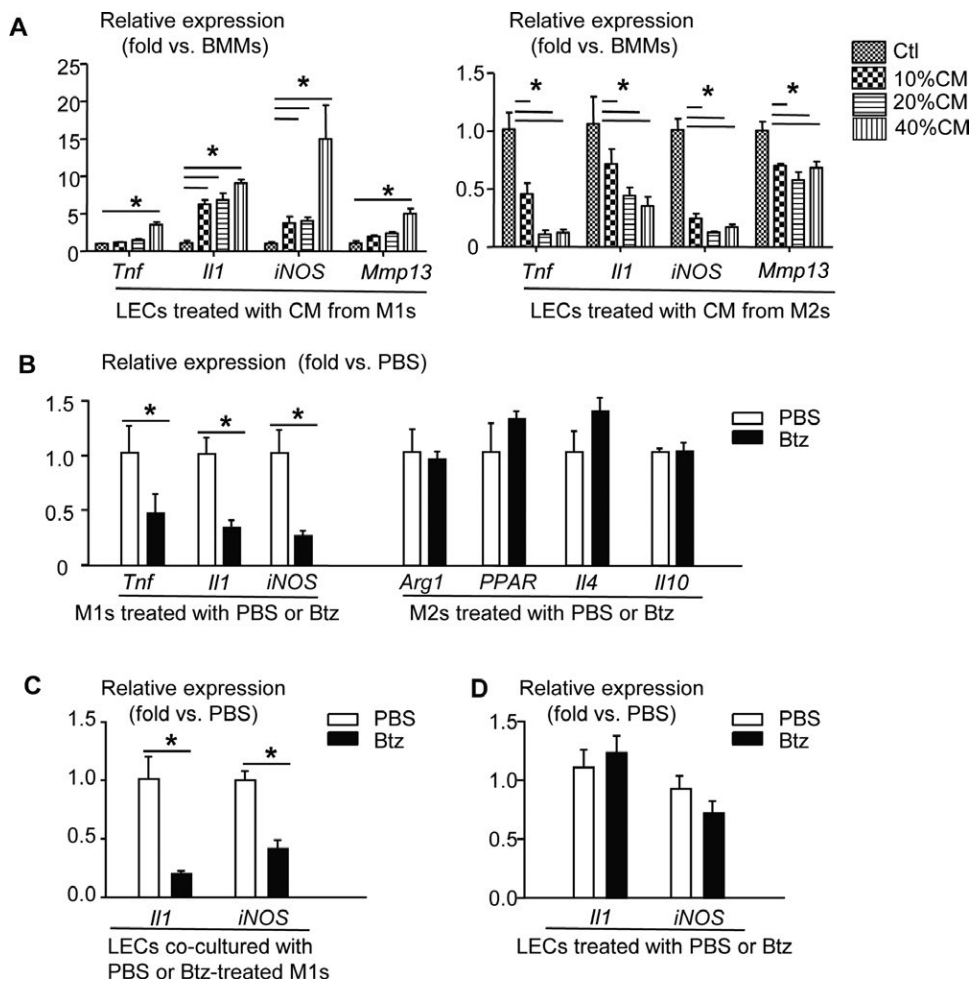
Figure 5. M1 macrophages promote expression of inflammatory genes by lymphatic endothelial cells (LECs), and these effects are inhibited by treatment with bortezomib (BTZ). **A,** Wild-type bone marrow–derived macrophages (BMMs) were treated with interleukin-1 (IL-1) or IL-4 to induce M1 or M2 macrophages, respectively. Cells were cultured for 24 hours to generate conditioned medium (CM). LECs from a murine LEC cell line were left untreated (control [Ctl]) or treated with different concentrations of M1- or M2-conditioned medium for 24 hours. Expression of inflammatory genes in LECs was determined by quantitative polymerase chain reaction (qPCR). Results are presented as the mean ± SD fold change relative to controls (set as 1.0) (n = 3 samples per group). * = $P < 0.05$ by analysis of variance. **B,** M1 or M2 macrophages were treated with phosphate buffered saline (PBS) or BTZ for 8 hours. Expression of M1 or M2 macrophage effector genes was examined by qPCR. Results are presented as the mean ± SD fold change relative to controls (set as 1.0) (n = 3 samples per group). **C,** M1 macrophages were pretreated with PBS or BTZ for 8 hours, and then cocultured with LECs for 24 hours. Expression of inflammatory genes by LECs was determined by qPCR. Results are presented as the mean ± SD fold change relative to controls (set as 1.0) (n = 4 samples per group). In **B** and **C,** * = $P < 0.05$ by Student's unpaired t-test. **D,** LECs were treated with PBS or BTZ for 8 hours. Expression of inflammatory genes was determined by qPCR. Results are presented as the mean ± SD fold change relative to controls (set as 1.0) (n = 3 samples per group).
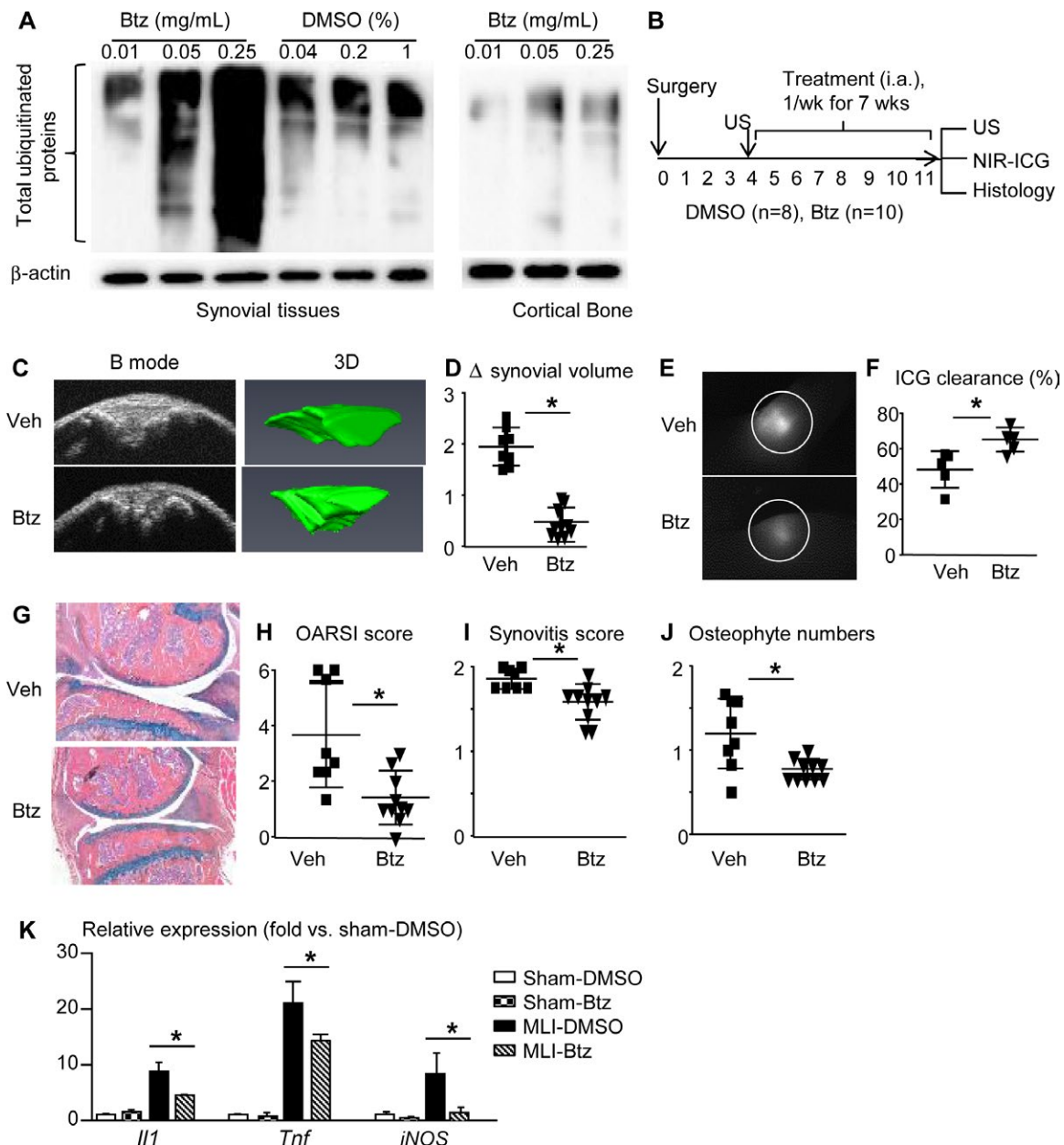
Figure 6. Bortezomib (BTZ) attenuates tissue damage, improves synovial lymphatic function, and reduces lymphatic endothelial cell (LEC) inflammation in the knee joints of mice with posttraumatic osteoarthritis induced by meniscal ligamentous injury (MLI). **A,** Different doses of BTZ or 1% DMSO (vehicle [Veh] control;) were injected intraarticularly into the knee joints of wild-type mice. Levels of total ubiquitinated proteins in the synovial tissue were examined by Western blotting at 4 hours postinjection. Cortical bone from the femur of the same joint was used as a control. **B,** Schematic illustration shows the experimental design, in which wild-type C57BL/6J mice received MLI surgery, and 4 weeks later were randomized to receive DMSO or BTZ (1 time per week by intraarticular injection for 7 weeks). **C,** Ultrasound (US) images of B-mode and 3-dimensional (3-D) reconstruction indicate the synovial volume in control and BTZ-treated mice at the end of treatment. **D,** Changes in synovial volume (in mm^3) are compared between groups. **E,** Indocyanine green (ICG) signal intensity was determined in the knee joints of mice 6 hours post–ICG administration. **F,** ICG clearance is compared between groups. In **D** and **F,** symbols represent individual mice; results are presented as the mean ± SD. **G,** Frozen synovial tissue sections were stained with Alcian blue–orange G for histopathologic assessment. Original magnification × 5. **H–J,** Osteoarthritis Research Society International (OARSI) histopathologic scores, synovitis scores, and osteophyte numbers were compared between groups. Results are presented as the mean ± SD of 8–10 mice per group. **K,** LECs from the synovium pooled from 4 joints were subjected to quantitative polymerase chain reaction for assessment of gene expression. Results are presented as the mean ± SD of 3 repeats. The fold change in expression was calculated relative to sham-operated, vehicle-treated mice (set as 1.0). * = $P < 0.05$ by Student's unpaired t-test. NIR = near-infrared dye.

An intervention protocol was used, with treatment starting at 4 weeks post-MLI. Before the treatment, we performed knee ultrasound to obtain synovial volume (21,22), and we then ran-domized the mice into either the BTZ treatment group (n = 10 mice) or the vehicle control group (n = 8 mice), based on their synovial volume. Mice received a weekly injection for 7 weeks.

Before termination, the mice were subjected to knee ultrasound, followed by NIR-ICG examination. The knees were harvested for histology (Figure 6B). Ultrasound imaging showed increased synovial volume in the vehicle-treated knee joints, with a mean ± SD fold increase of 1.95 ± 0.35. In contrast, the increase in synovial volume was much lower in BTZ-treated mouse knee joints (fold increase 0.48 ± 0.28) (Figures 6C and D).

NIR-ICG lymphatic imaging revealed that vehicle-treated joints had significantly reduced ICG clearance (mean ± SD 48 ± 9%), which was restored by BTZ treatment to an ICG clearance of 65 ± 6% (Figures 6E and F). The results of histologic analyses revealed that OARSI scores, synovitis scores, and osteophyte numbers were decreased in BTZ-treated mouse joints compared to controls (Figures 6G–J).

To determine whether BTZ reduces LEC inflammation, we treated MLI-operated and sham-operated mice with IA administration of BTZ or vehicle control, and compared the expression levels of inflammatory genes by synovial LECs among the groups (vehicle- and BTZ-treated sham-operated mice versus vehicle- and BTZ-treated mice with MLI-induced posttraumatic knee OA). Treatment with BTZ had no effect on LECs from sham-operated joints, but it significantly reduced the gene expression levels of Il1, Tnf, iNOS, and Mmp13 in LECs from MLI-operated joints with posttraumatic knee OA (Figure 6K). These data indicate that BTZ attenuates joint tissue damage and LEC inflammation and improves synovial lymphatic drainage in mice with experimental posttraumatic knee OA.

DISCUSSION

OA is associated with high levels of catabolic factors and inflammatory cells in the joint space and the soft tissues surrounding the joint, and yet the mechanisms responsible for clearance of these factors have not been well studied. Our previous study showed that lymphatic drainage is reduced in the joints of mice with MLI-induced posttraumatic knee OA, as observed following IA administration of the NIR dye ICG (5), suggesting that there is an association between synovial lymphatic drainage and posttraumatic knee OA. However, we do not know why lymphatic drainage is reduced or whether lymphatic vessel dysfunction is a sole consequence of inflammation, or if the synovial lymphatics system plays an active role in the pathogenesis of posttraumatic knee OA. In this study, we used mice with MLI-induced experimental posttraumatic knee OA and demonstrated that blockage of lymphatic function in the OA synovium resulted in increased joint tissue damage, high expression levels of inflammatory genes by OA synovial LECs, and increased numbers of macrophages with an M1 phenotype, which further promoted the expression of inflammatory genes by LECs. In addition, IA administration of BTZ decreased cartilage loss, attenuated LEC inflammation, and improved lymphatic drainage in the posttraumatic OA knee joints. Thus, BTZ may provide a new therapy for posttraumatic knee OA, as supported by our findings

suggesting that BTZ could improve synovial lymphatic function and protect against progressive joint degeneration in this disease.

Lymphangiogenesis requires the presence of the transcription factor Prox1 and the growth factor VEGF-C/VEGFR-3 signaling pathway (35,36). The VEGFR-3 neutralizing antibody has been used to investigate the effect of lymphatic blockage on the disease process and treatment in numerous preclinical studies, including our own study (20). Herein, we demonstrated that VEGFR-3 blockade exacerbates tissue damage and reduces synovial lymphatic drainage in mouse knee joints with MLI-induced posttraumatic OA (Figure 1). Thus, although our study cannot prove that lymphatic dysfunction leads to development of OA (because we treated mice that had already received MLI surgery), we demonstrated, for the first time, a negative association between lymphatic vessel function and joint injury in a mouse model of experimental OA. This makes sense, because our preliminary data previously demonstrated that MMP-13 protein is removed from the joints into the draining lymph nodes of mice with posttraumatic knee OA (data not shown).

The VEGFR-3 neutralizing antibody was given by IP injection. It may affect lymphatics systemically. This is unlikely, however, because this antibody mainly blocks newly formed lymphatic vessels, such as in tumor-induced (27) and inflammation-induced (20) lymphangiogenesis in mice. We did not find swelling or increased body weight in VEGFR-3 antibody–treated mice. In the future, we could damage lymphatic vessels locally using an ultrasound contrast agent, as has been previously described (37), and then examine its effect on the pathogenesis of OA and the clearance of catabolic factors.

Inflammation stimulates local lymphangiogenesis, but lymphatic vessels in inflamed areas do not function sufficiently and have slower lymph flow (24). Numerous lymphatic vessels are observed in the synovium of mice with MLI-induced posttraumatic knee OA, but these vessels have an impaired capacity to remove IA-injected ICG. Synovial LECs from these mice expressed high levels of iNOS (Figure 2), a phenotype similar to that found in LECs from TNF-Tg mice with RA (7). Lymph flow is controlled by active and passive forces placed on collecting lymphatic vessels via lymphatic muscle cells (38). Alternating contraction and relaxation of lymphatic muscle cells propels the lymph to draining lymph nodes and eventually to the venous circulation. Inducible NOS relaxes lymphatic muscle cells by producing an excess of nitric oxide. Thus, LECs from knee joints with posttraumatic OA may directly affect muscle cells by reducing their contractile function.

Another important finding of our study is that macrophages with the M1 phenotype promote expression of inflammatory factors by LECs (Figure 5). The contribution of macrophages or myeloid cells to lymphangiogenesis has been widely investigated (39–41). Macrophages produce factors, such as VEGF-C, to promote lymphangiogenesis (42). Depletion of macrophages ablates the prolymphangiogenesis effect (43). Macrophages may also function as precursors for lymphatic vessels, although this hypothesis has been challenged (44–46).

Macrophages are generally classified as proinflammatory M1 macrophages or antiinflammatory M2 macrophages. M2 macrophages are proangiogenic and prolymphangiogenic (11) in tumorigenesis. However, in age-related atherosclerosis, M1 macrophages, but not M2 macrophages, exacerbate atherosclerotic lesions (47), suggesting that M1 macrophages mediate tissue damage in the context of chronic inflammation. Zhang et al reported that skin macrophages have a predominant M1 phenotype in $Cox2^{-/-}$ mice fed with a high-salt diet. This was associated with decreased mature lymphatic ducts, dilated lymphatic vessels, and decreased lymphatic flow and lymphatic clearance (48,49). Our findings reveal another function for M1 macrophages—involving promotion of LECs to produce inflammatory factors via soluble factors present in conditioned medium. Currently, we do not know the identity of these soluble factors, but IL-1 and TNF, which are highly expressed by M1 macrophages, may be involved. Herein, we used cells that were induced in vitro to M1 and M2 activation states. However, it has been recognized for many years that these 2 states inadequately describe the complexity of macrophage responses within in vivo physiologic or pathologic conditions. Thus, more experiments, such as transcriptomic and systems biology analyses, are needed to further delineate the involvement of macrophage subsets in OA synovium.

The pathogenesis of OA involves multiple inflammatory pathways, and an agent that targets a single pathway, such as anti–IL-1 or anti-TNF drugs, may not be very effective (50,51). BTZ affects the ubiquitin-proteasome pathway that controls many inflammatory signaling proteins. Thus, BTZ may be more effective at inhibiting inflammation. However, our study has several limitations. First, joints contain many cell types. We do not have evidence to indicate a direct effect of BTZ on LECs or other cell types within the joint. We might be able to use a targeted approach by linking BTZ with anti-PDPN antibodies to deliver BTZ to LECs.

Second, we only examined 1 regimen for BTZ treatment, e.g., 4 weeks post-MLI and once a week administration. It is possible that other regimens may have better effects, such as giving the drug at an earlier stage or decreasing frequency.

Finally, we used a mouse model of experimental posttraumatic knee OA. Whether BTZ has an effect on other forms of OA, such as on age-related OA, requires additional study.

In summary, we used a combination of imaging, cell biology, and morphology in an experimental mouse model of posttraumatic knee OA and found that blockage of lymphangiogenesis accelerates joint tissue damage. Primary LECs isolated from the synovium of OA joints have an inflammatory phenotype, which is accompanied by a high number of macrophages that express M1 markers. In vitro, M1 macrophages promote production of inflammatory factors by LECs, an effect that is prevented by the proteasome inhibitor BTZ. Treatment with BTZ attenuates cartilage loss and expression of inflammatory factors by LECs, and improves lymphatic drainage in OA joints. These findings suggest a possible cellular mechanism for impaired synovial lymphatic function and a therapeutic potential of BTZ in the joints of subjects with posttraumatic knee OA.

AUTHOR CONTRIBUTIONS

All authors were involved in drafting the article or revising it critically for important intellectual content, and all authors approved the final version to be published. Dr. Xing had full access to all of the data in the study and takes responsibility for the integrity of the data and the accuracy of the data analysis.
Study conception and design. Wang, Lin, Xu, Sun, Bouta, Chen, Zuscik, Schwarz, Xing.
Acquisition of data. Wang, Lin, Xu, Sun, Bouta.
Analysis and interpretation of data. Wang, Lin, Xu, Sun, Bouta, Chen, Zuscik, Schwarz, Xing.

REFERENCES

1. Goldring MB, Goldring SR. Osteoarthritis. J Cell Physiol 2007; 213:626–34.
2. Sellam J, Berenbaum F. The role of synovitis in pathophysiology and clinical symptoms of osteoarthritis. Nat Rev Rheumatol 2010;6:625–35.
3. Dieterich LC, Seidel CD, Detmar M. Lymphatic vessels: new targets for the treatment of inflammatory diseases. Angiogenesis 2014;17:359–71.
4. Chakraborty S, Davis MJ, Muthuchamy M. Emerging trends in the pathophysiology of lymphatic contractile function. Semin Cell Dev Biol 2015;38:55–66.
5. Shi J, Liang Q, Zuscik M, Shen J, Chen D, Xu H, et al. Distribution and alteration of lymphatic vessels in knee joints of normal and osteoarthritic mice. Arthritis Rheumatol 2014;66:657–66.
6. Von der Weid PY, Rainey KJ. Review article: lymphatic system and associated adipose tissue in the development of inflammatory bowel disease. Aliment Pharmacol Ther 2010;32:697–711.
7. Liang Q, Ju Y, Chen Y, Wang W, Li J, Zhang L, et al. Lymphatic endothelial cells efferent to inflamed joints produce iNOS and inhibit lymphatic vessel contraction and drainage in TNF-induced arthritis in mice. Arthritis Res Ther 2016;18:62.
8. Liao S, Cheng G, Conner DA, Huang Y, Kucherlapati RS, Munn LL, et al. Impaired lymphatic contraction associated with immunosuppression. Proc Natl Acad Sci U S A 2011;108:18784–9.
9. Bouta EM, Kuzin I, de Mesy Bentley K, Wood RW, Rahimi H, Ji RC, et al. Treatment of tumor necrosis factor–transgenic mice with anti–tumor necrosis factor restores lymphatic contraction, repairs lymphatic vessels, and may increase monocyte/macrophage egress. Arthritis Rheumatol 2017;69:1187–93.
10. Biswas SK, Mantovani A. Macrophage plasticity and interaction with lymphocyte subsets: cancer as a paradigm. Nature Immunol 2010;10:889–96.
11. Quail DF, Joyce JA. Microenvironmental regulation of tumor progression and metastasis. Nat Med 2013;19:1423–37.
12. Fahy N, de Vries-van Melle ML, Lehmann J, Wei W, Grotenhuis N, Farrell E, et al. Human osteoarthritic synovium impacts chondrogenic differentiation of mesenchymal stem cells via macrophage polarisation state. Osteoarthritis Cartilage 2014;22:1167–75.
13. Kane RC, Bross PF, Farrell AT, Pazdur R. Velcade: U.S. FDA approval for the treatment of multiple myeloma progressing on prior therapy. Oncologist 2003;8:508–13.
14. Van der Heijden JW, Oerlemans R, Lems WF, Scheper RJ, Dijkmans BA, Jansen G. The proteasome inhibitor bortezomib inhibits the re-

lease of NFκB-inducible cytokines and induces apoptosis of activated T cells from rheumatoid arthritis patients. Clin Exp Rheumatol 2009;27:92–8.

15. Yannaki E, Papadopoulou A, Athanasiou E, Kaloyannidis P, Paraskeva A, Bougiouklis D, et al. The proteasome inhibitor bortezomib drastically affects inflammation and bone disease in adjuvant-induced arthritis in rats. Arthritis Rheum 2010;62:3277–88.

16. Hu W, Zhang W, Li F, Guo F, Chen A. Bortezomib prevents the expression of MMP-13 and the degradation of collagen type 2 in human chondrocytes. Biochem Biophys Res Commun 2014; 452:526–30.

17. Radwan M, Wilkinson DJ, Hui W, Destrument AP, Charlton SH, Barter MJ, et al. Protection against murine osteoarthritis by inhibition of the 26S proteasome and lysine-48 linked ubiquitination. Ann Rheum Dis 2015;74:1580–7.

18. Quan R, Huang Z, Yue Z, Xin D, Yang D, Pan J, et al. Effects of a proteasome inhibitor on the NF-κB signalling pathway in experimental osteoarthritis. Scand J Rheumatol 2013;42:400–7.

19. Hamada D, Sampson ER, Maynard RD, Zuscik MJ. Surgical induction of posttraumatic osteoarthritis in the mouse. Methods Mol Biol 2014;1130:61–72.

20. Guo R, Zhou Q, Proulx ST, Wood R, Ji RC, Ritchlin CT, et al. Inhibition of lymphangiogenesis and lymphatic drainage via vascular endothelial growth factor receptor 3 blockade increases the severity of inflammation in a mouse model of chronic inflammatory arthritis. Arthritis Rheum 2009;60:2666–76.

21. Xu H, Bouta EM, Wood RW, Schwarz EM, Wang Y, Xing L. Utilization of longitudinal ultrasound to quantify joint soft-tissue changes in a mouse model of posttraumatic osteoarthritis. Bone Res 2017;5:17012.

22. Bouta EM, Banik PD, Wood RW, Rahimi H, Ritchlin CT, Thiele RG, et al. Validation of power Doppler versus contrast-enhanced magnetic resonance imaging quantification of joint inflammation in murine inflammatory arthritis. J Bone Miner Res 2015;30: 690–4.

23. Zhou Q, Guo R, Wood R, Boyce BF, Liang Q, Wang YJ, et al. Vascular endothelial growth factor C attenuates joint damage in chronic inflammatory arthritis by accelerating local lymphatic drainage in mice. Arthritis Rheum 2011;63:2318–28.

24. Zhou Q, Wood R, Schwarz EM, Wang YJ, Xing L. Near-infrared lymphatic imaging demonstrates the dynamics of lymph flow and lymphangiogenesis during the acute versus chronic phases of arthritis in mice. Arthritis Rheum 2010;62:1881–9.

25. Glasson SS, Chambers MG, Van Den Berg WB, Little CB. The OARSI Histopathology Initiative: recommendations for histological assessments of osteoarthritis in the mouse. Osteoarthritis Cartilage 2010;18 Suppl 3:S17–23.

26. Hamada D, Maynard R, Schott E, Drinkwater CJ, Ketz JP, Kates SL, et al. Suppressive effects of insulin on tumor necrosis factor–dependent early osteoarthritic changes associated with obesity and type 2 diabetes mellitus. Arthritis Rheumatol 2016;68:1392–402.

27. Dar QA, Schott EM, Catheline SE, Maynard RD, Liu Z, Kamal F, et al. Daily oral consumption of hydrolyzed type 1 collagen is chondroprotective and anti-inflammatory in murine posttraumatic osteoarthritis. PloS One 2017;12:e0174705.

28. Sironi M, Conti A, Bernasconi S, Fra AM, Pasqualini F, Nebuloni M, et al. Generation and characterization of a mouse lymphatic endothelial cell line. Cell Tissue Res 2006;325:91–100.

29. Wang W, Wang H, Zhou X, Li X, Sun W, Dellinger M, et al. Lymphatic endothelial cells produce M-CSF, causing massive bone loss in mice. J Bone Miner Res 2017;32:939–50.

30. Sun W, Zhang H, Wang H, Chiu YG, Wang M, Ritchlin CT, et al. Targeting notch-activated M1 macrophages attenuates joint tissue

damage in a mouse model of inflammatory arthritis. J Bone Miner Res 2017;32:1469–80.

31. Noda Y, Amano I, Hata M, Kojima H, Sawa Y. Immunohistochemical examination on the distribution of cells expressed lymphatic endothelial marker podoplanin and LYVE-1 in the mouse tongue tissue. Acta Histochem Cytochem 2010;43:61–8.

32. Johnson LA, Prevo R, Clasper S, Jackson DG. Inflammation-induced uptake and degradation of the lymphatic endothelial hyaluronan receptor LYVE-1. J Biol Chem 2007;282:33671–80.

33. Johnson LA, Clasper S, Holt AP, Lalor PF, Baban D, Jackson DG. An inflammation-induced mechanism for leukocyte transmigration across lymphatic vessel endothelium. J Exp Med 2006;203:2763–77.

34. Nisato RE, Harrison JA, Buser R, Orci L, Rinsch C, Montesano R, et al. Generation and characterization of telomerase-transfected human lymphatic endothelial cells with an extended life span. Am J Pathol 2004;165:11–24.

35. Lohela M, Bry M, Tammela T, Alitalo K. VEGFs and receptors involved in angiogenesis versus lymphangiogenesis. Curr Opin Cell Biol 2009;21:154–65.

36. Karkkainen MJ, Haiko P, Sainio K, Partanen J, Taipale J, Petrova TV, et al. Vascular endothelial growth factor C is required for sprouting of the first lymphatic vessels from embryonic veins. Nat Immmunol 2004;5:74–80.

37. Bouta EM, Ju Y, Rahimi H, de Mesy-Bentley KL, Wood RW, Xing L, et al. Power Doppler ultrasound phenotyping of expanding versus collapsed popliteal lymph nodes in murine inflammatory arthritis. PloS One 2013;8:e73766.

38. Schmid-Schonbein GW. Microlymphatics and lymph flow. Physiol Rev 1990;70:987–1028.

39. Kerjaschki D. The crucial role of macrophages in lymphangiogenesis. J Clin Invest 2005;115:2316–9.

40. Zumsteg A, Christofori G. Myeloid cells and lymphangiogenesis. Cold Spring Harbor Perspect Med 2012;2:a006494.

41. Xing L, Ji RC. Lymphangiogenesis, myeloid cells and inflammation. Expert Rev Clin Immunol 2008;4:599–613.

42. Kataru RP, Jung K, Jang C, Yang H, Schwendener RA, Baik JE, et al. Critical role of CD11b+ macrophages and VEGF in inflammatory lymphangiogenesis, antigen clearance, and inflammation resolution. Blood 2009;113:5650–9.

43. Machnik A, Neuhofer W, Jantsch J, Dahlmann A, Tammela T, Machura K, et al. Macrophages regulate salt-dependent volume and blood pressure by a vascular endothelial growth factor-C-dependent buffering mechanism. Nat Med 2009;15:545–52.

44. Kerjaschki D, Huttary N, Raab I, Regele H, Bojarski-Nagy K, Bartel G, et al. Lymphatic endothelial progenitor cells contribute to de novo lymphangiogenesis in human renal transplants. Nat Med 2006;12:230–4.

45. Lee JY, Park C, Cho YP, Lee E, Kim H, Kim P, et al. Podoplanin-expressing cells derived from bone marrow play a crucial role in postnatal lymphatic neovascularization. Circulation 2010;122:1413–25.

46. Maruyama K, Ii M, Cursiefen C, Jackson DG, Keino H, Tomita M, et al. Inflammation-induced lymphangiogenesis in the cornea arises from CD11b-positive macrophages. J Clin Invest 2005;115:2363–72.

47. Couchie D, Vaisman B, Abderrazak A, Mahmood DF, Hamza MM, Canesi F, et al. Human plasma thioredoxin-80 increases with age and in apoE−/− mice induces inflammation, angiogenesis and atherosclerosis. Circulation 2017;136:464–75.

48. Zhang MZ, Yao B, Wang Y, Yang S, Wang S, Fan X, et al. Inhibition of cyclooxygenase-2 in hematopoietic cells results in salt-sensitive hypertension. J Clin Invest 2015;125:4281–94.

49. Stegbauer J, Coffman TM. Skin tight: macrophage-specific COX-2 induction links salt handling in kidney and skin. J Clin Invest 2015; 125:4008–10.

50. Chevalier X, Goupille P, Beaulieu AD, Burch FX, Bensen WG, Conrozier T, et al. Intraarticular injection of anakinra in osteoarthritis of the knee: a multicenter, randomized, double-blind, placebo-controlled study. Arthritis Rheum 2009;61:344–52.

51. Chevalier X, Ravaud P, Maheu E, Baron G, Rialland A, Vergnaud P, et al. Adalimumab in patients with hand osteoarthritis refractory to analgesics and NSAIDs: a randomised, multicentre, double-blind, placebo-controlled trial. Ann Rheum Dis 2015;74:1697–705.

Clinical Images: Osseous involvement in calcific tendinitis—unusual in the usual
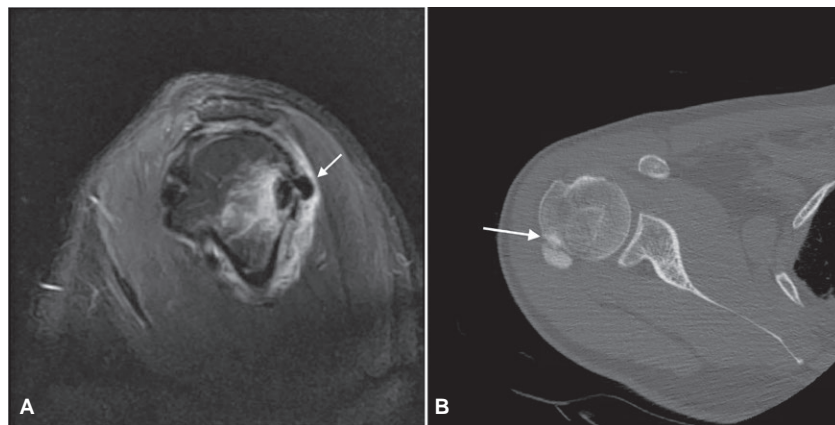
The patient, a 62-year-old man, was referred to us for ongoing right shoulder pain, particularly noticeable during performance of daily tasks. Physical examination demonstrated generalized pain with mobilization, more marked with external rotation, as well as limited abduction with a mechanical block at 60 degrees. Magnetic resonance imaging STIR sequences (**A**) revealed a low-signal-intensity structure at the footprint of the infraspinatus muscle (**arrow**) with an extra- and intraosseous component resembling an hourglass. Adjacent to the intraosseous component was hyperintensity of the bone marrow, consistent with edema, and a surrounding area of hyperintensity in the soft tissues, also representing edema. Computed axial tomography (**B**) demonstrated a homogeneous calcification with a region of mild adjacent cortical irregularity and a dense sclerotic region adjacent to the cortical area (**arrow**). Calcific tendinitis is a common condition caused by calcium hydroxyapatite deposition. In its usual presentation, calcific tendinitis is easily diagnosed, generally with radiography or ultrasound imaging, by the demonstration of calcification in classic locations (e.g., the tendon or the adjacent bursa). In exceptional cases, its imaging features will be unusually aggressive and involve underlying bony structures. These appearances may be confused with neoplastic processes and lead to further invasive investigations. Calcium hydroxyapatite deposition has been hypothesized to be due to decreased oxygen tension, leading to fibrocartilaginous metaplasia and subsequent mineralization. Osseous involvement is rare. Calcium hydroxyapatite deposition in tendons may produce focal hypervascularity, resulting in focal bone resorption at the enthesis. This process, associated with mechanical forces, may trigger cortical changes. A similar process is thought to occur when a periosteal reaction is present. In cases in which a combination of calcification and cystic lesions appears intramedullarly, calcium deposition paired with reparative response has been hypothesized.

Maria Pilar Aparisi Gómez, MBChB, FRANZCR iD
Auckland City Hospital
Auckland, New Zealand
  and Hospital Nueve de Octubre
  Valencia, Spain
Francisco Aparisi, MD, PhD
Hospital Nueve de Octubre
Valencia, Spain
Alberto Bazzocchi, MD, PhD
Rizzoli Orthopaedic Institute
Bologna, Italy

AMERICAN COLLEGE
OF RHEUMATOLOGY
EDUCATION · TREATMENT · RESEARCH

Three Multicenter, Randomized, Double-Blind, Placebo-Controlled Studies Evaluating the Efficacy and Safety of Ustekinumab in Axial Spondyloarthritis

Atul Deodhar,[1] Lianne S. Gensler,[2] Joachim Sieper,[3] Michael Clark,[4] Cesar Calderon,[4] Yuhua Wang,[4] Yiying Zhou,[4] Jocelyn H. Leu,[4] Kim Campbell,[4] Kristen Sweet,[4] Diane D. Harrison,[4] Elizabeth C. Hsia,[5] and Désirée van der Heijde[6]

Objective. To evaluate the efficacy and safety of ustekinumab in 3 randomized, placebo-controlled studies in patients with axial spondyloarthritis (SpA). Studies 1 and 2 included patients with radiographic axial SpA (anti–tumor necrosis factor [anti-TNF]–naive patients and patients with inadequate response or intolerance to anti-TNF, respectively); study 3 patients had nonradiographic axial SpA.

Methods. In all 3 studies, patients were randomly assigned (1:1:1) to receive subcutaneous ustekinumab at 45 mg or 90 mg or placebo up to 24 weeks, after which placebo-treated patients were rerandomized to receive ustekinumab at 45 mg or 90 mg. The primary end point in studies 1 and 2 was the proportion of patients who met the Assessment of SpondyloArthritis international Society criteria for 40% improvement in disease activity (achieved an ASAS40 response). The primary end point in study 3 was the proportion of patients who achieved an ASAS20 response. Other disease activity and safety measures were also evaluated. A week 24 analysis of study 1 was preplanned to determine continuation of studies 2 and 3.

Results. For study 1, the primary and major secondary end points were not met, and the study was discontinued. As a result, studies 2 and 3 were prematurely discontinued before they were fully enrolled. For all 3 studies, neither ustekinumab dose group demonstrated clinically meaningful improvement over placebo on key efficacy end points. The proportion of patients experiencing adverse events in the ustekinumab groups was consistent with that in previous studies.

Conclusion. In these 3 placebo-controlled trials, efficacy of ustekinumab in the treatment of axial SpA was not demonstrated. The safety profile was consistent with that of studies in other indications.

INTRODUCTION

Axial spondyloarthritis (SpA) is an immune-mediated systemic chronic inflammatory arthritis involving the axial skeleton that may involve peripheral joints. It is characterized by chronic inflammatory back pain (IBP), which typically has an insidious onset and improves with exercise but not rest (1). Axial SpA also manifests with sacroiliitis, spondylitis, and enthesitis, which may lead to ankylosis (1). Extraarticular manifestations include uveitis, inflammatory bowel disease, and psoriasis. Chronic inflamma-

tion in axial SpA can lead to bone loss and structural damage, including erosions and ankylosis of the sacroiliac (SI) joints and spine. This damage may lead to postural changes and mobility restriction resulting in functional impairment and decreased health-related quality of life (2,3). Patients with axial SpA include those with nonradiographic axial SpA (before the occurrence of definitive structural damage to the SI joints on radiography) and those with radiographic axial SpA. Patients with radiographic axial SpA and those with ankylosing spondylitis (AS) belong to the same subgroup, with slight differences in the exact definitions (4,5) (also see below).

Nonsteroidal antiinflammatory drugs (NSAIDs) are used to treat symptoms of axial SpA in many patients; however, conventional synthetic disease-modifying antirheumatic drugs (csDMARDs) or systemic glucocorticoids are ineffective for the axial component. Anti–tumor necrosis factor (anti-TNF) therapies are approved for use in AS globally and for nonradiographic axial SpA in many countries. More recently, a monoclonal antibody that inhibits interleukin-17A (IL-17A) was approved to treat adults with AS (6). Although these agents show efficacy in many patients with axial SpA, some patients do not respond adequately; thus, there is a need to target other mechanisms of action (7,8).

Axial SpA may be triggered by a combination of genetic and environmental factors. Axial SpA is strongly associated with HLA–B27, misfolding and accumulation of which can activate up-regulation of IL-23 production and induction of the Th17 axis (9). The IL-23/Th17 axis has gained attention recently as a possible inflammatory pathway for axial SpA (10,11), which suggests that IL-23 is involved in disease pathogenesis (12,13).

Ustekinumab, a human monoclonal antibody targeting the IL-12/23 p40 subunit, is effective in treating active psoriasis (14,15), Crohn's disease (16), and psoriatic arthritis (PsA) (17–20), including inhibition of radiographic progression, and has been shown to improve spondylitis symptoms in a subgroup of PsA patients with physician-reported spondylitis (21). A small, open-label study suggested preliminary efficacy of ustekinumab for the treatment of AS (8). Twenty patients with active AS received 90 mg ustekinumab at weeks 0, 4, and 16. Clinically meaningful improvements were noted at week 24, and significant improvements in inflammation were observed in magnetic resonance imaging (MRI) parameters (8). In the 3 randomized, placebo-controlled studies reported herein, efficacy and safety of ustekinumab were evaluated in patients with active axial SpA (radiographic or nonradiographic).

PATIENTS AND METHODS

Study design. Two parallel, phase III, multicenter, randomized, double-blind, placebo-controlled studies evaluated treatment with ustekinumab at 45 mg and 90 mg in patients with active radiographic axial SpA who had an inadequate response to or were intolerant of NSAIDs and who were naive to anti-TNF

therapy (study 1) or who were refractory (defined as having an inadequate response or intolerance) to a single anti-TNF agent (study 2). A third study (study 3) evaluated patients with active nonradiographic axial SpA who had an inadequate response to or were intolerant of NSAIDs and who could have been exposed to a single anti-TNF agent. These studies were conducted in accordance with the principles of the Declaration of Helsinki. Each patient gave written informed consent. An independent data monitoring committee regularly reviewed unblinded safety data. A list of investigators who randomized patients in the 3 trials is provided in Appendix A.

In all 3 studies, patients were randomly assigned (1:1:1) to receive subcutaneous (SC) administration of ustekinumab at 45 mg or 90 mg at weeks 0, 4, and 16 and then every 12 weeks or to receive placebo at weeks 0, 4, and 16. Placebo-treated patients were rerandomized at week 24 to receive ustekinumab at 45 mg or 90 mg at weeks 24 and 28 and then every 12 weeks. For studies 1 and 2, at week 16, patients in all 3 treatment groups who qualified for early escape (those with <10% improvement from baseline in both total back pain and morning stiffness measures at both week 12 and week 16) received open-label golimumab at 50 mg SC at week 16 and every 4 weeks thereafter through week 52. Final safety evaluations were to be performed at week 64 (study 2) and week 112 (study 1).

In study 3, patients in the placebo group who met early escape criteria were to be rerandomized at week 16 in a blinded manner to SC ustekinumab at 45 mg or 90 mg at weeks 16, 20, 28, and every 12 weeks thereafter through week 52. At week 24, all remaining placebo-treated patients crossed over to ustekinumab at either 45 mg or 90 mg at weeks 24 and 28, then every 12 weeks. All patients with inactive disease at both week 40 and week 52 were to be rerandomized at week 52 to either keep receiving ustekinumab or switch to placebo. The study was to continue to week 100.

Inclusion/exclusion criteria. A central reader assessed the presence or absence of radiographic sacroiliitis (according to the modified New York criteria for AS) for all 3 studies and the presence or absence of the ASAS/Outcome Measures in Rheumatology MRI group criteria for defining sacroiliitis by MRI (22) for study 3. In studies 1 and 2, eligible adult patients (age ≥18 years) fulfilled the modified New York criteria for AS (4). They also had active disease, defined as a Bath Ankylosing Spondylitis Disease Activity Index (BASDAI) (23) ≥4 and a visual analog scale score for total back pain ≥4 at screening and at baseline as well as a high-sensitivity C-reactive protein (hsCRP) level ≥0.3 mg/dl at screening. They also had an inadequate response to or intolerance of a single anti-TNF agent (patients in study 2) but were otherwise naive to biologic agents. Concomitant NSAIDs, glucocorticoids (≤10 mg prednisone equivalent per day), or the csDMARDs methotrexate, sulfasalazine, or hydroxychloroquine were permitted; however, doses of NSAIDs

and glucocorticoids were required to be stable for ≥2 weeks prior to baseline, and doses of csDMARDs were required to be stable for ≥4 weeks prior to baseline. Patients with complete ankylosis of the spine (assessed locally) were limited to 10% of the study population. Key exclusion criteria included other inflammatory diseases, active infection, uncontrolled concomitant diseases, and pregnancy.

For study 3, adults (ages 18–50 years) were eligible if they had active nonradiographic axial SpA that fulfilled the ASAS criteria for axial SpA (5) (back pain for ≥3 months and disease onset by age 45 years as well as evidence of active acute inflammation on MRI and ≥1 feature of SpA *or* HLA–B27 positive and ≥2 features of SpA) without radiographic sacroiliitis according to the modified New York criteria for AS (4). Patients without a positive MRI of the SI joints according to the ASAS definition required an elevated hsCRP ≥0.6 mg/dl at screening. All patients had active disease as defined in studies 1 and 2; patients could have been exposed to 1 anti-TNF agent.

Outcome assessments. *Primary and major secondary end points.* The primary end point was the proportion of patients who met the ASAS criteria for 40% improvement in disease activity (achieved an ASAS40 response) at week 24 in studies 1 and 2 and the proportion of patients who achieved an ASAS20 response at week 24 in study 3 (24–26). Major secondary end points were the proportions of patients who achieved an ASAS20 response (studies 1 and 2) and an ASAS40 response (study 3), the proportion of patients with 50% improvement in the BASDAI (a BASDAI50 response), change from baseline in the Bath Ankylosing Spondylitis Functional Index (BASFI) (27), and the proportion of patients with inactive disease according to the Ankylosing Spondylitis Disease Activity Score using the CRP level (an ASDAS-CRP score <1.3) (28).

Additional secondary end points. Additional secondary end points included changes from baseline in hsCRP level and ASDAS-CRP. A subset of patients from study 1 underwent MRI for spinal inflammation assessment using the Berlin MRI scoring method (29) (baseline and week 24, averaged scores of 2 central readers). During the double-blind period of studies 1, 2, and 3, serum samples were collected to evaluate ustekinumab pharmacokinetics, antibodies to ustekinumab, and/or biomarkers. Evaluation of the presence of antibodies to ustekinumab used a drug-tolerant enzyme chemiluminescent immunoassay in samples from patients who received ≥1 administration of ustekinumab and had ≥1 postadministration sample available.

Serum biomarkers were assayed using a Singulex system (IL-17A, IL-17F, IL-22, and IL-23), a Meso Scale Discovery Platform (matrix metalloproteinase 1 [MMP-1], MMP-3, MMP-9, interferon-γ [IFNγ], IL-12p70, IL-6, IL-8, TNFα, CRP, serum amyloid A [SAA], soluble intercellular adhesion molecule 1, and soluble vascular cell adhesion molecule 1), an R&D Systems Quantikine human enzyme-linked immunosorbent assay (CXCL13), and a

Cisbio human kit (S100 calcium binding protein A12). Biomarkers were evaluated in a subset of patients from studies 1 and 2, and clinical responders were oversampled versus the overall study population to increase statistical power for testing clinical response associations.

Due to discontinuation of the study, most secondary end points were only summarized for samples from study 1. Safety outcomes included the proportions of patients experiencing treatment-emergent adverse events (AEs) and serious AEs (SAEs) from baseline to the end of the study, along with clinical laboratory testing.

Statistical analysis. Sample sizes of all 3 studies were chosen to achieve 90% power to detect treatment differences between ustekinumab and placebo for the primary end point at a 2-sided significance level of 0.05. Sample size calculations were based on results from a ustekinumab investigator-initiated study and a certolizumab pegol axial SpA study (30). For study 1, the planned sample size calculation was based on anticipating an ASAS40 response of 40% in the ustekinumab group and 20% in the placebo group with n = 109 for each group. For study 2, the planned sample size calculation was based on an ASAS40 response of 30% in the ustekinumab group and 15% in the placebo group with n = 161 for each group. For study 3, the planned sample size calculation was based on the ASAS20 responses in the ustekinumab groups versus the placebo groups: 50% versus 35% in the anti-TNF inadequate responder group and 60% versus 40% in the other group (anti-TNF–naive and anti-TNF–experienced patients) with n = 130 for each group. It was preplanned to determine continuation of studies 2 and 3 based on the study 1 results at week 24.

For study 1, efficacy analyses were performed using the modified intent-to-treat (ITT) population, which included all patients who received ≥1 dose of study medication. Primary and major secondary end points were analyzed sequentially to control for multiplicity and were contingent on the success of the primary analysis.

Because studies 2 and 3 were terminated early based on study 1 results, a modified full analysis set was defined that included patients who were anticipated to have reached the week 24 visit. Additionally, only selected efficacy analyses through week 24, including primary and major secondary end points, were performed.

The following analysis rules were applied to all 3 studies. For dichotomous responder-type end points, patients with missing postbaseline responses or those who met treatment failure criteria (initiating new therapies or increasing concomitant medication doses for axial SpA or discontinuing study treatment due to lack of efficacy) were classified as nonresponders. Patients who entered early escape at week 16 were considered nonresponders for dichotomous end points at weeks 20 and 24; measurement values at those weeks were set as missing for continuous end

points. The Cochran-Mantel-Haenszel chi-square test was used to compare categorical variables. Generally, continuous parameters were compared using a repeated measures mixed model analysis with treatment group, strata, baseline value, visit week, and an interaction of treatment with visit week as independent variables. All statistical testing was performed at a 2-sided alpha level of 0.05. Patients who received ≥1 dose of study medication were included in safety analyses.

Serum proteins for biomarker analysis were assayed at weeks 0, 4, and 16 from a subset of patients from study 1 (n = 105 in ustekinumab treatment arms [pooled dose groups], n = 45 placebo-treated patients, n = 40 demographically matched healthy controls) and study 2 (n = 41 in ustekinumab treatment arms [pooled dose groups], n = 29 demographically matched healthy controls), with the exception of Th17 analytes, which

were measured only at baseline in a small subset of patients (n = 29 randomized to receive ustekinumab, n = 29 healthy controls). Significance was defined by $P < 0.05$ and absolute value of either fold change >1.2 or Pearson's correlation coefficient (r) of >0.25.

RESULTS

Patient disposition. Data were collected from July 2015 to September 2017. Patients were randomized at 58 sites in 7 countries for study 1, 114 sites in 19 countries for study 2, and 93 sites in 14 countries for study 3. The scheduled week 24 database lock and review of results for study 1 showed that the primary and major secondary end points were not met for either ustekinumab dose. As a result, the sponsor discontinued all 3 studies in May 2017.
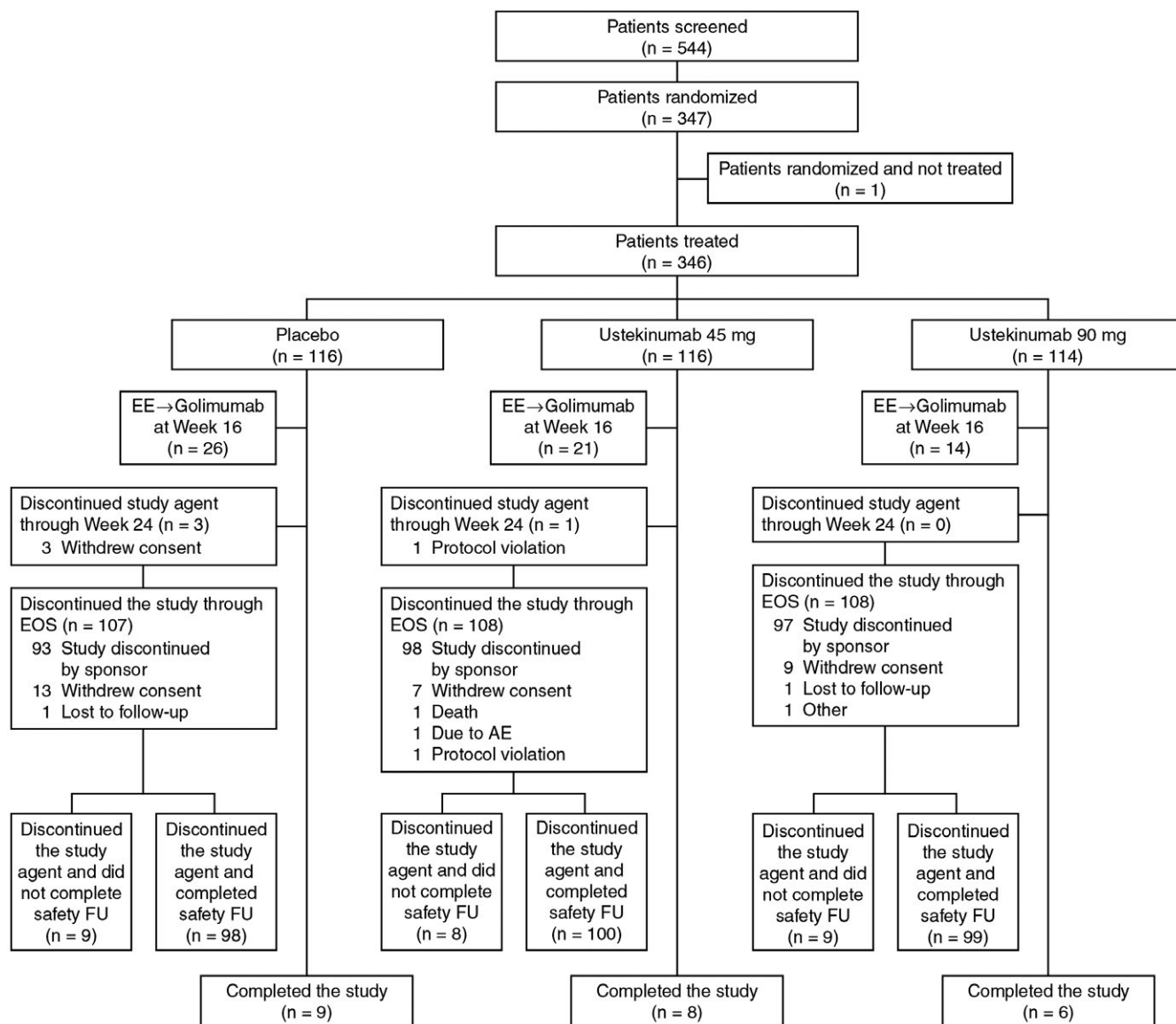
Figure 1. Patient disposition through week 24 for study 1 (anti–tumor necrosis factor–naive patients with ankylosing spondylitis). EE = early escape; EOS = end of study; AE = adverse event; FU = follow-up.

Table 1. Baseline demographic and disease characteristics of the patients in the 3 studies*

		Ustekinumab			
	Placebo	45 mg	90 mg	Combined	Total
Study 1 (anti-TNF–naive AS patients)†					
Age, years	38.3 ± 11.4	39.2 ± 10.5	39.5 ± 11.3	39.3 ± 10.9	39.0 ± 11.0
Men, no. (%)	101 (87.1)	93 (80.2)	100 (87.7)	193 (83.9)	294 (85.0)
White, no. (%)	86 (74.1)	84 (72.4)	82 (71.9)	166 (72.2)	252 (72.8)
IBP duration, years‡	10.6 ± 7.8	11.2 ± 8.2	10.5 ± 8.3	10.9 ± 8.2	10.8 ± 8.1
Years since AS diagnosis	6.6 ± 7.0	6.3 ± 7.1	6.3 ± 6.5	6.3 ± 6.8	6.4 ± 6.8
HLA–B27 positive, no. (%)	113 (97.4)	111 (95.7)	110 (96.5)	221 (96.1)	334 (96.5)
BASDAI, 0–10	7.4 ± 1.4	7.4 ± 1.3	7.3 ± 1.3	7.3 ± 1.3	7.4 ± 1.4
ASDAS-CRP‡	4.3 ± 0.8	4.3 ± 0.7	4.3 ± 0.9	4.3 ± 0.8	4.3 ± 0.8
ASAS components					
Patient's global assessment of disease activity, 0–10-cm VAS	7.5 ± 1.6	7.5 ± 1.6	7.6 ± 1.4	7.5 ± 1.5	7.5 ± 1.5
Total back pain, 0–10-cm VAS	7.6 ± 1.5	7.6 ± 1.4	7.7 ± 1.4	7.6 ± 1.4	7.6 ± 1.4
BASFI, 0–10	6.6 ± 2.2	6.8 ± 1.9	7.0 ± 1.6	6.9 ± 1.8	6.8 ± 1.9
Inflammation score§	7.5 ± 1.7	7.7 ± 1.5	7.7 ± 1.5	7.7 ± 1.5	7.6 ± 1.6
hsCRP, mg/dl¶	2.1 ± 2.1	2.1 ± 2.2	2.5 ± 3.1	2.3 ± 2.7	2.2 ± 2.5
Study 2 (AS patients with disease refractory to anti-TNF)†					
Age, years	40.8 ± 11.7	41.4 ± 11.3	41.5 ± 11.0	41.5 ± 11.2	41.2 ± 11.3
Men, no. (%)	80 (76.9)	88 (83.0)	92 (87.6)	180 (85.3)	260 (82.5)
White, no. (%)	82 (78.8)	84 (79.2)	84 (80.0)	168 (79.6)	250 (79.4)
IBP duration, years‡	13.8 ± 9.6	13.6 ± 8.1	15.3 ± 10.8	14.5 ± 9.6	14.3 ± 9.6
Years since AS diagnosis	7.8 ± 6.7	9.1 ± 7.9	9.6 ± 8.1	9.3 ± 8.0	8.8 ± 7.6
HLA–B27 positive, no. (%)	96 (92.3)	95 (89.6)	98 (93.3)	193 (91.5)	289 (91.7)
BASDAI, 0–10	7.5 ± 1.3	7.6 ± 1.4	7.5 ± 1.3	7.6 ± 1.3	7.5 ± 1.3
ASDAS-CRP‡	4.5 ± 0.8	4.4 ± 0.8	4.4 ± 0.8	4.4 ± 0.8	4.5 ± 0.8
ASAS components					
Patient's global assessment of disease activity, 0–10-cm VAS	8.1 ± 1.5	7.9 ± 1.4	7.9 ± 1.4	7.9 ± 1.4	8.0 ± 1.4
Total back pain, 0–10-cm VAS	7.8 ± 1.6	7.7 ± 1.5	7.8 ± 1.4	7.7 ± 1.4	7.8 ± 1.5
BASFI, 0–10	7.2 ± 1.6	6.9 ± 2.0	6.9 ± 1.7	6.9 ± 1.8	7.0 ± 1.8
Inflammation score§	7.8 ± 1.8	7.8 ± 1.9	7.8 ± 1.5	7.8 ± 1.7	7.8 ± 1.7
hsCRP, mg/dl¶	2.8 ± 3.2	2.6 ± 2.7	2.5 ± 2.5	2.5 ± 2.6	2.6 ± 2.8
Study 3 (patients with nonradiographic axial SpA)†					
Age, years	34.0 ± 8.8	33.9 ± 8.4	34.9 ± 9.1	34.4 ± 8.7	34.3 ± 8.7
Men, no. (%)	64 (55.2)	53 (44.9)	63 (51.6)	116 (48.3)	180 (50.6)
White, no. (%)	98 (84.5)	99 (83.9)	104 (85.2)	203 (84.6)	301 (84.6)
IBP duration, years‡	4.0 ± 4.6	4.3 ± 4.9	5.2 ± 5.9	4.8 ± 5.5	4.5 ± 5.2
Years since axial SpA diagnosis	1.4 ± 1.3	1.6 ± 1.5	1.6 ± 1.5	1.6 ± 1.5	1.5 ± 1.5
HLA–B27 positive, no. (%)	89 (76.7)	93 (79.5)	95 (77.9)	188 (78.7)	277 (78.0)

Table 1. *(Cont'd)*

| | Placebo | Ustekinumab | | | Total |
		45 mg	90 mg	Combined	
BASDAI, 0–10	7.3 ± 1.4	7.4 ± 1.4	7.4 ± 1.3	7.4 ± 1.3	7.4 ± 1.3
ASDAS-CRP‡	3.8 ± 0.9	3.7 ± 0.9	3.8 ± 0.9	3.8 ± 0.9	3.8 ± 0.9
ASAS components					
Patient's global assessment of disease activity, 0–10-cm VAS	7.6 ± 1.6	7.5 ± 1.5	7.5 ± 1.5	7.5 ± 1.5	7.5 ± 1.5
Total back pain, 0–10-cm VAS	7.5 ± 1.6	7.5 ± 1.6	7.6 ± 1.4	7.6 ± 1.5	7.6 ± 1.5
BASFI, 0–10	6.1 ± 2.2	6.2 ± 2.0	6.2 ± 2.0	6.2 ± 2.0	6.1 ± 2.0
Inflammation score§	7.3 ± 1.9	7.4 ± 1.8	7.4 ± 1.7	7.4 ± 1.7	7.4 ± 1.8
hsCRP, mg/dl¶	1.3 ± 2.0	1.3 ± 2.4	1.3 ± 2.1	1.3 ± 2.2	1.3 ± 2.1

* Except where indicated otherwise, values are the mean ± SD. Anti-TNF = anti–tumor necrosis factor; AS = ankylosing spondylitis; IBP = inflammatory back pain; ASDAS-CRP = Ankylosing Spondylitis Disease Activity Score using the C-reactive protein level; ASAS = Assessment of SpondyloArthritis international Society; VAS = visual analog scale; BASFI = Bath Ankylosing Spondylitis Functional Index; hsCRP = high-sensitivity CRP; SpA = spondyloarthritis.
† Study 1 included a total of 346 patients (116 treated with placebo, 116 treated with 45 mg ustekinumab, and 114 treated with 90 mg ustekinumab [total of 230 ustekinumab-treated patients combined]). Study 2 included a total of 315 patients (104 treated with placebo, 106 treated with 45 mg ustekinumab, and 105 treated with 90 mg ustekinumab [total of 211 ustekinumab-treated patients combined]). Study 3 included a total of 356 patients (116 treated with placebo, 118 treated with 45 mg ustekinumab, and 122 treated with 90 mg ustekinumab [total of 240 ustekinumab-treated patients combined]).
‡ Data missing at baseline for ≤2 patients.
§ Average of the last 2 questions of the Bath Ankylosing Spondylitis Disease Activity Index (BASDAI) concerning morning stiffness (0–10).
¶ Normal ≤0.287 mg/dl.

A total of 2,062 patients were screened, of whom 1,018 were randomized and 1,017 were treated (Figure 1; also see Supplementary Figures 1 and 2, available on the *Arthritis & Rheumatology* web site at http://onlinelibrary.wiley.com/doi/10.1002/art.40728/abstract). Safety data were evaluated for treated patients, and all 346 treated patients were evaluable for efficacy in study 1. Efficacy was evaluated in a subset of the modified ITT population for study 2 (n = 213, 44.1% of planned sample size) and study 3 (n = 250, 64.1% of planned sample size) as a result of sponsor-initiated early study termination.

Overall, in studies 1 and 2, respectively, 85% and 83% of patients were male, 73% and 79% were white, the mean age was 39.0 and 41.2 years, and the mean duration of IBP was 10.8 and 14.3 years. In study 3 overall, 51% of patients were male, 85% were white, the mean age was 34.3 years, and the mean duration of IBP was 4.5 years. Approximately 12% of patients in study 3 were anti-TNF experienced. Baseline demographics and disease characteristics are shown in Table 1. All patients in study 1 and study 2 met the modified New York criteria for AS, as specified in the protocol, and 92.8% and 93.7%, respectively, met the ASAS classification criteria for radiographic axial SpA (7.2% and 6.3% had IBP that started at or after age 45 years in study 1 and study 2, respectively, and therefore did not formally fulfill the ASAS axial SpA criteria).

The subset of patients included in the study 1 MRI analysis (n = 104) was primarily male (78%) and white (98%) and had a mean ± SD age of 38.2 ± 11.2 years, a mean ± SD duration of

IBP of 10.0 ± 8.4 years, and a mean ± SD hsCRP level of 2.7 ± 2.6 mg/dl. Mean baseline ASAS20/40 response component scores for this subset of patients ranged from 7.2 to 7.9.

Efficacy outcomes. Results for primary and major secondary end points for study 1 are shown in Figure 2 and Table 2. Those for studies 2 and 3 are shown in Table 2. In study 1 (patients naive to anti-TNF therapy), the primary end point (an ASAS40 response) and major secondary end points were not achieved. At week 16, early escape criteria were met by 22% of patients in the placebo group, 18% of patients in the ustekinumab 45 mg group, and 12% of patients in the ustekinumab 90 mg group. No patient met treatment failure criteria. The proportions of patients who achieved an ASAS40 response in the ustekinumab 45 mg (31%) and 90 mg (28%) groups and in the placebo group (28%) were not significantly different (Figure 2A). Neither ustekinumab dose group demonstrated improvement over placebo in achieving an ASAS20 response, a BASDAI50 response, inactive disease according to the ASDAS-CRP (a score <1.3), or mean change from baseline in the BASFI (Figures 2B and C). In general, secondary efficacy and health-related quality of life end points did not show meaningful differences between treatment groups. However, modest improvement was noted for the change in hsCRP level from baseline, which was generally greater in both ustekinumab groups than in the placebo group as early as week 4 through week 24. At week 24, mean changes from baseline in hsCRP level were numerically higher in the

ustekinumab-treated groups than in the placebo group (Table 2). Additionally, in the MRI substudy, the mean change from baseline in the Berlin MRI spine score for patients evaluated at week 24 was −0.6 for the ustekinumab 45 mg group, −1.2 for the ustekinumab 90 mg group, and −0.5 for the placebo group.

In study 2 (patients with disease refractory to a single anti-TNF agent), early study discontinuation prohibited valid statistical testing and formulating subsequent clinical conclusions. The proportion of patients with an ASAS40 response (the primary end point) in the ustekinumab 45 mg and 90 mg groups was 19% and 27%, respectively, and 12% in the placebo group. Similar patterns were noted for major secondary end points (Table 2). At week 24, mean changes from baseline in hsCRP level were not numerically higher in the ustekinumab-treated groups than in the placebo group (Table 2).

In study 3 (patients with nonradiographic axial SpA), 55% and 49% of patients in the ustekinumab 45 mg and 90 mg groups, respectively, achieved an ASAS20 response (the primary end point) versus 48% in the placebo group. Similar patterns were noted in major secondary end points (Table 2). At week 24, mean changes from baseline in hsCRP level were numerically higher in the ustekinumab-treated groups than in the placebo group (Table 2).

Safety. Through the end of week 24, the proportions of patients experiencing AEs in the ustekinumab groups were consistent across treatment groups in all 3 studies (Tables 3 and 4) and similar between the active treatment and placebo groups. No patient died, experienced a serious or opportunistic infec-

tion, or presented with malignancy or active tuberculosis. In all 3 studies, <2.0% of ustekinumab-treated patients had an injection site reaction; all were mild in severity.

In study 1, through week 24, 43% of patients in the placebo group and 40% in the combined ustekinumab groups had ≥1 AE. No patient in study 1 discontinued due to AEs through week 24 (Table 3). During this period, 2 placebo-treated patients reported an SAE (ischemic stroke and vertebrobasilar insufficiency). In the combined ustekinumab groups, 3 patients reported an SAE (subdural hematoma, osteoarthritis, and facial paralysis).

The proportion of patients reporting AEs through week 24 for study 2 (Table 3) and study 3 (Table 4) was similar to the proportion in study 1 (Table 3). In study 2, discontinuation due to an AE through week 24 occurred for 1 placebo-treated patient (back and musculoskeletal pain) and 3 ustekinumab-treated patients (worsening of AS, arthralgia, and back pain). During this period, 3 SAEs were reported in 3 placebo-treated patients (uterine prolapse, back pain, and myocardial ischemia), and 10 SAEs were reported in 7 ustekinumab-treated patients (upper abdominal pain, nausea, vomiting, obesity, uterine polyp, gastrointestinal hemorrhage, cholelithiasis, worsening of AS, rotator cuff syndrome, and cerebrovascular accident). In study 3, 1 ustekinumab-treated patient discontinued due to an AE (pustular psoriasis) through week 24. During this period, SAEs were reported for 2 placebo-treated patients (uveitis and worsening of axial SpA) and 3 ustekinumab-treated patients (inguinal hernia, chronic sinusitis, and ankle fracture).

For all 3 studies, through the end of the study (see Supplementary Tables 1 and 2, http://onlinelibrary.wiley.com/doi/
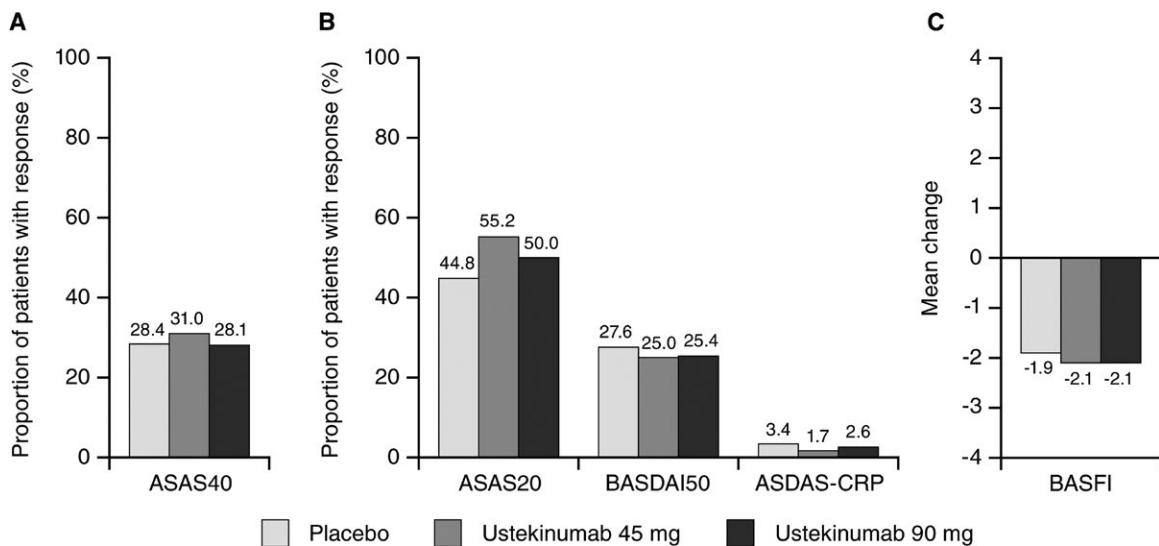
Figure 2. Primary and major secondary end points at week 24 for study 1 (anti–tumor necrosis factor–naive patients with ankylosing spondylitis). **A,** Primary end point: the proportion of patients who met the Assessment of SpondyloArthritis international Society criteria for 40% improvement in disease activity (achieved an ASAS40 response). **B,** Major secondary end points: the proportion of patients who achieved an ASAS20 response, the proportion of patients with 50% improvement in the Bath Ankylosing Spondylitis Disease Activity Index (a BASDAI50 response), and the proportion of patients with inactive disease according to the Ankylosing Spondylitis Disease Activity Score using the C-reactive protein level (an ASDAS-CRP score <1.3). **C,** Mean change from baseline in the Bath Ankylosing Spondylitis Functional Index (BASFI). There were no significant differences between either dose group and the placebo group.

Table 2. Primary, major secondary, and other selected end points at week 24 in the 3 studies*

| | Study 1 (anti-TNF–naive AS patients) | | | Study 2 (AS patients with disease refractory to anti-TNF) | | | Study 3 (patients with nonradiographic axial SpA) | | |
| | | Ustekinumab | | | Ustekinumab | | | Ustekinumab | |
	Placebo (n = 116)	45 mg (n = 116)	90 mg (n = 114)	Placebo (n = 73)	45 mg (n = 73)	90 mg (n = 67)	Placebo (n = 82)	45 mg (n = 83)	90 mg (n = 85)
ASAS40 response, no. (%)†	33 (28.4)	36 (31.0)	32 (28.1)	9 (12.3)	14 (19.2)	18 (26.9)	21 (25.6)	28 (33.7)	24 (28.2)
ASAS20 response, no. (%)†	52 (44.8)	64 (55.2)	57 (50.0)	20 (27.4)	23 (31.5)	25 (37.3)	39 (47.6)	46 (55.4)	42 (49.4)
BASDAI50 response, no. (%)	32 (27.6)	29 (25.0)	29 (25.4)	8 (11.0)	11 (15.1)	19 (28.4)	19 (23.2)	27 (32.5)	22 (25.9)
Inactive disease according to ASDAS-CRP, no. (%)	4 (3.4)	2 (1.7)	3 (2.6)	0	2 (2.7)	2 (3.0)	6 (7.3)	12 (14.5)	11 (12.9)
Change from baseline in ASDAS-CRP	−1.1 ± 1.1 (85)	−1.2 ± 1.0 (95)	−1.1 ± 1.0 (98)	−0.8 ± 1.0 (43)	−1.0 ± 1.1 (44)	−1.1 ± 1.1 (42)	−1.2 ± 1.1 (61)	−1.4 ± 1.4 (71)	−1.4 ± 1.2 (62)
Change from baseline in hsCRP, mg/dl	−0.4 ± 1.7 (87)	−0.7 ± 1.6 (95)	−0.9 ± 2.3 (98)	−0.4 ± 2.1 (43)	−0.1 ± 2.0 (44)	−0.3 ± 1.9 (43)	−0.4 ± 2.2 (61)	−0.6 ± 2.5 (71)	−1.0 ± 2.7 (62)
Change from baseline in BASFI	−1.9 ± 2.1 (88)	−2.1 ± 2.3 (95)	−2.1 ± 2.5 (99)	−1.3 ± 2.2 (44)	−1.7 ± 2.7 (44)	−2.2 ± 2.4 (42)	−2.1 ± 2.4 (61)	−2.3 ± 2.6 (72)	−1.9 ± 2.7 (63)

* Except where indicated otherwise, values are the mean ± SD (no. of patients). Anti-TNF = anti–tumor necrosis factor; AS = ankylosing spondylitis; SpA = spondyloarthritis; BASDAI50 response = 50% improvement in the Bath Ankylosing Spondylitis Disease Activity Index; ASDAS-CRP = Ankylosing Spondylitis Disease Activity Score using the C-reactive protein level; hsCRP = high-sensitivity CRP; BASFI = Bath Ankylosing Spondylitis Functional Index.
† For studies 1 and 2, 40% improvement in disease activity according to the Assessment of SpondyloArthritis international Society criteria (an ASAS40 response) was the primary end point, and achieving an ASAS20 response was a major secondary end point. For study 3, achieving an ASAS20 response was the primary end point, and achieving an ASAS40 response was a major secondary end point.

10.1002/art.40728/abstract), the safety profile was consistent with what was reported through week 24 (Tables 3 and 4). In study 1, after week 24, an additional 6 ustekinumab-treated patients reported 9 SAEs. In study 2, after week 24, an additional 3 ustekinumab-treated patients reported SAEs. In study 3, after week 24, an additional 7 ustekinumab-treated patients reported SAEs. Serious infections were reported for 2 patients in study 1 and 1 patient in study 3. No patient presented with malignancy or active tuberculosis. In study 1, after week 52, 1 patient (randomized to 45 mg ustekinumab then early escaped to golimumab) was reported to have a fatal SAE of blunt trauma. No deaths were reported for studies 2 or 3.

Pharmacokinetics and immunogenicity. After administration of ustekinumab at week 0 and week 4 then every 12 weeks in study 1, serum ustekinumab concentrations were dose proportional without evidence of accumulation in ustekinumab concentrations over time, which was similar to prior studies with ustekinumab in PsA. Ustekinumab concentrations were reviewed to confirm that patients received their assigned treatment (ustekinumab or placebo). Given the fixed dosing of ustekinumab, median ustekinumab concentrations were gener-

ally higher in the lower body weight quartiles than in the higher body weight quartiles. Patients with lower baseline hsCRP levels had higher median ustekinumab concentrations than those with higher baseline hsCRP levels. Through week 24, median ustekinumab concentrations were lower for ASAS40 nonresponders than for responders after receiving ustekinumab at 45 mg; however, median ustekinumab concentrations were similar between ASAS40 responders and nonresponders for those who received ustekinumab at 90 mg. ASAS20 and ASAS40 response rates were consistent across the 4 trough ustekinumab concentration quartiles.

Antibodies to ustekinumab were detected in 18% of 230 patients through week 24 using a validated drug-tolerant enzyme chemiluminescent immunoassay. Antibody peak titers were generally low, with 26 (11%) of 230 patients found to be positive for neutralizing antibodies. Patients positive for antibodies to ustekinumab had similar ASAS20 responses and higher ASAS40 responses than patients negative for antibodies to ustekinumab. No antibody-positive patients and 1 antibody-negative patient had an injection site reaction through week 24. Due to the early discontinuation, these analyses were not performed for studies 2 and 3.

Table 3. Summary of AEs through week 24 in studies 1 and 2*

	Placebo/early escape		Ustekinumab 45 mg/ early escape		Ustekinumab 90 mg/ early escape		Ustekinumab only combined†
	Placebo†	Placebo→ golimumab‡	45 mg only†	45 mg→ golimumab‡	90 mg only†	90 mg→ golimumab‡	
Study 1 (anti-TNF–naive AS patients)§							
Duration of follow-up, weeks	22.1	8.0	22.6	8.0	23.0	7.9	22.8
Exposure, number of administrations	2.8	2.0	2.8	2.0	2.9	2.0	2.8
Patients with ≥1 AE, no. (%)	50 (43.1)	1 (3.8)	46 (39.7)	4 (19.0)	46 (40.4)	2 (14.3)	92 (40.0)
Patients with ≥1 SAE, no. (%)	2 (1.7)	0	2 (1.7)	0	1 (0.9)	0	3 (1.3)
Patients with AE leading to discontinuation, no. (%)	0	0	0	0	0	0	0
Patients with ≥1 infections, no. (%)	19 (16.4)	0	18 (15.5)	2 (9.5)	24 (21.1)	1 (7.1)	42 (18.3)
Patients with ≥1 serious infections, no. (%)	0	0	0	0	0	0	0
Study 2 (AS patients with disease refractory to anti-TNF)§							
Duration of follow-up, weeks	19.4	7.9	19.5	8.1	19.9	8.1	19.7
Exposure, number of administrations	2.6	2.0	2.5	2.0	2.6	2.0	2.5
Patients with ≥1 AE, no. (%)	47 (45.2)	2 (9.5)	44 (41.5)	8 (38.1)	42 (40.0)	4 (20.0)	86 (40.8)
Patients with ≥1 SAE, no. (%)	1 (1.0)	2 (9.5)	2 (1.9)	0	5 (4.8)	0	7 (3.3)
Patients with AE leading to discontinuation, no. (%)	1 (1.0)	0	1 (0.9)	0	2 (1.9)	0	3 (1.4)
Patients with ≥1 infections, no. (%)	17 (16.3)	0	16 (15.1)	3 (14.3)	17 (16.2)	1 (5.0)	33 (15.6)
Patients with ≥1 serious infections, no. (%)	0	0	0	0	0	0	0

* Except where indicated otherwise, values are the mean. Anti-TNF = anti–tumor necrosis factor; AS = ankylosing spondylitis; SAE = serious adverse event.
† Includes all patients, but AEs for patients who escaped early at week 16 are only counted up to week 16.
‡ Includes only patients who escaped early at week 16. AEs are counted from early escape onward.
§ Study 1 included 116 patients treated with placebo (of whom 26 escaped early), 116 treated with 45 mg ustekinumab (of whom 21 escaped early), and 114 treated with 90 mg ustekinumab (of whom 14 escaped early). A total of 230 patients in study 1 were treated with ustekinumab. Study 2 included 104 patients treated with placebo (of whom 21 escaped early), 106 treated with 45 mg ustekinumab (of whom 21 escaped early), and 105 treated with 90 mg ustekinumab (of whom 20 escaped early). A total of 211 patients in study 2 were treated with ustekinumab.

Biomarker analysis. In study 1, 10 of 18 analytes tested at baseline were either correlated with disease activity (ASDAS) or were elevated compared with matched healthy controls. However, neither Th17 cytokines (IL-17A, IL-17F, IL-22, and IL-23) nor Th1 cytokines (IFNγ and IL-12p70) were dysregulated at baseline in AS patients compared with healthy controls (see Supplementary Table 3, http://onlinelibrary.wiley.com/doi/10.1002/art.40728/abstract). In study 2, overall, there was greater elevation of inflammatory cytokines compared with study 1, including the statistically significant dysregulation of IL-17A, MMP-3, and MMP-9 (but not IL-17F, IFNγ, or IL-12p70), which did not

reach statistical significance in study 1. Additionally, a higher fold change of SAA, CRP level, and TNFα was observed in the cohort from study 2. Although overall baseline levels of IL-17A were slightly higher in axial SpA patients enrolled in study 2 compared with healthy controls, there was no association with clinical response in this small sample.

In study 1, ustekinumab treatment had only a relatively minor impact on analytes at weeks 4 and 16, with only MMP-3, SAA, and IL-8 being significantly decreased. The decreases in these 3 analytes were independent of week 16 ASAS20 clinical response. In summary, in these cohorts, up-regulation of acute

Table 4. Summary of AEs through week 24 in study 3 (patients with nonradiographic axial SpA)*

	Placebo (n = 116)†	Placebo→ ustekinumab 45 mg (n = 10)‡	Placebo→ ustekinumab 90 mg (n = 10)‡	Ustekinumab 45 mg only (n = 118)	Ustekinumab 90 mg only (n = 122)	Ustekinumab only combined (n = 260)
Duration of follow-up, weeks	21.7	7.9	8.1	22.3	22.0	21.0
Exposure, number of administrations	3.3	1.9	1.9	2.8	2.7	2.7
Patients with ≥1 AE, no. (%)	52 (44.8)	1 (10.0)	3 (30.0)	57 (48.3)	58 (47.5)	119 (45.8)
Patients with ≥1 SAE, no. (%)	2 (1.7)	0	0	2 (1.7)	1 (0.8)	3 (1.2)
Patients with AE leading to discontinuation, no. (%)	0	0	0	0	1 (0.8)	1 (0.4)
Patients with ≥1 infections, no. (%)	26 (22.4)	1 (10.0)	1 (10.0)	22 (18.6)	30 (24.6)	54 (20.8)
Patients with ≥1 serious infections, no. (%)	0	0	0	0	0	0

* Except where indicated otherwise, values are the mean. SpA = spondyloarthritis; SAE = serious adverse event.
† Includes all patients, but AEs for patients who escaped early at week 16 are only counted up to week 16.
‡ Includes only patients who escaped early at week 16. AEs are counted from early escape onward.

inflammatory proteins (and MMPs) was seen, but very modest to no elevation of Th17/Th1 cytokines in the periphery was observed.

DISCUSSION

The patients in these 3 randomized, placebo-controlled, phase III studies demonstrated significant systemic inflammatory burden, as evidenced by mean disease activity scores and elevated hsCRP levels at baseline. Patients in study 3 (those with nonradiographic axial SpA) required a positive MRI or hsCRP ≥0.6 mg/dl at screening. Results from the week 24 database lock of study 1 showed no treatment effect between ustekinumab and placebo groups across primary and major secondary end points. Based on these results, the sponsor discontinued all 3 studies early. Not all patients in studies 2 and 3 reached the week 24 time point when the studies were discontinued, limiting the extent of those efficacy analyses. The efficacy data available through week 24 of studies 2 and 3 were inconclusive; however, no consistent trends of clinically relevant response were observed among primary and major secondary end points.

Because no formal phase II dose-ranging study was performed, it may be questioned whether the ustekinumab doses studied were too low to achieve clinical response in axial SpA. Median serum ustekinumab concentrations were lower for ASAS40 nonresponders compared with responders receiving the 45 mg dose but were similar for those receiving the 90 mg dose. However, no difference was seen in ASAS20 or ASAS40 response rates across the trough concentration quartiles. Also, studies 1 and 3 showed little difference between doses in the proportions of patients achieving primary and major secondary end points, with the lower dose (45 mg) having a slight numerical advantage in study 3. In study 2, there appeared to be a dose response, but the separation from placebo was limited, and it was not consistent across end points. The hsCRP level in the ustekinumab groups was modestly improved at most time points compared with placebo in studies 1 and 3, but not in study 2, which is in direct contrast to the hint of efficacy in clinical end points seen in study 2. The MRI differences from study 1 favored 90 mg slightly, while 45 mg and placebo were almost equivalent, which contrasts with the lack of clinical benefit demonstrated. Overall, these differences may represent chance variation over the program.

Blocking IL-12/IL-23p40 with ustekinumab has been shown to be efficacious in plaque psoriasis, PsA, and Crohn's disease (14–20), in which activation of the IL-23/IL-17 pathway has been reported (31–33). Despite both the scientific and clinical rationale for supporting initiation of these phase III studies of ustekinumab in axial SpA, including an open-label study of patients with AS (8) and improvement in PsA patients with physician-reported spondylitis (21), questions remain as to why ustekinumab was not effective. A recent review highlighted differences in axial disease in AS and PsA, suggesting that spondylitis may be driven by different mechanisms in these 2 diseases (34). While the immunopathogenesis of axial SpA remains unknown, the interplay of genetics (HLA–B27) with exposure to microbial triggers

originating from the gut or skin along with dysregulated innate and adaptive immune responses (the Th17 pathway) has been implicated (35). Although reports of up-regulation of the Th17 pathway in the spine and joints have been published (36,37), there is conflicting evidence regarding dysregulation of the IL-23/IL-17 axis in the serum of AS patients (38–40). In the biomarker subpopulation that was assayed, up-regulation of serum IL-17A was modestly increased only in study 2, but there was no baseline elevation in serum IL-12p70, IL-23, IFNγ, and IL-17A/F in axial SpA patients compared with healthy controls in either study. It is not clear how these findings relate to the lack of clinically relevant efficacy of ustekinumab observed in these studies. It should be noted that serum cytokine levels may not fully represent disease mechanisms present locally in the joints or spine.

The therapeutic success of TNF and IL-17 blockers in controlling axial SpA disease activity suggests that the etiology of axial SpA may involve both inflammatory and immune mechanisms. IL-23+ and IL-17+ cells, more so than IL-12+ cells, have been observed in the spine of patients with AS (36). Blockade of IL-12/IL-23p40 with ustekinumab did not show efficacy in AS, but neutralization of IL-17A is clinically effective (41), which suggests that the interplay between IL-12, IL-23, and IL-17 is complex in axial SpA and warrants further studies to understand the results. There may be synergistic or opposing effects of inhibiting IL-12 and IL-23 or sources of IL-17 secreted independently of Th17 cells. For example, there is evidence to suggest that innate γδ T cells secrete IL-17 independently of IL-23 to protectively maintain the integrity of the epithelial barrier and prevent excessive permeability after injury (42,43). Imbalances in immunopathogenic mechanisms driven by innate lymphoid cell populations may help explain the ineffectiveness of ustekinumab in axial SpA.

AEs reported in these studies were consistent with the known safety profile of ustekinumab (15,16,19,20). Through week 24, AE rates in the combined ustekinumab groups were similar to those in the placebo group in each study. Infections were the most common type of AE in all 3 studies. Through the end of the study, SAEs were reported by 3.2% of ustekinumab-treated patients, including 3 patients (0.3%) with serious infections. There were no opportunistic infections or malignancies during these studies.

Ustekinumab does not appear to be effective in the treatment of axial SpA. Additional research is needed to better understand the pathogenic mechanisms and the cytokine pathways that manifest as axial SpA. No new safety signals were identified, and the safety profile of ustekinumab in these populations was consistent with that observed in other indications.

ACKNOWLEDGMENTS

AUTHOR CONTRIBUTIONS

All authors were involved in drafting the article or revising it critically for important intellectual content, and all authors approved the final version to be published. Dr. Deodhar had full access to all of the data in the study and takes responsibility for the integrity of the data and the accuracy of the data analysis.

Study conception and design. Deodhar, Gensler, Sieper, Wang, Leu, Sweet, Harrison, Hsia, van der Heijde.
Acquisition of data. Deodhar, Clark, Calderon, Hsia.
Analysis and interpretation of data. Deodhar, Gensler, Sieper, Clark, Calderon, Wang, Zhou, Leu, Campbell, Sweet, Harrison, Hsia, van der Heijde.

ROLE OF THE STUDY SPONSOR

REFERENCES

1. Sieper J, van der Heijde D, Landewe R, Brandt J, Burgos-Vagas R, Collantes-Estevez E, et al. New criteria for inflammatory back pain in patients with chronic back pain: a real patient exercise by experts from the Assessment of SpondyloArthritis international Society (ASAS). Ann Rheum Dis 2009;68:784–8.

2. Sieper J, Poddubnyy D. Axial spondyloarthritis. Lancet 2017; 390:73–84.

3. Van der Horst-Bruinsma IE, Nurmohamed MT, Landewe RB. Comorbidities in patients with spondyloarthritis. Rheum Dis Clin North Am 2012;38:523–38.

4. Van der Linden S, Valkenburg HA, Cats A. Evaluation of diagnostic criteria for ankylosing spondylitis: a proposal for modification of the New York criteria. Arthritis Rheum 1984;27:361–8.

5. Rudwaleit M, van der Heijde D, Landewe R, Listing J, Akkoc N, Brandt J, et al. The development of Assessment of SpondyloArthritis international Society classification criteria for axial spondyloarthritis (part II): validation and final selection. Ann Rheum Dis 2009;68:777–83.

6. Cosentyx (secukinumab) [package insert]. East Hanover (NJ): Novartis Pharmaceutical; 2016. URL: https://www.accessdata.fda.gov/drugsatfda_docs/label/2016/125504s001s002lbl.pdf.

7. Akkoc N, Can G, D'Angelo S, Padula A, Olivieri I. Therapies of early, advanced, and late onset forms of axial spondyloarthritis, and the need for treat to target strategies. Curr Rheumatol Rep 2017;19:8.

8. Poddubnyy D, Hermann KG, Callhoff J, Listing J, Sieper J. Ustekinumab for the treatment of patients with active ankylosing spondyli-

tis: results of a 28-week, prospective, open-label, proof-of-concept study (TOPAS). Ann Rheum Dis 2014;73:817–23.

9. Colbert RA, Tran TM, Layh-Schmitt G. HLA-B27 misfolding and ankylosing spondylitis. Mol Immunol 2014;57:44–51.

10. Wellcome Trust Case Control Consortium, Australo-Anglo-American Spondylitis Consortium, Burton PR, Clayton DG, Cardon LR, Craddock N, et al. Association scan of 14,500 nonsynonymous SNPs in four diseases identifies autoimmunity variants. Nat Genet 2007;39:1329–37.

11. Shen H, Goodall JC, Hill Gaston JS. Frequency and phenotype of peripheral blood Th17 cells in ankylosing spondylitis and rheumatoid arthritis. Arthritis Rheum 2009;60:1647–56.

12. Jandus C, Bioley G, Rivals JP, Dudler J, Speiser D, Romero P. Increased numbers of circulating polyfunctional Th17 memory cells in patients with seronegative spondylarthritides. Arthritis Rheum 2008;58:2307–17.

13. Hreggvidsdottir HS, Noordenbos T, Baeten DL. Inflammatory pathways in spondyloarthritis. Mol Immunol 2014;57:28–37.

14. Leonardi CL, Kimball AB, Papp KA, Yeilding N, Guzzo C, Wang Y, et al. Efficacy and safety of ustekinumab, a human interleukin-12/23 monoclonal antibody, in patients with psoriasis: 76-week results from a randomised, double-blind, placebo-controlled trial (PHOENIX 1). Lancet 2008;371:1665–74.

15. Papp KA, Langley RG, Lebwohl M, Krueger GG, Szapary P, Yeilding N, et al. Efficacy and safety of ustekinumab, a human interleukin-12/23 monoclonal antibody, in patients with psoriasis: 52-week results from a randomised, double-blind, placebo-controlled trial (PHOENIX 2). Lancet 2008;371:1675–84.

16. Feagan BG, Sandborn WJ, Gasink C, Jacobstein D, Lang Y, Friedman JR, et al. Ustekinumab as induction and maintenance therapy for Crohn's disease. N Engl J Med 2016;375:1946–60.

17. Kavanaugh A, Puig L, Gottlieb AB, Ritchlin C, Li S, Wang Y, et al. Maintenance of clinical efficacy and radiographic benefit through two years of ustekinumab therapy in patients with active psoriatic arthritis: results from a randomized, placebo-controlled Phase III trial. Arthritis Care Res (Hoboken) 2015;67:1739–49.

18. Kavanaugh A, Ritchlin C, Rahman P, Puig L, Gottlieb AB, Li S, et al. Ustekinumab, an anti-IL-12/23 p40 monoclonal antibody, inhibits radiographic progression in patients with active psoriatic arthritis: results of an integrated analysis of radiographic data from the phase 3, multicentre, randomised, double-blind, placebo-controlled PSUMMIT-1 and PSUMMIT-2 trials. Ann Rheum Dis 2014;73:1000–6.

19. McInnes IB, Kavanaugh A, Gottlieb AB, Puig L, Rahman P, Ritchlin C, et al. Efficacy and safety of ustekinumab in patients with active psoriatic arthritis: 1 year results of the phase 3, multicentre, double-blind, placebo-controlled PSUMMIT 1 trial. Lancet 2013;382:780–9.

20. Ritchlin C, Rahman P, Kavanaugh A, McInnes IB, Puig L, Li S, et al. Efficacy and safety of the anti-IL-12/23 p40 monoclonal antibody, ustekinumab, in patients with active psoriatic arthritis despite conventional non-biological and biological anti-tumour necrosis factor therapy: 6-month and 1-year results of the phase 3, multicentre, double-blind, placebo-controlled, randomised PSUMMIT 2 trial. Ann Rheum Dis 2014;73:990–9.

21. Kavanaugh A, Puig L, Gottlieb AB, Ritchlin C, You Y, Li S, et al. Efficacy and safety of ustekinumab in psoriatic arthritis patients with peripheral arthritis and physician-reported spondylitis: post-hoc analyses from two phase III, multicentre, double-blind, placebo-controlled studies (PSUMMIT-1/PSUMMIT-2). Ann Rheum Dis 2016;75:1984–8.

22. Rudwaleit M, Jurik AG, Hermann KG, Landewé R, van der Heijde D, Baraliakos X, et al. Defining active sacroiliitis on magnetic resonance imaging (MRI) for classification of axial spondyloarthritis: a consensual approach by the ASAS/OMERACT MRI group. Ann Rheum Dis 2009;68:1520–7.

23. Garrett S, Jenkinson T, Kennedy LG, Whitelock H, Gaisford P, Calin A. A new approach to defining disease status in ankylosing spondylitis: the Bath Ankylosing Spondylitis Disease Activity Index. J Rheumatol 1994;21:2286–91.

24. Anderson JJ, Baron G, van der Heijde D, Felson DT, Dougados M. Ankylosing spondylitis assessment group preliminary definition of short-term improvement in ankylosing spondylitis. Arthritis Rheum 2001;44:1876–86.

25. Sieper J, Rudwaleit M, Baraliakos X, Brandt J, Braun J, Burgos-Vargas R, et al. The assessment of SpondyloArthritis international Society (ASAS) handbook: a guide to assess spondyloarthritis. Ann Rheum Dis 2009;68 Suppl 2:ii1–44.

26. Van der Heijde D, Sieper J, Maksymowych WP, Dougados M, Burgos-Vargas R, Landewe R, et al. 2010 update of the international ASAS recommendations for the use of anti-TNF agents in patients with axial spondyloarthritis. Ann Rheum Dis 2011;70:905–8.

27. Calin A, Garrett S, Whitelock H, Kennedy LG, O'Hea J, Mallorie P, et al. A new approach to defining functional ability in ankylosing spondylitis: the development of the Bath Ankylosing Spondylitis Functional Index. J Rheumatol 1994;21:2281–5.

28. Machado P, Landewe R, Lie E, Kvien TK, Braun J, Baker D, et al. Ankylosing Spondylitis Disease Activity Score (ASDAS): defining cut-off values for disease activity states and improvement scores. Ann Rheum Dis 2011;70:47–53.

29. Braun J, Baraliakos X, Golder W, Hermann KG, Listing J, Brandt J, et al. Analysing chronic spinal changes in ankylosing spondylitis: a systematic comparison of conventional x rays with magnetic resonance imaging using established and new scoring systems. Ann Rheum Dis 2004;63:1046–55.

30. Landewe R, Braun J, Deodhar A, Dougados M, Maksymowych WP, Mease PJ, et al. Efficacy of certolizumab pegol on signs and symptoms of axial spondyloarthritis including ankylosing spondylitis: 24-week results of a double-blind randomised placebo-controlled Phase 3 study. Ann Rheum Dis 2014;73:39–47.

31. Alunno A, Carubbi F, Cafaro G, Pucci G, Battista F, Bartoloni E, et al. Targeting the IL-23/IL-17 axis for the treatment of psoriasis and psoriatic arthritis. Expert Opin Biol Ther 2015;15:1727–37.

32. Catana CS, Berindan Neagoe I, Cozma V, Magdas C, Tabaran F, Dumitrascu DL. Contribution of the IL-17/IL-23 axis to the pathogenesis of inflammatory bowel disease. World J Gastroenterol 2015;21:5823–30.

33. Hawkes JE, Chan TC, Krueger JG. Psoriasis pathogenesis and the development of novel targeted immune therapies. J Allergy Clin Immunol 2017;140:645–53.

34. Feld J, Chandran V, Haroon N, Inman R, Gladman D. Axial disease in psoriatic arthritis and ankylosing spondylitis: a critical comparison. Nat Rev Rheumatol 2018;14:363–71.

35. Ranganathan V, Gracey E, Brown MA, Inman RD, Haroon N. Pathogenesis of ankylosing spondylitis - recent advances and future directions. Nat Rev Rheumatol 2017;13:359–67.

36. Appel H, Maier R, Bleil J, Hempfing A, Loddenkemper C, Schlichting U, et al. In situ analysis of interleukin-23– and interleukin-12–positive cells in the spine of patients with ankylosing spondylitis. Arthritis Rheum 2013;65:1522–9.

37. Appel H, Maier R, Wu P, Scheer R, Hempfing A, Kayser R, et al. Analysis of IL-17+ cells in facet joints of patients with spondyloarthritis suggests that the innate immune pathway might be of greater relevance than the Th17-mediated adaptive immune response. Arthritis Res Ther 2011;13:R95.

38. Wendling D, Cedoz JP, Racadot E. Serum and synovial fluid levels of p40 IL12/23 in spondyloarthropathy patients. Clin Rheumatol 2009;28:187–90.

39. Romero-Sanchez C, Jaimes DA, Londono J, De Avila J, Castellanos JE, Bello JM, et al. Association between Th-17 cytokine profile and

clinical features in patients with spondyloarthritis. Clin Exp Rheumatol 2011;29:828–34.

40. Sherlock JP, Joyce-Shaikh B, Turner SP, Chao CC, Sathe M, Grein J, et al. IL-23 induces spondyloarthropathy by acting on ROR-gt+ CD3+CD4-CD8- entheseal resident T cells. Nat Med 2012;18:1069–76.

41. Baeten D, Baraliakos X, Braun J, Sieper J, Emery P, van der Heijde D, et al. Anti-interleukin-17A monoclonal antibody secukinumab in treatment of ankylosing spondylitis: a randomised, double-blind, placebo-controlled trial. Lancet 2013;382:1705–13.

42. Lee JS, Tato CM, Joyce-Shaikh B, Gulen MF, Cayatte C, Chen Y, et al. Interleukin-23-independent IL-17 production regulates intestinal epithelial permeability. Immunity 2015;43:727–38.

43. Maxwell JR, Zhang Y, Brown WA, Smith CL, Byrne FR, Fiorino M, et al. Differential roles for interleukin-23 and interleukin-17 in intestinal immunoregulation. Immunity 2015;43:739–50.

APPENDIX A: INVESTIGATORS WHO RANDOMIZED PATIENTS IN THE USTEKINUMAB–AXIAL SpA TRIALS

The following investigators randomized patients in the 3 trials: Frederico Ariel, Cecilia Adma Asnal, Alberto Berman, Gustavo Citera, Graciela Rodriguez, and Veronica Gabriela Savio (Argentina); Paul Bird, Hedley Griffiths, David Nicholls, Maureen Rischmueller, and Jane Zochling (Australia); Kurt De Vlam, Michel Malaise, Adrien Nzeusseu Toukap, Filip Van den Bosch, and Johan Vanhoof (Belgium); Rubens Bonfiglioli, Mauro Keiserman, Antonio Scafuto Scotton, Ricardo Xavier, and Antonio Carlos Ximenes (Brazil); Assen Atanasov, Ivan Goranov, Ivan Kazmin, Rodina Nestorova Licheva, Nikolay Nikolov, Boycho Oparanov, and Rumen Stoilov (Bulgaria); Louis Bessette and Jude Rodrigues (Canada); Ladislav Bortilik, Eva Dokoupilova, Zdenek Dvoarak, Dagmar Galatikova, Petr Nemec, Lucie Podrazilova, Gabriela Simkova, Zuzana Stejfova, Radka Moravcova, and Petr Vitek (Czech Republic); Alain Cantagrel, Athan Baillet, Beatrice Banneville, Bernard Combe, Maxime Breban, Minh Nguyen, and Philippe Goupille (France); Juergen Braun, Andrea Everding, Joern Kekow, Ramona Koenig, Andrea Rubbert-Roth, Joachim Sieper, and Torsten Witte (Germany); Attila Bartha, Edit Drescher, Kata Kerekes, Attila Kovacs, Judit Pulai, Bernadette Rojkovich, Sandor Szanto, and Edit Toth (Hungary); Hilario Avila, Igancio Garcia de la Torre, Fedra Irazoque, Marco Maradiaga, and Cesar Pacheco (Mexico); Marek Brzosko, Anna Dudek, Slawomir Jeka, Marek Krogulec, Brygida Kwiatkowska, Piotr Wiland, Rafal Wojciechowski, and Agnieszka Zielinska (Poland); Helena Santos (Portugal); Olga Bugrova, Valery Christyakov, Vladimir Gorbunov, Elena Ilivanova, Elena Zemerova, Rima Kamalova, Tatyana Kameneva, Galina Macievskaya, Irina Marusenko, Alexey Maslyansky, Svetlana Myasoedova, Leisan Myasoutova, Boris Nemtsov, Olga Nesmeyanova, Tatyana Plaksina, Tatyana Pokrovskaya, Svetlana Polyakova, Andrey Rebrov, Liudmila Savina, Svetlana Smakotina, Marina Stanislav, Olga Ukhanova, Irina Vinogradova, and Elena Zonova (Russia); Han Joo Baek, Tae-Hwan Kim, ChangKeun Lee, SangHeon Lee, Sang-Hoon Lee, Shin-Seok Lee, Sung-Hwan Park, YeongWook Song, and Chang-Hee Suh (Republic of Korea); Juan Amarelo Ramos, Franciso Javier Blanco, Eduardo Collantes, Miguel Consuelo Diaz, Maria Luz Garcia Vivar, Jordi Gratacos, and Xavier Juanola (Spain); Der-Yuan Chen, Hsiang-Cheng Chen, Kun-Hung Chen, Ying-Chou Chen, Ying-Ming Chiu, Shue-Fen Luo, Shih-Tzu Tsai, Jui-Cheng Tseng, Cheng-Chung Wei, and Meng-Yu Weng (Taiwan); Orest Abrahamovych, Dmytro Reshotko, Oleksandr Golovchenko, Ihor Hospodarsky, Oleg Iaremenko, Olena Levchenko, Oleksandr Dudnyk, Olena Garmish, Olena Grishyna, Galyna Protsenko, Dmytro Rekalov, Svitlana Smiyan, Mykola Stanislavchuk, Svitlana Trypilka, Vira Tseluyko, Samvel Turianytsia, Viktoriya Vasylets, Nataliya Virstyuk, and Yaroslav Kleban (Ukraine); Coziana Ciurtin, Karl Gaffney, Wiranthi Gunasekera, Kirsten Mackay, Jon Packham, Raj Sengupta, and Hasan Tahir (United Kingdom); Jacob Aelion, Ralph Bennett, Atul Deodhar, Julio Gonzalez-Paoli, Robert M. Griffin, Jr., Michael Grisanti, Jyothi Mallepalli, Eric Peters, Joy Schechtman, and Atul Singhal (United States).

AMERICAN COLLEGE
OF RHEUMATOLOGY
EDUCATION · TREATMENT · RESEARCH

Effect of Achieving Minimal Disease Activity on the Progression of Subclinical Atherosclerosis and Arterial Stiffness: A Prospective Cohort Study in Psoriatic Arthritis

Isaac T. Cheng,[1] Qing Shang,[1] Edmund K. Li,[1] Priscilla C. Wong,[1] Emily W. Kun,[2] Mei Yan Law,[3] Ronald M. Yip,[4] Isaac C. Yim,[5] Billy T. Lai,[5] Shirley K. Ying,[6] Kitty Y. Kwok,[7] Martin Li,[1] Tena K. Li,[1] Tracy Y. Zhu,[1] Jack J. Lee,[8] Mimi M. Chang,[1] Cheuk-Chun Szeto,[1] Bryan P. Yan,[1] Alex P. Lee,[1] and Lai-Shan Tam[1]

Objective. To investigate the effects of achieving minimal disease activity (MDA) on the progression of subclinical atherosclerosis and arterial stiffness in patients with psoriatic arthritis (PsA).

Methods. A total of 101 consecutive patients with PsA were recruited for this prospective cohort study. All patients received protocolized treatment targeting MDA for a period of 2 years. High-resolution carotid ultrasound and arterial stiffness markers were assessed annually. The primary outcome measure was the effect of achieving MDA at 12 months (MDA group) on the progression of subclinical atherosclerosis over a period of 24 months. Secondary objectives were to compare the changes in arterial stiffness markers over 24 months between the MDA and non-MDA groups, as well as the changes in subclinical atherosclerosis and arterial stiffness markers in patients who achieved MDA at each visit from month 12 through month 24 (sustained MDA [sMDA]).

Results. Ninety PsA patients (mean ± SD age 50 ± 11 years, 58% male [n = 52]) who completed 24 months of follow-up were included in this analysis. Fifty-seven patients (63%) had achieved MDA at 12 months. Subclinical atherosclerosis and arterial stiffness outcomes were similar between the MDA and non-MDA groups. Forty-one patients (46%) achieved sMDA. As shown by multivariate analysis, achieving sMDA had a protective effect on plaque progression (odds ratio 0.273 [95% confidence interval 0.088–0.846], $P = 0.024$), and less of an increase in total plaque area, mean intima-media thickness, and augmentation index values after adjustment for covariates.

Conclusion. Our results support the recommendation that once MDA is achieved, it should ideally be maintained for a prolonged period in order to prevent progression of carotid atherosclerosis and arterial stiffness in patients with PsA.

INTRODUCTION

Incidence of myocardial infarction is increased in patients with psoriatic arthritis (PsA), rheumatoid arthritis (RA), and possibly ankylosing spondylitis compared to the general population (1). Cardiovascular (CV) risk assessment is recommended for these patients at least once every 5 years, so that lifestyle advice and CV disease (CVD) preventive treatment can be initiated when indicated (2). Screening for asymptomatic atherosclerotic plaques by carotid ultrasound has been recommended as part of the CV risk evaluation in patients with RA, as the presence of carotid plaques is associated with poor CVD-free survival and is strongly linked to a future diagnosis of acute coronary syndrome (3). Similar to patients with RA, patients with PsA also had a greater burden of subclinical carotid atherosclerosis (4–8). Increased intima-media thickening (IMT) significantly correlated with traditional risk factors (4–7) and disease-related parameters (4,5). Indeed, exposure to an increased burden of inflammation is associated with more severe atherosclerosis (9) and arterial stiffness (10) in patients with PsA, which may be mediated by traditional CV risk factors.

PsA may predispose patients to accelerated atherosclerosis through a number of mechanisms, including chronically elevated

inflammatory cytokine levels, a higher prevalence of traditional CVD risk factors (11), and the impact of pharmacotherapies. Markers of disease activity, as reflected by prior use of medication, a high erythrocyte sedimentation rate (ESR) at presentation, and evidence of radiologic damage, were associated with increased CV mortality in these patients (12). Thus, it is possible that effective immunosuppression may interfere with the inflammation underlying both synovitis and atherosclerosis.

In PsA, criteria for minimal disease activity (MDA) have been developed and validated (13). Achieving MDA by these criteria results in less radiographic damage in the long term (14). While achieving MDA may result in significant benefits in articular disease (15), little is known about its effect on extraarticular disease, including CVD risk. Previous studies linked the suppression of inflammation using anti–tumor necrosis factor (anti-TNF) agents with a favorable effect on carotid atherosclerosis (8,16,17) and arterial stiffness (18) in patients with PsA. However, whether this positive impact is specifically related to blocking TNF, or is due to a nonspecific effect from suppression of inflammation, cannot be differentiated. We hypothesized that abrogation of inflammation in PsA patients achieving MDA through a protocolized treatment strategy may prevent progression of subclinical atherosclerosis and arterial stiffness over a period of 2 years.

PATIENTS AND METHODS

Inclusion and exclusion criteria. A total of 101 consecutive patients with PsA attending the outpatient clinic of the Prince of Wales Hospital, age >18 years and fulfilling the Classification of Psoriatic Arthritis (CASPAR) criteria (19), were recruited into this cohort study from April 2014 to October 2015. Patients were excluded if they met any 1 of the following criteria: 1) having a history of overt CVD (including myocardial infarction, angina, stroke, and transient ischemic attack), 2) taking antiplatelet agents (including aspirin, clopidogrel, etc.), hydroxymethylglutaryl-coenzyme A reductase inhibitors (statins), or angiotensin-converting enzyme inhibitors that would interfere with vascular outcomes, 3) having significant comorbidities, including severe renal impairment or severe deranged liver function, or 4) being a woman of childbearing potential who was pregnant, breastfeeding, or not using an effective method of contraception. Patients were not eligible if they were taking glucocorticoids at a dosage of >10 mg/day.

Treatment protocol. All participants received 2 years of protocolized treatment (see Supplementary Figure 1, available on the *Arthritis & Rheumatology* web site at http://onlinelibrary.wiley. com/doi/10.1002/art.40695/abstract), with the aim of achieving MDA. When a patient did not achieve the treatment goal after 4 months of therapy, the treatment was escalated to the next level according to the protocol, unless the patient declined further treatment or the toxic effects of the treatment precluded this approach.

The study was approved by the Ethics Committee of the Chinese University of Hong Kong, with written informed consent provided by all participants. The study was conducted in accordance with the Declaration of Helsinki.

Clinical assessments. Assessments conducted at each visit included the following: pain, the physician's and patient's global assessment, the tender joint count (TJC; 68 joints assessed) and swollen joint count (SJC; 66 joints assessed), the Maastricht Ankylosing Spondylitis Enthesitis Score (range 1–13) (20), and the number of digits with dactylitis. The following instruments were used to measure joint and skin disease activity: the Bath Ankylosing Spondylitis Disease Activity Index (21), the Modified Health Assessment Questionnaire (M-HAQ) (22), the Disease Activity Index for Psoriatic Arthritis (23), body surface area (BSA) affected by psoriasis, and the Psoriasis Activity and Severity Index (PASI) (24).

MDA was used for the assessment of the treatment efficacy end point. The MDA criteria assess 7 domains, with the following cutoffs: TJC ≤1, SJC ≤1, enthesitis count ≤1, skin score ≤1 (or BSA ≤3%), function score ≤0.5 (measured by the HAQ) (25), patient's global assessment ≤20 on a 100-mm visual analog scale (VAS), and patient-reported pain ≤15 on a 100-mm VAS. If 5 of the 7 cutoffs for these domains were met, then the patient was classified as having MDA. Anthropomorphic measurements included body height, body weight, waist and hip circumferences, and blood pressure. The number of joints irreversibly damaged was assessed at baseline and annually. Patient information regarding menopausal status, smoking and drinking habits, history of diabetes mellitus, hypertension, dyslipidemia, overt CVD, and family history of CVD was obtained at baseline. Treatment history was retrieved from case notes or elicited during the clinical assessment.

Laboratory assessments and markers of inflammation. Laboratory assessments were conducted at baseline, every 4 months, and at the end of the study. These tests included complete blood cell count, liver and renal function tests, ESR, C-reactive protein level, fasting blood glucose level, lipid profile (total cholesterol, low-density lipoprotein cholesterol, high-density lipoprotein cholesterol, triglycerides), fibrinogen level, and uric acid level.

Carotid IMT and plaque. Carotid IMT and plaque were assessed at baseline, 12 months, and 24 months (7). Carotid IMT was measured by an experienced cardiologist (QS) who was blinded with regard to all clinical information, using a high-resolution B-mode EPIQ7 ultrasound machine (Philips) and a Philips L12-3 30 MHz linear vascular probe (broadband linear array transducer). The IMT was measured offline in the distal common carotid artery, carotid bulb, and proximal internal carotid artery using dedicated Philips Xcelera Cardiology Enterprise Viewer Client 4 software. The mean and maximal IMT values of 6 arterial segments were calculated for further analysis. Plaque was defined as a localized thick-

Table 1. Characteristics of the patients at baseline and month 24*

	Baseline (n = 90)	Month 24 (n = 90)	P
Disease activity			
Tender joint count, 0–68	3 (1–6)	0 (0–1)	<0.001
Swollen joint count, 0–66	1 (0–2)	0 (0–1)	0.020
Damaged joint count, 0–68	2 (0–6)	3 (0–9)	0.003
Dactylitis, 0–20	0 (0–0)	0 (0–0)	0.209
MASES enthesitis, 0–13	0 (0–2)	0 (0–1)	0.841
VAS pain, 0–100 mm	35 (20–60)	10 (5–30)	<0.001
Patient's global assessment, 0–100 mm	50 (30–70)	15 (10–30)	<0.001
Physician's global assessment, 0–100 mm	30 (15–48)	2 (0–8)	<0.001
ESR, mean ± SD mm/hour	29 ± 22	25 ± 18	0.034
CRP, mean ± SD mg/dl	7.7 ± 10.6	4.4 ± 6.4	<0.001
DAPSA, 0–64	19 (13–32)	7 (4–14)	<0.001
PASI, 0–72	3.4 (0.6–7.6)	1.0 (0–3.2)	<0.001
HAQ total score, 0–3	0.38 (0–0.88)	0.13 (0–0.5)	0.001
Achieved MDA, no. (%)	15 (16.7)	62 (68.9)	<0.001
Traditional CV risk factors			
Body weight, mean ± SD kg	69.6 ± 15.2	70.2 ± 15.5	0.188
BMI, mean ± SD kg/m^2	25.6 ± 4.8	25.9 ± 4.8	0.142
Systolic blood pressure, mean ± SD mm Hg	125 ± 18	124 ± 15	0.761
Diastolic blood pressure, mean ± SD mm Hg	79 ± 11	77 ± 10	0.095
Waist-to-hip ratio, mean ± SD	0.92 ± 0.06	0.92 ± 0.07	0.522
Abdominal obesity, no. (%)	59 (65.6)	61 (67.8)	0.832
Hypertension, no. (%)	28 (31.1)	33 (36.7)	0.063
Diabetes mellitus, no. (%)	11 (12.2)	15 (16.7)	0.219
Dyslipidemia, no. (%)	18 (20.0)	21 (23.3)	0.250
Plasma total cholesterol, mean ± SD mmoles/liter	5.0 ± 0.9	5.0 ± 0.9	0.752
Plasma HDL cholesterol, mean ± SD mmoles/liter	1.4 ± 0.4	1.4 ± 0.4	0.345
Plasma LDL cholesterol, mean ± SD mmoles/liter	3.0 ± 0.8	3.0 ± 0.8	0.639
Plasma total triglyceride, mean ± SD mmoles/liter	1.4 ± 0.9	1.5 ± 1.0	0.122
Plasma fasting glucose, mean ± SD mmoles/liter	5.3 ± 1.4	5.6 ± 1.5	0.160
Smoking, no. (%)	14 (15.6)	15 (16.7)	0.999
Framingham Risk Score, mean ± SD	9.5 ± 8.0	11 ± 9.2	**0.003**
Medication, no. (%)			
Antihypertensive drugs	20 (22.2)	29 (32.2)	**0.052**
Oral hypoglycemic agents	8 (8.9)	10 (11.5)	**0.999**
NSAIDs	48 (53.3)	37 (41.1)	**<0.001**
Prednisolone	1 (1.1)	0 (0.0)	–
csDMARDs	51 (56.7)	62 (68.9)	**<0.001**
bDMARDs	16 (17.8)	28 (31.1)	**0.010**

* Except where indicated otherwise, values are the median (interquartile range). MASES = Maastricht Ankylosing Spondylitis Enthesitis Score; VAS = visual analog scale; ESR = erythrocyte sedimentation rate; CRP = C-reactive protein; DAPSA = Disease Activity in Psoriatic Arthritis; PASI = Psoriatic Area and Severity Index; HAQ = Health Assessment Questionnaire; MDA = minimal disease activity; CV = cardiovascular; BMI = body mass index; HDL = high-density lipoprotein; LDL = low-density lipoprotein; NSAIDs = nonsteroidal antiinflammatory drugs; csDMARDs = conventional synthetic disease-modifying antirheumatic drugs; bDMARDs = biologic DMARDs.

ening of >1.2 mm that did not uniformly involve the whole artery. Progression of plaque was defined as an incident plaque in a segment without plaque before or an increased number of plaques in a segment. The reproducibility of IMT was 0.97 (7). The total plaque area (TPA) was measured as described previously (26). The plane for measurement of each plaque was chosen by reviewing the video of the ultrasound scan to find the largest extent of plaque as seen on the longitudinal view. TPA was recorded as the sum of the areas of all plaques in the right and left carotid arteries. Reading of the ultrasound scans obtained at baseline and at follow-up was performed concurrently by a single reader (ITC) who was aware of the temporal order of the images but was blinded with regard to the clinical data. The change in TPA was calculated by subtracting the baseline TPA from the follow-up TPA. The intra-observer intraclass correlation coefficient for TPA was 0.94 (27).

Pulse wave velocity (PWV) and pulse wave analysis (PWA). Arterial stiffness was measured by PWV and the augmentation index value at baseline, 12 months, and 24 months (28). PWA was performed using a SphygmoCor device (Vicorder; SMT Medical) with a tonometer probe at the right radial artery. The central aortic arterial pulse wave is transferred from the peripheral arterial pulse wave automatically. Since the augmentation index value for an individual patient varies by heart rate, it is standardized to a heart rate of 75 beats per minute. Ankle–brachial PWV was assessed non-invasively in subjects in the supine position, with a dedicated tonometry system (VP-2000; Omron Healthcare) as described previously. All PWA measurements were made by the same skilled operator (QS). Intraobserver reliability was 0.86 (28).

Outcome measures. The primary outcome measure was the effect of achieving MDA at 12 months (MDA group) on the progression of subclinical atherosclerosis over a period of 24 months compared to those who did not achieve MDA (non-MDA group). Secondary outcome measures included 1) changes in arterial stiffness markers over a period of 24 months between the MDA group and the non-MDA group and 2) changes in subclinical atherosclerosis and arterial stiffness markers over a period of 24 months between patients who achieved sMDA (sMDA group) and those who did not (non-sMDA group). Sustained MDA was defined as having achieved MDA at every visit between month 12 and month 24 (i.e., months 12, 16, 20, and 24). Additional analyses were performed to investigate the time-averaged achievement of MDA on vascular outcomes. The time-averaged achievement of MDA was determined by calculating the area under the curve of whether the patient had achieved MDA at each visit of the total follow-up period divided by the follow-up period.

Statistical analysis. Statistical analyses were performed using an SPSS version 24.0 software package.

Descriptive statistics, including frequency, percentage, mean and SD, and median and interquartile (IQR) range, were used for demographic and clinical variables. Comparisons in demographic and clinical characteristics at baseline and changes over 2 years between 2 groups were performed using the chi-square test, independent-sample *t*-test, and Mann-Whitney U test, depending on the distribution of data. Univariate analysis was performed to look for potential variables (Table 1) that may predict the changes in vascular parameters, including IMT, PWV, augmentation index values, and TPA and progression of plaque. Chi-square tests were performed to analyze the association between the use of nonsteroidal antiinflammatory drugs (NSAIDs), conventional synthetic disease-modifying antirheumatic drugs (csDMARDs), and biologic DMARDs (bDMARDs) and the achievement of MDA at each clinic visit. The vascular effects of achieving MDA at 12 months, achieving sMDA from month 12 through month 24, or time-averaged achievement of MDA were analyzed using multivariate linear or logistic regression models with adjustment for covariates (including the baseline covariates listed in Table 1 that we associated with progression in the vascular parameters from univariate analyses with a *P* value of less than 0.1, baseline vascular parameters, and the use of DMARDs and NSAIDs). A 2-tailed probability *P* value of less than 0.05 was considered significant.

RESULTS

A total of 101 patients were recruited; of these, 90 patients (mean ± SD age 50 ± 11 years, 57.8% male [n = 52], disease duration 9.9 ± 9.0 years) had a repeat carotid ultrasound and augmentation index, and were included in the final analysis for carotid plaque, IMT, and augmentation index progression, while 87 patients had a second PWV measurement (Figure 1).

Table 1 summarizes the clinical features and traditional CV risk factors of the patients at baseline and at month 24. Significant improvement in disease activity was observed in the whole cohort after 2 years. MDA was achieved by 15 (17%), 57 (63%), and 62 (69%) of patients at baseline, at 1 year, and at 2 years, respectively (Figure 2). No statistically significant changes in traditional CV risk factors were observed, except for an increase in the Framingham Risk Score, which was most likely due to the increase in age.

Treatments. The use of csDMARDs increased from 57% at baseline and reached a peak of 75% at month 12, and then decreased to 69% at month 24. The use of bDMARDs increased from 18% at baseline to 31% at month 24 (Figure 3A). The use of NSAIDs decreased at baseline from 53% to 41% at month 24.

MDA and compliance with the protocol. The proportion of subjects reaching MDA increased progressively throughout the study period (Figure 2). On average, MDA was achieved in 53%
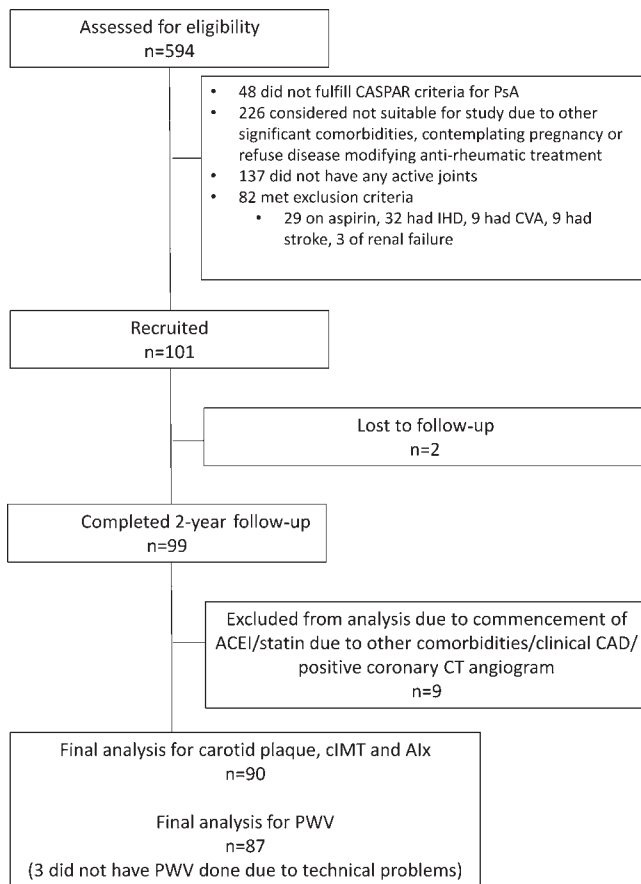
Figure 1. Study flow diagram. CASPAR = Classification of Psoriatic Arthritis Study Group; PsA = psoriatic arthritis; IHD = ischemic heart disease; CVA = cerebrovascular accident; ACEI = angiotensin-converting enzyme inhibitor; CAD = coronary artery disease; CT = computed tomography; cIMT = carotid intima-media thickness; AIx = augmentation index; PWV = pulse wave velocity.

of the visits. Treatment was escalated to the next level in 84% of visits when MDA was not met. The reasons for non-escalation of treatment are summarized in Supplementary Table 1, available

on the *Arthritis & Rheumatology* web site at http://onlinelibrary. wiley.com/doi/10.1002/art.40695/abstract.

MDA and treatment utilization. We next analyzed the relationship of MDA status and the use of medication at each visit separately. Altogether, there were a total of 769 patient visits. Among all the visits when patients were treated with bDMARDs (n = 216), a significantly higher proportion of them had achieved MDA (60% versus 40%; $P = 0.005$). Among all the visits when patients had achieved MDA (n = 397), fewer patients required treatment with NSAIDs (30% versus 70%; $P < 0.001$). Use of csDMARDs was not significantly associated with MDA (see Supplementary Table 2, available at http://onlinelibrary.wiley.com/doi/10.1002/art.40695/abstract).

Serious a Adverse events. Seven episodes of serious adverse events (SAEs) were reported (see Supplementary Table 3, available at http://onlinelibrary.wiley.com/doi/10.1002/art.40695/abstract). All 7 episodes of SAEs required hospitalization, with none of the events being life-threatening. No previously undescribed SAEs or deaths were observed.

Achieving MDA at month 12 and progression of vascular parameters over 24 months. Fifty-seven of the subjects (63%) had achieved MDA at month 12 (MDA group). Baseline traditional CV risk factors were similar between the 2 groups (see Supplementary Table 2, available at http://onlinelibrary.wiley.com/doi/10.1002/art.40695/abstract). The MDA group had lower disease activity at baseline, probably because a higher proportion of patients was already taking bDMARDs. The prevalence of NSAID use was significantly lower (Supplementary Table 4).

At month 24, the MDA group had significantly less progression as shown on the augmentation index, while the changes in mean and maximum IMT, PWV, TPA, and plaque progression were similar between the 2 groups (Table 2). Nonetheless, the differences in the change in the augmentation index
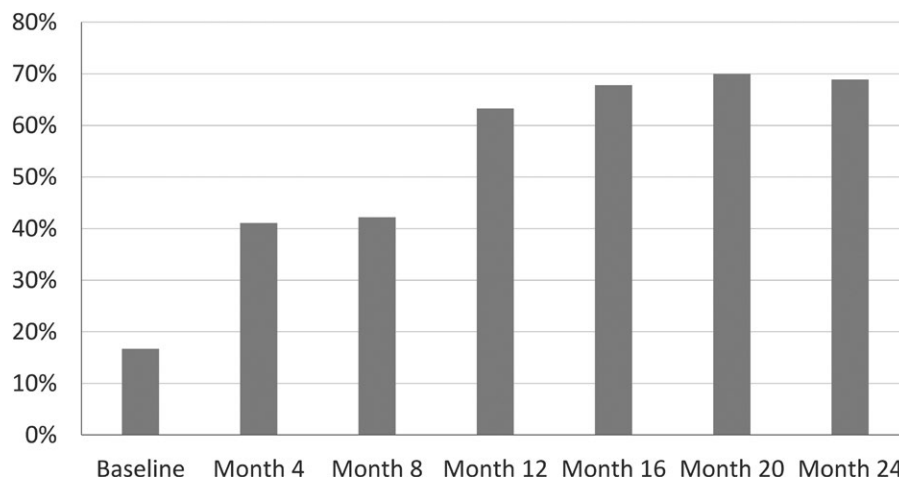
Figure 2. Proportion of subjects achieving minimum disease activity across the study period.
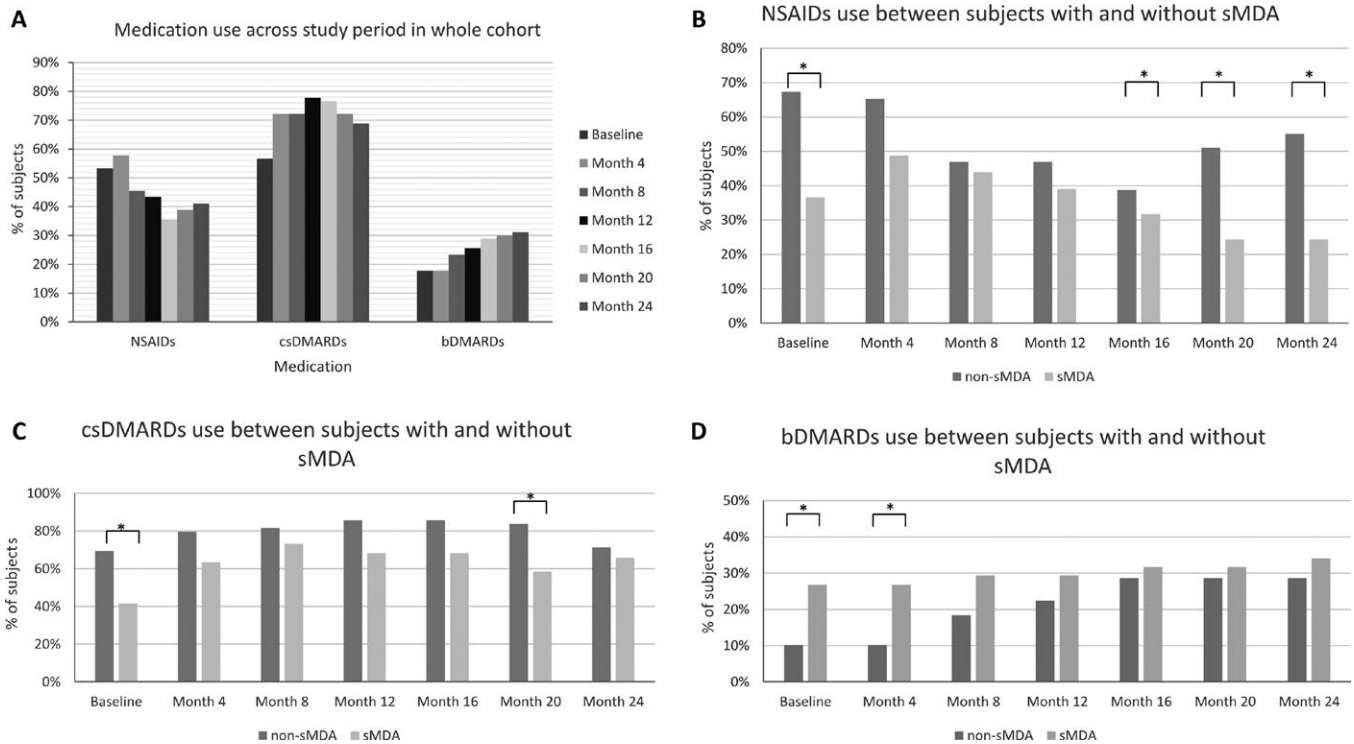
Figure 3. Different treatment regimens of the patients throughout the study period. **A**, Overall medication use throughout the study period. **B–D,** Treatment with nonsteroidal antiinflammatory drugs (NSAIDs) (**B**), conventional synthetic disease-modifying antirheumatic drugs (csDMARDs) (**C**), and biologic DMARDs (bDMARDs) (**D**) in patients with sustained minimal disease activity (sMDA group) and patients without sMDA (non-sMDA group). * = $P < 0.05$.

became insignificant after adjustment for baseline differences and csDMARD use throughout the 2 years (data not shown).

Achieving sustained MDA from month 12 to month 24 and progression of vascular parameters over 24 months. Forty-one patients (46%) achieved sMDA from month 12 to month 24. At baseline, patients in the sMDA group had lower disease activity, and a higher proportion of patients had already achieved MDA compared to those who did not achieve sMDA (see Supplementary Table 5, available at http://onlinelibrary.wiley.com/doi/10.1002/art.40695/abstract). A significantly higher proportion of subjects in the sMDA group were taking bDMARDs, while fewer patients were taking NSAIDs and csDMARDs (Figure 3). Traditional CV risk factors were similar between the 2 groups, except that the sMDA group had fewer smokers (Supplementary Table 5). After 24 months, fewer patients in the sMDA group required NSAIDs (Figure 3B).

The vascular parameters were similar between the 2 groups at baseline (Table 2). A total of 34 of 90 patients (38%) had plaque progression. Plaque progression was observed less frequently in the sMDA group than in the non-sMDA group, but the difference did not quite reach significance in univariate analysis. Regression analysis revealed that achieving sMDA was associ-

ated with a protective effect on plaque progression (odds ratio [OR] 0.273 [95% confidence interval (95% CI) 0.088, 0.846], $P = 0.024$), increase in TPA ($\beta = -3.919$ [95% CI -7.181, -0.657], $P = 0.019$), mean IMT ($\beta = -0.037$ [95% CI -0.066, -0.007], $P = 0.014$), and the augmentation index ($\beta = -3.059$ [95% CI -6.067, -0.051], $P = 0.046$), as well as a trend suggesting improvement in PWV ($\beta = -71.4$ [95% CI -143.2, 0.2], $P = 0.051$) (Table 3).

Vascular effect of time-averaged achievement of MDA. The median (IQR) number of visits in MDA for the whole cohort was 4 (2–5). There was a trend suggesting that patients with an increasing number of visits in MDA had a lower risk of plaque progression (OR 0.851 [95% CI 0.696, 1.040], $P = 0.116$). Similar trends were observed for the changes in mean and maximum IMT, PWV, and augmentation index (data not shown). Subjects with plaque progression had a lower time-averaged achievement of MDA, though the difference was not significant (48% versus 58.5%; $P = 0.138$). In multivariate regression analysis, an increase in the time-averaged achievement of MDA was only marginally associated with a lower risk of plaque progression after adjusting for baseline covariates (OR 0.982 [95% CI 0.965, 0.999], $P = 0.044$). No significant association was found with other vascular parameters (data not shown). Overall, there was no association between the change in vascular parameters and clinical or labo-

Table 2. Subclinical atherosclerosis and arterial stiffness outcomes in patients according to MDA status at month 12 and whether patients achieved sMDA*

	Did not achieve MDA at month 12 (n = 33)	Achieved MDA at month 12 (n = 57)	P	Did not achieve sMDA (n = 49)	Achieved sMDA (n = 41)	P
Subclinical atherosclerosis						
Carotid IMT, mean ± SD mm						
Baseline	0.63 ± 0.10	0.66 ± 0.12	0.316	0.64 ± 0.10	0.66 ± 0.13	0.264
Month 24	0.62 ± 0.09	0.63 ± 0.92	0.555	0.63 ± 0.08	0.62 ± 0.10	0.760
Change	0.02 ± 0.07	0.03 ± 0.07	0.398	−0.01 ± 0.08	−0.04 ± 0.06	0.031
Maximum carotid IMT, mean ± SD mm						
Baseline	0.77 ± 0.14	0.80 ± 0.17	0.320	0.77 ± 0.15	0.81 ± 0.18	0.660
Month 24	0.73 ± 0.13	0.75 ± 0.13	0.589	0.75 ± 0.12	0.74 ± 0.14	0.083
Change	0.03 ± 0.13	0.05 ± 0.15	0.532	−0.02 ± 0.14	−0.08 ± 0.15	0.083
Presence of carotid plaque, no. (%)						
Baseline	14 (42.4)	18 (31.6)	0.300	18 (36.7)	14 (34.1)	0.798
Month 24	18 (54.5)	32 (56.1)	0.883	29 (59.2)	21 (51.2)	0.449
Any plaque progression	13 (39.4)	21 (36.8)	0.810	22 (44.9)	12 (29.3)	0.128
Total plaque area, median (IQR) mm^2						
Baseline	0 (0–9.1)	0 (0–6)	0.383	0 (0–6)	0 (0–7.5)	0.962
Month 24	7.0 (0–18.1)	6.5 (0–12.7)	0.630	7.5 (0–16)	1.3 (0–13)	0.458
Change	0 (0.8)	0 (0–6.5)	0.761	0.1 (0–10.4)	0 (0–6.45)	0.103
Arterial stiffness						
Augmentation index, mean ± SD %						
Baseline	23 ± 7	24 ± 8	0.436	23 ± 7	14 ± 9	0.620
Month 24	26 ± 8	24 ± 9	0.180	26 ± 8	23 ± 9	0.151
Change	3 ± 8	0 ± 8	0.032	3 ± 7	−1 ± 9	**0.043**
PWV, mean ± SD cm/second						
Baseline	1,512 ± 252	1,472 ± 213	0.437	1,515 ± 249	1,455 ± 198	**0.223**
Month 24	1,527 ± 275	1,459 ± 196	0.180	1,530 ± 265	1,432 ± 169	**0.042**
Change	15 ± 220	−15 ± 162	0.469	13 ± 211	−23 ± 152	**0.357**

* MDA = minimal disease activity; sMDA = sustained MDA; IMT = intima-media thickness; IQR = interquartile range; PWV = pulse wave velocity.

ratory parameters of disease activity (see Supplementary Table 6, available at http://onlinelibrary.wiley.com/doi/10.1002/art.40695/abstract).

DISCUSSION

This is the first longitudinal study to demonstrate that effective control of systemic inflammation in PsA patients who achieved sMDA was associated with less progression of subclinical atherosclerosis and arterial stiffness compared to those who did not achieve sMDA. The data in the study support the European League Against Rheumatism recommendation that disease activity should be controlled optimally in order to lower CVD risk in patients with PsA (2). After 2 years of protocol-driven, treat-to-target therapy, the proportion of patients achieving MDA increased from 16.7% at baseline to 63.3% at 12 months and to

68.9% at 24 months. The proportion of patients achieving MDA in our cohort at months 12 and 24 was similar to that in other observational studies in patients treated with anti-TNF agents (44–64%) (29). A previous studies demonstrated that 60% of patients had achieved MDA on at least 1 visit and 34% had achieved MDA on consecutive visits for at least 12 months (30), which is similar to the results from the current study (55% and 46%, respectively). Data from the current study confirm that when using a treat-to-target strategy, MDA is indeed an achievable target, even in a health care system with limited resources.

The most important finding in this study is that long-term control of inflammation is essential in preventing the progression of subclinical atherosclerosis and arterial stiffness, independent of traditional CV risk factors. A single instance of achieving MDA at month 12 has no impact on the progression of subclinical atherosclerosis and vascular stiffness. Time-

Table 3. Multivariate analysis for the change in mean maximal IMT, augmentation index, PWV, any plaque progression, and change in TPA*

	Multivariate analysis	
	Value	P
Plaque progression, OR (95% CI)†		
Age	1.069 (1.009, 1.131)	0.023
PGA, baseline	0.964 (0.936, 0.993)	0.016
Plasma LDL cholesterol, baseline	2.628 (1.310, 5.493)	0.007
bDMARD use at baseline	0.110 (0.018, 0.652)	0.015
Achieved sustained MDA	0.273 (0.088, 0.846)	0.024
Change in TPA, β (95% CI)‡		
BMI, kg/m^2, baseline	−0.428 (−0.760, −0.096)	0.012
Plasma LDL cholesterol, baseline	2.828 (0.723, 4.932)	0.009
Achieved sustained MDA	−3.919 (−7.181, −0.657)	0.019
Change in mean IMT, β (95% CI)§		
bDMARD use throughout the year	−0.034 (−0.065, −0.004)	0.028
Achieved sustained MDA	−0.037 (−0.066, −0.007)	0.014
Change in maximal IMT, β (95% CI)¶		
Age	0.003 (0.000, 0.005)	0.038
CRP, baseline	0.002 (0.000, 0.005)	0.036
NSAID use, baseline	0.122 (0.045, 0.199)	0.003
Maximum IMT, baseline	−0.455 (−0.646, −0.264)	<0.001
Change in PWV, β (95% CI)#		
Age	4.953 (0.919, 8.986)	0.017
PWV, baseline	−0.483 (−0.676, −0.289)	<0.001
Achieved sustained MDA	−71.4 (−143.2, 0.2)	0.051
Change in augmentation index, β (95% CI)**		
Male sex	3.332 (0.105, 6.560)	0.043
Achieved sustained MDA	−3.059 (−6.067, −0.051)	0.046

* TPA = total plaque area; OR = odds ratio; 95% CI = 95% confidence interval.
† Adjusted for age, sex, baseline deformed joint count, physician's global assessment (PGA) score, plasma total triglyceride, total cholesterol, and low-density lipoprotein (LDL) cholesterol levels, use of biologic disease-modifying antirheumatic drugs (bDMARDs), and presence of carotid plaque at baseline.
‡ Adjusted for age, sex, baseline body mass index (BMI), visual analog scale pain score, patient's global assessment score, plasma total triglyceride, total cholesterol, and LDL cholesterol levels, and use of conventional synthetic DMARDs (csDMARDs).
§ Adjusted for disease duration, baseline C-reactive protein (CRP) level, Framingham Risk Score, use of nonsteroidal antiinflammatory drugs (NSAIDs), and use of bDMARDs throughout the year.
¶ Adjusted for age, sex, baseline CRP level, waist-to-hip ratio, plasma total cholesterol and, LDL cholesterol levels, use of NSAIDs, and maximum intima-media thickness (IMT).
# Adjusted for age, sex, baseline abdominal obesity, and pulse wave velocity (PWV).
** Adjusted for age, sex, baseline augmentation index, and use of csDMARDs throughout the year.

averaged achievement of MDA represented the percentage of time when the patient exhibited MDA throughout the study period, while sMDA demonstrated the prolonged control of disease activity over consecutive visits. These findings suggest that stable low disease activity over a prolonged period of time may have a significant protective effect against CVD in patients with PsA compared to those patients with intermittent flares.

Previous studies have focused on the vascular effects of anti-TNF treatment in PsA, which were associated with reduced progression of carotid atherosclerosis (8,16,17) and

arterial stiffness (18), as well as with improvement in vascular inflammation (17). A protective effect of anti-TNF agents, as compared to csDMARDs, was greater than when compared to no systemic therapy (17). In fact, treatment with csDMARDs was associated with the progression of atherosclerosis (16,17). Those studies were unable to determine whether the vascular effects were due to suppression of inflammation or to the blockade of the specific pathways. In the present study, we observed that achieving sMDA had a protective effect on carotid atherosclerosis and arterial stiffness, a finding that was independent of the use of bDMARDs, suggesting that con-

trolling disease activity using various combinations of conventional and bDMARDs may be useful in improving CV risk in these patients.

A previous study of PsA showed the superiority in achieving clinical outcomes of a treat-to-target strategy compared with routine care (15). We investigated further to explore whether aiming at sMDA could lead to a better vascular outcome. A recent study showed that low disease activity (LDA) is sufficient to achieve a protective effect against CVD in RA (31). Apparently, remission defined as a Disease Activity Score in 28 joints (32) of <2.6 has no additional protective effect against CVD when compared to LDA. Data from that study, as well as from our study, showed that patients who are able to achieve and maintain MDA in PsA or LDA in RA during follow-up may be less likely to experience flares of uncontrolled, sustained, high systemic inflammation, which is a contributing factor to atherosclerosis and CVD. Patients with PsA with very active disease at diagnosis, with a poor treatment response and more frequent flares as a result, may form a subgroup within the PsA population that is particularly at risk for developing CVD, thereby significantly contributing to the excess CVD risk in this population. The idea that achieving sMDA reduces the risk of clinical CV events in PsA remains to be confirmed in large-scale prospective studies.

In both PsA and psoriasis patients, a higher burden of atherosclerotic plaques correlated with the measure of inflammatory burden, disease activity scores, and traditional risk factors (33). A previous study demonstrated that in PsA patients, an increase in TPA was associated with the highest PASI score recorded in the first 3 years of follow-up ($P = 0.02$) (22). The baseline median (IQR) PASI score in the current cohort was 3.4 (0.6–7.6), and most of the patients (71%) had mild psoriasis (PASI score <10). Therefore, our data on subclinical atherosclerosis applied mainly to patients with mild psoriasis. Another psoriatic disease cohort from Toronto with mild psoriasis (mean ± SD PASI score 1.9 ± 2.6) treated with anti-TNF agents also exhibited a reduced rate of atherosclerosis progression in men (17). However, a pilot study in subjects with severe psoriasis vulgaris demonstrated reduced carotid IMT in patients without preexisting carotid plaques after anti-TNF therapy, suggesting that these findings may also be applicable to patients with severe psoriasis (34). Future studies need to address the question of whether achieving MDA may prevent atherosclerosis progression in patients with severe psoriasis.

There are a few strengths in our study. To date, this is the first study to investigate a treat-to-target strategy to reduce CV risk. Also, this is one of the largest prospective studies to assess the impact of control of inflammation on 2 different phenotypic features of atherosclerosis in PsA, thereby providing insights about the effect of suppression of inflammation on early (arterial stiffness) and late (carotid plaque) phases of atherogenesis. Limitations of our study include the fact that, in Hong Kong, the cost of bDMARDs is not reimbursed by the government. As a result, most patients treated with bDMARDs paid the cost of the medication out-of-pocket. This may explain why some patients could not afford treatment with bDMARDs after treatment failure with csDMARDs. In PsA/psoriasis, limited evidence suggests that systemic therapies are associated with a decrease in all-CV-event risk (35). Whether early initiation of bDMARDs, compared to csDMARDs, would improve CV outcome would need to be addressed in future studies. A second limitation of our study is the use of surrogate end points instead of actual CV events. There are few studies suggesting that carotid IMT (36), plaque (37), and PWV (38) are good surrogates of future CVD events, specifically in patients with RA. Nonetheless, we have reported a modest association between carotid atherosclerosis and coronary atherosclerosis in patients with PsA (39).

In conclusion, effective control of systematic inflammation by achieving sMDA was associated with less progression in subclinical atherosclerosis and arterial stiffness in patients with PsA. Our results strengthen the evidence supporting use of tight control (treat-to-target) strategies in daily clinical practice in order to achieve MDA in PsA patients, with the additional goal of reducing CVD risk.

AUTHOR CONTRIBUTIONS

REFERENCES

1. Schieir O, Tosevski C, Glazier RH, Hogg-Johnson S, Badley EM. Incident myocardial infarction associated with major types of arthritis in the general population: a systematic review and meta-analysis. Ann Rheum Dis 2017;76:1396–404.

2. Agca R, Heslinga SC, Rollefstad S, Heslinga M, McInnes IB, Peters MJ, et al. EULAR recommendations for cardiovascular disease risk management in patients with rheumatoid arthritis and other forms of inflammatory joint disorders: 2015/2016 update. Ann Rheum Dis 2017;76:17–28.

3. Ajeganova S, de Faire U, Jogestrand T, Frostegård J, Hafström I. Carotid atherosclerosis, disease measures, oxidized low-density lipoproteins, and atheroprotective natural antibodies for cardiovascular disease in early rheumatoid arthritis: an inception cohort study. J Rheumatol 2012;39:1146–54.

4. Kimhi O, Caspi D, Bornstein NM, Maharshak N, Gur A, Arbel Y, et al. Prevalence and risk factors of atherosclerosis in patients with psoriatic arthritis. Semin Arthritis Rheum 2007;36:203–9.

5. Gonzalez-Juanatey C, Llorca J, Amigo-Diaz E, Dierssen T, Martin J, Gonzalez-Gay MA. High prevalence of subclinical atherosclerosis in psoriatic arthritis patients without clinically evident cardiovascular disease or classic atherosclerosis risk factors. Arthritis Rheum 2007;57:1074–80.

6. Eder L, Zisman D, Barzilai M, Laor A, Rahat M, Rozenbaum M, et al. Subclinical atherosclerosis in psoriatic arthritis: a case-control study. J Rheumatol 2008;35:877–82.

7. Tam LS, Shang Q, Li EK, Tomlinson B, Chu TT, Li M, et al. Subclinical carotid atherosclerosis in patients with psoriatic arthritis. Arthritis Rheum 2008;59:1322–31.

8. Di Minno MN, Iervolino S, Peluso R, Scarpa R, Di Minno G, and the CaRRDs Study Group. Carotid intima-media thickness in psoriatic arthritis: differences between tumor necrosis factor-α blockers and traditional disease-modifying antirheumatic drugs. Arterioscler Thromb Vasc Biol 2011;31:705–12.

9. Eder L, Thavaneswaran A, Chandran V, Cook R, Gladman DD. Increased burden of inflammation over time is associated with the extent of atherosclerotic plaques in patients with psoriatic arthritis. Ann Rheum Dis 2015;74:1830–5.

10. Shen J, Shang Q, Li EK, Leung YY, Kun EW, Kwok LW, et al. Cumulative inflammatory burden is independently associated with increased arterial stiffness in patients with psoriatic arthritis: a prospective study. Arthritis Res Ther 2015;17:75.

11. Zhu TY, Li EK, Tam LS. Cardiovascular risk in patients with psoriatic arthritis. Int J Rheumatol 2012;2012:714321.

12. Gladman DD, Farewell VT, Wong K, Husted J. Mortality studies in psoriatic arthritis: results from a single outpatient center. II. Prognostic indicators for death. Arthritis Rheum 1998;41:1103–10.

13. Coates LC, Fransen J, Helliwell PS. Defining minimal disease activity in psoriatic arthritis: a proposed objective target for treatment. Ann Rheum Dis 2010;69:48–53.

14. Coates LC, Helliwell PS. Validation of minimal disease activity criteria for psoriatic arthritis using interventional trial data. Arthritis Care Res (Hoboken) 2010;62:965–9.

15. Coates LC, Moverley AR, McParland L, Brown S, Navarro-Coy N, O'Dwyer JL, et al. Effect of tight control of inflammation in early psoriatic arthritis (TICOPA): a UK multicentre, open-label, randomised controlled trial. Lancet 2015;386:2489–98.

16. Tam LS, Li EK, Shang Q, Tomlinson B, Li M, Leung YY, et al. Tumour necrosis factor α blockade is associated with sustained regression of carotid intima-media thickness for patients with active psoriatic arthritis: a 2-year pilot study. Ann Rheum Dis 2011;70:705–6.

17. Eder L, Joshi AA, Dey AK, Cook R, Siegel EL, Gladman DD, et al. Association of tumor necrosis factor inhibitor treatment with reduced indices of subclinical atherosclerosis in patients with psoriatic disease. Arthritis Rheumatol 2018;70:408–16.

18. Angel K, Provan SA, Fagerhol MK, Mowinckel P, Kvien TK, Atar D. Effect of 1-year anti-TNF-α therapy on aortic stiffness, carotid atherosclerosis, and calprotectin in inflammatory arthropathies: a controlled study. Am J Hypertens 2012;25:644–50.

19. Taylor W, Gladman D, Helliwell P, Marchesoni A, Mease P, Mielants H, et al. Classification criteria for psoriatic arthritis: development of new criteria from a large international study. Arthritis Rheum 2006;54:2665–73.

20. Heuft-Dorenbosch L, Spoorenberg A, van Tubergen A, Landewe R, van ver Tempel H, Mielants H, et al. Assessment of enthesitis in ankylosing spondylitis. Ann Rheum Dis 2003;62:127–32.

21. Garrett S, Jenkinson T, Kennedy LG, Whitelock H, Gaisford P, Calin A. A new approach to defining disease status in ankylosing spondylitis: the Bath Ankylosing Spondylitis Disease Activity Index. J Rheumatol 1994;21:2286–91.

22. Pincus T, Summey JA, Soraci SA Jr, Wallston KA, Hummon NP. Assessment of patient satisfaction in activities of daily living using a modified Stanford Health Assessment Questionnaire. Arthritis Rheum 1983;26:1346–53.

23. Schoels M, Aletaha D, Funovits J, Kavanaugh A, Baker D, Smolen JS. Application of the DAREA/DAPSA score for assessment of disease activity in psoriatic arthritis. Ann Rheum Dis 2010;69:1441–7.

24. Fredriksson T, Pettersson U. Severe psoriasis: oral therapy with a new retinoid. Dermatologica 1978;157:238–44.

25. Fries JF, Spitz PW, Kraines RG, Holman HR. Measurement of patient outcome in arthritis. Arthritis Rheum 1980;23:137–45.

26. Spence JD. Ultrasound measurement of carotid plaque as a surrogate outcome for coronary artery disease. Am J Cardiol 2002;89:10–5.

27. Eder L, Jayakar J, Shanmugarajah S, Thavaneswaran A, Pereira D, Chandran V, et al. The burden of carotid artery plaques is higher in patients with psoriatic arthritis compared with those with psoriasis alone. Ann Rheum Dis 2013;72:715–20.

28. Tam LS, Shang Q, Li EK, Wong S, Li RJ, Lee KL, et al. Serum soluble receptor for advanced glycation end products levels and aortic augmentation index in early rheumatoid arthritis: a prospective study. Semin Arthritis Rheum 2012;42:333–45.

29. Gossec L, McGonagle D, Korotaeva T, Lubrano E, de Miguel E, Ostergaard M, et al. Minimal disease activity as a treatment target in psoriatic arthritis: a review of the literature. J Rheumatol 2018;45:6–13.

30. Coates LC, Cook R, Lee KA, Chandran V, Gladman DD. Frequency, predictors, and prognosis of sustained minimal disease activity in an observational psoriatic arthritis cohort. Arthritis Care Res (Hoboken) 2010;62:970–6.

31. Arts EE, Fransen J, den Broeder AA, van Riel P, Popa CD. Low disease activity (DAS28</=3.2) reduces the risk of first cardiovascular event in rheumatoid arthritis: a time-dependent Cox regression analysis in a large cohort study. Ann Rheum Dis 2017;76:1693–9.

32. Prevoo ML, Van 't Hof MA, Kuper HH, van Leeuwen MA, de van Putte LB, van Riel PL. Modified disease activity scores that include twenty-eight–joint counts: development and validation in a prospective longitudinal study of patients with rheumatoid arthritis. Arthritis Rheum 1995;38:44–8.

33. Sobchak C, Eder L. Cardiometabolic disorders in psoriatic disease. Curr Rheumatol Rep 2017;19:63.

34. Jokai H, Szakonyi J, Kontar O, Marschalko M, Szalai K, Karpati S, et al. Impact of effective tumor necrosis factor-α inhibitor treatment on arterial intima-media thickness in psoriasis: results of a pilot study. J Am Acad Dermatol 2013;69:523–9.

35. Roubille C, Richer V, Starnino T, McCourt C, McFarlane A, Fleming P, et al. The effects of tumour necrosis factor inhibitors, methotrexate, non-steroidal anti-inflammatory drugs and corticosteroids on cardiovascular events in rheumatoid arthritis, psoriasis and psoriatic arthritis: a systematic review and meta-analysis. Ann Rheum Dis 2015;74:480–9.

36. Gonzalez-Juanatey C, Llorca J, Martin J, Gonzalez-Gay MA. Carotid intima-media thickness predicts the development of cardiovascular events in patients with rheumatoid arthritis. Semin Arthritis Rheum 2009;38:366–71.

37. Evans MR, Escalante A, Battafarano DF, Freeman GL, O'Leary DH, del Rincón I. Carotid atherosclerosis predicts incident acute coronary syndromes in rheumatoid arthritis. Arthritis Rheum 2011;63:1211–20.

38. Ikdahl E, Rollefstad S, Wibetoe G, Olsen IC, Berg IJ, Hisdal J, et al. Predictive value of arterial stiffness and subclinical carotid atherosclerosis for cardiovascular disease in patients with rheumatoid arthritis. J Rheumatol 2016;43:1622–30.

39. Cheng TH, Shang Q, Li EK, Wong KT, Lee AP, Szeto CC, Tam LS. Increased carotid intima-media thickness can discriminate significant coronary artery stenosis by coronary CT angiogram in patients with psoriatic arthritis [abstract]. Ann Rheum Dis 2017;76 Suppl 2:956.

AMERICAN COLLEGE
OF RHEUMATOLOGY
EDUCATION · TREATMENT · RESEARCH

Psychosis in Systemic Lupus Erythematosus: Results From an International Inception Cohort Study

John G. Hanly,[1] Qiuju Li,[2] Li Su,[2] Murray B. Urowitz,[3] Caroline Gordon,[4] Sang-Cheol Bae,[5] Juanita Romero-Diaz,[6] Jorge Sanchez-Guerrero,[3] Sasha Bernatsky,[7] Ann E. Clarke,[8] Daniel J. Wallace,[9] David A. Isenberg,[10] Anisur Rahman,[10] Joan T. Merrill,[11] Paul R. Fortin,[12] Dafna D. Gladman,[3] Ian N. Bruce,[13] Michelle Petri,[14] (iD) Ellen M. Ginzler,[15] M. A. Dooley,[16] Kristjan Steinsson,[17] Rosalind Ramsey-Goldman,[18] Asad A. Zoma,[19] Susan Manzi,[20] Ola Nived,[21] Andreas Jonsen,[21] Munther A. Khamashta,[22] Graciela S. Alarcón,[23] Ronald F. van Vollenhoven,[24] Cynthia Aranow,[25] Meggan Mackay,[25] Guillermo Ruiz-Irastorza,[26] Manuel Ramos-Casals,[27] S. Sam Lim,[28] Murat Inanc,[29] Kenneth C. Kalunian,[30] Soren Jacobsen,[31] Christine A. Peschken,[32] Diane L. Kamen,[33] Anca Askanase,[34] Chris Theriault,[1] and Vernon Farewell[2]

Objective. To determine, in a large, multiethnic/multiracial, prospective inception cohort of patients with systemic lupus erythematosus (SLE), the frequency, attribution, clinical, and autoantibody associations with lupus psychosis and the short- and long-term outcomes as assessed by physicians and patients.

Methods. Patients were evaluated annually for 19 neuropsychiatric (NP) events including psychosis. Scores on the Systemic Lupus Erythematosus Disease Activity Index 2000, the Systemic Lupus International Collaborating Clinics/American College of Rheumatology Damage Index, and the Short Form 36 (SF-36) were recorded. Time to event and linear regressions were used as appropriate.

Results. Of 1,826 SLE patients, 88.8% were female and 48.8% were Caucasian. The mean ± SD age was 35.1 ± 13.3 years, the mean ± SD disease duration was 5.6 ± 4.2 months, and the mean ± SD follow-up period was 7.4 ± 4.5 years. There were 31 psychotic events in 28 of 1,826 patients (1.53%), and most patients had a single event (26 of 28 [93%]). In the majority of patients (20 of 25 [80%]) and events (28 of 31 [90%]), psychosis was attributed to SLE, usually either in the year prior to or within 3 years of SLE diagnosis. Positive associations (hazard ratios [HRs] and 95% confidence intervals [95% CIs]) with lupus psychosis were previous SLE NP events (HR 3.59 [95% CI 1.16–11.14]), male sex (HR 3.0 [95% CI 1.20–7.50]), younger age at SLE diagnosis (per 10 years) (HR 1.45 [95% CI 1.01–2.07]), and African ancestry (HR 4.59 [95% CI 1.79–11.76]). By physician assessment, most psychotic events resolved by the second annual visit following onset, in parallel with an improvement in patient-reported SF-36 summary and subscale scores.

Conclusion. Psychosis is an infrequent manifestation of NPSLE. Generally, it occurs early after SLE onset and has a significant negative impact on health status. As determined by patient and physician report, the short- and long-term outlooks are good for most patients, although careful follow-up is required.

INTRODUCTION

Neuropsychiatric (NP) events are one of the features of systemic lupus erythematosus (SLE), but their frequency and attribution to SLE or other causes is variable. Overall, approximately one-third are caused directly by SLE (1), but for individual manifestations this varies between 0% and 100% (2,3). The outcome for individual NPSLE manifestations, especially rare NP events, is derived from observational cohorts of well-characterized patients followed up over prolonged periods.

One of the rarer NP events is lupus psychosis, which is part of both the American College of Rheumatology (ACR) (4) and the Systemic Lupus International Collaborating Clinics (SLICC) (5) classification criteria for SLE. Characterized by delusions and hallucinations, it is a dramatic presentation of NPSLE (6,7). It is one of the few manifestations of nervous system disease in SLE associated, although inconsistently, with a lupus-specific autoantibody against ribosomal P (8–10). The infrequent occurrence of psychosis has limited the number of clinical studies, and most consist of case series obtained by review of medical records. In the present study of lupus psychosis, we determined its frequency, attribution, clinical, and autoantibody associations and the outcome assessed by physicians and patients in a large, multiethnic/multiracial, prospective inception cohort of SLE patients.

PATIENTS AND METHODS

Research study network. The study was conducted by the SLICC (11), a network of 53 investigators in 43 academic medical centers in 16 countries. The current study involved 31 centers in 10 countries. Data were collected per protocol at enrollment and annually, submitted to the coordinating center in Halifax, Nova Scotia, Canada, and entered into an Access database. Appropriate procedures ensured data quality, management, and security. The Nova Scotia Health Authority central zone Research Ethics Board, Halifax, and each of the participating centers' institutional research ethics review boards approved the study.

Patients. Patients fulfilled the ACR classification criteria for SLE (4), which served as the date of diagnosis, and provided written informed consent. Enrollment was permitted up to 15 months following the diagnosis. Demographic variables, education, and medication history were recorded. Lupus-related variables included the Systemic Lupus Erythematosus Disease Activity Index 2000 (SLEDAI-2K) (12) and the SLICC/ACR Damage Index (SDI) (13). Laboratory testing required to determine the SLEDAI-2K and SDI scores was done at each center.

NP events. An enrollment window extended from 6 months prior to the diagnosis of SLE up to the actual enrollment date. NP events were characterized within this window using the ACR case definitions for 19 NP syndromes (14). The clinical diagnosis was supported by investigations, if warranted, as per the guidelines. Patients were reviewed annually within a 6-month window around the assessment date. New NP events and the status of previous NP events since the last study visit were determined at each assessment.

The ACR case definition for psychosis (14) includes the following: 1) delusions or hallucinations without insight; 2) causing clinical distress or impairment in social, occupational, or other relevant areas of functioning; 3) disturbance should not occur exclusively during delirium; and 4) not better accounted for by another mental disorder. Recurring episodes of psychosis and other NP events within the enrollment window or within a follow-up assessment period were recorded once for that period of observation.

University, Montreal, Quebec, Canada; [8]Ann E. Clarke, MD, MSc: University of Calgary, Calgary, Alberta, Canada; [9]Daniel J. Wallace, MD: Cedars-Sinai Medical Center and David Geffen School of Medicine at University of California, Los Angeles; [10]David A. Isenberg, MD, Anisur Rahman, MD, PhD: University College London, London, UK; [11]Joan T. Merrill, MD: Oklahoma Medical Research Foundation, Oklahoma City; [12]Paul R. Fortin, MD, MPH: CHU de Québec, Université Laval, Quebec City, Quebec, Canada; [13]Ian N. Bruce, MD: University of Manchester and Manchester University NHS Foundation Trust, Manchester, UK; [14]Michelle Petri, MD: Johns Hopkins University School of Medicine, Baltimore, Maryland; [15]Ellen M. Ginzler, MD, MPH: SUNY Downstate Medical Center, Brooklyn, New York; [16]M. A. Dooley, MD, MPH: University of North Carolina, Chapel Hill; [17]Kristjan Steinsson, MD: Landspitali University Hospital, Reykjavik, Iceland; [18]Rosalind Ramsey-Goldman, MD, DrPH: Northwestern University, Chicago, Illinois; [19]Asad A. Zoma, MD: Hairmyres Hospital, East Kilbride, Scotland, UK; [20]Susan Manzi, MD, MPH: Lupus Center of Excellence, Allegheny Health Network, Pittsburgh, Pennsylvania; [21]Ola Nived, MD, PhD, Andreas Jonsen, MD, PhD: Lund University, Lund, Sweden; [22]Munther A. Khamashta, MD: St Thomas' Hospital, King's College London School of Medicine, London, UK; [23]Graciela S. Alarcón, MD, MPH: University of Alabama at Birmingham; [24]Ronald F. van Vollenhoven, MD: Karolinska Institute, Stockholm, Sweden; [25]Cynthia Aranow, MD, Meggan Mackay, MD: Feinstein Institute for Medical Research, Manhasset, New York; [26]Guillermo Ruiz-Irastorza, MD: Hospital Universitario Cruces, University of the Basque Country, Barakaldo, Spain; [27]Manuel Ramos-Casals, MD: Hospital Clínic, Barcelona, Spain; [28]S. Sam

Lim, MD, MPH: Emory University School of Medicine, Atlanta, Georgia; [29]Murat Inanc, MD: Istanbul University, Istanbul, Turkey; [30]Kenneth C. Kalunian, MD: University of California San Diego School of Medicine, La Jolla; [31]Soren Jacobsen, MD, DMSc: Rigshospitalet, Copenhagen University Hospital, Copenhagen, Denmark; [32]Christine A. Peschken, MD: University of Manitoba, Winnipeg, Manitoba, Canada; [33]Diane L. Kamen, MD: Medical University of South Carolina, Charleston; [34]Anca Askanase, MD, MPH: Hospital for Joint Diseases, New York University, New York, New York.

The date of the first episode was taken as the onset of the event. Once an NP event had resolved, a subsequent event of the same type was recorded as a new event.

Attribution of NP events. Decision rules used to determine the attribution of NP events were similar to those reported in other publications concerning the SLICC NPSLE inception cohort (15,16). We considered 3 factors. The first was the temporal onset of NP event(s) in relation to the diagnosis of SLE, and the second concerned concurrent non-SLE factor(s), such as potential causes ("exclusions") or contributing factors ("associations") for each NP syndrome in the glossary for the ACR case definitions of NP events (14). For psychosis, the prespecified potential alternative causes (exclusions) were 1) primary psychotic disorder unrelated to SLE (e.g., schizophrenia), 2) substance- or drug-induced psychotic disorder, and 3) psychologically mediated reaction to SLE (brief reactive psychosis with major stressor); the prespecified potential contributing factors (associations) were 1) marked psychosocial stress and 2) corticosteroids. For the third and final factor, we identified "common" NP events in normal population controls as described by Ainiala et al (17). These included isolated headaches, anxiety, and mild depression (mood disorders failing to meet criteria for "major depressive-like episodes"), mild cognitive impairment (deficits in less than 3 of the 8 specified cognitive domains), and polyneuropathy without electrophysiologic confirmation. Using these 3 factors, we used 2 attribution decision rules of different stringency (models A and B) (15,16).

Attribution model A (most stringent). NP events that had their onset within the enrollment window *and* had no exclusions or associations *and* were not one of the NP events identified by Ainiala et al (17) were attributed to SLE.

Attribution model B (least stringent). NP events that had their onset within 10 years of the diagnosis of SLE and were still present within the enrollment window *and* had no exclusions *and* were not one of the NP events identified by Ainiala et al (17) were attributed to SLE.

By definition, all NP events attributed to SLE using model A were similarly attributed using model B. Events that did not fulfill these criteria were classified as non-SLE NP events.

Outcome of psychosis. For every NP event, a physician-generated 7-point Likert scale was completed at each follow-up assessment until resolution of the event or patient demise (1 = patient demise, 2 = much worse, 3 = worse, 4 = no change, 5 = improved, 6 = much improved, 7 = resolved) (18). A patient-generated Short Form 36 (SF-36) questionnaire was also completed at each assessment and provided subscale scores, mental component summary (MCS) and physical component summary (PCS) scores (18,19) that were unavailable to physicians at their assessments.

Autoantibodies. Plasma lupus anticoagulant, serum IgG anticardiolipin, anti–β_2-glycoprotein I, anti–ribosomal P (anti-P), and anti–NR2 glutamate receptor antibodies were measured at the Oklahoma Medical Research Foundation, as described (20–23).

Statistical analysis. Since there were only 15 patients with psychosis attributed to SLE by model A, we used attribution model B and Cox regression to analyze time to first SLE psychosis. This included onset of NP events prior to SLE diagnosis in order to capture all NP events potentially related to the risk of psychosis.

Hazard ratios (HRs) and 95% confidence intervals (95% CIs) were calculated. Covariates examined included sex, race/ethnicity, SLICC sites, postsecondary education, number of ACR criteria at enrollment (excluding neurologic disorder), SDI (without NP variables), other concurrent NP events, and, as continuous variables, age at SLE diagnosis, disease duration (in years), and SLEDAI-2K score (without NP variables). Binary variables indicating autoantibodies present at baseline and follow-up assessments were defined when available. Time-varying variables, other than those related to autoantibodies, were updated at each assessment. When examining the time-varying version of the autoantibody variables, autoantibody data in the period before enrollment were imputed by their values at enrollment, while autoantibody data at follow-up assessments were imputed by the last observation carried forward method. Kaplan-Meier estimates of the survivor function for the time until resolution of psychosis were calculated. For analyses of longitudinal SF-36 subscale and summary scores, linear regression with generalized estimating equations allowed for correlation of observations within patients, and adjustment variables included time/visit, sex, age at SLE diagnosis, race/ethnicity/location, education, SLEDAI-2K and SDI scores (without NP variables), corticosteroids, antimalarials, and immunosuppressant use since last assessment.

RESULTS

Patient recruitment and assessments. A total of 1,826 patients were recruited between October 1999 and December 2011, from centers in the US (n = 539 [29.5%]), Europe (n = 477 [26.1%]), Canada (n = 418 [22.9%]), Mexico (n = 223 [12.2%]), and Asia (n = 169 [9.3%]) (Table 1). The number of patient assessments varied from 1 to 19 with a mean ± SD follow-up period of 7.4 ± 4.5 years, and final assessment follow-up was in March 2017.

NP manifestations. NP events (≥1) occurred in 951 of 1,826 patients (52.1%), and 488 of 1,826 patients (26.7%) had ≥2 events during the study period. There were 1,902 unique NP events, encompassing all 19 NP syndromes in the ACR case definitions (14). The proportion of NP events attributed to SLE varied from 17.8% (attribution model A) to 31.1% (attribution model B)

Table 1. Demographics, clinical features, medications, and autoantibodies in the 1,826 patients at enrollment*

Sex, no. (%)	
Female	1,622 (88.8)
Male	204 (11.2)
Age, years	35.1 ± 13.3
Race/ethnicity, no. (%)	
Caucasian	891 (48.8)
African	306 (16.8)
Hispanic	282 (15.4)
Asian	275 (15.1)
Other	72 (3.9)
Marital status, no. (%)	
Single	818 (44.9)
Married	766 (42.0)
Other	238 (13.1)
Postsecondary education, no. (%)	1,064 (61.9)
Disease duration, months	5.6 ± 4.2
ACR SLE criteria met	4.9 ± 1.1
ACR SLE criteria, no. (%)	
Malar rash	660 (36.1)
Discoid rash	227 (12.4)
Photosensitivity	652 (35.7)
Oral/nasal ulcers	677 (37.1)
Serositis	502 (27.5)
Arthritis	1,368 (74.9)
Renal disorder	510 (27.9)
Neurologic disorder	88 (4.8)
Hematologic disorder	1,129 (61.8)
Immunologic disorder	1,392 (76.2)
Antinuclear antibody positivity	1,731 (94.8)
SLEDAI-2K score	5.3 ± 5.4

Table 1. *(Cont'd)*

SLICC/ACR Damage Index score†	0.32 ± 0.74
Medications, no. (%)	
Corticosteroids	1,284 (70.3)
Antimalarials	1,231 (67.4)
Immunosuppressants	732 (40.1)
ASA	261 (14.3)
Antidepressants	183 (10.0)
Warfarin	99 (5.4)
Anticonvulsants	80 (4.4)
Antipsychotics	12 (0.7)
Autoantibody positivity, no./total no. (%)	
Lupus anticoagulant	241/1,174 (20.5)
Anticardiolipin	138/1,142 (12.1)
Anti–β_2-glycoprotein I	163/1,142 (14.3)
Anti–ribosomal P	112/1,136 (9.9)
Anti–NR2 glutamate receptor	130/1,064 (12.2)

* Except where indicated otherwise, values are the mean ± SD. SLEDAI-2K = Systemic Lupus Erythematosus Disease Activity Index 2000; ASA = acetylsalicylic acid.
† The Systemic Lupus International Collaborating Clinics/American College of Rheumatology (SLICC/ACR) Damage Index score was not available for 1,057 patients at the enrollment visit when disease duration was <6 months.

and occurred in 13.3% of patients (model A) to 21.1% of patients (model B). Of the 1,902 unique NP events, 1,742 (91.6%) involved the central nervous system and 160 (8.4%) involved the peripheral nervous system (14). The classification of events as diffuse and focal was 1,471 (77.3%) and 431 (22.7%), respectively (16).

Psychosis. Among 28 of 1,826 patients with psychosis (1.53%), 26 of 28 (93%) had a single psychotic event, while 1 patient had 2 discrete events and 1 patient had 3 discrete events. The majority of patients had psychosis attributed to SLE (15 of 28 [54%] using attribution model A and 25 of 28 [89%] using attribution model B). Patients with lupus psychosis (model B) were located in centers in Europe (9 patients), Canada (6 patients), the US (5 patients), Mexico (4 patients), and Asia (1 patient). There was no significant association between location and risk of SLE psychosis (P = 0.53 in Cox regression) taking into account the

number of patients and the duration of follow-up at each site. The majority of patients with lupus psychosis (20 of 25 [80%]) had their first episode either in the year prior to or within 3 years following the diagnosis of SLE (Figure 1). There were 31 psychotic events, of which 16 of 31 (52%) and 28 of 31 (90%) were attributed to SLE using attribution models A and B, respectively. The earliest psychotic episode occurred 2 months prior to the diagnosis of SLE.

Clinical and laboratory associations with lupus psychosis. Using Cox regression, we looked for associations with the risk of the first episode of psychosis attributed to SLE using attribution model B. Univariate analysis revealed positive associations with male sex (HR 2.58 [95% CI 1.04–6.41]), younger age at diagnosis (per 10 years) (HR 1.36 [95% CI 1.0–1.88]), African ancestry (HR 4.80 [95% CI 1.86–12.40]), in particular for patients outside the US (HR 5.53 [95% CI 1.86–16.42]), concurrent other central (HR 3.86 [95% CI 1.27–11.70]) or diffuse (HR 6.36 [95% CI 2.12–19.12]) NP events (mood disorder, acute confusional state) attributed to SLE, and presence of anti-P antibodies at the enrollment visit into the cohort (HR 3.31 [95% CI 1.19–9.21]) and over time (HR 3.13 [95% CI 1.15–8.56]).

Important variables identified in univariate analyses, in particular for African patients outside the US, were included in multivariate analyses, excluding antibody variables due to reduced sample size consequent to missing data (Table 2). The significant positive associations with lupus psychosis were similar, namely, prior SLE NP events (HR 3.59 [95% CI 1.16–
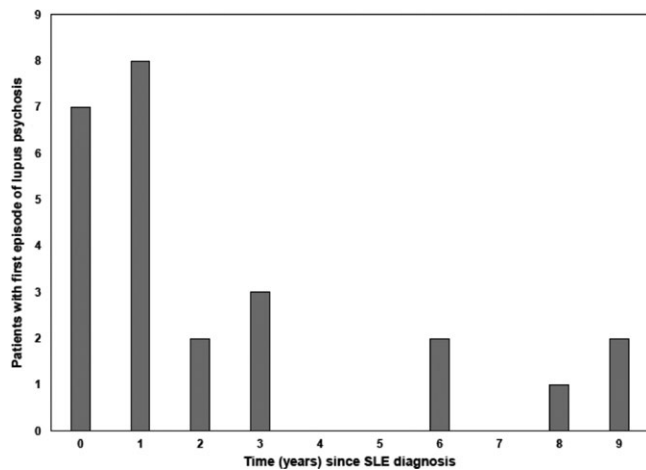
Figure 1. Relationship between the time of onset of lupus psychosis and diagnosis of systemic lupus erythematosus (SLE).

11.14]), male sex (HR 3.0 [95% CI 1.20–7.50]), younger age at SLE diagnosis (per 10 years) (HR 1.45 [95% CI 1.01–2.07]), and African ancestry (HR 4.59 [95% CI 1.79–11.76]). Further, after adjustment for the demographic predictors in Table 2 (sex, age at SLE diagnosis, and race/ethnicity), anti-P antibodies at enrollment (HR 2.29 [95% CI 0.81–6.46], *P* = 0.11) and over time (HR 2.17 [95% CI 0.79–5.97], *P* = 0.13) were no longer significantly associated with the risk of lupus psychosis.

Treatment of SLE psychosis. The treatment of individual patients was at the discretion of their attending rheumatologists and was predicated on the overall needs of the patient and not only on the psychotic event. The following therapies

were used during the time of the first psychotic events: corticosteroids in 23 of 28 patients (82.1%) with a mean ± SD dose of prednisone of 21.9 ± 14.9 mg/day, immunosuppressants (cyclophosphamide, azathioprine, methotrexate, mycophenolate mofetil) in 17 of 28 patients (60.7%), biologic agents in 1 of 28 patients (3.6%), antipsychotic drugs in 19 of 28 patients (67.9%), antidepressants in 11 of 28 patients (39.3%), and either/both antipsychotic drugs and antidepressants in 22 of 28 patients (78.6%). In 13 of 28 patients (46.4%), corticosteroids had been started prior to the onset of psychosis with a mean ± SD dose of 20.3 ± 13.6 mg/day.

Clinical outcome and health-related quality of life (HRQoL) in patients with lupus psychosis. A summary of physician assessments of outcome of lupus psychosis is illustrated in Figure 2. More than 80% of the psychotic events had resolved by the second annual assessment following onset of the event (Figure 2A). Likewise, the maximum and minimum Likert scores over the duration of follow-up illustrate that the majority of psychotic events either improved or resolved during the period of observation (Figure 2B).

The mean ± SD SF-36 PCS and MCS scores are shown in Figure 3A for 4 patient groups. Group 1 consisted of patients with onset of lupus psychosis since last assessment or with an ongoing psychotic event (n = 29 visits). Group 2 consisted of patients with onset of other NP events since last assessment or ongoing other NP event(s), including non-SLE psychosis (n = 3,379 visits). Group 3 consisted of patients with no NP events since last assessment and no ongoing NP event(s) but with a history of previous NP event(s) (n = 2,180 visits). Group 4 consisted of patients who never

Table 2. Predictors of lupus psychosis by multivariate analysis*

Predictor, factor level	HR (95% CI)	*P*
Other concurrent NP events		
No concurrent NP events	1	
Any unresolved NP events attributed to SLE	3.59 (1.16–11.14)	0.027†
Any unresolved NP events not attributed to SLE but no events attributable to SLE	0.89 (0.21–3.82)	0.087†
Global test	–	0.082
Sex		
Female	1	
Male	3.0 (1.20–7.50)	0.019†
Younger age at SLE diagnosis (per 10 years)	1.45 (1.01–2.07)	0.044†
Race		
Caucasian	1	
African	4.59 (1.79–11.76)	0.002†
Asian and other	0.93 (0.24–3.64)	0.913†
Hispanic	1.37 (0.39–4.85)	0.622†
Global test	–	0.005

* HR = hazard ratio; 95% CI = 95% confidence interval; NP = neuropsychiatric; SLE = systemic lupus erythematosus.
† By Wald's test.
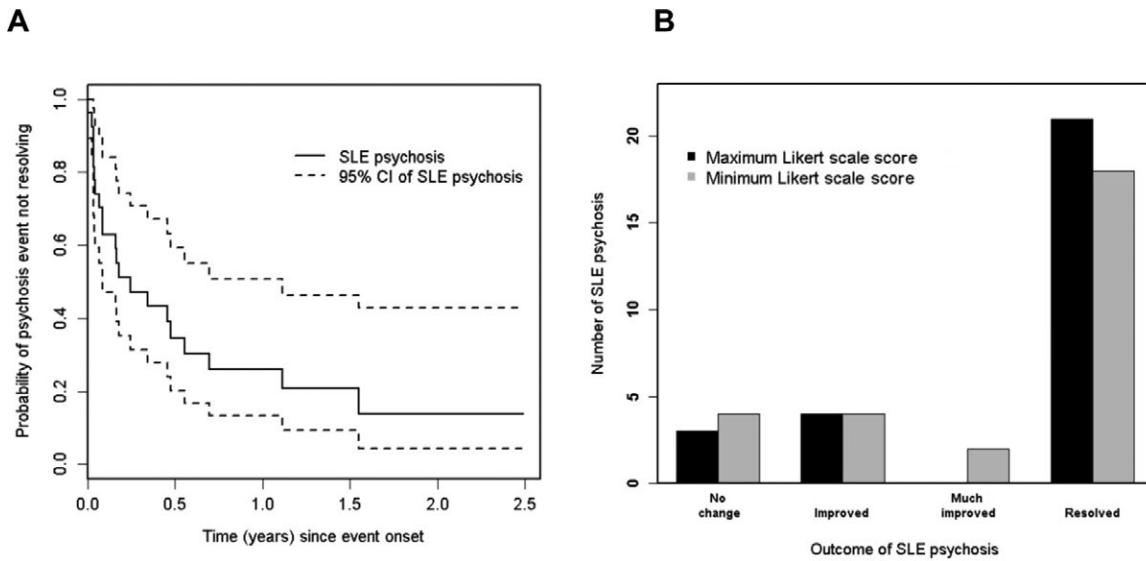
Figure 2. Physician-determined outcome of lupus psychosis. **A,** Survival curve for resolution. **B,** Likert scale scores. The highest and lowest scores over the duration of follow-up are shifted to the right, indicating improvement. SLE = systemic lupus erythematosus; 95% CI = 95% confidence interval.

had NP event(s) (n = 5,893 visits). The lowest summary scores were in groups 1 and 2 (global $P < 0.0001$ in the multivariate analyses), and the negative impact on HRQoL affected all 8 subscales of the SF-36 as shown in the accompanying spidergram (Figure 3B).

To determine if there was a persistent change in HRQoL following physician-determined resolution of lupus psychosis, patient-generated SF-36 scores were compared in 2 groups. The psychosis group consisted of patients with onset of lupus psy-

chosis since last assessment up to its resolution (n = 29 visits). The resolved group consisted of patients with resolution of lupus psychosis up to their last follow-up visit or recurrence of psychosis (n = 112 visits). If the psychotic event had both onset and resolution in the same interval prior to assessment, SF-36 scores at that assessment were included only in the psychosis group. As illustrated in Figure 4A, there was substantial improvement both in MCS scores (mean difference 7.01) and in PCS scores (mean
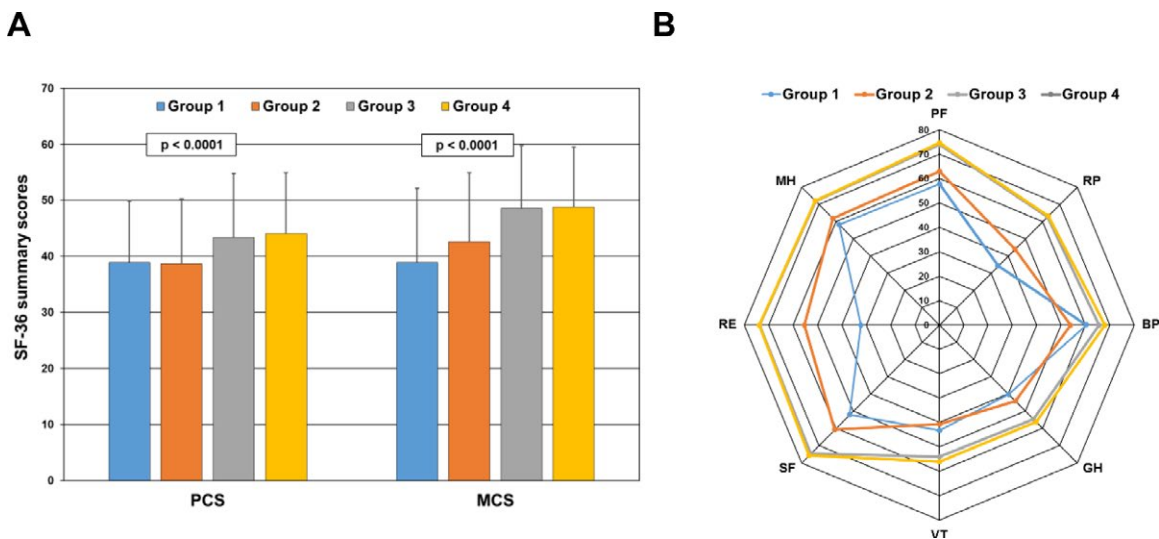
Figure 3. Association of Short Form 36 (SF-36) summary and subscale scores with lupus psychosis. **A,** Mean ± SD physical component summary (PCS) and mental component summary (MCS) scores in 4 groups of patients with systemic lupus erythematosus (SLE). Group 1 consisted of patients with onset of lupus psychosis since last assessment or with an ongoing psychotic event (n = 29 visits). Group 2 consisted of patients with onset of other neuropsychiatric (NP) events since last assessment or ongoing other NP event(s), including non-SLE psychosis (n = 3,379 visits). Group 3 consisted of patients with no NP events since last assessment and no ongoing NP event(s) but with a history of previous NP event(s) (n = 2,180 visits). Group 4 consisted of patients who never had NP event(s) (n = 5,893 visits). The numbers of assessments contributing to each bar are aggregated for patients over time. Global *P* values in the multivariate analyses are shown. **B,** Comparison of individual subscale scores in the same 4 patient groups. SF-36 subscales are as follows: PF = physical function; RP = role physical; BP = bodily pain; GH = general health; VT = vitality; SF = social function; RE = role emotion; MH = mental health.
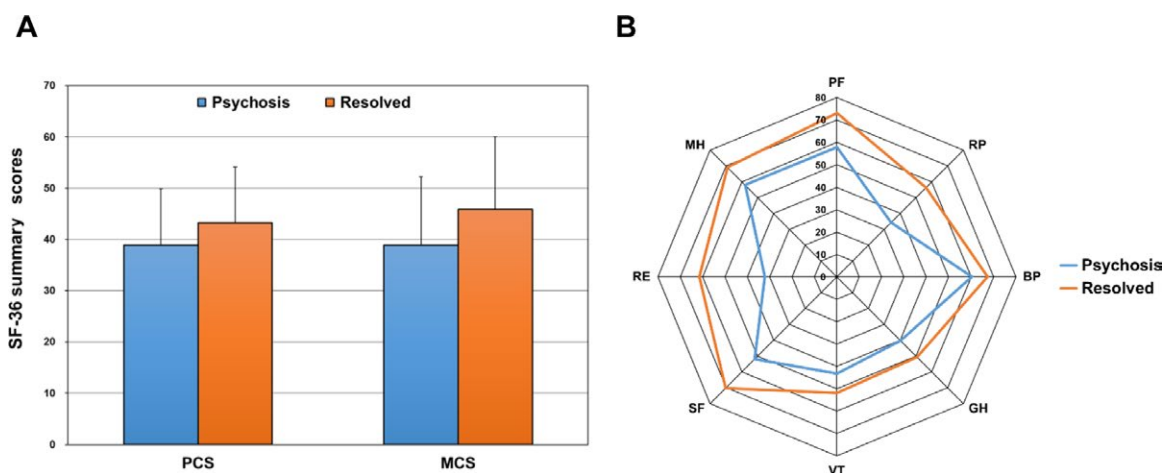
Figure 4. Long-term change in Short Form 36 (SF-36) summary and subscale scores following resolution of lupus psychosis. **A,** Mean ± SD physical component summary (PCS) and mental component summary (MCS) scores in 2 groups of patients with systemic lupus erythematosus. The psychosis group consisted of patients with onset of lupus psychosis since last assessment up to its resolution (n = 29 visits). The resolved group consisted of patients with resolution of lupus psychosis up to their last follow-up visit or recurrence of psychosis (n = 112 visits). If the psychotic event had both onset and resolution in the same interval prior to assessment, SF-36 scores at that assessment were included only in the psychosis group. The numbers of assessments contributing to each bar are aggregated for patients over time. **B,** Comparison of individual subscale scores in the same 2 patient groups. SF-36 subscales are as follows: PF = physical function; RP = role physical; BP = bodily pain; GH = general health; VT = vitality; SF = social function; RE = role emotion; MH = mental health.

difference 4.34) and in all subscales of the SF-36 (Figure 4B) concurrent with resolution of lupus psychosis.

DISCUSSION

In a large international inception cohort study of SLE patients, we have prospectively documented the frequency, associations, and outcomes of psychotic events during a mean follow-up period of 7.4 years. Our findings confirm and expand upon the results of previous cross-sectional and historical studies of psychosis in SLE (6–8,24,25). The majority of psychotic events were directly attributed to SLE, had a tendency to occur early in the course of the disease, and were more frequent in male patients. Psychosis was also more frequent in patients of African ancestry, as is also the case for non-SLE patients with the same race/ethnicity (26). The outcome of lupus psychosis, as determined by both physicians and patients, was positive and emphasizes the importance of diagnosing and treating this rare manifestation of NPSLE.

Studies of NPSLE conducted prior to the introduction in 1999 of the ACR case definitions for NPSLE did not have a uniform definition for psychosis. Using the ACR case definition, the frequency of psychosis has been reported to vary between 0% and 17.1% (6,17,27–30), and in our study it was 1.53% (28 of 1,826 patients). Using a well-defined process for determining attribution, we confirmed that the majority of psychotic events were due to SLE. In keeping with other NPSLE events and with other severe SLE manifestations such as nephritis (31), there was a tendency for psychosis to occur early in the disease course, usually within the first 3 years following the diagnosis of SLE. Univariate analysis identified significant associations between lupus psychosis and

anti-P antibodies, although following adjustment for demographic variables, the 95% CIs around HRs were wide and included the null value, precluding a definitive conclusion regarding association of these autoantibodies with psychosis. This is consistent with an earlier report on NP events in the SLICC inception cohort (32).

The potential role of corticosteroids must also be considered. In the current study, exposure to corticosteroids prior to lupus psychosis occurred in less than half of the initial events. As per the ACR case definition for psychosis (14), the concurrent use of corticosteroids at the onset of psychosis was identified as an association rather than as a firm exclusion, indicating uncertainty about the role of corticosteroids in individual cases and to allow flexibility for determining attribution. Although NP symptoms have been reported with all types and doses of corticosteroids (33), including psychosis following intraarticular steroid injections (34,35), in general the dose of corticosteroids is the most important risk factor. In the Boston Collaborative Drug Surveillance Program (36), the frequency of psychiatric symptoms of any type was 18.6% in patients receiving >80 mg/day of prednisone, 4.6% in patients receiving 40–80 mg/day, and 1.3% in those receiving <40 mg/day. In the current study, exposure to corticosteroids prior to lupus psychosis was in the lowest of these dose ranges.

Although the somatic toxicities of corticosteroids are well described, the literature on NP effects is sparse. Their reported frequency varies widely from 2% to 60% (36–38), and symptoms include affective, behavioral, and cognitive manifestations (33). Moreover, the term "steroid psychosis" has been used to capture a heterogeneous group of NP effects and is not supported by validated diagnostic criteria, and previous studies

have included many patients who were not psychotic. The ACR case definition for psychosis (14), used in the current study, is based on the Diagnostic and Statistical Manual of Mental Disorders, Fourth Edition (DSM-IV) (39). In a previous study of 2,069 patients who received corticosteroids, only 3 (0.14%) developed psychosis according to DSM-IV criteria (40).

One of the major advantages of our prospective study was the ability to document the short-term impact and long-term outcome of lupus psychosis from the perspectives of both the physician and the patient. In keeping with previous studies (6,7), the physician assessments indicated resolution in the majority of cases with very few recurrences. Using a previously validated approach to measure the clinical outcome of NP events in SLE (18), we used summary and subscale scores of the SF-36 to assess the patient perspective. This is important because physician and patient assessment of outcome for other manifestations of SLE (41) and some NP events (42) may be discrepant. Although the greatest impact was on MCS scores, it was apparent that all subscales of the SF-36 were negatively impacted in patients with lupus psychosis. However, following treatment and in keeping with physician assessment of outcome, the patient-generated SF-36 scores showed a remarkable reversal when averaged over time.

There are some limitations to the current study. First, the small number of patients with lupus psychosis limited our ability to precisely estimate potential associations with clinical or laboratory variables of interest. However, most of the previous studies have had an even smaller sample size, and the SLICC cohort is the largest inception cohort of SLE patients. Second, specialized investigations such as advanced neuroimaging or cytokine profiling of cerebrospinal fluid were not routinely performed but were left to the discretion of individual investigators, which reflects what is done in clinical practice, a key component of our overall SLICC protocol. Third, the observational cohort study design precludes determination of optimal therapeutic regimens for lupus psychosis but instead reflects current standard of care. Despite these limitations, the study provides encouraging data on the outcome of this rare but potentially devastating manifestation of NPSLE.

AUTHOR CONTRIBUTIONS

All authors were involved in drafting the article or revising it critically for important intellectual content, and all authors approved the final version to be published. Dr. Hanly had full access to all of the data in the study and takes responsibility for the integrity of the data and the accuracy of the data analysis.

Study conception and design. Hanly, Urowitz, Gordon, Romero-Diaz, Clarke, Merrill, Fortin, Gladman, Bruce, Petri, Zoma, Nived, Khamashta, Alarcón, Askanase, Farewell.

Acquisition of data. Hanly, Urowitz, Gordon, Bae, Romero-Diaz, Sanchez-Guerrero, Bernatsky, Clarke, Wallace, Isenberg, Rahman, Merrill, Fortin, Gladman, Bruce, Petri, Ginzler, Dooley, Steinsson, Ramsey-Goldman, Zoma, Manzi, Nived, Khamashta, Alarcón, van

Vollenhoven, Aranow, Mackay, Ruiz-Irastorza, Ramos-Casals, Lim, Inanc, Kalunian, Jacobsen, Peschken, Kamen, Askanase, Theriault.

Analysis and interpretation of data. Hanly, Li, Su, Urowitz, Gordon, Romero-Diaz, Bernatsky, Clarke, Wallace, Fortin, Bruce, Zoma, Jonsen, Khamashta, Alarcón, van Vollenhoven, Inanc, Askanase, Farewell.

REFERENCES

1. Hanly JG. Diagnosis and management of neuropsychiatric SLE. Nat Rev Rheumatol 2014;10:338–47.

2. Bortoluzzi A, Fanouriakis A, Appenzeller S, Costallat L, Scire CA, Murphy E, et al. Validity of the Italian algorithm for the attribution of neuropsychiatric events in systemic lupus erythematosus: a retrospective multicentre international diagnostic cohort study. BMJ Open 2017;7:e015546.

3. Hanly JG. Avoiding diagnostic pitfalls in neuropsychiatric lupus: the importance of attribution. Lupus 2017;26:497–503.

4. Hochberg MC, for the Diagnostic and Therapeutic Criteria Committee of the American College of Rheumatology. Updating the American College of Rheumatology revised criteria for the classification of systemic lupus erythematosus [letter]. Arthritis Rheum 1997;40:1725.

5. Petri M, Orbai AM, Alarcon GS, Gordon C, Merrill JT, Fortin PR, et al. Derivation and validation of the Systemic Lupus International Collaborating Clinics classification criteria for systemic lupus erythematosus. Arthritis Rheum 2012;64:2677–86.

6. Appenzeller S, Cendes F, Costallat LT. Acute psychosis in systemic lupus erythematosus. Rheumatol Int 2008;28:237–43.

7. Pego-Reigosa JM, Isenberg DA. Psychosis due to systemic lupus erythematosus: characteristics and long-term outcome of this rare manifestation of the disease. Rheumatology (Oxford) 2008;47:1498–502.

8. Bonfa E, Golombek SJ, Kaufman LD, Skelly S, Weissbach H, Brot N, et al. Association between lupus psychosis and anti-ribosomal P protein antibodies. N Engl J Med 1987;317:265–71.

9. Karassa FB, Afeltra A, Ambrozic A, Chang DM, De Keyser F, Doria A, et al. Accuracy of anti–ribosomal P protein antibody testing for the diagnosis of neuropsychiatric systemic lupus erythematosus: an international meta-analysis. Arthritis Rheum 2006;54:312–24.

10. Viana VT, Durcan L, Bonfa E, Elkon KB. Ribosomal P antibody: 30 years on the road. Lupus 2017;26:453–62.

11. Isenberg D, Ramsey-Goldman R. Systemic Lupus International Collaborating Group—onwards and upwards? Lupus 2006;15:606–7.

12. Gladman DD, Ibanez D, Urowitz MB. Systemic Lupus Erythematosus Disease Activity Index 2000. J Rheumatol 2002;29:288–91.

13. Gladman D, Ginzler E, Goldsmith C, Fortin P, Liang M, Urowitz M, et al. The development and initial validation of the Systemic Lupus International Collaborating Clinics/American College of Rheumatology Damage Index for systemic lupus erythematosus. Arthritis Rheum 1996;39:363–9.

14. ACR Ad Hoc Committee on Neuropsychiatric Lupus Nomenclature. The American College of Rheumatology nomenclature and case definitions for neuropsychiatric lupus syndromes. Arthritis Rheum 1999;42:599–608.

15. Hanly JG, Urowitz MB, Sanchez-Guerrero J, Bae SC, Gordon C, Wallace DJ, et al. Neuropsychiatric events at the time of diagnosis of systemic lupus erythematosus: an international inception cohort study. Arthritis Rheum 2007;56:265–73.

16. Hanly JG, Urowitz MB, Su L, Sanchez-Guerrero J, Bae SC, Gordon C, et al. Short-term outcome of neuropsychiatric events in systemic lupus erythematosus upon enrollment into an international inception cohort study. Arthritis Rheum 2008;59:721–9.

17. Ainiala H, Hietaharju A, Loukkola J, Peltola J, Korpela M, Metsanoja R, et al. Validity of the new American College of Rheumatology criteria for neuropsychiatric lupus syndromes: a population-based evaluation. Arthritis Rheum 2001;45:419–23.

18. Hanly JG, Urowitz MB, Jackson D, Bae SC, Gordon C, Wallace DJ, et al. SF-36 summary and subscale scores are reliable outcomes of neuropsychiatric events in systemic lupus erythematosus. Ann Rheum Dis 2011;70:961–7.

19. Thumboo J, Fong KY, Ng TP, Leong KH, Feng PH, Thio ST, et al. Validation of the MOS SF-36 for quality of life assessment of patients with systemic lupus erythematosus in Singapore. J Rheumatol 1999;26:97–102.

20. Merrill JT, Zhang HW, Shen C, Butman BT, Jeffries EP, Lahita RG, et al. Enhancement of protein S anticoagulant function by β2-glycoprotein I, a major target antigen of antiphospholipid antibodies: β2-glycoprotein I interferes with binding of protein S to its plasma inhibitor, C4b-binding protein. Thromb Haemost 1999;81:748–57.

21. Merrill JT, Shen C, Gugnani M, Lahita RG, Mongey AB. High prevalence of antiphospholipid antibodies in patients taking procainamide. J Rheumatol 1997;24:1083–8.

22. Erkan D, Zhang HW, Shriky RC, Merrill JT. Dual antibody reactivity to β2-glycoprotein I and protein S: increased association with thrombotic events in the antiphospholipid syndrome. Lupus 2002;11:215–20.

23. Hanly JG, Urowitz MB, Siannis F, Farewell V, Gordon C, Bae SC, et al. Autoantibodies and neuropsychiatric events at the time of systemic lupus erythematosus diagnosis: results from an international inception cohort study. Arthritis Rheum 2008;58:843–53.

24. Chau SY, Mok CC. Factors predictive of corticosteroid psychosis in patients with systemic lupus erythematosus. Neurology 2003;61:104–7.

25. Mok CC, Lau CS, Wong RW. Treatment of lupus psychosis with oral cyclophosphamide followed by azathioprine maintenance: an open-label study. Am J Med 2003;115:59–62.

26. Schwartz RC, Blankenship DM. Racial disparities in psychotic disorder diagnosis: a review of empirical literature. World J Psychiatry 2014;4:133–40.

27. Brey RL, Holliday SL, Saklad AR, Navarrete MG, Hermosillo-Romo D, Stallworth CL, et al. Neuropsychiatric syndromes in lupus: prevalence using standardized definitions. Neurology 2002;58:1214–20.

28. Hanly JG, Fisk JD, McCurdy G, Fougere L, Douglas JA. Neuropsychiatric syndromes in patients with systemic lupus erythematosus and rheumatoid arthritis. J Rheumatol 2005;32:1459–6.

29. Sanna G, Bertolaccini ML, Cuadrado MJ, Laing H, Mathieu A, Hughes GR. Neuropsychiatric manifestations in systemic lupus erythematosus: prevalence and association with antiphospholipid antibodies. J Rheumatol 2003;30:985–92.

30. Sibbitt WL Jr, Brandt JR, Johnson CR, Maldonado ME, Patel SR, Ford CC, et al. The incidence and prevalence of neuropsychiatric syndromes in pediatric onset systemic lupus erythematosus. J Rheumatol 2002;29:1536–42.

31. Hanly JG, O'Keeffe AG, Su L, Urowitz MB, Romero-Diaz J, Gordon C, et al. The frequency and outcome of lupus nephritis: results from an international inception cohort study. Rheumatology (Oxford) 2016;55:252–62.

32. Hanly JG, Urowitz MB, Su L, Bae SC, Gordon C, Clarke A, et al. Autoantibodies as biomarkers for the prediction of neuropsychiatric events in systemic lupus erythematosus. Ann Rheum Dis 2011;70:1726–32.

33. Dubovsky AN, Arvikar S, Stern TA, Axelrod L. The neuropsychiatric complications of glucocorticoid use: steroid psychosis revisited. Psychosomatics 2012;53:103–15.

34. Robinson DE, Harrison-Hansley E, Spencer RF. Steroid psychosis after an intra-articular injection. Ann Rheum Dis 2000;59:927.

35. Baloch N. Steroid psychosis: a case report. Br J Psychiatry 1974;124:545–6.

36. The Boston Collaborative Drug Surveillance Program. Acute adverse reactions to prednisone in relation to dosage. Clin Pharmacol Ther 1972;13:694–8.

37. Bolanos SH, Khan DA, Hanczyc M, Bauer MS, Dhanani N, Brown ES. Assessment of mood states in patients receiving long-term corticosteroid therapy and in controls with patient-rated and clinician-rated scales. Ann Allergy Asthma Immunol 2004;92:500–5.

38. Lewis DA, Smith RE. Steroid-induced psychiatric syndromes: a report of 14 cases and a review of the literature. J Affect Disord 1983;5:319–32.

39. Diagnostic and statistical manual of mental disorders. 4th ed. Washington, DC: American Psychiatric Association; 1994.

40. Wada K, Yamada N, Sato T, Suzuki H, Miki M, Lee Y, et al. Corticosteroid-induced psychotic and mood disorders: diagnosis defined by DSM-IV and clinical pictures. Psychosomatics 2001;42:461–6.

41. Golder V, Ooi JJ, Antony AS, Ko T, Morton S, Kandane-Rathnayake R, et al. Discordance of patient and physician health status concerns in systemic lupus erythematosus. Lupus 2018;27:501–6.

42. Hanly JG, Li Q, Su L, Urowitz MB, Gordon C, Bae SC, et al. Cerebrovascular events in systemic lupus erythematosus. Arthritis Care Res (Hoboken) 2018;70:1478–87.

Long-Term Clinical Outcomes in a Cohort of Adults With Childhood-Onset Systemic Lupus Erythematosus

N. Groot,[1] D. Shaikhani,[2] Y. K. O. Teng,[3] K. de Leeuw,[4] M. Bijl,[5] R. J. E. M. Dolhain,[6] E. Zirkzee,[7] R. Fritsch-Stork,[8] I. E. M. Bultink,[9] (iD) and S. Kamphuis[2]

Objective. Childhood-onset systemic lupus erythematosus (SLE) is a severe, lifelong, multisystem autoimmune disease. Long-term outcome data are limited. This study was undertaken to identify clinical characteristics and health-related quality of life (HRQoL) of adults with childhood-onset SLE.

Methods. Patients participated in a single study visit comprising a structured history and physical examination. Disease activity (scored using the SLE Disease Activity Index 2000 [SLEDAI-2K]), damage (scored using the Systemic Lupus International Collaborating Clinics/American College of Rheumatology Damage Index [SDI]), and HRQoL (scored using the Short Form 36 Health Survey) were assessed. Medical records were reviewed.

Results. In total, 111 childhood-onset SLE patients were included; the median disease duration was 20 years, 91% of patients were female, and 72% were white. Disease activity was low (median SLEDAI-2K score 4), and 71% of patients received prednisone, hydroxychloroquine (HCQ), and/or other disease-modifying antirheumatic drugs. The vast majority of new childhood-onset SLE–related manifestations developed within 2 years of diagnosis. Damage such as myocardial infarctions began occurring after 5 years. Most patients (62%) experienced damage, predominantly in the musculoskeletal, neuropsychiatric, and renal systems. Cerebrovascular accidents, renal transplants, replacement arthroplasties, and myocardial infarctions typically occurred at a young age (median age 20 years, 24 years, 34 years, and 39 years, respectively). Multivariate logistic regression analysis showed that damage accrual was associated with disease duration (odds ratio [OR] 1.15, $P < 0.001$), antiphospholipid antibody positivity (OR 3.56, $P = 0.026$), and hypertension (OR 3.21, $P = 0.043$). Current HCQ monotherapy was associated with an SDI score of 0 (OR 0.16, $P = 0.009$). In this cohort, HRQoL was impaired compared to the overall Dutch population. The presence of damage reduced HRQoL scores in 1 domain. High disease activity (SLEDAI-2K score ≥8) and changes in physical appearance strongly reduced HRQoL scores (in 4 of 8 domains and 7 of 8 domains, respectively).

Conclusion. The majority of adults with childhood-onset SLE in this large cohort developed significant damage at a young age and had impaired HRQoL without achieving drug-free remission, illustrating the substantial impact of childhood-onset SLE on future life.

INTRODUCTION

Systemic lupus erythematosus (SLE) is a lifelong, multisystem autoimmune disease, known for its highly heterogeneous clinical presentation and waxing–waning disease course. Childhood-onset SLE, defined as SLE with onset at age <18 years (1), represents 10–20% of all SLE cases and has a mean age at onset of 11–12 years (2,3). Childhood-onset SLE is a rare disease, with an incidence rate of 0.3–0.9 per 100,000 patient-years and a prevalence of 1.89–25.7 per

100,000 children worldwide (4–6). Similar to SLE in adults, childhood-onset SLE is seen more often in nonwhite individuals and girls (female:male ratio 4–5:1). Disease manifestations differ among ethnicities, but clinical outcomes such as disease activity and damage tend to be similar among patients when data are corrected for socioeconomic status (7–10).

Although survival rates for childhood-onset SLE patients have greatly improved, morbidity is still high, and questions from children and parents regarding the future course of the disease are difficult to answer (7,11). Long-term follow-up studies of childhood-onset SLE are limited and often have low patient numbers and/or include patients with relatively short disease duration; thus, detailed evidence regarding development of new organ involvement and damage over time is lacking (7,12–17). Overall, these studies show that the majority of adolescents and young adults with childhood-onset SLE still have active disease, receive immunosuppressive drugs, and steadily accrue damage during their disease (7,11,12,18,19).

Only 1 North American cohort study of both childhood-onset SLE and adult-onset SLE patients has included a large number of childhood-onset SLE patients (n = 90) with a long disease duration (mean 16.5 years) and compared outcomes of the 2 diseases (18). In that study, structured telephone interviews were used to collect patient-reported clinical outcomes, of which only significant renal outcomes could be validated by chart review. At the time of interview, childhood-onset SLE patients had lower disease activity and were more likely to have ever received and currently receive glucocorticoids and disease-modifying antirheumatic drugs (DMARDs) when compared to adult-onset SLE patients (18). This was also observed in a cohort in which outcomes were compared between childhood-onset SLE patients, adult-onset SLE patients, and late-onset SLE patients with a disease duration of 12 years (19). In the North American cohort of adult-onset and childhood-onset SLE patients, the latter was shown to be an independent risk factor for mortality (11). Due to the nature of that cohort study (which relied primarily on patient-reported clinical outcomes), data regarding development of damage could not be included.

In children with childhood-onset SLE, health-related quality of life (HRQoL) has been shown to be impaired compared to healthy peers, which has been at least partially attributed to disease activity and damage (20,21). There were no data available regarding HRQoL in adult patients with childhood-onset SLE or pertaining to the specific factors that could influence HRQoL in these patients.

In the present study (the Childhood-Onset SLE in The Netherlands [CHILL-NL] study), we aimed to assess the disease burden of childhood-onset SLE in The Netherlands. In this report, we describe the clinical characteristics of adults with childhood-onset SLE, focusing on disease course and damage accrual over time, in association with HRQoL.

PATIENTS AND METHODS

Patients. All childhood-onset SLE patients who were >18 years old, had been treated in any Dutch hospital, and met the American College of Rheumatology (ACR) criteria for SLE (22,23) were eligible for inclusion in the CHILL-NL study. Rheumatologists, immunologists, nephrologists, hematologists, and neurologists in all 88 Dutch hospitals were contacted. Private practices were not contacted, as there are very few in The Netherlands. Moreover, as SLE is a systemic disease and hospital diagnostics are essential for optimal treatment, rheumatologists in private practices do not typically treat SLE patients. All medical specialists in secondary or tertiary hospitals were contacted via email and informational flyers. They were asked to identify SLE patients in their care who were diagnosed as having childhood-onset SLE prior to their 18th birthday, and to ask if these patients were interested in participating in a study on long-term outcomes. The study was also promoted by the Dutch SLE patient organization (the National Association for Lupus, APS, Scleroderma, and MCTD [NVLE]) both in their magazine and on their web site (24). Due to the study design, data regarding mortality in childhood-onset SLE or clinical characteristics of deceased patients could not be retrieved reliably; therefore, we only report data on surviving patients. The Research Ethics Board of the Erasmus University Medical Center approved the study (MEC-2013-163), and written informed consent was obtained from all patients.

Data collection. The CHILL-NL team designed the study with the help of a patient panel (n = 5). Patients were seen for a single 1.5-hour study visit at the Erasmus University Medical Center. If patients were unable to travel, the study visit was performed at the hospital of their choice. During the study visit, an extensive medical history was obtained using structured data collection forms and (validated) questionnaires. Data regarding demographics, current health, disease activity, damage, disease onset and progression over time, and current and previous medication use were collected. A physical examination was performed, blood and urine were collected, and patients completed questionnaires regarding HRQoL, effects of medication use (on physical appearance, physical health, or mental health [with a yes/no option and a request for elaboration]), education and employment, fertility and family planning, fatigue, depression, and coping and resilience (25–30). For this report, a selection of the data (i.e., disease activity, medication use, disease manifestations over time, damage, and HRQoL) was used. Medical information was requested from all hospitals where patients had previously received care. Clinical data collected during the study visit were supplemented and verified through the retrieved medical history. Only data that could be verified in medical records were reported.
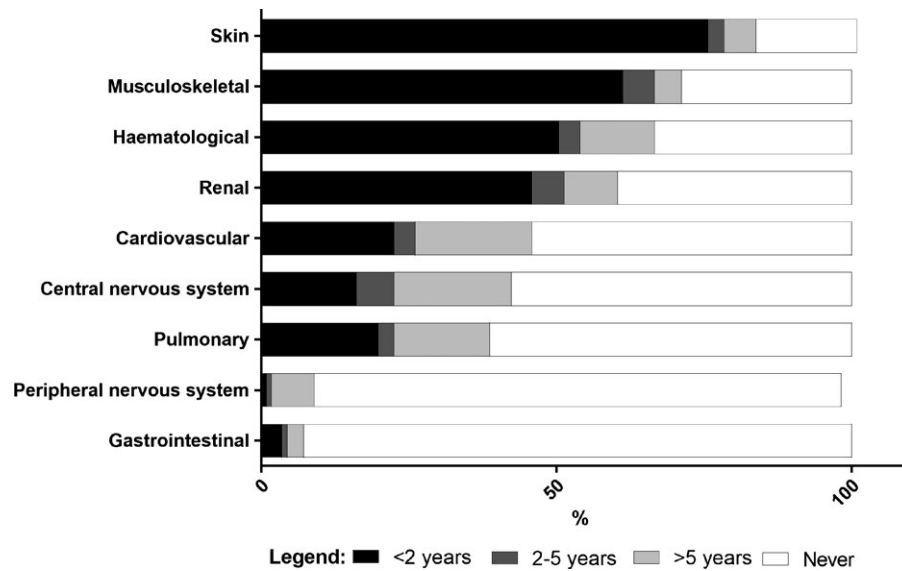
Figure 1. First occurrence of disease manifestations (by organ system) over time since diagnosis of childhood-onset systemic lupus erythematosus (SLE). Skin category includes malar rash, discoid rash, ulcers, photosensitivity, cutaneous vasculitis, and other ongoing inflammatory SLE-related rashes. Musculoskeletal category includes arthritis and myositis. Hematologic category includes hemolytic anemia, thrombocytopenia, leukopenia, lymphopenia, neutropenia, and thrombotic thrombocytopenic purpura. Renal category includes persistent proteinuria and lupus nephritis. Cardiovascular category includes pericarditis, myocarditis, endocarditis, myocardial infarction, angina pectoris, cerebrovascular accident, transient ischemic attack, arterial thrombosis, venous thrombosis, and embolus. Central nervous system category includes aseptic meningitis, cerebrovascular disease, demyelinating disease, lupus headache, myelopathy, chorea, convulsions, acute confusional state, anxiety disorder, mood disorder, and psychosis. Pulmonary category includes pleuritis, pneumonia, fibrosis, shrinking lung, pulmonary arterial hypertension, and interstitial lung disease. Peripheral nervous system category includes autonomous nervous system disorder, mononeuropathy, myasthenia gravis, Guillain-Barré syndrome, cranial nerve neuropathy, plexopathy, and polyneuropathy. Gastrointestinal category includes peritonitis, pancreatitis, autoimmune hepatitis, and liver cirrhosis.

Demographics. Data regarding demographic characteristics such as age, sex, self-reported ethnicity, and area of residence were collected by structured questionnaires. Categories of ethnicity included African/Caribbean, Arabic, Asian, Hispanic, white, and mixed.

Diagnosis, disease manifestations, and damage over time. Data on which components of ACR SLE criteria and/or SLE International Collaborating Clinics (SLICC) SLE criteria patients met were recorded, in addition to any childhood-onset SLE–related manifestations at diagnosis (22,23,31). Definitions of disease manifestations are described in Figure 1. Disease duration was defined as years between date of diagnosis (as reported in medical records) and study visit. Based on findings in previous studies, disease manifestations of childhood-onset SLE over time were recorded according to 6 predefined time frames: 1) never, 2) prior to diagnosis, 3) at diagnosis, 4) <2 years since diagnosis, 5) 2–5 years since diagnosis, and 6) >5 years since diagnosis (7,32,33). Age at first myocardial infarction, renal transplantation, cerebrovascular accident (CVA), and/or replacement arthroplasty was obtained from medical records. Specific disease manifestations such as antibody positivity were recorded as positive or negative if found in medical records and as unknown if not mentioned in the records. Nephrotic syndrome was recorded as present if clinical manifes-

tations (edema, proteinuria [3–3.5 gm/24 hours], and hypoalbuminemia [<25 gm/liter]) were present, or if medical records included a nephrotic syndrome diagnosis. Hypertension was recorded as present if blood pressure was >140/90 mm Hg on repeated examinations, or if medical records included a hypertension diagnosis.

Disease activity and medication use. Disease activity was assessed using the SLE Disease Activity Index 2000 (SLEDAI-2K) (34). High disease activity was defined by a SLEDAI-2K score of ≥8 (35,36). Additionally, patients were asked to rate their disease activity on a visual analog scale (VAS), ranging from 0 (no disease activity) to 100 (very high disease activity). Medication use was classified as current use, previous use, and never used. Glucocorticoids and hydroxychloroquine (HCQ) were considered separately. Non-HCQ DMARDs included azathioprine, cyclosporine, cyclophosphamide, leflunomide, methotrexate, mycophenolate mofetil, rituximab, and tacrolimus. All other medication use, including antiepileptic medication, antihypertensive drugs such as angiotensin-converting enzyme (ACE) inhibitors and angiotensin II receptor blockers (ARBs), and coumarins was also recorded. During the study visit, patients were asked if there were any medications that had affected them in terms of their physical appearance, physical health, or mental health, and in what ways they were affected.

Damage assessment. Disease damage was assessed using the SLICC/ACR Damage Index (SDI) (37). Presence of damage was defined by an SDI score of ≥1. For damage that had a specific temporal component (i.e., cognitive impairment or renal impairment present for ≥6 months), it was recorded if the item was found in 2 consecutive reports from the medical records.

Assessment of health-related quality of life. HRQoL was assessed using the Short Form 36 (SF-36), which includes 36 questions about 8 health domains: physical functioning, social functioning, role limitations due to physical problems, role limitations due to emotional problems, mental health, vitality, bodily pain, and general health perception (25). Patient HRQoL scores were compared to those from the general population in The Netherlands. Effects on HRQoL from the following factors were assessed: disease activity (low [SLEDAI-2K score ≤4], intermediate [5–7], or high [≥8]) (35), SLEDAI-2K items concerning changes in physical appearance (i.e., ongoing inflammatory rash and/or alopecia), and damage.

Statistical analysis. Group comparisons were made using the Mann-Whitney U test or the Kruskal-Wallis test, where applicable. One-sample *t*-tests were used for comparisons with normative data from the Dutch population. Logistic regression analysis was performed to assess associations of individual variables and the development of damage. Selection of these variables was based on a literature review (38). Presence of damage was defined as the outcome of interest, and predetermined variables were covariates in the model. Variables with an individual *P* value of <0.1 were used to build the multivariable model, using a hierarchical entry method. In the final, most parsimonious model, variables with associations at a *P* value of <0.05 were considered to contribute. To assess goodness of fit, the Hosmer-Lemeshow test was used, and residual statistics (i.e., Cook's distance for standardized residuals, deviance, and leverage) were analyzed. All analyses were performed using IBM SPSS Statistics version 22.

RESULTS

Patient inclusion. Patients were enrolled in the CHILL-NL study from November 2013 until April 2016. Eighty-eight secondary and tertiary hospitals were contacted. Doctors from 18 hospitals confirmed having adult patients with childhood-onset SLE under their care and sent contact information for 121 patients to the study team. An additional 15 patients contacted the study team via NVLE. Of these 136 patients, 111 patients (82%) were seen for a single study visit (see Supplementary Figure 1, on the *Arthritis & Rheumatology* web site at http://onlinelibrary.wiley.com/doi/10.1002/art.40697/abstract). Most study participants (69%) were treated in a tertiary center (Supplementary Figure 1). As an example of the proportion of patients treated at a certain site

who participated in the study, 17 of the 23 current patients with childhood-onset SLE (74%) at the Erasmus University Medical Center participated in the CHILL-NL study. Forty percent of patients in the study lived within the vicinity of the Erasmus University Medical Center; residences of the remaining patients were equally distributed over the rest of the country.

Demographic and disease characteristics of the patients. The median age at study visit was 33 years, with a median disease duration of 20 years (Table 1). Patients were divided into 3 diagnostic eras according to year of diagnosis, which ranged from 1959 to 2013. The number of patients among the 3 groups was evenly distributed, with 33% of patients diagnosed before 1990. The most common elements of the ACR criteria met by patients at diagnosis were antinuclear antibody positivity, immunologic features, and arthritis (see Supplementary Figure 2, http://onlinelibrary.wiley.com/doi/10.1002/art.40697/abstract). Almost all participants were female (91%). The majority of patients were white (72%), while 10% were African/Caribbean, 7% Asian, 3% Hispanic, 1% Arabic, and 7% of mixed heritage. Due to the majority of patients being white, ethnicity was presented as a binary category: white and nonwhite. Age at onset and disease duration were similar across these ethnic groups.

Treatment. The vast majority of patients (68%) were taking glucocorticoids and/or non-HCQ DMARDs at the time of the study visit (Table 1). Fifty-six patients (51%) were taking glucocorticoids (with or without non-HCQ DMARDs), and 76 patients (68%) were taking HCQ (of whom 29% were being treated with HCQ monotherapy). Sixty-five percent of patients were taking other non-antiinflammatory medications, including antihypertensive drugs (such as ACE inhibitors and ARBs) (51%), statins (14%), coumarins (14%), acetylsalicylic acid (12%), antidepressants (8%), antiepileptic drugs (5%), and erythropoietin (5%). When asked about the effects of medication use on physical appearance, physical health, or mental health, the majority of patients reported negative effects. The largest impact reported was physical appearance (89% of patients), which was perceived negatively by 93% of patients. Patients also reported a negative impact on physical health (36%) and mental health (28%). Effects on physical appearance (e.g., weight gain) and on mental health (e.g., mood swings) were mostly attributed to prednisone use. Effects on physical health (e.g., nausea) were mostly attributed to non-HCQ DMARDs.

Disease activity. At the study visit, recorded disease activity was relatively low (median SLEDAI-2K score 4 and median VAS score 13). Low complement levels (32%), skin rashes (14%), and proteinuria (13%) were the most commonly recorded SLEDAI-2K items. No difference was found between

Table 1. Patient characteristics at the study visit*

Female	101 (91)
Ethnicity	
White	80 (72)
Nonwhite	31 (28)
Age at diagnosis, median (range) years	14 (4–17)
Age at study visit, median (range) years	33 (18–65)
Disease duration, median (range) years	20 (1–55)
Era of diagnosis	
Prior to 1990	37 (33)
Between 1990 and 2000	38 (34)
After 2000	36 (32)
Disease activity	
SLEDAI-2K, median (range) score	4 (0–16)
SLEDAI ≤4	72 (65)
SLEDAI 5–7	23 (21)
SLEDAI ≥8	16 (14)
Patient-reported VAS, median (range) score	13 (0–95)
Current glucocorticoids/non-HCQ DMARDs use†‡	75 (68)
Glucocorticoids with non-HCQ DMARDs	40 (53)
Glucocorticoids only	16 (21)
Non-HCQ DMARDs only	15 (20)
2 non-HCQ DMARDs with or without glucocorticoids	4 (5)
Current HCQ use‡	76 (68)
HCQ with non-HCQ DMARDs/glucocorticoids	54 (71)
HCQ monotherapy	22 (29)
No HCQ, glucocorticoids, or non-HCQ DMARDs	14 (13)§
SDI, median (range)	1 (0–8)
SDI ≥1	69 (62)
Infections requiring IV antibiotics (ever)‡	50 (45)
1 occurrence	26 (52)
>1 occurrence	24 (48)

* Except where indicated otherwise, values are the number (%) of patients. SLEDAI-2K = Systemic Lupus Erythematosus Disease Activity Index 2000; VAS = visual analog scale; HCQ = hydroxychloroquine; SDI = Systemic Lupus International Collaborating Clinics/American College of Rheumatology Damage Index.
† More information regarding specific disease-modifying antirheumatic drug (DMARD) use can be found in Supplementary Table 3, on the *Arthritis & Rheumatology* web site at http://onlinelibrary.wiley.com/doi/10.1002/art.40697/abstract.
‡ Percentages below are based on the number of patients receiving the treatment (n = 75 or 76) or the number of patients with infections requiring intravenous (IV) antibiotics (n = 50), rather than the full cohort of 111 patients.
§ More information regarding these 14 patients can be found in Supplementary Table 4.

the SLEDAI-2K scores of patients receiving glucocorticoids and/or non-HCQ DMARDs, patients receiving HCQ monotherapy, and patients not receiving glucocorticoids, non-HCQ DMARDs, or HCQ monotherapy (P = 0.177 by Kruskal-Wallis test).

Infections. During their disease course, almost half of the patients (45%) had been admitted to the hospital due to infections that required intravenous antibiotic therapy. Forty-eight percent of these patients were admitted more than once (Table 1).

Disease manifestations and damage over time. The organ systems that were most frequently involved were the skin (e.g., malar or discoid rash, cutaneous vasculitis), musculoskeletal system (primarily arthritis), hematologic system (e.g., hemolytic anemia, leukopenia), and renal system (e.g., lupus nephritis). The vast majority of new manifestations in these organ systems developed within 2 years of diagnosis (Figure 1). Cardiovascular, pulmonary, and central nervous system (CNS) manifestations occurred in the short term and long term. Within 2 years of diagnosis, pericarditis, pleuritis, and epilepsy were the most common manifestations within these organ systems, while 5 years after diagnosis damage was most prevalent (e.g., myocardial infarction and CVA). Manifestations in the peripheral nervous system and gastrointestinal system were uncommon and mainly occurred ≥5 years after diagnosis.

Disease damage. Renal, neuropsychiatric, and musculoskeletal damage were the most prevalent types of damage (Figure 2A). In total, 62% percent of patients had developed disease damage, and the percentage of patients with damage increased over time (Figure 2B). Musculoskeletal damage (e.g., avascular necrosis, deforming/erosive arthritis), neuropsychiatric damage (primarily cognitive impairment, often combined with seizures requiring treatment of >6 months), and renal damage (e.g., end-stage renal disease) were the most prevalent types of damage across disease duration categories (Figure 2C and Supplementary Table 1, http://onlinelibrary.wiley.com/doi/10.1002/art.40697/abstract).

Notably, after 10–20 years, when childhood-onset SLE patients were in their 20s and 30s, more than half experienced significant damage (Figure 2C, and Supplementary Table 1). Seven childhood-onset SLE patients (5%) experienced a CVA (at a median age of 20 years). Sixteen patients (24%) who had renal involvement during their disease subsequently developed damage (Supplementary Table 2, http://onlinelibrary.wiley.com/doi/10.1002/art.40697/abstract). Of these 16 patients, 38% received a renal transplant (median age 24 years), and 1 patient was undergoing dialysis. Six patients underwent replacement arthroplasty in 1 joint, and 4 patients received >1 joint replacement; the median age at first joint replacement was 34 years (Supplementary Table 2). Five patients experienced a myocardial infarction (at a median age of 39 years), and 3 of them underwent coronary bypass surgery.

Factors related to the development of damage. Logistic regression analysis was performed, and odds ratios (ORs) and 95% confidence intervals (95% CIs) were calcu-
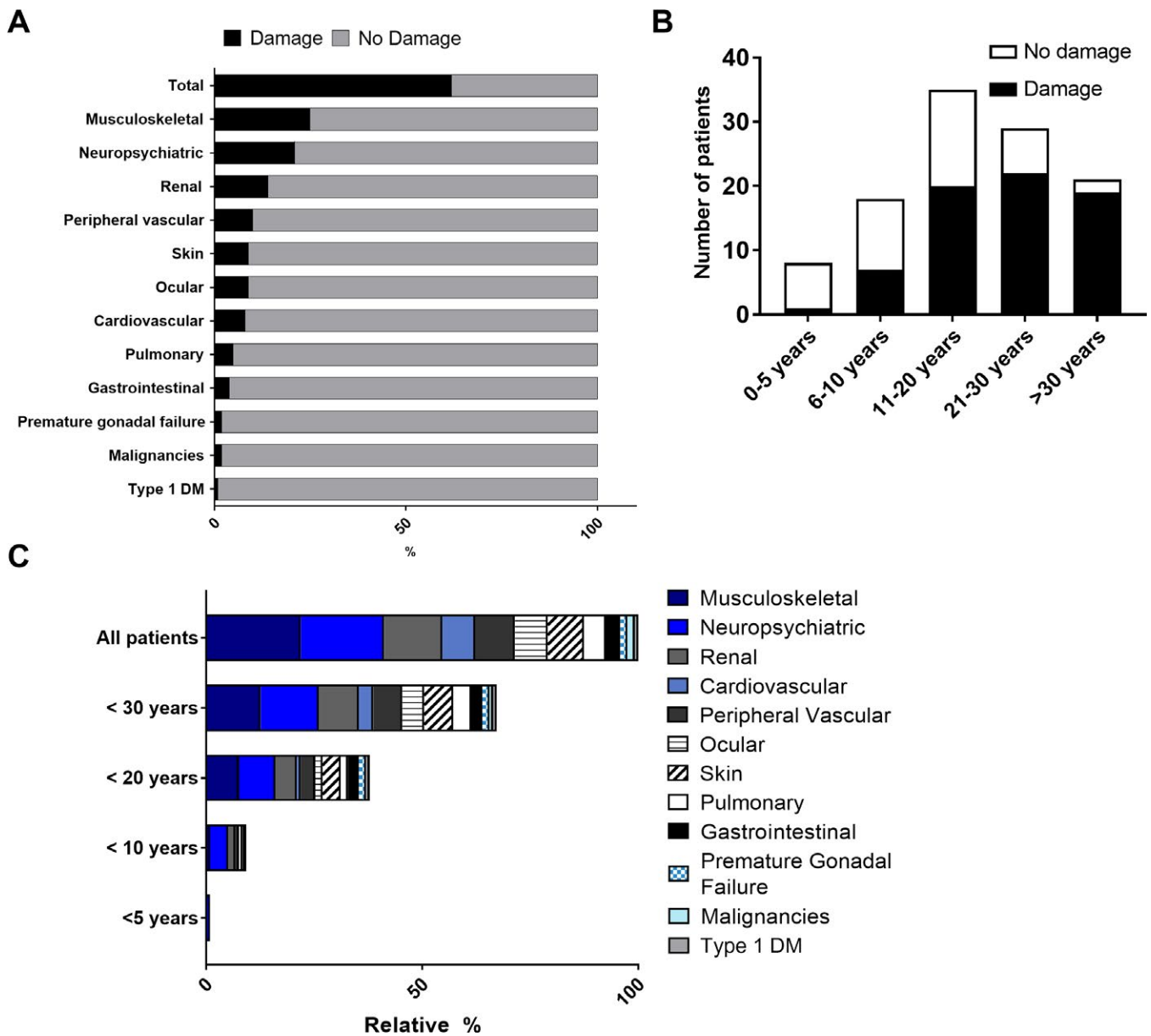
Figure 2. Childhood-onset systemic lupus erythematosus–related damage defined by a Systemic Lupus International Collaborating Clinics/American College of Rheumatology Damage Index score of ≥1. **A,** Percentage of patients with damage according to organ system. **B,** Number of patients with and without damage, by disease duration category. **C,** Percentage of cumulative specific organ damage relative to the sum of damage scores in all organ systems, displayed by disease duration category. DM = diabetes mellitus.

lated to assess associations between individual variables and development of damage (Table 2). The univariate analysis showed longer disease duration; additionally, antiphospholipid antibody (aPL) positivity, infections requiring hospitalization (ever), the presence of hypertension (ever), and the presence of nephrotic syndrome (ever) were associated with the presence of damage. Neither sex nor ethnicity showed a significant association with the presence of damage. Current HCQ monotherapy was associated with the absence of damage. In the multivariate analysis, disease duration (OR 1.147 [95% CI 1.077–1.227], $P < 0.001$), hypertension (OR 3.214 [95% CI

1.040–9.932], $P = 0.043$), and aPL positivity (OR 3.559 [95% CI 1.161–10.908], $P = 0.026$) were significantly associated with presence of damage, and current HCQ monotherapy (OR 0.162 [95% CI 0.042–0.633], $P = 0.009$) was again associated with the absence of damage. No differences in number or type of organ systems involved or in antiinflammatory medication use were found between patients currently receiving HCQ monotherapy and other patients.

Health-related quality of life. HRQoL as measured by the SF-36 at study visit was lower in adults with childhood-

Table 2. Binary logistic regression analysis of variables associated with damage as the outcome measure*

Predictor (no. of patients)	Univariate analysis			Multivariate analysis		
	β†	OR (95% CI)	P	β†	OR (95% CI)	P
Disease duration (111)	0.107	1.113 (1.057–1.171)	<0.001	0.139	1.147 (1.077–1.227)	<0.001
No. of ACR criteria elements met at diagnosis (111)	0.036	1.037 (0.786–1.367)	0.798	–	–	–
Age at diagnosis (111)	−0.70	0.933 (0.811–1.072)	0.322	–	–	–
Use of DMARDs/glucocorticoids with or without HCQ (75)						
Compared to HCQ monotherapy (22)	−1.259	0.283 (0.103–0.776)	0.014	−1.818	0.162 (0.042–0.633)	0.009
Compared to no HCQ, glucocorticoids, or non-HCQ DMARDs (14)	−0.185	0.831 (0.251–2.747)	0.761	−0.942	0.390 (0.085–1.787)	0.225
White (80) compared to nonwhite (31)	0.754	2.215 (0.847–5.329)	0.108‡	–	–	–
Female (101) compared to male (10)	−0.964	0.381 (0.077–1.888)	0.237‡	–	–	–
aPL negativity (44)						
Compared to aPL positivity (48)	0.990	2.692 (1.130–6.417)	0.025	1.269	3.559 (1.161–10.908)	0.026
Compared to unknown aPL status (19)	0.539	1.714 (0.569–5.169)	0.338	0.264	1.302 (0.333–5.092)	0.704
No renal involvement ever (44)						–
Compared to renal involvement within 2 years of diagnosis (50)	0.663	1.94 (0.839–4.490)	0.121‡	–	–	
Compared to renal involvement after 2 years (17)	0.784	2.191 (0.660–7.268)	0.200‡			
No CNS involvement ever (78)						
Compared to CNS involvement within 2 years of diagnosis (9)	1.023	7.515 (1.595–35.423)	0.214‡			
Compared to CNS involvement after 2 years of diagnosis (24)	0.266	2.088 (0.826–5.276)	0.591‡			
Nephrotic syndrome (24) compared to no nephrotic syndrome ever (87)	1.738	5.687 (1.578–20.488)	0.008	0.932	–	0.242§
Hospitalization (50) compared to no hospitalization due to infection ever (61)	0.505	1.656 (1.098–2.500)	0.016	0.393	–	0.456§
Hypertension (71) compared to no hypertension ever (40)	1.522	4.583 (1.792–11.715)	0.001	1.167	3.214 (1.040–9.932)	0.043

* OR = odds ratio; 95% CI = 95% confidence interval; ACR = American College of Rheumatology; DMARDs = disease-modifying antirheumatic drugs; HCQ = hydroxychloroquine; aPL = antiphospholipid antibody; CNS = central nervous system.
† Regression coefficient.
‡ A cutoff of P <0.100 was set to select the variables for multivariate logistic regression. As such, these covariates were not incorporated in the multivariate model.
§ These covariates did not improve the fit of the model and were therefore not used for the final multivariate model.

onset SLE in 6 of the 8 assessed domains when compared to the Dutch population (Figure 3A). Low disease activity, defined as a SLEDAI score of ≤4, positively affected HRQoL (Figure 3B). A more detailed evaluation of SLEDAI-2K items concerning changes in physical appearance (e.g., ongoing inflammatory rash and/or alopecia [n = 25]) revealed a clearly negative impact on HRQoL in 7 of 8 domains (Figure 3C). Notably, HRQoL scores in these patients were similar to or even lower than those of patients with high disease activity (SLEDAI-2K ≥8), even though only 24% of patients with changes in physical appearance had high disease activity. An active renal component as defined by the SLEDAI-2K (n

= 14) did not affect HRQoL. No differences in HRQoL scores were observed between white and nonwhite patients (data not shown). Notably, in 7 of the 8 domains, HRQoL scores did not differ between patients with damage and those without; significantly lower scores in patients with damage were observed only in the physical functioning domain (Figure 3D). Additionally, physical functioning domain scores of patients with very long disease durations (>30 years) were worse compared to those of patients with short disease durations (<10 years). On the other hand, mental health domain scores improved over time, with higher scores in patients with a long disease duration (data not shown).
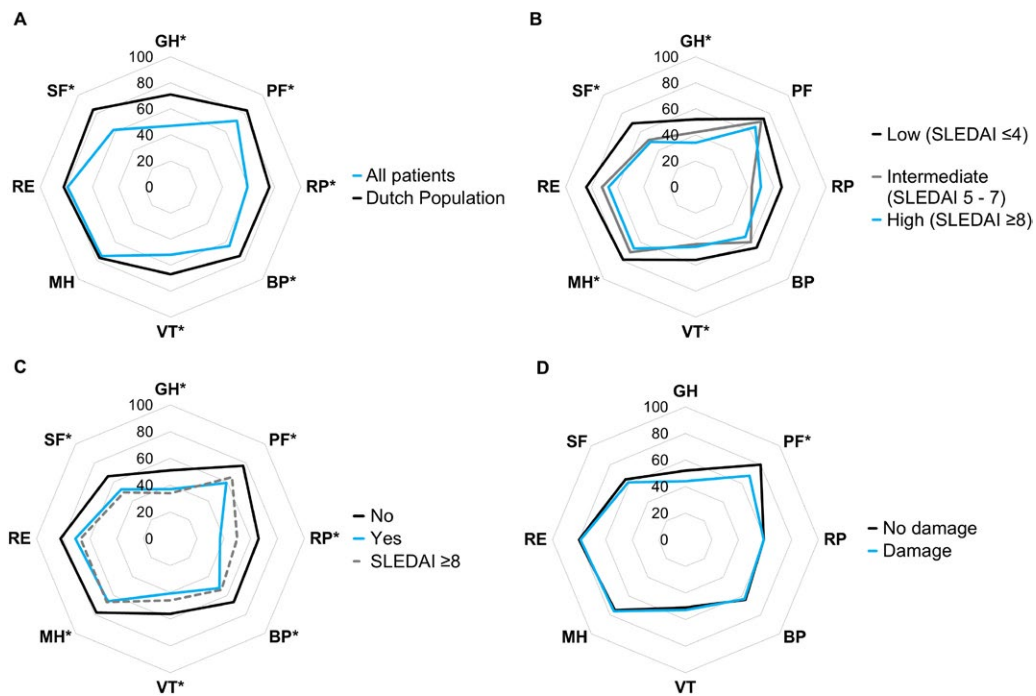
Figure 3. Health-related quality of life expressed as mean Short Form 36 (SF-36) health survey scores per domain. Spidergrams (63) show mean scores within each domain of the SF-36, ranging from 0 (worst) to 100 (best). **A,** SF-36 scores of childhood-onset systemic lupus erythematosus (SLE) patients versus those of the overall Dutch population. **B,** SF-36 scores of patients with low SLE Disease Activity Index 2000 (SLEDAI-2K) scores (≤4), intermediate scores (5–7), and high scores (≥8). **C,** SF-36 scores of patients with affirmative responses to questions about effects on physical appearance (e.g., ongoing inflammatory rash and/or alopecia) versus patients without these symptoms and patients with SLEDAI-2K scores ≥8. **D,** SF-36 scores of patients with damage (Systemic Lupus International Collaborating Clinics/American College of Rheumatology Damage Index [SDI] score ≥1) versus patients without damage (SDI score 0). GH = general health perception domain; PF = physical functioning domain; RP = role limitations due to physical problems domain; BP = bodily pain domain; VT = vitality domain; MH = mental health domain; RE = role limitations due to emotional problems domain; SF = social functioning domain. * = P < 0.05. Color figure can be viewed in the online issue, which is available at http://onlinelibrary.wiley.com/doi/10.1002/art.40697/abstract.

DISCUSSION

This is the first study to report data on disease manifestations over time, damage, and HRQoL in a large cohort of predominantly white adult patients with childhood-onset SLE with very long disease duration. Most patients had low disease activity but still took DMARDs and/or glucocorticoids 20 years after diagnosis. More than half of the patients also took medications to treat noninflammatory disease or damage-related symptoms. Clearly, drug-free remission remains difficult to achieve, and current DMARDs are not effective enough to be taken without glucocorticoids in many patients. Indeed, half of the patients in our cohort were still taking glucocorticoids with or without DMARDs, which was also reported in cohorts that included patients with childhood-onset SLE or adult-onset SLE patients with a mean disease duration of 12–16 years (18,19). This is concerning, as glucocorticoids are associated with the development of damage (39). Patients in the CHILL-NL cohort were eager to limit glucocorticoid use, as nearly all reported negative experiences with prednisone, especially with regard to their physical appearance and/or

mental well-being. Although our findings may be influenced by recall bias, they illustrate the perceived impact of glucocorticoid use on a patient's well-being, emphasizing the need for the development of new treatment strategies that can limit or even eliminate glucocorticoid use.

Most organ systems became involved within the first 2 years of diagnosis, and thereafter hardly any new childhood-onset SLE–related manifestations occurred in organ systems not previously affected. This finding was also reported in 2 childhood-onset SLE cohorts, but these cohorts had a mean disease duration of only 4 years (32,40). After 5 years of disease, our study demonstrated that the nature of disease manifestations shifts to damage (such as myocardial infarction) instead of primary disease–related manifestations (such as pericarditis or epilepsy). This shift has also been observed in adult-onset SLE patients (41–44), and there has been a push for preventative screening measures for cardiovascular damage and healthy lifestyle advice (i.e., guidance on healthy diet, regular exercise, abstinence from smoking). A study that examined laboratory markers of cardiovascular risk in adolescents with childhood-onset SLE showed that disease duration and signs of renal injury (e.g., proteinuria, history of hypertension)

were associated with these markers (45). As has also been shown by others (12,18), we found in the present study that cardiovascular damage begins when childhood-onset SLE patients are in their 20s and early 30s, so prevention strategies must be considered during transition to adult care, especially in patients with renal involvement. Because infections are common and related to mortality in childhood-onset SLE patients (46,47), infection prevention by vaccination should be encouraged (48,49).

The majority of our patients had developed damage by their mid-20s, and this percentage increased with longer disease duration. The musculoskeletal system, kidneys, and CNS were the most frequently affected, as in other childhood-onset SLE studies, though those studies involved patients with limited disease duration (5–10 years) (13,15,16,19,50). The only available studies of damage in patients with a mean disease duration of ≥20 years were performed in adult-onset SLE (50,51). Reported frequency and characteristics of damage in these cohorts were similar to the results in the CHILL-NL cohort. However, the mean age at diagnosis in the adult-onset SLE cohorts was 31 years (50,51), versus 14 years in our study, which likely explains why most patients with childhood-onset SLE began to develop significant damage in their early 20s. This is further supported by reports from 2 North American childhood-onset SLE cohorts (mean disease durations of 5 years and 16.5 years) that described myocardial infarction in childhood-onset SLE patients in their 20s and 30s (12,18).

Disease duration was the main variable associated with the development of damage in the CHILL-NL cohort, followed by aPL positivity and hypertension (Table 2), and this has been consistently demonstrated in many other childhood-onset SLE studies (13,15,50–53). Presence of damage did not differ between white and nonwhite patients in our study, but other studies have shown conflicting results regarding ethnicity and development of damage (7,9,12). Similar socioeconomic status among white and nonwhite patients could possibly explain the lack of association of ethnicity with damage (7–11). Due to the low number of men included, this study was underpowered to assess associations of sex with damage.

Current HCQ monotherapy was associated with the absence of damage, although no information regarding the duration of HCQ monotherapy was recorded. Therefore, we cannot be sure of a causal relationship between current HCQ monotherapy and mild disease. This is further highlighted by the lack of association of organ involvement and antiinflammatory medication use (ever) between the patients currently receiving HCQ monotherapy and other patients. Longitudinal cohort studies are necessary to further clarify this issue.

Notably, the association of damage with disease duration also reflects past and current treatment modalities. Patients with long disease duration may have developed more damage over time due to treatment strategies that are now uncommon, and more recently diagnosed patients may have had the benefit of improved treatment strategies that led to less damage. The cross-sectional design of this study does not allow us to isolate the positive effects of improved treatment modalities from the negative effects of disease duration on the development of damage.

This is the first study assessing HRQoL in childhood-onset SLE patients after they have reached adulthood. HRQoL was reduced in most domains when compared to the overall Dutch population. Other studies in children with childhood-onset SLE and adult-onset SLE patients also showed that patients had an impaired HRQoL (21,54–56), and HRQoL scores were similar or even lower when compared to patients with other chronic illnesses (54–57). A possible explanation for the similar mental and emotional health scores of the CHILL-NL cohort as compared to those of the overall Dutch population (Figure 3) might be the development of resilience at a young age to the emotional impact of the disease, as perceived HRQoL can be affected by different styles of coping (58).

High disease activity (SLEDAI-2K ≥8) had a significant negative effect on HRQoL, which is supported by other studies (20,21,57,59). Interestingly, an even larger negative effect was seen with regard to factors affecting physical appearance. Indeed, 2 other studies showed that changes in physical appearance (e.g., obesity, skin involvement) were associated with reduced HRQoL (60,61). Surprisingly, in the CHILL-NL cohort, the presence of damage barely affected HRQoL, with only scores in the physical functioning domain significantly reduced. However, other studies showed a negative association of damage with HRQoL (21,52). This discrepancy might be explained by the heterogeneous nature of damage that can differ between cohorts, but also by the development of coping styles in childhood-onset SLE patients, who may have learned at an earlier age to adjust their lifestyle according to damage.

The CHILL-NL study has several strengths. It is a large cohort, and all patients were seen in person, providing the opportunity to verify disease activity and damage by laboratory analysis and physical examination. Medical records were retrieved for all patients, by which all reported outcomes were verified. The lack of studies in adults with childhood-onset SLE demonstrates the challenge in identifying patients after they transfer to adult care. Even in a report from a North American cohort that included outcomes in adult childhood-onset SLE patients, the study was not designed to specifically recruit adults with childhood-onset SLE (62). The present study describes verified disease characteristics and HRQoL in the largest cohort of childhood-onset SLE patients with very long disease duration.

The limitations of the CHILL-NL study must also be addressed. First, the number of patients who were not interested in participating in the study (and as such were not referred to the study team) was unknown. It must be noted that the patients included in this study are not a random selection of the total childhood-onset SLE population in The Netherlands. Patients from both ends of the severity spectrum (i.e. those with severe disease and those with mild disease) who do not visit a physician regularly will be missed in this cross-sectional study. Patients with high disease activity or severe damage may not have partic-

ipated in the study due to participation being seen as too taxing. To overcome this limitation, we offered to travel to the patient if they indicated that travel distance was seen as a barrier. Of the patients who were referred to the study team, the vast majority participated in the study. Second, due to the cross-sectional nature of the study, deceased patients were not included. As disease severity is a risk factor for mortality (11,50), it is possible that our study had a bias toward less severe disease. Third, data for this study were collected retrospectively, and information may have been missed. We chose only to report disease characteristics that could be verified with medical records, and no data could be collected from deceased patients. Consequently, it is likely that the results from the CHILL-NL study will underrepresent the severity of the disease. These limitations illustrate the need for longitudinal cohorts in which childhood-onset SLE patients are followed up even after they transfer to adult care (12).

In conclusion, the CHILL-NL study shows that childhood-onset SLE has a major impact on adult life. This is the first study to provide insight into the HRQoL and the development of disease manifestations and damage over time in adults with childhood-onset SLE. Childhood-onset SLE–related manifestations developed mostly within 2 years of diagnosis, with a shift to development of damage 5 years after diagnosis. Major medical complications (i.e., renal transplants, CVA, myocardial infarction) occurred at a young age. These results demonstrate the need for optimal control over disease activity and preventative screening measures (particularly cardiovascular) beginning before age 30 to facilitate a better disease prognosis. HRQoL scores of adults with childhood-onset SLE are affected by factors other than disease activity or damage alone. By identifying and addressing these factors, such as physical appearance and coping styles, HRQoL may be improved.

AUTHOR CONTRIBUTIONS

All authors were involved in drafting the article or revising it critically for important intellectual content, and all authors approved the final version to be published. Ms Groot had full access to all of the data in the study and takes responsibility for the integrity of the data and the accuracy of the data analysis.

Study conception and design Groot, Shaikhani, Kamphuis.

Acquisition of data Groot, Teng, de Leeuw, Bijl, Dolhain, Zirkzee, Fritsch-Stork, Bultink, Kamphuis.

Analysis and interpretation of data Groot, Kamphuis.

REFERENCES

1. Silva CA, Avcin T, Brunner HI. Taxonomy for systemic lupus erythematosus with onset before adulthood. Arthritis Care Res (Hoboken) 2012;64:1787–93.

2. D'Cruz DP, Khamashta MA, Hughes GR. Systemic lupus erythematosus. Lancet 2007;369:587–96.

3. Levy DM, Kamphuis S. Systemic lupus erythematosus in children and adolescents. Pediatr Clin North Am 2012;59:345–64.

4. Hiraki LT, Feldman CH, Liu J, Alarcon GS, Fischer MA, Winkelmayer WC, et al. Prevalence, incidence, and demographics of systemic lupus erythematosus and lupus nephritis from 2000 to 2004 among children in the US Medicaid beneficiary population. Arthritis Rheum 2012;64:2669–76.

5. Kamphuis S, Silverman ED. Prevalence and burden of pediatric-onset systemic lupus erythematosus. Nat Rev Rheumatol 2010;6:538–46.

6. Pineles D, Valente A, Warren B, Peterson MG, Lehman TJ, Moorthy LN. Worldwide incidence and prevalence of pediatric onset systemic lupus erythematosus. Lupus 2011;20:1187–92.

7. Miettunen PM, Ortiz-Alvarez O, Petty RE, Cimaz R, Malleson PN, Cabral DA, et al. Gender and ethnic origin have no effect on longterm outcome of childhood-onset systemic lupus erythematosus. J Rheumatol 2004;31:1650–4.

8. Levy DM, Peschken CA, Tucker LB, Chedeville G, Huber AM, Pope JE, et al. Influence of ethnicity on childhood-onset systemic lupus erythematosus: results from a multiethnic multicenter Canadian cohort. Arthritis Care Res (Hoboken) 2013;65:152–60.

9. Hiraki LT, Benseler SM, Tyrrell PN, Harvey E, Hebert D, Silverman ED. Ethnic differences in pediatric systemic lupus erythematosus. J Rheumatol 2009;36:2539–46.

10. Alarcon GS. Multiethnic lupus cohorts: what have they taught us? Reumatol Clin 2011;7:3–6.

11. Hersh AO, Trupin L, Yazdany J, Panopalis P, Julian L, Katz P, et al. Childhood-onset disease as a predictor of mortality in an adult cohort of patients with systemic lupus erythematosus. Arthritis Care Res (Hoboken) 2010;62:1152–9.

12. Lim LS, Pullenayegum E, Feldman B, Lim L, Gladman DD, Silverman E. From childhood to adulthood: the trajectory of damage in patients with childhood-onset systemic lupus erythematosus. Arthritis Care Res (Hoboken) 2018;70:750–7.

13. Brunner HI, Silverman ED, To T, Bombardier C, Feldman BM. Risk factors for damage in childhood-onset systemic lupus erythematosus: cumulative disease activity and medication use predict disease damage. Arthritis Rheum 2002;46:436–44.

14. Descloux E, Durieu I, Cochat P, Vital-Durand D, Ninet J, Fabien N, et al. Influence of age at disease onset in the outcome of paediatric systemic lupus erythematosus. Rheumatology (Oxford) 2009;48:779–84.

15. Ravelli A, Duarte-Salazar C, Buratti S, Reiff A, Bernstein B, Maldonado-Velazquez MR, et al. Assessment of damage in juvenile-onset systemic lupus erythematosus: a multicenter cohort study. Arthritis Rheum 2003;49:501–7.

16. Watson L, Leone V, Pilkington C, Tullus K, Rangaraj S, McDonagh JE, et al. Disease activity, severity, and damage in the UK Juvenile-Onset Systemic Lupus Erythematosus Cohort. Arthritis Rheum 2012;64:2356–65.

17. Koutsonikoli A, Trachana M, Heidich AB, Galanopoulou V, Pratsidou-Gertsi P, Garyphallos A. Dissecting the damage in Northern Greek patients with childhood-onset systemic lupus erythematosus: a retrospective cohort study. Rheumatol Int 2015;35:1225–32.

18. Hersh AO, von Scheven E, Yazdany J, Panopalis P, Trupin L, Julian L, et al. Differences in long-term disease activity and treatment of adult patients with childhood- and adult-onset systemic lupus erythematosus. Arthritis Rheum 2009;61:13–20.

19. Sousa S, Goncalves MJ, Ines LS, Eugenio G, Jesus D, Fernandes S, et al. Clinical features and long-term outcomes of systemic lupus erythematosus: comparative data of childhood, adult and late-onset disease in a national register. Rheumatol Int 2016;36:955–60.

20. Moorthy LN, Baldino ME, Kurra V, Puwar D, Llanos A, Peterson MG, et al. Relationship between health-related quality of life, disease activity and disease damage in a prospective international multicenter cohort of childhood onset systemic lupus erythematosus patients. Lupus 2017;26:255–65.

21. Brunner HI, Higgins GC, Wiers K, Lapidus SK, Olson JC, Onel K, et al. Health-related quality of life and its relationship to patient disease course in childhood-onset systemic lupus erythematosus. J Rheumatol 2009;36:1536–45.

22. Tan EM, Cohen AS, Fries JF, Masi AT, McShane DJ, Rothfield NF, et al. The 1982 revised criteria for the classification of systemic lupus erythematosus. Arthritis Rheum 1982;25:1271–7.

23. Hochberg MC, for the Diagnostic and Therapeutic Criteria Committee of the American College of Rheumatology. Updating the American College of Rheumatology revised criteria for the classification of systemic lupus erythematosus [letter]. Arthritis Rheum 1997;40:1725.

24. National Association for Lupus, APS, Scleroderma, and MCTD. URL: https://www.nvle.org/.

25. Aaronson NK, Muller M, Cohen PD, Essink-Bot ML, Fekkes M, Sanderman R, et al. Translation, validation, and norming of the Dutch language version of the SF-36 Health Survey in community and chronic disease populations. J Clin Epidemiol 1998;51:1055–68.

26. Krupp LB, LaRocca NG, Muir-Nash J, Steinberg AD. The fatigue severity scale: application to patients with multiple sclerosis and systemic lupus erythematosus. Arch Neurol 1989;46:1121–3.

27. Brandtstadter J, Renner G. Tenacious goal pursuit and flexible goal adjustment: explication and age-related analysis of assimilative and accommodative strategies of coping. Psychol Aging 1990;5:58–67.

28. Beck AT, Steer RA. Internal consistencies of the original and revised Beck Depression Inventory. J Clin Psychol 1984;40:1365–7.

29. Wallston KA. The validity of the multidimensional health locus of control scales. J Health Psychol 2005;10:623–31.

30. Evers AW, Kraaimaat FW, van Lankveld W, Jongen PJ, Jacobs JW, Bijlsma JW. Beyond unfavorable thinking: the illness cognition questionnaire for chronic diseases. J Consult Clin Psychol 2001;69:1026–36.

31. Petri M, Orbai AM, Alarcon GS, Gordon C, Merrill JT, Fortin PR, et al. Derivation and validation of the Systemic Lupus International Collaborating Clinics classification criteria for systemic lupus erythematosus. Arthritis Rheum 2012;64:2677–86.

32. Hiraki LT, Benseler SM, Tyrrell PN, Hebert D, Harvey E, Silverman ED. Clinical and laboratory characteristics and long-term outcome of pediatric systemic lupus erythematosus: a longitudinal study. J Pediatr 2008;152:550–6.

33. Brunner HI, Gladman DD, Ibanez D, Urowitz MD, Silverman ED. Difference in disease features between childhood-onset and adult-onset systemic lupus erythematosus. Arthritis Rheum 2008;58:556–62.

34. Gladman DD, Ibanez D, Urowitz MB. Systemic lupus erythematosus disease activity index 2000. J Rheumatol 2002;29:288–91.

35. Campos LM, Silva CA, Aikawa NE, Jesus AA, Moraes JC, Miraglia J, et al. High disease activity: an independent factor for reduced immunogenicity of the pandemic influenza a vaccine in patients with juvenile systemic lupus erythematosus. Arthritis Care Res (Hoboken) 2013;65:1121–7.

36. Iaccarino L, Bettio S, Reggia R, Zen M, Frassi M, Andreoli L, et al. Effects of belimumab on flare rate and expected damage progression in patients with active systemic lupus erythematosus. Arthritis Care Res (Hoboken) 2017;69:115–23.

37. Gladman D, Ginzler E, Goldsmith C, Fortin P, Liang M, Urowitz M, et al. The development and initial validation of the Systemic Lupus International Collaborating Clinics/American College of Rheumatology Damage Index for systemic lupus erythematosus. Arthritis Rheum 1996;39:363–9.

38. Sutton EJ, Davidson JE, Bruce IN. The systemic lupus international collaborating clinics (SLICC) damage index: a systematic literature review. Semin Arthritis Rheum 2013;43:352–61.

39. Zonana-Nacach A, Barr SG, Magder LS, Petri M. Damage in systemic lupus erythematosus and its association with glucocorticoids. Arthritis Rheum 2000;43:1801–8.

40. Tan JH, Hoh SF, Win MT, Chan YH, Das L, Arkachaisri T. Childhood-onset systemic lupus erythematosus in Singapore: clinical phenotypes, disease activity, damage, and autoantibody profiles. Lupus 2015;24:998–1005.

41. Tselios K, Sheane BJ, Gladman DD, Urowitz MB. Optimal monitoring for coronary heart disease risk in patients with systemic lupus erythematosus: a systematic review. J Rheumatol 2016;43:54–65.

42. Ballocca F, D'Ascenzo F, Moretti C, Omede P, Cerrato E, Barbero U, et al. Predictors of cardiovascular events in patients with systemic lupus erythematosus (SLE): a systematic review and meta-analysis. Eur J Prev Cardiol 2015;22:1435–41.

43. Agca R, Heslinga SC, Rollefstad S, Heslinga M, McInnes IB, Peters MJ, et al. EULAR recommendations for cardiovascular disease risk management in patients with rheumatoid arthritis and other forms of inflammatory joint disorders: 2015/2016 update. Ann Rheum Dis 2017;76:17–28.

44. Bultink IE, Turkstra F, Diamant M, Dijkmans BA, Voskuyl AE. Prevalence of and risk factors for the metabolic syndrome in women with systemic lupus erythematosus. Clin Exp Rheumatol 2008;26:32–8.

45. Ardoin SP, Schanberg LE, Sandborg C, Yow E, Barnhart HX, Mieszkalski K, et al. Laboratory markers of cardiovascular risk in pediatric SLE: the APPLE baseline cohort. Lupus 2010;19:1315–25.

46. Hashkes PJ, Wright BM, Lauer MS, Worley SE, Tang AS, Roettcher PA, et al. Mortality outcomes in pediatric rheumatology in the US. Arthritis Rheum 2010;62:599–608.

47. Joo YB, Park SY, Won S, Bae SC. Differences in clinical features and mortality between childhood-onset and adult-onset systemic lupus erythematosus: a prospective single-center study. J Rheumatol 2016;43:1490–7.

48. Heijstek MW, Ott de Bruin LM, Bijl M, Borrow R, van der Klis F, Kone-Paut I, et al. EULAR recommendations for vaccination in paediatric patients with rheumatic diseases. Ann Rheum Dis 2011;70:1704–12.

49. Naveau C, Houssiau FA. Pneumococcal sepsis in patients with systemic lupus erythematosus. Lupus 2005;14:903–6.

50. Chambers SA, Allen E, Rahman A, Isenberg D. Damage and mortality in a group of British patients with systemic lupus erythematosus followed up for over 10 years. Rheumatology (Oxford) 2009;48:673–5.

51. Taraborelli M, Cavazzana I, Martinazzi N, Lazzaroni MG, Fredi M, Andreoli L, et al. Organ damage accrual and distribution in systemic lupus erythematosus patients followed-up for more than 10 years. Lupus 2017;26:1197–1204.

52. Legge A, Doucette S, Hanly JG. Predictors of organ damage progression and effect on health-related quality of life in systemic lupus erythematosus. J Rheumatol 2016;43:1050–6.

53. Bruce IN, O'Keeffe AG, Farewell V, Hanly JG, Manzi S, Su L, et al. Factors associated with damage accrual in patients with systemic lupus erythematosus: results from the Systemic Lupus International Collaborating Clinics (SLICC) Inception Cohort. Ann Rheum Dis 2015;74:1706–13.

54. Jolly M. How does quality of life of patients with systemic lupus erythematosus compare with that of other common chronic illnesses? J Rheumatol 2005;32:1706–8.

55. Wolfe F, Michaud K, Li T, Katz RS. EQ-5D and SF-36 quality of life measures in systemic lupus erythematosus: comparisons with rheumatoid arthritis, noninflammatory rheumatic disorders, and fibromyalgia. J Rheumatol 2010;37:296–304.

56. Alarcon GS, McGwin G Jr, Uribe A, Friedman AW, Roseman JM, Fessler BJ, et al. Systemic lupus erythematosus in a multiethnic lupus cohort (LUMINA). XVII. Predictors of self-reported health-related quality of life early in the disease course. Arthritis Rheum 2004;51:465–74.

57. Ruperto N, Buratti S, Duarte-Salazar C, Pistorio A, Reiff A, Bernstein B, et al. Health-related quality of life in juvenile-onset systemic lupus erythematosus and its relationship to disease activity and damage. Arthritis Rheum 2004;51:458–64.

58. Rinaldi S, Ghisi M, Iaccarino L, Zampieri S, Ghirardello A, Sarzi-Puttini P, et al. Influence of coping skills on health-related quality of life in patients with systemic lupus erythematosus. Arthritis Rheum 2006;55:427–33.

59. Chaigne B, Chizzolini C, Perneger T, Trendelenburg M, Huynh-Do U, Dayer E, et al. Impact of disease activity on health-related quality of life in systemic lupus erythematosus—a cross-sectional analysis of the Swiss Systemic Lupus Erythematosus Cohort Study (SSCS). BMC Immunol 2017;18:17.

60. Mina R, Klein-Gitelman MS, Nelson S, Eberhard BA, Higgins G, Singer NG, et al. Effects of obesity on health-related quality of life in juvenile-onset systemic lupus erythematosus. Lupus 2015;24:191–7.

61. Ishiguro M, Hashizume H, Ikeda T, Yamamoto Y, Furukawa F. Evaluation of the quality of life of lupus erythematosus patients with cutaneous lesions in Japan. Lupus 2014;23:93–101.

62. Yelin E, Trupin L, Katz P, Criswell L, Yazdany J, Gillis J, et al. Work dynamics among persons with systemic lupus erythematosus. Arthritis Rheum 2007;57:56–63.

63. Strand V, Crawford B, Singh J, Choy E, Smolen JS, Khanna D. Use of "spydergrams" to present and interpret SF-36 health-related quality of life data across rheumatic diseases. Ann Rheum Dis 2009;68:1800–4.

Suppressive Regulation by MFG-E8 of Latent Transforming Growth Factor β–Induced Fibrosis via Binding to αv Integrin: Significance in the Pathogenesis of Fibrosis in Systemic Sclerosis

Chisako Fujiwara, Akihito Uehara, Akiko Sekiguchi, Akihiko Uchiyama, Sahori Yamazaki, Sachiko Ogino, Yoko Yokoyama, Ryoko Torii, Mari Hosoi, Chiaki Suto, Katsuhiko Tsunekawa, Masami Murakami, Osamu Ishikawa, and Sei-ichiro Motegi

Objective. Several studies have demonstrated that the secreted glycoprotein and integrin ligand milk fat globule–associated protein with epidermal growth factor– and factor VIII–like domains (MFG-E8) negatively regulates fibrosis in the liver, lungs, and respiratory tract. However, the mechanisms and roles of MFG-E8 in skin fibrosis in systemic sclerosis (SSc) have not been characterized. We undertook this study to elucidate the role of MFG-E8 in skin fibrosis in SSc.

Methods. We assessed expression of MFG-E8 in the skin and serum in SSc patients. We examined the effect of recombinant MFG-E8 (rMFG-E8) on latent transforming growth factor β (TGFβ)–induced gene/protein expression in SSc fibroblasts. We examined the effects of deficiency or administration of MFG-E8 on fibrosis mouse models.

Results. We demonstrated that MFG-E8 expression around dermal blood vessels and the serum MFG-E8 level in SSc patients (n = 7 and n = 44, respectively) were lower than those in healthy individuals (n = 6 and n = 28, respectively). Treatment with rMFG-E8 significantly inhibited latent TGFβ–induced expression of type I collagen, α-smooth muscle actin, and CCN2 in SSc fibroblasts (n = 3–8), which suggested that MFG-E8 inhibited activation of latent TGFβ as well as TGFβ signaling via binding to αv integrin. In a mouse model of bleomycin-induced fibrosis (n = 5–8) and in a TSK mouse model (a genetic model of SSc) (n = 5–10), deficient expression of MFG-E8 significantly enhanced both pulmonary and skin fibrosis, and administration of rMFG-E8 significantly inhibited bleomycin-induced dermal fibrosis.

Conclusion. These results suggest that vasculopathy-induced dysfunction of pericytes and endothelial cells, the main cells secreting MFG-E8, may be associated with the decreased expression of MFG-E8 in SSc and that the deficient inhibitory regulation of latent TGFβ–induced skin fibrosis by MFG-E8 may be involved in the pathogenesis of SSc and may be a therapeutic target for fibrosis in SSc patients.

INTRODUCTION

Systemic sclerosis (SSc) is a connective tissue disorder characterized by the development of fibrosis in the skin and internal organs, vascular disorders, and autoimmunity (1,2). SSc patients develop various vasculopathy-induced vascular disorders, such as Raynaud's phenomenon, abnormal nailfold capillaries, and digital ulcers (1,3,4). Vascular disorders precede the onset of fibrosis, and vasculopathy is thought to be a primary event in the pathogenesis of SSc (1,2). It is believed that vasculopathy induces dysfunction of endothelial cells (ECs) and pericytes, hypoxia, and overproduction of endothelin 1, resulting in the activation of fibroblasts around damaged vessels and the induction of fibrosis (2,5). However, the underlying mechanism of fibrosis induction by vasculopathy remains unknown.

Milk fat globule–associated protein with epidermal growth factor (EGF)– and factor VIII–like domains (MFG-E8) is a secreted glycoprotein composed of 2 N-terminal EGF-like domains and 2 C-terminal discoidin-like domains that are homologous to

blood coagulation factors 5 and 8 (6,7). One EGF-like domain contains the RGD domain that binds to αvβ3/β5 integrin, and the C-domains bind to phosphatidylserine and type I collagen (8,9). MFG-E8 accelerates phagocytosis of apoptotic cells by bridging phosphatidylserine in apoptotic cells and αvβ3/β5 integrin in phagocytes, resulting in the suppression of inflammatory responses (10–12). We previously found that pericytes and mesenchymal stem cells (MSCs) secrete large amounts of MFG-E8 and that pericyte- and MSC-derived MFG-E8 promotes angiogenesis in intractable diabetic wounds, cutaneous ischemia-reperfusion injury, and melanoma tumors (13–18).

Regarding the regulation of fibrosis by MFG-E8, it has been reported that the expression of MFG-E8 was decreased in cirrhotic liver tissue; recombinant MFG-E8 (rMFG-E8) inhibited the expression of transforming growth factor β receptor type I (TGFβRI) by binding to αvβ3 integrin on human hepatic stellate cells, resulting in the inhibition of TGFβ signaling in vitro; and injection of rMFG-E8 into mice had an antifibrotic effect on thioacetamide-induced liver fibrosis in vivo (19). However, it remains unknown how MFG-E8 regulates skin fibrosis in SSc.

It has been reported that MFG-E8 is implicated in the pathogenesis of autoimmune disorders, such as systemic lupus erythematosus (SLE) and rheumatoid arthritis (RA). The serum MFG-E8 level in SLE patients was higher than that in healthy individuals (20), and aged MFG-E8–knockout (KO) mice developed glomerulonephritis and showed antinuclear antibody (ANA) production (21). Serum MFG-E8 levels in RA patients and arthritic mice were significantly lower than those in healthy controls, and MFG-E8–KO mice exhibited exacerbated arthritis (22).

TGFβ, a pivotal cytokine in fibrosis, is secreted from cells as a large latent complex composed of bioactive peptide of TGFβ and latency-associated protein, which in turn binds to latent TGFβ binding protein. Secreted latent TGFβ is stored in the extracellular matrix (ECM), and activated TGFβ is released by the binding of the RGD sequence in the latent TGFβ complex to αvβ1, αvβ3, αvβ5, αvβ6, and αvβ8 integrins (23,24). In SSc fibroblasts, overexpression of αvβ5 integrin leads to the activation of TGFβ1 and skin fibrosis (25). Furthermore, SSc-like skin fibrosis, ANA production, and TGFβ signaling activation were demonstrated in fibrillin 1 mutant mice in which the RGD domain of fibrillin 1 was changed to an RGE domain, resulting in inhibition of the binding of fibrillin to αv integrin (26). These findings strongly suggest that the binding between αv integrin on fibroblasts and latent TGFβ complex might be implicated in the pathogenesis of skin fibrosis in SSc.

MFG-E8 binds to αvβ3/β5 integrin via the RGD domain, which suggests that MFG-E8 might be associated with the pathogenesis of skin fibrosis in SSc through modulation of the interaction between αv integrin and latent TGFβ. However, the roles of MFG-E8 in the pathogenesis of skin fibrosis in SSc have not been investigated. In this study, we examined the expression of MFG-E8 in fibrotic lesions and the serum MFG-E8 level in SSc patients, and we analyzed the effects of the addition of MFG-E8 on latent

TGFβ–induced fibrosis in fibroblasts in vitro. Furthermore, we assessed the effect of MFG-E8 depletion or injection on skin fibrosis in a mouse model of bleomycin-induced fibrosis and in a TSK mouse model, which are experimental models of SSc.

MATERIALS AND METHODS

Patients. All of the SSc patients fulfilled the American College of Rheumatology/European League Against Rheumatism 2013 classification criteria (27). The serum samples were obtained from 44 Japanese patients with SSc (35 women and 9 men, mean ± SD age 60.0 ± 2.1 years) and 28 age-, race-, and sex-matched healthy volunteers. Twenty-eight patients were classified as having limited cutaneous SSc and 16 were classified as having diffuse cutaneous SSc (dcSSc) according to LeRoy et al (28). Skin sclerosis was assessed using the modified Rodnan skin thickness score (29). We obtained human dermal fibroblasts by performing skin biopsies on affected dorsal forearm areas of dcSSc patients and age-, race-, and sex-matched healthy volunteers. For immunohistochemical staining of MFG-E8, we obtained human skin tissues in the same way from 7 dcSSc patients and 6 age-, race-, and sex-matched healthy volunteers. The study was approved by the Institutional Review Board and the local research ethics committee of Gunma University and was conducted according to the principles of the Declaration of Helsinki.

Immunohistochemistry and immunofluorescence staining. Frozen sections (4 μm thick) of human skin were fixed in 4% paraformaldehyde (PFA) in phosphate buffered saline (PBS) at room temperature for 1 hour. Dermal fibroblasts from SSc patients were seeded in 8-well culture slides (BD Biosciences), and cells were either left untreated or treated with latent TGFβ1 (2 ng/ml; R&D Systems) with or without rMFG-E8 (100 ng/ml; R&D Systems) for 24 hours and fixed in 4% PFA at room temperature for 1 hour. After being blocked with 3% skim milk–PBS supplemented with 5% normal goat serum for 30 minutes at room temperature, skin tissues or cells were stained with mouse anti-human MFG-E8 polyclonal antibody (R&D Systems), rabbit anti-CD31 antibody (Abcam), and anti–α-smooth muscle actin (anti–α-SMA) antibody (Sigma) followed by staining with Alexa Fluor 488– or Alexa Fluor 568–conjugated secondary antibodies (Invitrogen). Tissues or cells were mounted in ProLong Gold antifade reagent (Invitrogen). Immunofluorescence images were collected and visualized with an FV10i-DOC confocal laser scanning microscope (Olympus).

Sections (4 μm thick) of mouse skin or lung embedded in paraffin were stained with hematoxylin and eosin (H&E) or Masson's trichrome. Skin fibrosis was quantified by measuring the thickness of the dermis, which was defined as the distance from the epidermal–dermal junction to the dermal–subcutaneous junction, at 6 randomly selected microscopic fields. Lung fibrosis was quantified by lung fibrosing score as described previously (30). Lung fibrosis was graded on a scale of 0 to

8 by examining 10 randomly selected fields. The criteria for grading lung fibrosis were as follows: grade 0 = normal lung; grade 1 = minimal fibrous thickening of alveolar or bronchiolar walls; grade 3 = moderate thickening of walls without obvious damage to lung architecture; grade 5 = increased fibrosis with definite damage to lung structure and formation of fibrous bands or small fibrous masses; grade 7 = severe distortion of structure and large fibrous area; grade 8 = total fibrous obliteration of the field. Grades 2, 4, and 6 were used as intermediate pictures between the aforementioned criteria.

For immunohistochemical staining, tissue sections of human or mouse skin were treated for antigen retrieval with a pressure cooker for 10 minutes at 121°C. After blocking using Peroxidase Blocking (Dako) for 5 minutes and Protein Block (Dako) for 10 minutes, the sections were incubated with mouse anti-human MFG-E8 polyclonal antibody, anti–α-SMA antibody, anti-CD3 antibody (Abcam), anti-CD68 antibody (Bio-Rad), anti-CD31 antibody (BD Biosciences), and anti-NG2 polyclonal antibody (Millipore). After washing, the sections were incubated with a horseradish peroxidase–labeled polymer-conjugated secondary antibody (EnVision+; Dako). Finally, color was developed with 3,3′-diaminobenzidine tetrahydrochloride. Numbers of α-SMA+, CD3+, CD68+, CD31+, and NG2+ cells in the dermis were determined by counting in 6 random microscopic fields in 3 mice per group.

Reverse transcriptase–polymerase chain reaction analysis. To examine the effect of rMFG-E8 on TGFβ- or latent TGFβ–induced fibrosis in SSc fibroblasts, the cells were pretreated with rMFG-E8 (100 ng/ml) for 1 hour and then stimulated with TGFβ1 (2 ng/ml; R&D Systems) or latent TGFβ (2 ng/ml) for 24 hours. To examine the effect of RGD-MFG-E8-Ig or RGE-MFG-E8-Ig on latent TGFβ–induced fibrosis–related gene expression, NIH3T3 fibroblasts were pretreated with RGD-MFG-E8-Ig or RGE-MFG-E8-Ig (100 ng/ml) for 1 hour and then stimulated with latent TGFβ (2 ng/ml) for 12 hours. RGD-MFG-E8-Ig and RGE-MFG-E8-Ig were generated and used as previously described (31). RGD-MFG-E8-Ig is a fusion protein that consists of the N-terminal EGF-like domains (E1 and E2) and the linker region fused with the hinge-containing Fc region of human IgG1 (31). RGE-MFG-E8-Ig is the corresponding point mutant of MFG-E8-Ig in which aspartic acid (D) in the RGD motif is replaced by glutamic acid (E) (for further details, see Supplementary Materials and Methods, available on the *Arthritis & Rheumatology* web site at http://onlinelibrary.wiley.com/doi/10.1002/art.40701/abstract).

Western blot assay. Western blot analyses were performed according to previously described protocols (31,32). To examine the effect of rMFG-E8 on TGFβ- or latent TGFβ–induced fibrosis–related protein expression in SSc fibroblasts, the cells were pretreated with rMFG-E8 (100 ng/ml) for 1 hour and then stimulated with TGFβ1 (2 ng/ml) or latent TGFβ (2 ng/ml) for 48

hours. To examine the effect of RGD-MFG-E8-Ig or RGE-MFG-E8-Ig on latent TGFβ–induced fibrosis–related protein expression, NIH3T3 fibroblasts were pretreated with RGD-MFG-E8-Ig or RGE-MFG-E8-Ig (100 ng/ml) for 1 hour and then stimulated with latent TGFβ (2 ng/ml) for 12 hours (for further details, see Supplementary Materials and Methods, http://onlinelibrary.wiley.com/doi/10.1002/art.40701/abstract).

Mouse model of bleomycin-induced fibrosis and TSK mouse model. Dermal fibrosis was induced in 8-week-old C57BL/6 mice (Japan SLC) with injections of bleomycin. Injections of 300 μl of bleomycin (Nippon Kayaku) at a concentration of 1 mg/ml were given 5 times per week for 2 weeks as previously described (33,34). Injections of 300 μl of PBS were used as controls for treatment with bleomycin. To examine the effect of rMFG-E8, mice received subcutaneously 400 ng/day rMFG-E8 dissolved in 50 μl of PBS or PBS alone 5 times per week for 2 weeks. MFG-E8–KO C57BL/6 mice were generated, characterized, and genotyped as previously described (13,15,16,18,35). MFG-E8–KO mice were generated by interbreeding homozygous animals carrying the targeted MFG-E8 allele. TSK mice (TSK/+: B6.Cg-Fbn1^{Tsk}/J), which had genetic mutations in fibrillin 1, were purchased from The Jackson Laboratory. MFG-E8 wild-type TSK (WT TSK/+) mice and MFG-E8–KO TSK (MFG-E8$^{-/-}$TSK/+) mouse littermates were generated by crossing MFG-E8$^{+/-}$TSK/+ parents. Mice ages 8–12 weeks were used for all experiments. Mice were bred and maintained in the Institute of Experimental Animal Research of Gunma University under specific pathogen–free conditions. All experiments were approved by the Gunma University Animal Care and Experimentation Committee and carried out in accordance with approved guidelines.

Quantitative assessment of collagen content. Total soluble collagen in the skin was quantified using a Sircol collagen assay (Biocolor) according to the manufacturer's protocol and the previously described protocols (36).

Measurement of serum levels of MFG-E8, ANAs, and anti–topoisomerase I (anti–topo I). A specific enzyme-linked immunosorbent assay (ELISA) kit (R&D Systems) was used to measure serum MFG-E8 levels according to the manufacturer's protocol. ANAs were assessed with an indirect immunofluorescence kit using HEp-2 substrate cells (Medical and Biological Laboratories) as described (37). To measure anti–topo I, a specific ELISA kit (Medical and Biological Laboratories) was used according to the manufacturer's protocol.

Statistical analysis. *P* values were calculated by Student's *t*-test or one-way analysis of variance followed by the Bonferroni post hoc test for multiple comparisons. Data are reported as the mean ± SEM.

RESULTS

Decreased expression of MFG-E8 in ECs and peri-cytes/vascular smooth muscle cells (VSMCs) of lesional skin and low serum MFG-E8 levels in SSc patients. We first examined the expression of MFG-E8 in the sclerotic skin lesions of SSc patients and healthy individuals by immunofluorescence staining. In the skin of healthy individuals, MFG-E8 staining was mainly observed in and around CD31+ vascular ECs, especially being colocalized with α-SMA+ pericytes and VSMCs (Figure 1A). Dermal fibroblasts in normal skin were slightly positive for MFG-E8 staining. In contrast, MFG-E8 staining around blood vessels in
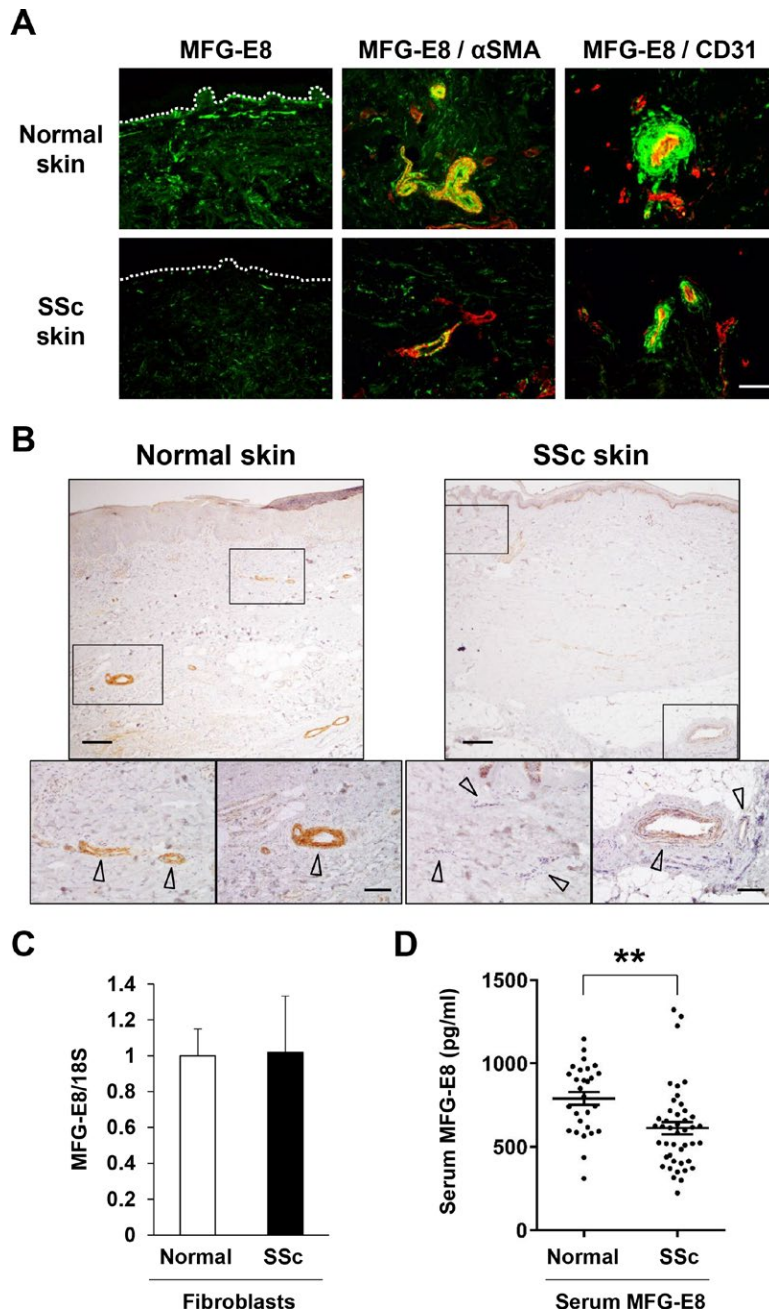
Figure 1. Decreased expression of milk fat globule–associated protein with epidermal growth factor– and factor VIII–like domains (MFG-E8) in endothelial cells (ECs) and pericytes/vascular smooth muscle cells (VSMCs) of lesional skin as well as low serum MFG-E8 levels in patients with systemic sclerosis (SSc). **A,** Representative immunofluorescence staining of MFG-E8, α-smooth muscle actin–positive (α-SMA+) pericytes/VSMCs, and CD31+ vascular ECs in the dermis of SSc patients and normal individuals. **Dotted line** is the border of the epidermis and the dermis. Bar = 50 μm. **B,** Top, Representative immunohistochemical staining of MFG-E8 in the skin of SSc patients and normal individuals. Bottom, Representative MFG-E8 staining in dermal small vessels (**arrowheads**). Boxed areas at top are shown at higher magnification at bottom. Bars = 200 μm at top; 100 μm at bottom. **C,** Expression of mRNA for MFG-E8 in fibroblasts from 4 healthy individuals and 5 SSc patients. The mRNA level in normal fibroblasts was assigned a value of 1. Values are the mean ± SEM. **D,** Serum MFG-E8 levels in 44 SSc patients and 28 normal individuals. Symbols represent individual subjects; bars show the mean ± SEM. ** = $P < 0.01$.

skin lesions of SSc patients was reduced compared with that in normal skin (Figure 1A). The extent of MFG-E8 staining in dermal fibroblasts from SSc patients was nearly the same as that in normal skin fibroblasts. Immunohistochemistry indicated that MFG-E8 staining around capillaries and small blood vessels in the dermis was reduced in the skin of SSc patients (Figure 1B; also see Supplementary Table 1 and Supplementary Figure 1, http://online

library.wiley.com/doi/10.1002/art.40701/abstract). There was no difference in expression of messenger RNA (mRNA) for MFG-E8 between normal and SSc cultured fibroblasts (Figure 1C). In addition, serum MFG-E8 levels in SSc patients were significantly lower than those in healthy individuals (Figure 1D). These results suggest that MFG-E8 expression in ECs and pericytes/VSMCs in the skin and serum MFG-E8 levels might be decreased in SSc patients.

Figure 2. Recombinant milk fat globule–associated protein with epidermal growth factor– and factor VIII–like domains (rMFG-E8) inhibits latent transforming growth factor β (TGFβ)–induced fibrosis–related gene/protein expression in fibroblasts from patients with systemic sclerosis (SSc). **A–C,** Expression of mRNA for type I collagen (**A**), α-smooth muscle actin (α-SMA) (**B**), and CCN2 (**C**) in SSc fibroblasts either left untreated or treated with latent TGFβ with or without rMFG-E8 (n = 5–8 donors). **D** and **E,** Protein levels of type I collagen and α-SMA (**D**) and p-Smad2 (**E**) in SSc fibroblasts either left untreated or treated with latent TGFβ with or without rMFG-E8 (n = 3 donors). Quantification of relative levels was accomplished via densitometry using ImageJ software (National Institutes of Health). **F,** Immunofluorescence staining of α-SMA in SSc fibroblasts either left untreated or treated with latent TGFβ with or without rMFG-E8. Bar = 50 μm. **G** and **H,** Expression of mRNA for TGFβ receptor type I (TFGβRI) (**G**) and TFGβRII (**H**) in SSc fibroblasts either left untreated or treated with latent TGFβ with or without rMFG-E8 (n = 3–4 donors). Values are the mean ± SEM relative to mRNA and protein levels in untreated fibroblasts (set to 1). * = $P < 0.05$; ** = $P < 0.01$.

Recombinant MFG-E8 inhibits latent TGFβ–induced fibrosis–related gene/protein expression but not TGFβ-induced fibrosis–related gene/protein expression in SSc fibroblasts. It is well known that latent TGFβ binds to αv integrin, and thereafter active TGFβ is released from the latent complex (23,24). Since MFG-E8 binds to αv integrin, we hypothesized that rMFG-E8 might affect TGFβ signaling by interfering with TGFβ activation. Therefore, we next examined the effect of rMFG-E8 addition on latent TGFβ–induced fibrosis–related gene/protein expression in SSc fibroblasts. Type I collagen is the major ECM in the dermis of skin, and it is overexpressed in sclerotic skin lesions in SSc (38). Myofibroblasts are primarily involved in fibrosis by overproducing the ECM, and they express α-SMA. The number of α-SMA+ myofibroblasts is increased in sclerotic skin lesions in SSc (38). CCN2 (also known as connective tissue growth factor) is the member of the CCN family of matricellular proteins associated with fibrosis (39). CCN2 is overexpressed in SSc fibroblasts and plays an important role in the production and maintenance of fibrotic lesions in SSc (40). In SSc fibroblasts, latent TGFβ enhanced expression of mRNA for type I collagen, α-SMA, and CCN2, and this was significantly inhibited upon addition of rMFG-E8 (Figures 2A–C). Furthermore, the elevated protein levels of type I collagen, α-SMA, and p-Smad2 induced by latent TGFβ were significantly inhibited by rMFG-E8 treatment (Figures 2D and E).

Akt activates various cell functions such as proliferation, migration, and adhesion, leading to the enhancement of fibrosis. In SSc fibroblasts, p-Akt induced by latent TGFβ was also significantly inhibited by rMFG-E8 treatment (see Supplementary Figure 2A, http://onlinelibrary.wiley.com/doi/10.1002/art.40701/abstract). Focal adhesion kinase (FAK) is important for cell adhesion. Phosphorylated FAK induced by latent TGFβ was slightly inhibited by rMFG-E8 treatment, but this difference did not reach statistical significance (see Supplementary Figure 2B). Immunofluorescence staining indicated that latent TGFβ–induced α-SMA expression in SSc fibroblasts was inhibited by rMFG-E8 (Figure 2F). Expression of mRNA for TGFβRI and TGFβRII in SSc fibroblasts treated with latent TGFβ was not inhibited by rMFG-E8 (Figures 2G and H).

We next examined whether rMFG-E8 also inhibits TGFβ-induced fibrosis–related gene/protein expression in SSc fibroblasts. The TGFβ-induced increases in expression of mRNA for type I collagen, α-SMA, and CCN2 were not inhibited by the addition of rMFG-E8 (see Supplementary Figures 3A–C, http://onlinelibrary.wiley.com/doi/10.1002/art.40701/abstract). Furthermore, TGFβ-induced increases in protein levels of type I collagen, α-SMA, and p-Smad2 were not inhibited by rMFG-E8 treatment (see Supplementary Figures 3D and E), although the expression of type I collagen, α-SMA, and CCN2 tended to be increased by rMFG-E8 treatment. The expression of TGFβRI and TGFβRII in SSc fibroblasts treated with TGFβ was not affected by rMFG-E8 (see Supplementary Figures 3F and G). These results suggest that rMFG-E8 inhibits latent TGFβ–induced fibrosis– related gene/protein expression but not TGFβ-induced fibrosis–related gene/protein expression in SSc fibroblasts.

MFG-E8 inhibits latent TGFβ–induced fibrosis–related gene/protein expression by binding to αv integrin via the RGD domain in fibroblasts. We next examined the effects of RGD-MFG-E8-Ig and RGE-MFG-E8-Ig on latent TGFβ–induced fibrosis–related gene/protein expression in NIH3T3 fibroblasts. We have previously reported that RGE-MFG-E8-Ig, the corresponding RGE point mutant, cannot bind to αv integrin on cultured cells (31). In the present study, we found that RGD-MFG-E8-Ig significantly inhibited latent TGFβ–induced expression of mRNA for type I collagen and CCN2, while RGE-MFG-E8-Ig did not (Figures 3A and C). Furthermore, latent TGFβ–induced protein expression of type I collagen was inhibited by RGD-MFG-E8-Ig but not by RGE-MFG-E8-Ig (Figure 3D). We did not observe obvious differences in α-SMA expression between RGD-MFG-E8-Ig– and RGE-MFG-E8-Ig–treated fibroblasts (Figures 3B and D). These results suggest that the inhibitory action of MFG-E8 on latent TGFβ–induced fibrosis–related gene/protein expression might be competitively mediated by the binding of the RGD domain of MFG-E8 to αv integrin in fibroblasts.

Bleomycin-induced skin and pulmonary fibrosis are exacerbated by deficiency of MFG-E8. To assess the role of MFG-E8 in tissue fibrosis in vivo, we examined bleomycin-induced skin and pulmonary fibrosis in MFG-E8 WT and MFG-E8–KO C57BL/6 mice. Bleomycin-induced dermal thickness in MFG-E8–KO mice was significantly increased compared with that in WT mice (Figures 4A and C). The amount of bleomycin-induced dermal collagen was significantly larger in MFG-E8–KO mice than in WT mice, as indicated by Masson's trichrome staining (Figure 4B). In addition, bleomycin-induced pulmonary fibrosis in MFG-E8–KO mice was significantly more intense than that in WT mice (Figures 4D–F). Expression of mRNA for type I collagen, CCN2, and α-SMA in lesional skin was significantly increased in bleomycin-treated MFG-E8–KO mice compared to bleomycin-treated WT mice (Figure 4G). Expression of mRNA for TGFβ and interleukin-6 (IL-6) tended to be higher in bleomycin-treated MFG-E8–KO mice, but the differences did not reach statistical significance (Figure 4G). The number of α-SMA+ myofibroblasts in the skin of bleomycin-treated MFG-E8–KO mice was increased, while the numbers of CD3+ T cells, CD68+ macrophages, CD31+ ECs, and NG2+ pericytes in the 2 groups were not significantly different (Figures 4H and I). These results suggest that MFG-E8 negatively regulates bleomycin-induced skin and pulmonary fibrosis in mice.

Skin and pulmonary fibrosis in TSK/+ mice are exacerbated by deficiency of MFG-E8. We further examined skin and pulmonary fibrosis in MFG-E8 WT TSK/+ mice and MFG-E8⁻/⁻TSK/+ mice to assess the role of MFG-E8 in
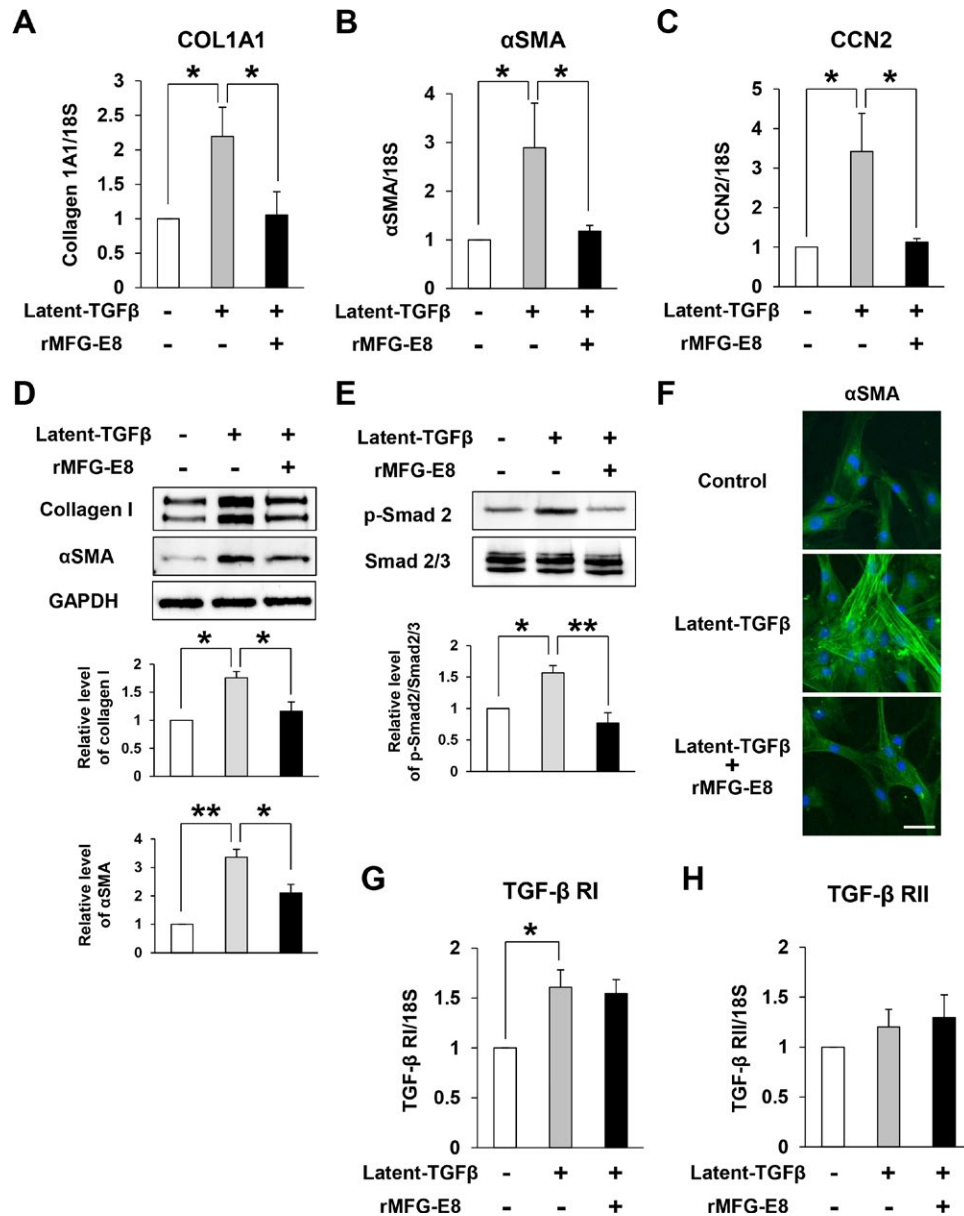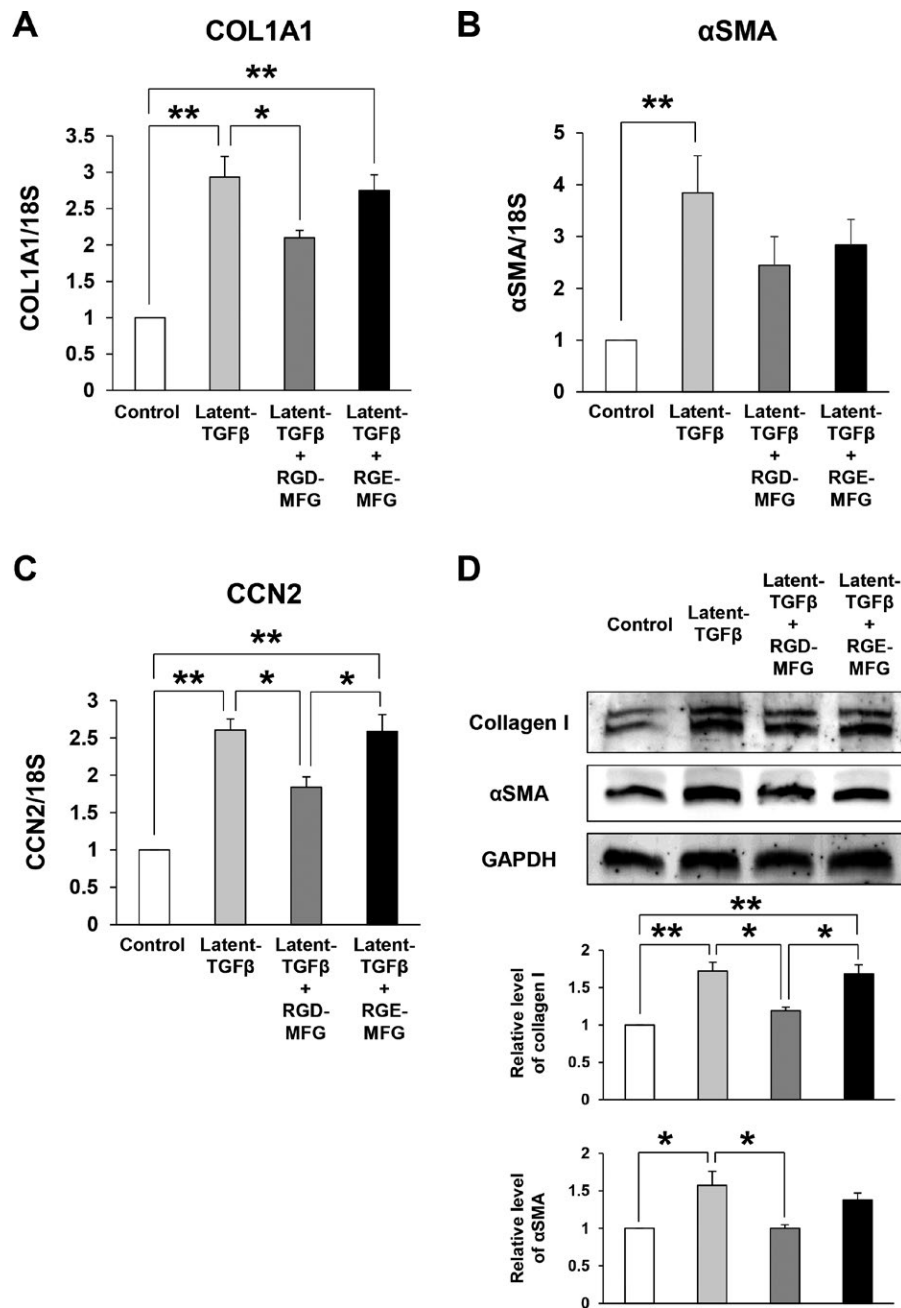
Figure 3. Milk fat globule–associated protein with epidermal growth factor– and factor VIII–like domains (MFG-E8) inhibits latent transforming growth factor β (TGFβ)–induced fibrosis–related gene/protein expression by binding to αv integrin through the RGD domain in fibroblasts. **A–C,** Expression of mRNA for type I collagen (**A**), α-smooth muscle actin (α-SMA) (**B**), and CCN2 (**C**) in NIH3T3 fibroblasts either left untreated or treated with latent TGFβ with or without RGD-MFG-E8-Ig (RGD-MFG) or RGE-MFG-E8-Ig (RGE-MFG) (n = 3 donors). **D,** Protein levels of type I collagen and α-SMA in fibroblasts either left untreated or treated with latent TGFβ with or without RGD-MFG-E8-Ig or RGE-MFG-E8-Ig (n = 3 donors). Quantification of relative levels was accomplished via densitometry using ImageJ software (National Institutes of Health). Values are the mean ± SEM relative to mRNA and protein levels in untreated fibroblasts (set to 1). * = $P < 0.05$; ** = $P < 0.01$.

tissue fibrosis in vivo. TSK mice spontaneously develop skin fibrosis because of a partial in-frame duplication in the fibrillin 1 gene, and they are known as an experimental model of SSc (41–43). The hypodermal thickness in MFG-E8$^{-/-}$TSK/+ mice was significantly increased compared with that in MFG-E8 WT TSK/+ mice (Figures 5A–C). H&E and Masson's trichrome staining of the lungs indicated that infiltration of inflammatory

cells and lung fibrosis in MFG-E8$^{-/-}$TSK/+ mice were also enhanced (Figures 5D and E). Lung fibrosing scores were significantly higher in MFG-E8$^{-/-}$TSK/+ mice than in MFG-E8 WT TSK/+ mice (Figure 5F). The numbers of α-SMA+ myofibroblasts, CD3+ T cells, and CD68+ macrophages in the lungs of MFG-E8$^{-/-}$TSK/+ mice were significantly higher than those in the lungs of MFG-E8 WT TSK/+ mice (Figure 5G).
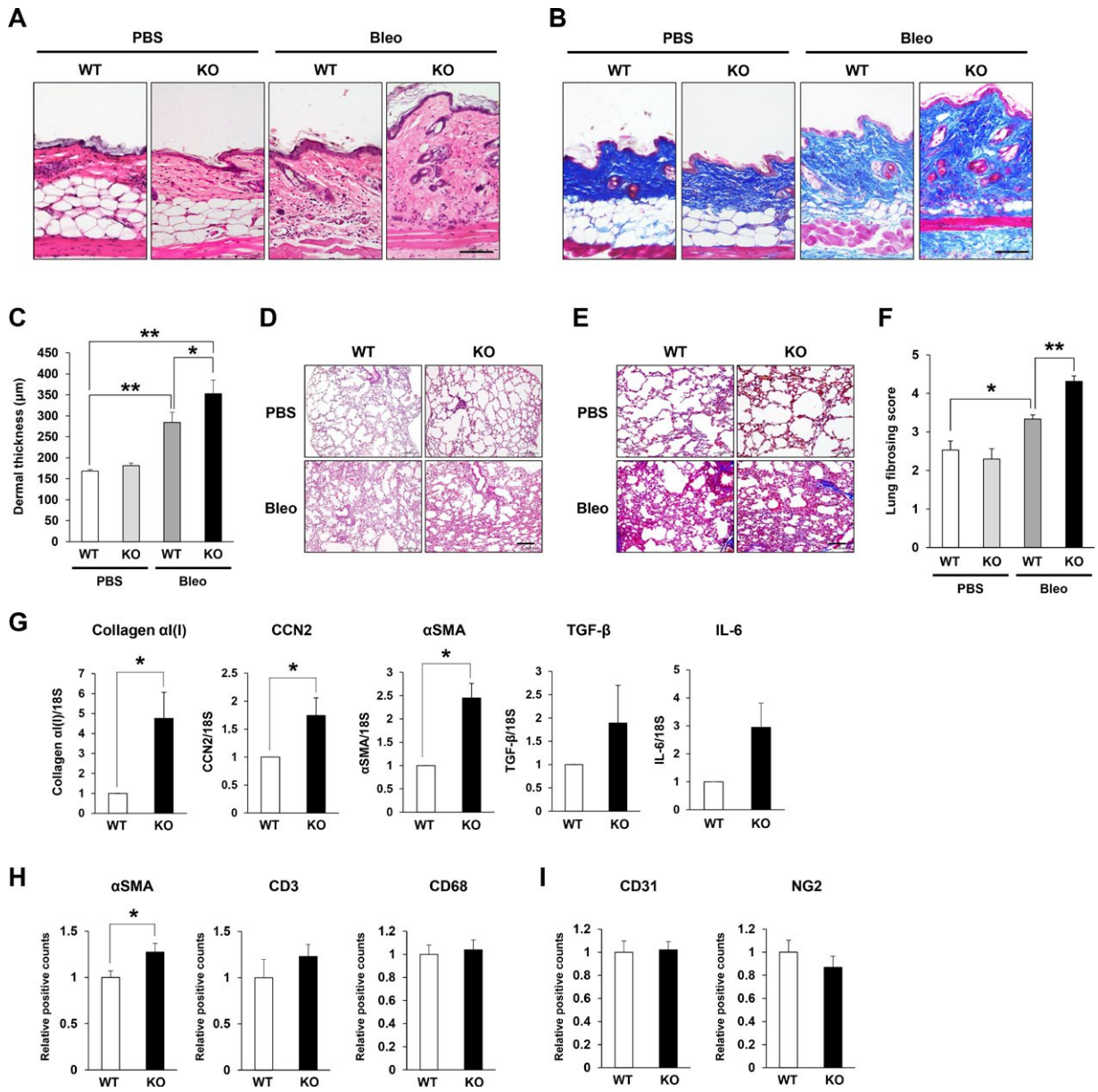
Figure 4. Exacerbation of bleomycin (Bleo)–induced skin and pulmonary fibrosis by deficiency of milk fat globule–associated protein with epidermal growth factor– and factor VIII–like domains (MFG-E8). **A**, **B**, **D**, and **E,** Representative images of hematoxylin and eosin staining (**A** and **D**) or Masson's trichrome staining (**B** and **E**) of the skin (**A** and **B**) and lung (**D** and **E**) of MFG-E8 wild-type (WT) or MFG-E8–knockout (KO) C57BL/6 mice treated with subcutaneous injections of phosphate buffered saline (PBS) or bleomycin. Bars = 100 μm in **A**, **B**, and **E**; 50 μm in **D**. **C,** Quantification of dermal thickness (n = 5–8 mice per group). **F,** Quantification of pulmonary fibrosis (n = 6 mice per group). **G,** Expression of mRNA for type I collagen, CCN2, α-smooth muscle actin (α-SMA), transforming growth factor β (TGFβ), and interleukin-6 (IL-6) in the skin of bleomycin-treated MFG-E8 WT mice or MFG-E8–KO mice (n = 3 per group), determined using quantitative reverse transcriptase–polymerase chain reaction. **H** and **I,** Numbers of α-SMA+ myofibroblasts, CD3+ T cells, and CD68+ macrophages (**H**) and CD31+ endothelial cells and NG2+ pericytes (**I**) in the dermis (n = 3 mice per group). In **C** and **F**, values are the mean ± SEM. In **G–I**, values are the mean ± SEM relative to mRNA levels and cell counts in WT mice (set to 1). * = $P < 0.05$; ** = $P < 0.01$.

IL-6 signaling is also recognized as being involved in the development and progression of fibrosis in SSc (32,44). Expression of mRNA for type I collagen and IL-6 in the lungs of MFG-E8$^{-/-}$TSK/+ mice was significantly higher than that in the lungs of MFG-E8 WT TSK/+ mice (Figure 5H). TSK mice produce specific autoantibodies, including ANAs and anti–topo I, that can also be shown in SSc patients (43). In our study, serum levels of ANAs and anti–topo I were significantly higher in MFG-E8$^{-/-}$TSK/+ mice than in MFG-E8 WT TSK/+ mice (Figure 5I).

These results suggest that MFG-E8 negatively regulates fibrosis and infiltration of inflammatory cells in the skin and lungs as well as autoantibody production in TSK mice.
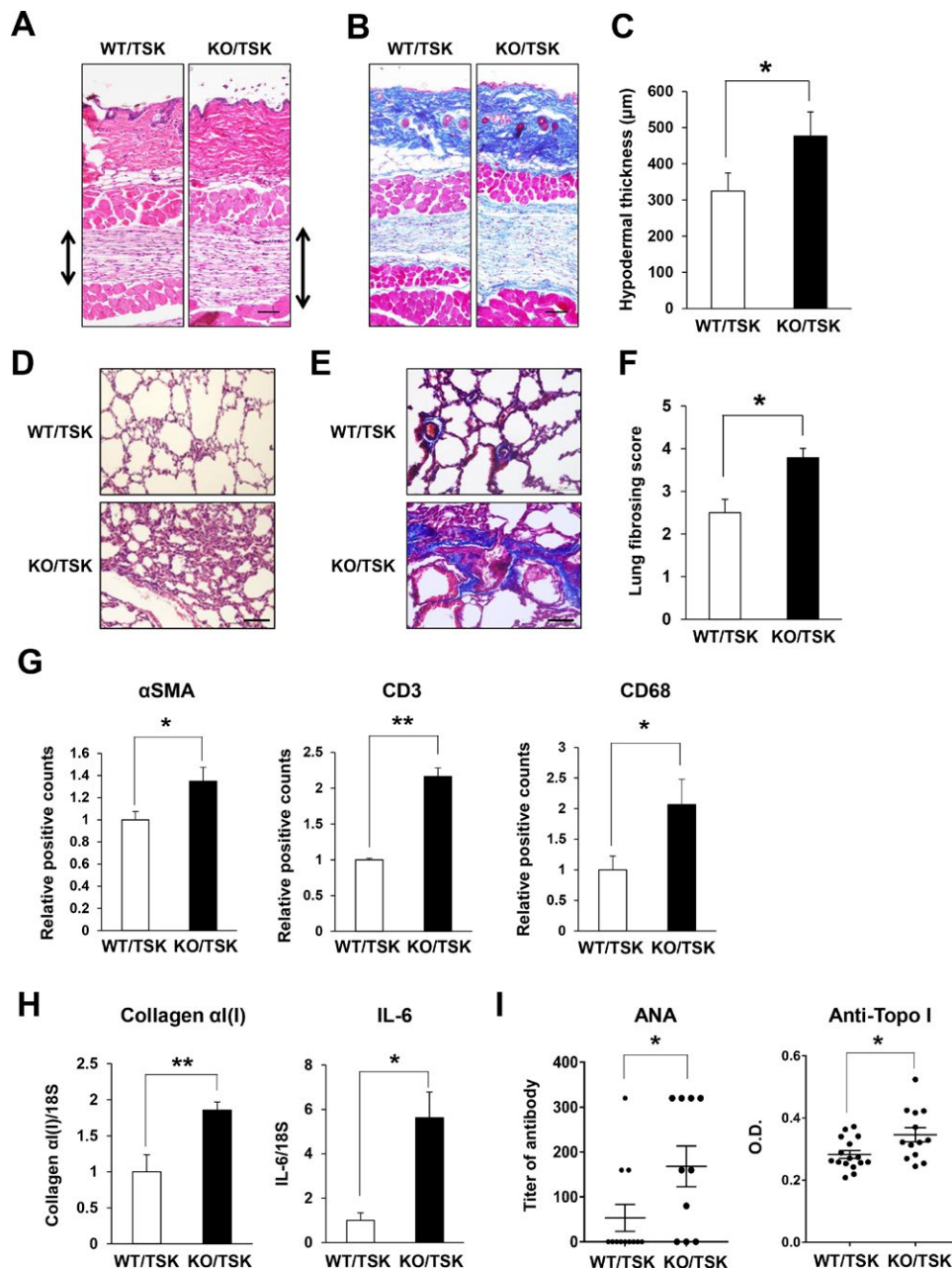
Figure 5. Exacerbation of skin and pulmonary fibrosis in TSK mice by deficiency of milk fat globule–associated protein with epidermal growth factor– and factor VIII–like domains (MFG-E8). **A**, **B**, **D**, and **E,** Representative images of hematoxylin and eosin staining (**A** and **D**) or Masson's trichrome staining (**B** and **E**) of the skin (**A** and **B**) and lung (**D** and **E**) of MFG-E8 wild-type TSK (WT/TSK) mice and MFG-E8–knockout TSK (KO/TSK) mice. Bars = 50 μm in **A**, **B**, and **D**; 100 μm in **E**. **C,** Quantification of hypodermal thickness in mice (n = 5 per group). **F,** Quantification of pulmonary fibrosis in mice (n = 10 per group). **G,** Numbers of α-smooth muscle actin–positive (α-SMA+) myofibroblasts, CD3+ T cells, and CD68+ macrophages in the lung (n = 3 mice per group). **H,** Expression of mRNA for type I collagen and interleukin-6 (IL-6) in the lung (n = 3 mice per group), determined using quantitative reverse transcriptase–polymerase chain reaction. **I,** Serum levels of antinuclear antibodies (ANAs) and anti–topoisomerase I (anti–topo I) in mice (n = 10–16 per group). In **C** and **F**, values are the mean ± SEM. In **G** and **H**, values are the mean ± SEM relative to cell counts and mRNA levels in WT TSK mice (set to 1). In **I**, symbols represent individual mice; bars show the mean ± SEM. * = $P < 0.05$; ** = $P < 0.01$.

Administration of rMFG-E8 significantly inhibits bleomycin-induced dermal fibrosis in mice. Finally, we examined the effect of rMFG-E8 injection on bleomycin-induced dermal fibrosis in mice. Bleomycin-enhanced dermal thick-ness was significantly inhibited by the subcutaneous injection of rMFG-E8 (Figures 6A and B). Masson's trichrome staining revealed that bleomycin-induced dermal fibrosis was signifi-cantly suppressed by rMFG-E8 injection (Figure 6C). In addition,

the increase in the amount of collagen in the skin induced by bleomycin treatment was also inhibited by rMFG-E8 injection (Figure 6D). The increase in the numbers of α-SMA+ myofibroblasts, CD68+ macrophages, and CD3+ T cells in lesional skin in bleomycin-treated mice was significantly decreased by rMFG-E8 injection (Figure 6E). These results suggest that rMFG-E8 acts to inhibit bleomycin-induced skin fibrosis in vivo.

DISCUSSION

We previously reported that MFG-E8 is mainly expressed in ECs and pericytes/VSMCs in human and mouse skin (15). In human and mouse melanoma tumors, MFG-E8 is also mainly expressed by pericytes/pericyte precursors, and MFG-E8 enhances angiogenesis and tumor growth (13,18). In the present
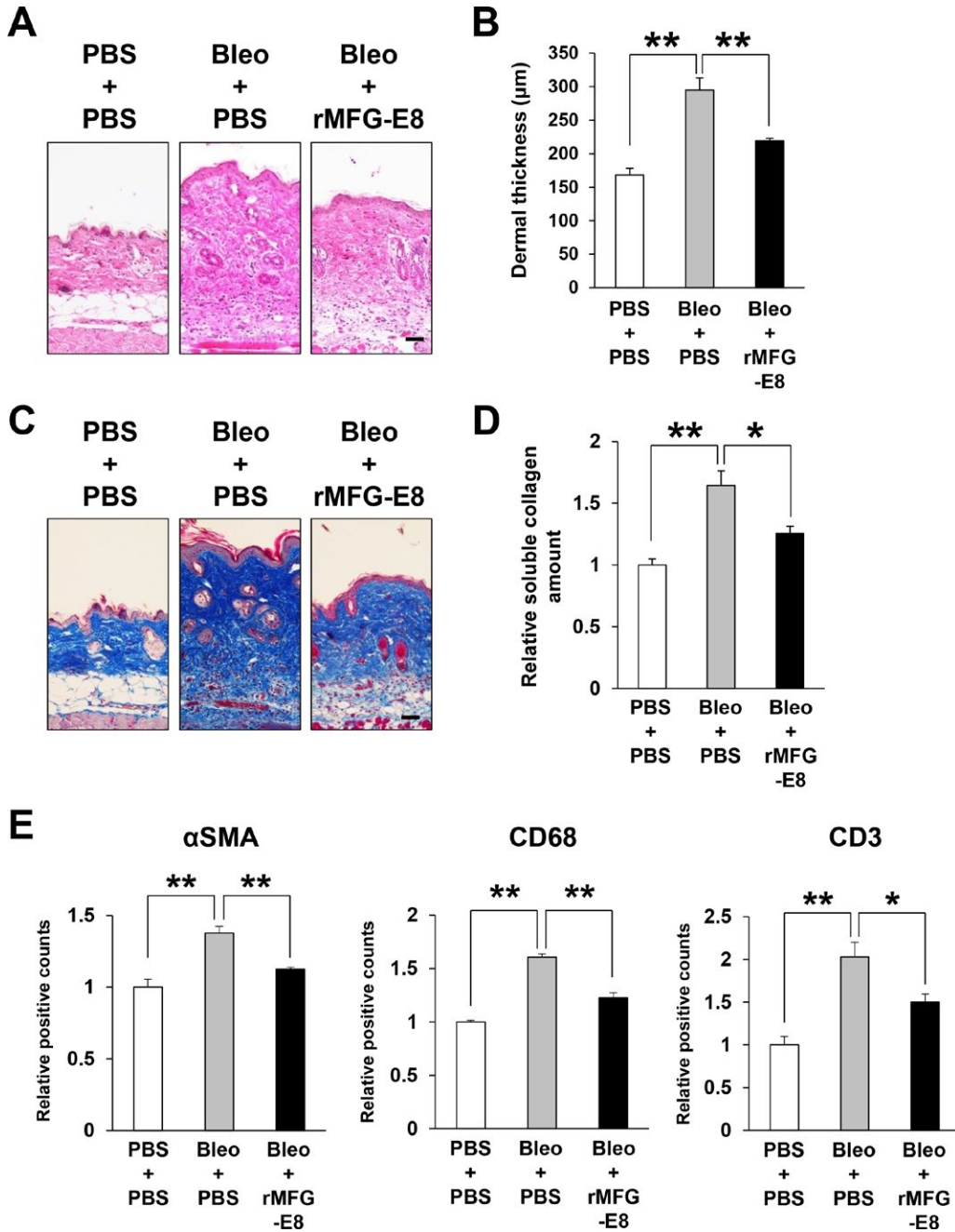
Figure 6. Significant inhibition of bleomycin (Bleo)–induced dermal fibrosis in mice by administration of recombinant milk fat globule–associated protein with epidermal growth factor– and factor VIII–like domains (rMFG-E8). **A** and **C,** Representative images of hematoxylin and eosin staining (**A**) or Masson's trichrome staining (**C**) of the skin of mice treated with subcutaneous injections of phosphate buffered saline (PBS) or bleomycin, or treated with subdermal injections of rMFG-E8 or PBS. Bars = 50 μm. **B,** Quantification of dermal thickness in mice (n = 10 per group). **D,** Quantification of soluble collagen amount in skin tissue (n = 7 mice per group). **E,** Numbers of α-smooth muscle actin–positive (α-SMA+) myofibroblasts, CD68+ macrophages, and CD3+ T cells in the dermis (n = 4–6 mice per group). In **B,** values are the mean ± SEM. In **D** and **E,** values are the mean ± SEM relative to soluble collagen amount and cell counts in mice injected both subcutaneously and subdermally with PBS. * = $P < 0.05$; ** = $P < 0.01$.

study, we found that MFG-E8 expression in ECs and pericytes/ VSMCs was reduced in sclerotic skin lesions of SSc patients. It has been suggested that vasculopathy and dysfunction of ECs might be associated with the development of skin fibrosis in SSc patients (1,2). Additionally, it has been reported that numbers of pericytes/ VSMCs in all types of blood vessels in lesional skin are decreased in SSc patients (2,25,45). Collectively, vasculopathy-induced dysfunction of and reduction in ECs and pericytes/VSMCs might be associated with decreased expression of MFG-E8 in lesional skin of SSc patients. Similar to our results, expression of MFG-E8 was reduced in smooth muscle cells around fibrosing respiratory tracts of asthma patients as well as in cirrhotic livers (19,46), which suggests that reduced expression of MFG-E8 might be involved in the pathogenesis of fibrosis in various organs and tissues.

It is considered that the binding of latent TGFβ complex to αv integrin is necessary to release an active form of TGFβ. For example, in SSc fibroblasts, αv integrin was found to be overexpressed and to consequently increase the activation of TGFβ, resulting in enhancement of TGFβ signaling and fibrosis in vitro (25). In addition, using fibrillin 1 mutant mice, enhancement of skin fibrosis was found to be caused by modulation of binding between αv integrin and latent TGFβ (26). In our study, we determined that rMFG-E8 inhibited latent TGFβ–enhanced TGFβ signaling and fibrosis in SSc fibroblasts. Furthermore, we confirmed that the inhibition of latent TGFβ–enhanced TGFβ signaling by rMFG-E8 was partly mediated via the interaction of the RGD domain of MFG-E8 with αv integrin on fibroblasts.

With respect to inhibition of TGFβ signaling by MFG-E8, An et al reported that rMFG-E8 inhibited TGFβ-enhanced TGFβ signaling and fibrosis in hepatic stellate cells through inhibition of TGFβRI expression (19). However, we could not confirm inhibition of TGFβ-enhanced TGFβ signaling by rMFG-E8 in SSc fibroblasts. In addition, expression of mRNA for TGFβRI and TGFβRII in SSc fibroblasts was not inhibited by rMFG-E8 in our study, which suggests that inhibition of latent TGFβ–enhanced TGFβ signaling in SSc fibroblasts by rMFG-E8 might not depend on inhibition of TGFβR expression.

Consistent with our findings, it has been reported that MFG-E8–KO mice develop exaggerated pulmonary fibrosis upon intratracheal bleomycin administration owing to a defect in collagen removal by macrophages (9). Although skin fibrosis was not examined in that previous study, we found that bleomycin-induced skin fibrosis in MFG-E8–KO mice was significantly exacerbated compared with that in WT mice and that expression of mRNA for type I collagen and numbers of α-SMA+ myofibroblasts in the skin of bleomycin-treated MFG-E8–KO mice were enhanced, suggesting that overproduction of collagen from myofibroblasts may be associated with enhancement of skin fibrosis in MFG-E8–KO mice.

We demonstrated that skin and pulmonary fibrosis in TSK mice were exacerbated by deficiency of MFG-E8. Our results suggest that MFG-E8 might negatively regulate fibrosis and inflamma-

tory cell infiltration in the skin and lungs as well as autoantibody production in TSK mice. Although a tandem duplication within the fibrillin 1 gene has been suggested to cause the TSK phenotype (41–43), the mechanisms of pathogenesis of fibrosis in TSK mice are still unknown. Activation of TGFβ signaling possibly plays an important role in the pathogenesis of fibrosis in TSK mice (47,48). Our results suggest that deficiency of MFG-E8 might enhance the release of active TGFβ from latent TGFβ complex in TSK mice, leading to exacerbation of fibrosis. However, the precise mechanisms underlying the increase in fibrosis in TSK mice caused by MFG-E8 deficiency require further study.

We demonstrated that administration of rMFG-E8 significantly inhibited bleomycin-induced dermal fibrosis in mice. These in vivo results are consistent with our in vitro results, which suggest that MFG-E8 might have therapeutic potential by inhibiting TGFβ signaling under pathogenic conditions. Consistent with our results, it has been reported that rMFG-E8 administration inhibited thioacetamide-induced liver fibrosis in mice and reduced the number of α-SMA+ myofibroblasts (19), warranting that rMFG-E8 may have therapeutic potential for fibrosis in several organs.

In conclusion, we have, for the first time, demonstrated that MFG-E8 inhibited latent TGFβ–enhanced TGFβ signaling and fibrosis mediated by the interaction of the RGD domain in MFG-E8 with αv integrin in SSc fibroblasts. Vasculopathy may be responsible for the reduced MFG-E8 expression in ECs and pericytes/ VSMCs in sclerotic skin lesions, and this reduction may be related to poor angiogenesis and prominent dermal fibrosis around blood vessels. Our in vivo findings suggest that MFG-E8 might negatively regulate skin and pulmonary fibrosis in bleomycin-treated mice and TSK mice. A deficient antifibrotic effect of MFG-E8 may be involved in the pathogenesis of SSc, and integrin-modulating therapy, such as administration of rMFG-E8, could be promising for the treatment of fibrosis in SSc.

AUTHOR CONTRIBUTIONS

REFERENCES

1. Denton CP, Khanna D. Systemic sclerosis. Lancet 2017;390:1685–99.
2. Trojanowska M. Cellular and molecular aspects of vascular dysfunction in systemic sclerosis. Nat Rev Rheumatol 2010;6:453–60.
3. Motegi S, Toki S, Hattori T, Yamada K, Uchiyama A, Ishikawa O. No association of atherosclerosis with digital ulcers in Japanese patients

with systemic sclerosis: evaluation of carotid intima-media thickness and plaque characteristics. J Dermatol 2014;41:604–8.

4. Motegi S, Yamada K, Toki S, Uchiyama A, Kubota Y, Nakamura T, et al. Beneficial effect of botulinum toxin A on Raynaud's phenomenon in Japanese patients with systemic sclerosis: a prospective, case series study. J Dermatol 2016;43:56–62.

5. Kuwana M, Okazaki Y, Yasuoka H, Kawakami Y, Ikeda Y. Defective vasculogenesis in systemic sclerosis. Lancet 2004;364:603–10.

6. Ogura K, Nara K, Watanabe Y, Kohno K, Tai T, Sanai Y. Cloning and expression of cDNA for O-acetylation of GD3 ganglioside. Biochem Biophys Res Commun 1993;225:932–8.

7. Stubbs JD, Lekutis C, Singer KL, Bui A, Yuzuki D, Srinivasan U, et al. cDNA cloning of a mouse mammary epithelial cell surface protein reveals the existence of epidermal growth factor-like domains linked to factor VIII-like sequences. Proc Natl Acad Sci U S A 1990;87:8417–21.

8. Andersen MH, Berglund L, Rasmussen JT, Peterson TE. Bovine PAS-6/7 binds α v β 5 integrins and anionic phospholipids through two domains. Biochemistry 1997;36:5441–6.

9. Atabai K, Jame S, Azhar N, Kuo A, Lam M, McKleroy W, et al. MFG-E8 diminishes the severity of tissue fibrosis in mice by binding and targeting collagen for uptake by macrophages. J Clin Invest 2009;119:3713–22.

10. Asano K, Miwa M, Miwa K, Hanayama R, Nagase H, Nagata S, et al. Masking of phosphatidylserine inhibits apoptotic cell engulfment and induces autoantibody production in mice. J Exp Med 2004;200:459–67.

11. Hanayama R, Tanaka M, Miwa K, Shinohara A, Iwamatsu A, Nagata S. Identification of a factor that links apoptotic cells to phagocytes. Nature 2002;417:182–7.

12. Jinushi M, Sato M, Kanamoto A, Itoh A, Nagai S, Koyasu S, et al. Milk fat globule epidermal growth factor-8 blockade triggers tumor destruction through coordinated cell-autonomous and immune-mediated mechanisms. J Exp Med 2009;206:1317–26.

13. Motegi S, Leitner WW, Lu M, Tada Y, Sárdy M, Wu C, et al. Pericyte-derived MFG-E8 regulates pathologic angiogenesis. Arterioscler Thromb Vasc Biol 2011;31:2024–34.

14. Motegi S, Ishikawa O. Mesenchymal stem cells: the roles and functions in cutaneous wound healing and tumor growth. J Dermatol Sci 2017;86:83–9.

15. Uchiyama A, Yamada K, Ogino S, Yokoyama Y, Takeuchi Y, Udey MC, et al. MFG-E8 regulates angiogenesis in cutaneous wound healing. Am J Pathol 2014;184:1981–90.

16. Uchiyama A, Yamada K, Perera B, Ogino S, Yokoyama Y, Takeuchi Y, et al. Protective effect of MFG-E8 after cutaneous ischemia-reperfusion injury. J Invest Dermatol 2015;135:1157–65.

17. Uchiyama A, Motegi S, Sekiguchi A, Fujiwara C, Perera B, Ogino S, et al. Mesenchymal stem cells-derived MFG-E8 accelerates diabetic cutaneous wound healing. J Dermatol Sci 2017;86:187–97.

18. Yamada K, Uchiyama A, Uehara A, Perera B, Ogino S, Yokoyama Y, et al. MFG-E8 drives melanoma growth by stimulating mesenchymal stromal cell-induced angiogenesis and M2 polarization of tumor-associated macrophages. Cancer Res 2016;76:4283–92.

19. An SY, Jang YJ, Lim HJ, Han J, Lee J, Lee G, et al. Milk fat globule-EGF factor 8, secreted by mesenchymal stem cells, protects against liver fibrosis in mice. Gastroenterology 2017;152:1174–86.

20. Kishi C, Motegi S, Ishikawa O. Elevated serum MFG-E8 level is possibly associated with the presence of high-intensity cerebral lesions on magnetic resonance imaging in patients with systemic lupus erythematosus. J Dermatol 2017;44:783–8.

21. Hanayama R, Tanaka M, Miyasaka K, Aozasa K, Koike M, Uchiyama Y, et al. Autoimmune disease and impaired uptake of apoptotic cells in MFG-E8-deficient mice. Science 2004;304:1147–50.

22. Albus E, Sinningen K, Winzer M, Thiele S, Baschant U, Hannemann A, et al. Milk fat globule-epidermal growth factor 8 (MFG-E8) is a novel anti-inflammatory factor in rheumatoid arthritis in mice and humans. J Bone Miner Res 2016;31:596–605.

23. Robertson IB, Rifkin DB. Unchaining the beast: insights from structural and evolutionary studies on TGFβ secretion, sequestration, and activation. Cytokine Growth Factor Rev 2013;24:355–72.

24. Henderson NC, Arnold TD, Katamura Y, Giacomini MM, Rodriguez JD, McCarty JH, et al. Targeting of αv integrin identifies a core molecular pathway that regulates fibrosis in several organs. Nat Med 2013;19:1617–24.

25. Asano Y, Ihn H, Yamane K, Jinnin M, Tamaki K. Increased expression of integrin αvβ5 induces the myofibroblastic differentiation of dermal fibroblasts. Am J Pathol 2006;168:499–510.

26. Gerber EE, Gallo EM, Fontana SC, Davis EC, Wigley FM, Huso DL, et al. Integrin-modulating therapy prevents fibrosis and autoimmunity in mouse models of scleroderma. Nature 2013;503:126–30.

27. Van den Hoogen F, Khanna D, Fransen J, Johnson SR, Baron M, Tyndall A, et al. 2013 classification criteria for systemic sclerosis: an American College of Rheumatology/European League Against Rheumatism collaborative initiative. Arthritis Rheum 2013;65: 2737–47.

28. LeRoy EC, Black C, Fleischmajer R, Jablonska S, Krieg T, Medsger TA Jr, et al. Scleroderma (systemic sclerosis): classification, subsets and pathogenesis. J Rheumatol 1988;15:202–5.

29. Clements P, Lachenbruch P, Seibold J, White B, Weiner S, Martin R, et al. Inter and intraobserver variability of total skin thickness score (modified Rodnan TSS) in systemic sclerosis. J Rheumatol 1995;22:1281–5.

30. Ashcroft T, Simpson JM, Timbrell V. Simple method of estimating severity of pulmonary fibrosis on a numerical scale. J Clin Pathol 1988;41:467–70.

31. Motegi S, Garfield S, Feng X, Sárdy M, Udey MC. Potentiation of platelet-derived growth factor receptor-β signaling mediated by integrin-associated MFG-E8. Arterioscler Thromb Vasc Biol 2011;31:2653–64.

32. Uehara A, Motegi S, Yamada K, Uchiyama A, Perera B, Toki S, et al. Mechanistic insight into the norepinephrine-induced fibrosis in systemic sclerosis. Sci Rep 2016;6:34012.

33. Yamamoto T, Takagawa S, Katayama I, Yamazaki K, Hamazaki Y, Shinkai H, et al. Animal model of sclerotic skin. I: local injections of bleomycin induce sclerotic skin mimicking scleroderma. J Invest Dermatol 1999;112:456–62.

34. Yokoyama Y, Sekiguchi A, Fujiwara C, Uchiyama A, Uehara A, Ogino S, et al. Inhibitory regulation of skin fibrosis in systemic sclerosis by apelin/APJ signaling. Arthritis Rheumatol 2018;70:1661–72.

35. Neutzner M, Lopez T, Feng X, Bergmann-Leitner ES, Leitner WW, Udey MC. MFG-E8/lactadherin promotes tumor growth in an angiogenesis-dependent transgenic mouse model of multistage carcinogenesis. Cancer Res 2007;67:6777–85.

36. Thoua NM, Derrett-Smith EC, Khan K, Dooley A, Shi-Wen X, Denton CP. Gut fibrosis with altered colonic contractility in a mouse model of scleroderma. Rheumatology (Oxford) 2012;51:1989–98.

37. Sato S, Hasegawa M, Fujimoto M, Tedder TF, Takehara K. Quantitative genetic variation in CD19 expression correlates with autoimmunity. J Immunol 2000;165:6635–43.

38. Pattanaik D, Brown M, Postlethwaite BC, Postlethwaite AE. Pathogenesis of systemic sclerosis. Front Immunol 2015;6:272.

39. Heng EC, Huang Y, Black SA Jr, Trackman PC. CCN2, connective tissue growth factor, stimulates collagen deposition by gingival fibroblasts via module 3 and α6- and β1 integrins. J Cell Biochem 2006;98:409–20.

40. Denton CP, Abraham DJ. Transforming growth factor-β and connective tissue growth factor: key cytokines in scleroderma pathogenesis. Curr Opin Rheumatol 2001;13:505–11.

41. Saito E, Fujimoto M, Hasegawa M, Komura K, Hamaguchi Y, Kaburagi Y, et al. CD19-dependent B lymphocyte signaling thresholds influence skin fibrosis and autoimmunity in the tight-skin mouse. J Clin Invest 2002;109:1453–62.

42. Siracusa LD, McGrath R, Ma Q, Moskow JJ, Manne J, Christner PJ, et al. A tandem duplication within the fibrillin 1 gene is associated with the mouse tight skin mutation. Genome Res 1996;6:300–13.

43. Yamamoto T. Animal model of systemic sclerosis. J Dermatol 2010;37:26–41.

44. Khan K, Xu S, Nihtyanova S, Derrett-Smith E, Abraham D, Denton CP, et al. Clinical and pathological significance of interleukin 6 overexpression in systemic sclerosis. Ann Rheum Dis 2012;71:1235–42.

45. Motegi S, Sekiguchi A, Fujiwara C, Toki S, Ishikawa O. Possible association of elevated serum collagen type IV level with skin sclerosis in systemic sclerosis. J Dermatol 2017;44:167–72.

46. Kudo M, Khalifeh Soltani SM, Sakuma SA, McKleroy W, Lee TH, Woodruff PG, et al. MFG-E8 suppresses airway hyperresponsiveness in asthma by regulating smooth muscle contraction. Proc Natl Acad Sci U S A 2013;110:660–5.

47. McGaha T, Saito S, Phelps RG, Gordon R, Noben-Trauth N, Paul WE, et al. Lack of skin fibrosis in tight skin (TSK) mice with targeted mutation in the interleukin-4R α and transforming growth factor-β genes. J Invest Dermatol 2001;116:136–43.

48. McGaha TL, Phelps RG, Spiera H, Bona C. Halofuginone, an inhibitor of type-I collagen synthesis and skin sclerosis, blocks transforming-growth-factor-β-mediated SMAD3 activation in fibroblasts. J Invest Dermatol 2002;118:461–70.

AMERICAN COLLEGE
OF RHEUMATOLOGY
EDUCATION · TREATMENT · RESEARCH

Presentation and Disease Course of Childhood-Onset Versus Adult-Onset Takayasu Arteritis

Florence A. Aeschlimann,[1] Lillian Barra,[2] Roaa Alsolaimani,[2] Susanne M. Benseler,[3] Diane Hebert,[1] Nader Khalidi,[4] Ronald M. Laxer,[1] Damien Noone,[1] Christian Pagnoux,[5] Marinka Twilt,[3] and Rae S. M. Yeung[1]

Objective. To compare the clinical features, efficacy and safety of treatment regimens, and outcomes of childhood- and adult-onset Takayasu arteritis (TAK).

Methods. The study was designed as a retrospective cohort study comparing patients with childhood-onset TAK (from 1986 onward) to patients with adult-onset TAK (from 1988 onward) who were followed up until 2014 or 2015 at 4 centers in Ontario, Canada. Demographic, clinical, laboratory, and angiographic features, treatment regimens, and outcomes were recorded throughout the course of the disease. Disease activity and damage scores were completed retrospectively.

Results. Twenty-nine children and 48 adults (median age at diagnosis 12.1 years and 31.2 years, respectively) were included. A lower predominance of females was observed among the childhood-onset TAK cohort (76% versus 100% of patients with adult-onset TAK; $P < 0.01$), and children had a shorter delay to diagnosis (median 6.0 months versus 12.2 months for adults; $P = 0.03$). The distribution of vascular involvement was also different, with children having significantly more aortic and renal artery involvement and a higher frequency of arterial hypertension. Relapses in the first year after diagnosis were common both in children (39%) and in adults (28%). Two children, but no adults, died.

Conclusion. Childhood-onset TAK has a lower female predominance and a higher frequency of aortic and renal involvement compared to adult-onset TAK. Relapses and disease burden were high in both groups, corroborating the need for careful monitoring of disease activity and aggressive therapeutic management.

INTRODUCTION

Takayasu arteritis (TAK) is an idiopathic granulomatous vasculitis of the aorta with its major branches predominantly affecting young women before the age of 40 years (1). In up to 30% of patients with TAK, the disease manifests for the first time in childhood (2–4). TAK is associated with a high morbidity and increased mortality in both children and adults (1,5,6). The clinical presentation of TAK is highly variable, reflecting the pattern of vascular involvement. Early in the disease course, symptoms may be nonspecific; thus, the diagnosis can be challenging and diagnostic delay is common (7,8).

Differences in disease expression of TAK between children and adults, including the sex ratio of affected patients,

the frequency of vascular involvement, and the disease course, have been reported (2,9). Patients with childhood-onset TAK and those with adult-onset TAK have been compared in China and Brazil (2,9). Given that geographic or ethnic variations in disease presentation have been reported (1), we investigated childhood-onset and adult-onset TAK cohorts in a North American population in order to compare disease features at the time of clinical presentation, the efficacy and safety of treatment regimens, and outcomes at follow-up.

PATIENTS AND METHODS

Design. The study was designed as a retrospective cohort study involving patients with TAK (all from Canada) who

[1]Florence A. Aeschlimann, MD, MPH, Diane Hebert, MD, Ronald M. Laxer, MD, Damien Noone, MB, BCh, BAO, MSc, Rae S. M. Yeung, MD, PhD: The Hospital for Sick Children and University of Toronto, Toronto, Ontario, Canada; [2]Lillian Barra, MD, MPH, Roaa Alsolaimani, MD: St. Joseph's Health Care London and University of Western Ontario, London, Ontario, Canada; [3]Susanne M. Benseler, MD, PhD, Marinka Twilt, MD, PhD: Alberta Children's Hospital and University of Calgary, Calgary, Alberta, Canada; [4]Nader Khalidi,

MD: St. Joseph's Healthcare and McMaster University, Hamilton, Ontario, Canada; [5]Christian Pagnoux, MD, MPH: Mount Sinai Hospital and University of Toronto, Toronto, Ontario, Canada.

Drs. Aeschlimann and Barra contributed equally to this work.

Address correspondence to Rae S. M. Yeung, MD, PhD, The Hospital for Sick Children, Division of Rheumatology, 555 University Avenue, Toronto, Ontario M5G 1X8, Canada. E-mail: rae.yeung@sickkids.ca.

were receiving care at the Hospital for Sick Children (SickKids, Toronto, Ontario), Mount Sinai Hospital (Toronto, Ontario), St. Joseph's Health Care (London, Ontario), or St. Joseph's Healthcare (Hamilton, Ontario). All of these participating institutions are tertiary care hospitals with specialty vasculitis centers.

All children with TAK who were followed up at the Hospital for Sick Children between 1986 and 2015 were identified from the institutional rheumatology database. All adult patients with TAK were included in the study beginning in 1988 (Mount Sinai Hospital) or 1990 (St. Joseph's Health Care, London and St. Joseph's Healthcare, Hamilton) up to 2014 if they had 1 baseline visit and at least 1 follow-up visit at any of the 3 centers. Two patients with childhood-onset TAK were diagnosed and followed up at adult centers, but were included in the pediatric cohort. Childhood-onset TAK was diagnosed in patients with a disease onset at age ≤18 years who met either the American College of Rheumatology (ACR) criteria for vasculitis (patients diagnosed prior to 2009) or the European League against Rheumatism (EULAR)/Pediatric Rheumatology International Trials Organization (PRINTO)/Pediatric Rheumatology European Society (PRES) classification criteria for TAK (patients diagnosed after 2009) (10–12). Adult-onset TAK was diagnosed in patients with a disease onset at age >18 years. Diagnosis was based on the ACR criteria for TAK or expert opinion (12).

The study was approved by the local institutional research ethics boards (REB approval numbers 1000012364, 102078, and 15-034-C).

Data collection. Data were collected separately from the pediatric and adult cohorts using standardized forms at the time of diagnosis, at 6 months' follow-up, at the time of relapse within the first year after diagnosis, and at the last follow-up. Data included demographic features, medical history, features of TAK at the time of clinical presentation, laboratory and imaging investigations, treatment (drugs and interventions), and adverse outcomes (defined as relapse, death, or complications). The location of vascular involvement was obtained from various angiographic studies, including conventional angiography, computed tomography angiography (CTA), and magnetic resonance angiography (MRA). Vascular lesions deemed indicative of active or worsening disease were defined as the occurrence of new or worsening narrowing, occlusion, aneurysm, dilatation, dissection, or both vessel wall thickening and post–contrast enhancement of vessel wall inflammation.

Results of vascular imaging were recorded when performed within 1 month of the predefined data collection time points for children and within 3 months for adults. Complications included the following: 1) events related to disease activity, such as stroke, blindness, cardiac involvement (myocardial infarction, congestive heart failure, cor pulmonale, aortic coarctation, and aortic valve/aneurysm repair), end-stage ischemic limb, renal complications (end-stage renal disease, nephrectomy), and mesenteric ischemia; 2) medication-related events, such as severe infections, defined as infections that are life-threatening or

requiring hospital admission, drug-induced hepatitis requiring discontinuation of the drug, and allergic drug reaction; and 3) events resulting from atherosclerosis (in adult patients with TAK), which may have been related to chronic systemic inflammation or other risk factors for cardiovascular disease.

Age-specific definitions were used for arterial hypertension, hemoglobin levels, and creatinine levels. Arterial hypertension was defined as blood pressure ≥95th percentile for age in children, and a systolic blood pressure of ≥140 mm Hg in adults. A blood pressure discrepancy of ≥10 mm Hg between limbs was considered abnormal both in children and in adults. In children, abnormal hemoglobin and creatinine levels were based on age-specific limits provided by the institution's laboratory. A hemoglobin level of ≤110 gm/liter and creatinine level of ≥120 μmoles/liter was considered abnormal in adults. The types of assays and normal ranges for the level of C-reactive protein (CRP) varied between sites and over the course of the study, and therefore median CRP values could not be reported.

Assessment of disease relapse, activity, and inactivity. The presence of relapse, active disease, and inactive disease was retrospectively assessed (by FAA and SMB in patients with childhood-onset TAK; by LB and RA in patients with adult-onset TAK). For both groups, disease relapse was defined as the occurrence of new or worsening clinical symptoms attributable to TAK. Relapse also included a new or worsening lesion identified on vascular imaging, which was usually performed in a patient because clinical symptoms were present or acute-phase reactant levels were increased. Active disease was defined as ongoing clinical symptoms and/or elevation of acute-phase reactant levels attributable to TAK (and not explained otherwise), as was determined by the treating physician. In children, active disease was also diagnosed based on vascular imaging findings alone (vessel wall inflammation, based on both post–contrast enhancement and vessel wall thickening), whereas vascular imaging was not necessarily performed in asymptomatic adults. Inactive disease was defined as the absence of symptoms attributable to active vasculitis, normal acute-phase reactant levels, and the absence of imaging findings of active disease (as defined above).

Disease activity was additionally assessed using the validated Pediatric Vasculitis Disease Activity Score (PVAS) in children or Birmingham Vasculitis Activity Score (BVAS) in adults (13,14), as well as the 2010 Indian Takayasu Arteritis Clinical Activity Score (ITAS2010) (15). The ITAS2010 is a disease activity measurement tool that captures clinical manifestations attributable to TAK that were new or worse within the 3 months prior to clinical presentation (15). Although the ITAS2010 has been specifically developed to assess disease activity in patients with TAK, it has not been validated in children (15).

The PVAS was completed prospectively during each patient's visits since 2009. For visits before 2009, the PVAS was retrospectively assessed by 2 independent reviewers (FAA and SMB). The

BVAS was retrospectively scored in all adults (by LB and RA or by CP or NK), and the ITAS2010 was assessed both in children (by FAA and SMB) and in adults (by LB and RA or by CP or NK) (15).

Disease damage was evaluated retrospectively using the Pediatric Vasculitis Damage Index (PVDI) in children or the Vasculitis Damage Index (VDI) in adults (16). The PVDI and VDI are disease damage assessment tools that capture irreversible cumulative disease- and treatment-related damage that has been present for more than 3 months (16). For the purpose of this study, only items caused by the disease itself were included.

Statistical analysis. Statistical analyses were performed using SAS version 9.4 (SAS Institute). Categorical variables were presented as frequencies, and groups were compared using Fisher's exact test. Odds ratios (ORs) and their 95% confidence intervals (95% CIs) were computed. Continuous variables were reported as median values with interquartile ranges (IQRs) and compared using the Wilcoxon rank sum test. Trajectories of disease activity (PVAS/BVAS and ITAS2010 scores) were analyzed using linear mixed-effects models. Missing data were not included in the analyses (no imputations for missing data were performed). P values less than 0.05 were considered significant.

RESULTS

Characteristics of the study population at the time of TAK diagnosis. The study included 29 patients with childhood-onset TAK and 48 patients with adult-onset TAK. All of the patients with childhood-onset TAK met the EULAR/PRINTO/PRES classification criteria for childhood TAK. Two adult patients did not fulfill the ACR criteria for TAK but were diagnosed based on expert opinion, including a 22-year-old woman who presented with myocardial infarction and elevated inflammation markers and who had ascending aortic wall thickening and post–contrast enhancement of vessel wall inflammation evident on MRA, and a 47-year-old woman with carotidynia, weight loss, a subclavian bruit with an elevation in the erythrocyte sedimentation rate, and imaging findings consistent with TAK (subclavian stenosis and aortic wall thickening without significant atherosclerosis). Seven of the patients with childhood-onset TAK (24%) were male, while all of the adult patients were female (P < 0.01). The duration from the time of symptom onset to diagnosis was shorter in children compared to adults (median 6.0 months versus 12.2 months; P = 0.03). An overview of the patients' demographic and clinical features is presented in Table 1.

The clinical and laboratory features of the enrolled patients at the time of diagnosis are summarized in Table 2. Fewer children

Table 1. Demographic and clinical characteristics at the time of diagnosis in the childhood-onset and adult-onset TAK cohorts*

Feature	Childhood-onset TAK (n = 29)	Adult-onset TAK (n = 48)
Female	22 (76)	48 (100)†
Age at diagnosis, median (IQR) years	12.1 (9.8–13.8)	31.2 (26.9–40.1)
Age at symptom onset, median (IQR) years	10.8 (9.4–13.1)	26.9 (22.0–36.3)
Diagnostic delay, median (IQR) months	6.0 (3.0–13.2)	12.2 (4.5–36.5)‡
Follow-up duration, median (IQR) years	2.6 (1.8–6.4)	3.9 (2.3–6.6)
Race or ethnicity		
Caucasian	9 (31)	20 (42)
Asian	4 (14)	4 (8)
Black	3 (10)	3 (6)
Indian	2 (7)	9 (19)
Hispanic	2 (7)	3 (6)
First Nations	2 (7)	0
Middle Eastern	2 (7)	1 (2)
Not available	5 (17)	8 (17)
Comorbidity		
Inflammatory bowel disease	2 (7)	6 (13)
Rheumatic disease§	2 (7)	2 (4)
Cardiovascular disease	0	3 (6)
Tuberculosis	3 (10)	1 (2)

* Except where indicated otherwise, values are the number (%) of patients. IQR = interquartile range.
† P < 0.01 versus childhood-onset Takayasu arteritis (TAK).
‡ P = 0.03 versus childhood-onset TAK.
§ Rheumatic diseases included IgA vasculitis, psoriatic arthritis, rheumatoid arthritis, and systemic lupus erythematosus.

Table 2. Clinical presentation and laboratory characteristics at the time of diagnosis in the childhood-onset and adult-onset TAK cohorts*

Presenting feature	Childhood-onset TAK (n = 29)	Adult-onset TAK (n = 48)	P	OR (95% CI)
Constitutional				
Malaise	14 (48)	21 (44)	0.81	–
Weight loss	8 (28)	7 (15)	0.24	–
Fever	5 (17)	5 (10)	0.49	–
Night sweats	1 (3)	5 (10)	0.40	–
Lymphadenopathy	3 (10)	2 (4)	0.36	–
Cardiovascular				
Claudication of the extremities	6 (21)	22 (46)	0.03	0.31 (0.11–0.89)
Lower extremities	5 (17)	6 (13)	0.74	–
Upper extremities	1 (3)	20 (42)	<0.01	0.05 (0.01–0.40)
Decreased or absent pulse	17 (59)	34 (71)	0.32	–
Both lower extremities	12 (41)	1 (2)	<0.01	33.18 (4.01–274.76)
Both upper extremities	0	13 (27)	<0.01	–
Limb ischemia	1 (3)	6 (13)	0.24	–
Bruits	17 (59)	29 (60)	1.00	–
Blood pressure discrepancy	20/23 (87)	31/47 (66)	0.09	–
Carotidynia	1 (3)	8 (17)	0.14	–
Angina	2 (7)	2 (4)	0.63	–
Myocardial infarction	2 (7)	2 (4)	0.63	–
Neurologic				
Headache	11 (38)	10 (21)	0.12	–
Dizziness	5 (17)	4 (8)	0.28	–
Stroke/TIA	3 (10)	3 (6)	0.67	–
Syncope	4 (14)	4 (8)	0.47	–
Seizure	2 (7)	1 (2)	0.55	–
Gastrointestinal				
Nonspecific abdominal pain	4 (14)	3 (6)	0.42	–
Ischemic abdominal pain	2 (7)	0	0.14	–
Renal				
Arterial hypertension	17 (59)	15 (31)	0.03	3.12 (1.20–8.13)
Pulmonary				
Chest pain	3 (10)	11 (23)	0.23	–
Shortness of breath	4 (14)	7 (15)	0.99	–
Cutaneous	2 (7)	11 (23)	0.11	–
Ocular	5 (17)	6 (13)	0.74	–
Musculoskeletal				
Arthritis/arthralgias	2 (7)	14 (29)	0.02	0.18 (0.04–0.86)
Laboratory features				
Elevated ESR	21/26 (81)	36/46 (78)	0.99	–
ESR, median (IQR) mm/hour	35 (18–64)	45 (30–55)	0.86	–
Elevated CRP	15/20 (75)	28/38 (74)	0.99	–
Anemia	20/28 (71)	18/34 (53)	0.19	–
Increased creatinine level	2/24 (8)	1/33 (3)	0.57	–

* Except where indicated otherwise, values are the number (%) of patients or the number/total number assessed (%). Odds ratios (ORs) with 95% confidence intervals (95% CIs) are presented for those features that were significantly different (*P* < 0.05) in children compared to adults. TAK = Takayasu arteritis; TIA = transient ischemic attack; ESR = erythrocyte sedimentation rate; IQR = interquartile range.

had claudication of the extremities, specifically the upper extremities, compared to adults. However, children were more likely to have decreased pulses of the lower extremities ($P < 0.01$). Arterial hypertension was more frequent, and arthritis/arthralgias were less frequent, in children compared to adults.

All subjects underwent vascular imaging prior to or at the time of diagnosis. The type of imaging modality used differed between the 2 groups (Table 3). Involvement of the aorta and renal arteries was more common in children. These differences were not significantly associated with ethnicity (data not shown). Cardiac investigations were inconsistently performed. Electro-

cardiography revealed atrial or ventricular hypertrophy in 6 of the 20 children assessed compared to none of the 20 adults assessed ($P = 0.02$); 4 of 15 children had structural defects evident on echocardiogram, such as left ventricular hypertrophy, as compared to none of the 24 adults assessed ($P = 0.02$).

Medical treatments and vascular interventions. At the time of diagnosis, 24 (83%) of 29 children were deemed to have active disease compared to 39 (81%) of 48 adults ($P = 0.74$), and these children were started on a treatment regimen with immunosuppressive agents. The disease activity scores at the time of diagnosis and over follow-up are presented in Table 4.

Various treatment regimens were prescribed for induction of remission (Table 5). Compared to adults, fewer children received glucocorticoids alone, but more often received glucocorticoids in combination with methotrexate or glucocorticoids in combination with cyclophosphamide. There was no significant difference in the prescription of other immunosuppressive or biologic therapies. The disease activity scores in children and adults did not differ between any of the treatment groups (data not shown).

Antiplatelet treatment was prescribed in 16 (55%) of 29 children and 29 (62%) of 47 adults ($P = 0.64$). Anticoagulation therapy was given to 6 (21%) of 29 children and 3 (6%) of 47 adults ($P = 0.08$). More children than adults received antihypertensive drugs (66% versus 28% of adults; $P < 0.01$). No difference between children and adults was found in the prescription patterns of calcium and vitamin D (17 of 29 children and 23 of 48 adults) or lipid-lowering agents (0 of 29 children and 4 of 48 adults).

Vascular interventions at the time of disease presentation or diagnosis were performed with similar frequency in children (7 interventions in 6 of 29 children) and adults (13 interventions in 12 of 48 adults), including stenting (0 of 29 children and 6 of 48 adults), embolectomy (1 child and 1 adult), valve repair (0 children

Table 3. Imaging modality used and site of vascular involvement at the time of diagnosis in children and adults with TAK*

	Childhood-onset TAK (n = 29)	Adult-onset TAK (n = 48)
Imaging modality		
Conventional angiography	9 (31)	2 (4)†
MRA	11 (38)	14 (29)†
CTA	5 (17)	20 (42)†
MRA and CTA	1 (3)	9 (19)†
Various imaging combinations	3 (10)	3 (6)†
Vascular site		
Aorta (arch, thoracic, or abdominal)	28/29 (97)‡	35 (73)†
Carotid artery	14/26 (54)	31 (65)
Vertebral artery	4/24 (17)	11 (23)
Subclavian artery	13/25 (52)	36 (75)
Coronary artery	3/25 (12)	5 (10)
Pulmonary artery	4/25 (16)	5 (10)
Central nervous system artery	1/18 (6)	2 (4)
Splanchnic vessels	14/26 (54)	15 (31)
Renal artery	21/29 (72)§	14 (29)†
Iliac artery	7/23 (30)	NA¶

* Frequencies of paired arteries (right/left) are presented as one combined value. Values are the number (%) of patients or the number/total number assessed (%). For the childhood-onset Takayasu arteritis (TAK) cohort, the number of children with available information is presented per individual vessels. MRA = magnetic resonance angiography; CTA = computed tomography angiography.
† $P < 0.01$ versus childhood-onset TAK.
‡ Odds ratio (OR) 10.40 (95% confidence interval [95% CI] 1.28–84.40) for likelihood of specific vascular site involvement in children compared to adults.
§ OR 6.38 (95% CI 2.29–17.77) for likelihood of specific vascular site involvement in children compared to adults.
¶ Imaging for iliac artery involvement was inconsistently performed in adults, and therefore data were not available (NA) for the adult-onset TAK cohort.

Table 4. Disease activity scores at baseline, 6 months, and last follow-up in children and adults with TAK*

	Childhood-onset TAK (n = 29)	Adult-onset TAK (n = 48)
PVAS/BVAS		
At baseline	10 (7–17)	3 (2–4)
At 6 months	0 (0–0)	1 (0–2)
At last follow-up	0 (0–0)	0 (0–0)
ITAS2010		
At baseline	12 (7–15)	10 (7–12)
At 6 months	0 (0–3)	0 (0–2)
At last follow-up	0 (0–0)	0 (0–0)

* Values are the median (interquartile range). The Pediatric Vasculitis Disease Activity Score (PVAS) in children and Birmingham Vasculitis Activity Score (BVAS) in adults have a score range of 0–63. The 2010 Indian Takayasu Arteritis Clinical Activity Score (ITAS2010) ranges from 0 to 51. TAK = Takayasu arteritis.

Table 5. Treatment regimens at baseline, 6 months, and last follow-up in children and adults with TAK*

Treatment	At diagnosis			6-months' follow-up			Last follow-up		
	Children (n = 29)	Adults (n = 48)	P	Children (n = 25)	Adults (n = 47)	P	Children (n = 27)	Adults (n = 41)	P
No immunosuppression	5 (17)	9 (19)	0.99	4 (16)	6 (13)	0.73	6 (22)	12 (29)	0.58
GC only	5 (17)	24 (50)	<0.01†	3 (12)	12 (26)	0.23	1 (4)	8 (20)	0.08
GC + CYC	5 (17)	1 (2)	0.03‡	1 (4)	1 (2)	0.99	1 (4)	0	0.40
GC + MTX	11 (38)	7 (15)	0.03§	12 (48)	19 (40)	0.62	5 (19)	9 (22)	0.99
GC + anti-TNF¶	3 (10)	0	0.05	3 (12)	2 (4)	0.33	8 (30)	2 (5)	0.01#
GC + AZA**	0	6 (13)	0.08	2 (8)	7 (15)	0.48	3 (11)	3 (7)	0.68
GC + MMF**	0	1 (2)	0.99	0	0	NA	1 (4)	1 (2)	0.99
GC + ABA	0	0	NA	0	0	NA	0	1 (2)	NA
GC + LEF	0	0	NA	0	0	NA	0	3 (7)	0.27
GC + TCZ¶	0	0	NA	0	0	NA	2 (7)	2 (5)	0.99

* Values are the number (%) of patients. CYC = cyclophosphamide; MMF = mycophenylate mofetil; NA = not applicable; ABA = abatacept; TCZ = tocilizumab.
† Odds ratio (OR) 0.25 (95% confidence interval [95% CI] 0.08–0.75) for the likelihood of receiving the specific treatment.
‡ OR 9.79 (95% CI 1.08–88.60) for the likelihood of receiving the specific treatment.
§ OR 3.58 (95% CI 1.19–10.73) for the likelihood of receiving the specific treatment.
¶ All patients received another immunosuppressive agent in addition to the anti–tumor necrosis factor (anti-TNF) inhibitor: either methotrexate (MTX), leflunomide (LEF), or azathioprine (AZA).
# OR 8.21 (95% CI 1.59–42.48) for the likelihood of receiving the specific treatment.
** At last follow-up, 1 adult patient was additionally treated with MTX. At the 6-month follow-up, the median glucocorticoid (GC) dose was 0.38 mg/kg/day (interquartile range [IQR] 0.28–0.72) for children and 20 mg/day (IQR 10–35) for adults; at last follow-up, children were receiving glucocorticoid treatment at a median dose of 0.21 mg/kg/day (IQR 0.09–0.35), while adults were receiving a median glucocorticoid dose of 5 mg/day prednisone equivalent (IQR 5–5). Over the study period, the use of biologic agents increased: 27% of the children and 8% of adults were diagnosed as having Takayasu arteritis (TAK) prior to the year 2000 (none treated with biologic agents during this time), and 48% of children and 52% of adults were diagnosed between 2000 and 2009, of whom 36% of children compared to 16% of adults were treated with biologic agents (P = 0.24); the remaining patients were diagnosed between 2010 and 2015 and of these, 86% of children compared to 21% of adults were treated with biologic agents (P < 0.01).

and 3 adults), angioplasty (3 children and 1 adult), and bypass grafting (axillary femoral and renal vasculature bypass grafting in 1 child each and coronary bypass grafting in 2 adults). The vessels on which vascular interventions were most frequently performed were the renal arteries in children (3 of 7 procedures), and the coronary arteries in adults (5 of 13 procedures).

Disease course. In total, 11 (46%) of 24 children and 29 (74%) of 39 adults who had active disease at baseline did not have active disease at 6 months' follow-up (P = 0.22). Disease activity scores decreased from the time of diagnosis to 6 months (Table 4). Repeat imaging at 6 months of follow-up was available for 8 of 24 children and 17 of 39 adults. Among the 8 children assessed over 6 months, the imaging findings remained unchanged in 5 patients, and new lesions became apparent in 3 patients. Among the 17 adults assessed over 6 months, imaging findings indicated improvement in disease activity in 3 patients, remained unchanged in 5 patients, and showed new lesions in 9 patients. At 6 months, 21 (80%) of 25 children and 41 (85%) of 47 adults remained on treatment with glucocorticoids with or without another immunosuppressive agent (Table 5).

During the 12-month period after diagnosis, relapses were observed in a total of 11 (39%) of 28 surviving children and 13

(28%) of 47 adults (P = 0.32). Children were more likely to experience a disease relapse with constitutional symptoms, while the most common symptoms of relapse in adults were headaches and carotidynia. Major complications within the first year after diagnosis were equally common among the 2 groups. Stroke occurred in 3 children (10%) and 3 adults (6%). Blindness developed in 1 child (3%) and 1 adult (2%). Cardiac complications were documented in 3 children (10%) and 9 adults (19%). Severe limb ischemia was found in none of the children, but in 3 adult patients (6%). End-stage renal disease or nephrectomy occurred in 2 children (7%) and 2 adults (4%). Severe infections were more common in children (17% versus 2% of adults; OR 9.58, 95% CI 1.06–85.75). No statistically significant difference was found in the frequency of drug-induced hepatitis or allergic drug reactions.

Two children (7%) died within a few months after diagnosis: a 13-year-old girl died of uncontrollable disease and a left middle cerebral arterial infarction resulting from a ventricular thrombus and multiorgan failure 12 days after diagnosis, and a 4-year-old boy died 4 months after diagnosis following a disease flare with massive intestinal ischemia. None of the adult patients died.

At last follow-up (median 2.6 years in children and 3.9 years in adults), 18 (67%) of 27 children and 36 (88%) of 41 adults were considered to have inactive disease (P = 0.06). There were

no further deaths. None of the children, but 15 of 41 patients with adult-onset TAK had repeat imaging available at last follow-up. Among these adult patients, the imaging findings remained unchanged from those obtained previously in 11 patients, had improved in 2 patients, and had worsened with occurrence of new lesions in 2 patients.

Furthermore, at last follow-up, 21 (81%) of 26 children and 29 (71%) of 41 adults were taking glucocorticoids alone or in combination with another immunosuppressive drug (Table 5). More children than adults were receiving treatment with tumor necrosis factor (TNF) inhibitors at last follow-up; due to the small sample size, this analysis could not be adjusted for the duration of follow-up. No statistically significant difference was found in the prescription of other immunosuppressive medications.

Accrued disease damage was more severe in children than in adults. The PVDI in children was a median score of 4 (IQR 3–6), whereas the VDI in adults was a median score of 2 (IQR 2–3) (the maximum cumulative scores for the PVDI and VDI are 68 and 59 points, respectively).

DISCUSSION

This is the first study to describe the presentation and disease course of childhood-onset and adult-onset TAK in North America. We found that there were fewer female patients in the childhood-onset TAK cohort. Moreover, children more frequently had vascular involvement of the aorta and renal arteries, and arterial hypertension at presentation. In contrast, adults more commonly presented with vascular involvement of the subclavian arteries, claudication, and decreased pulses of the upper extremities as well as arthritis/arthralgias.

Disease burden was high in both groups. Relapses during the first year after diagnosis were common in children (39%) and adults (28%). Two children died within a few months after diagnosis. At 6 months and last follow-up, children were more likely to have active disease and to be treated with TNF inhibitors.

There was a higher proportion of male patients in the childhood-onset TAK cohort. It has been reported that in some ethnicities, there is a higher proportion of male patients than female patients with TAK (17,18), but the difference in the affected sex ratio that we observed between children and adults was not attributable to ethnicity (data not shown). A similar lower female predominance has been reported previously in some studies of childhood-onset TAK compared to adult TAK cohorts (2,9). Lower proportions of female patients have also been reported in other childhood-onset inflammatory and autoimmune diseases, where the affected sex ratio difference has been attributed to differences in hormone status (19,20). However, to our knowledge, possible underlying causal mechanisms of this sex ratio difference have not yet been investigated. In TAK, the available data are inconclusive, because other large TAK cohort studies did not find an age-related predominance of the disease in either sex (4,21).

We documented a heterogeneous clinical phenotype in both cohorts, reflecting the variable underlying pattern of vascular inflammation. Children more frequently presented with vasculitis of the large branches of the abdominal aorta, including renal artery lesions, contributing to increased arterial hypertension, which is similar to the results of a Brazilian study comparing childhood-onset and adult-onset TAK (9). In other pediatric TAK series (5–7), including 1 cohort from North America (22), high frequencies of hypertension have been reported, and the presence of arterial hypertension has previously been associated with unfavorable outcomes in TAK (7,18). Thus, recognition and appropriate management of arterial hypertension is critical.

Adults in our TAK cohort, on the other hand, more frequently presented with subclavian artery lesions, claudication, and decreased pulses of the upper extremities. Our findings are consistent with data from previous studies, in which high proportions of upper extremity involvement were reported in adult patients with TAK who were predominantly white (9,23–25). It has previously been hypothesized that the arterial disease begins in the left subclavian artery and subsequently extends to other sites (26). However, subclavian artery lesions were documented in only about one-half of the childhood-onset TAK cohort, and therefore may not necessarily represent the initial location of vascular inflammation in all TAK patients.

In children, the diagnostic delay was shorter than that observed in adults. Potential reasons for this discrepancy are differences in the type and severity of symptoms, as well as attitudes of patients and physicians toward symptoms. Many of the early symptoms of TAK are nonspecific. For example, neck and limb pain in adults may be attributed to mechanical or degenerative musculoskeletal disease, and adults may be less likely than children to seek out medical attention. Adults are more likely than children to present with arthritis, of which the differential diagnosis is broad and includes conditions that are much more common than TAK. Conversely, children who are more likely to have TAK involvement below the diaphragm commonly present with hypertension, prompting further investigations for secondary causes, which can identify the inflammatory vascular disease. In adults, vascular disease and its complications may be attributed to other causes or comorbidities, including hypertension, diabetes, smoking-related vascular disease, or atherosclerosis. In our study, children had higher disease activity scores at presentation compared to adults, suggesting a more widespread and/or severe disease. However, the components of these scores are different in the pediatric and adult versions, and therefore preclude direct comparison.

Children less frequently achieved inactive disease both at 6 months (46% versus 74% of adults) and at last follow-up (67% versus 88% of adults), and had a nominally higher frequency of death (7% versus none of the adults) and frequency of relapse (39% versus 28% of adults) during the first year after diagnosis. The components of composite disease activity scores

(PVAS and BVAS) are different in the pediatric and adult versions, and therefore cannot be directly compared. More severe and refractory disease in childhood-onset TAK has been reported by Jales-Neto et al (9) and in other autoimmune diseases with onset in childhood (27). It is possible that some of the underlying pathogenic mechanisms in children are different from those in adults (28). Various studies have shown the critical role of specific cytokine profiles and immunologic pathways in the promotion of vascular inflammation and disease activity in patients with TAK (29,30). Furthermore, genetic factors are known to play an important role in the pathophysiology of TAK (31–33). However, none of these potential causes underlying the differences in disease activity between children and adults with TAK have yet been evaluated in comparative studies. To summarize, we found some differences between the 2 cohorts that could be suggestive of a more severe disease course in children, but these differences were not statistically significant.

Treatment regimens for initial induction of remission were different between children and adults. Whereas adults were most often treated with systemic glucocorticoids alone, children received systemic glucocorticoids in combination with methotrexate or cyclophosphamide. In addition, anti-TNF therapy at follow-up was more commonly given to children than to adults. These differences in treatment may reflect differences in the clinical characteristics, disease severity, and physician's and patient's preferences, as well as the lack of treatment guidelines for TAK or the difficulties in accessing certain drugs.

This study is limited by its retrospective design, with its associated biases and missing data. The cohorts were designed and the data collected separately; therefore, some variables were not identical. The sample size was small and findings were descriptive. The study lacked power to detect more subtle differences. Because the study involved multiple comparisons, false-positive results were possible, and multivariable analyses to determine predictors of outcomes could not be performed due to the sample size. Nevertheless, this pediatric cohort represents one of the largest reported worldwide.

Diagnosis and monitoring of disease activity remains challenging in TAK, as disease-specific biomarkers are lacking and noninvasive imaging modalities, such as MRA and CTA, have a limited ability to accurately assess vessel wall inflammation. In adults, differentiating between TAK-related ischemic complications and atherosclerotic complications is difficult. Finally, given the frequently observed diagnostic delay, some patients classified as having adult-onset TAK may have had disease onset in childhood.

In conclusion, childhood-onset TAK was characterized by a lower female predominance and a higher frequency of renal involvement and arterial hypertension, while adults more commonly presented with involvement of the subclavian arteries, upper extremity symptoms, and arthritis/arthralgias. Larger studies are needed to confirm these differences. The frequency of relapses and the disease burden were high in both groups, corroborating

the need for careful monitoring of disease activity and aggressive therapeutic management in order to prevent mortality and long-term morbidity. The optimal methods for monitoring and treating patients with TAK will require further study.

ACKNOWLEDGMENT

AUTHOR CONTRIBUTIONS

All authors were involved in drafting the article or revising it critically for important intellectual content, and all authors approved the final version to be published. Dr. Yeung had full access to all of the data in the study and takes responsibility for the integrity of the data and the accuracy of the data analysis.
Study conception and design. Aeschlimann, Barra, Alsolaimani, Benseler, Hebert, Khalidi, Laxer, Noone, Pagnoux, Twilt, Yeung.
Acquisition of data. Aeschlimann, Barra, Alsolaimani, Benseler, Hebert, Khalidi, Laxer, Noone, Pagnoux, Twilt, Yeung.
Analysis and interpretation of data. Aeschlimann, Barra, Alsolaimani, Benseler, Hebert, Khalidi, Laxer, Noone, Pagnoux, Twilt, Yeung.

REFERENCES

1. Mason JC. Takayasu arteritis–advances in diagnosis and management. Nat Rev Rheumatol 2010;6:406–15.
2. Cong XL, Dai SM, Feng X, Wang ZW, Lu QS, Yuan LX, et al. Takayasu's arteritis: clinical features and outcomes of 125 patients in China. Clin Rheumatol 2010;29:973–81.
3. Kerr GS, Hallahan CW, Giordano J, Leavitt RY, Fauci AS, Rottem M, et al. Takayasu arteritis. Ann Intern Med 1994;120:919–29.
4. Watanabe Y, Miyata T, Tanemoto K. Current clinical features of new patients with Takayasu arteritis observed from cross-country research in Japan: age and sex specificity. Circulation 2015;132:1701–9.
5. Eleftheriou D, Varnier G, Dolezalova P, McMahon AM, Al-Obaidi M, Brogan PA. Takayasu arteritis in childhood: retrospective experience from a tertiary referral centre in the United Kingdom. Arthritis Res Ther 2015;17:36.
6. Goel R, Kumar TS, Danda D, Joseph G, Jeyaseelan V, Surin AK, et al. Childhood-onset Takayasu arteritis–experience from a tertiary care center in South India. J Rheumatol 2014;41:1183–9.
7. Brunner J, Feldman BM, Tyrrell PN, Kuemmerle-Deschner JB, Zimmerhackl LB, Gassner I, et al. Takayasu arteritis in children and adolescents. Rheumatology (Oxford) 2010;49:1806–14.
8. Terao C, Yoshifuji H, Mimori T. Recent advances in Takayasu arteritis. Int J Rheum Dis 2014;17:238–47.
9. Jales-Neto LH, Levy-Neto M, Bonfa E, de Carvalho JF, Pereira RM. Juvenile-onset Takayasu arteritis: peculiar vascular involvement and more refractory disease. Scand J Rheumatol 2010;39:506–10.
10. Bloch DA, Michel BA, Hunder GG, McShane DJ, Arend WP, Calabrese LH, et al. The American College of Rheumatology 1990 criteria for the classification of vasculitis: patients and methods. Arthritis Rheum 1990;33:1068–73.
11. Ozen S, Pistorio A, Iusan SM, Bakkaloglu A, Herlin T, Brik R, et al. EULAR/PRINTO/PRES criteria for Henoch–Schönlein purpura, childhood polyarteritis nodosa, childhood Wegener granulomatosis and childhood Takayasu arteritis: Ankara 2008. Part II: final classification criteria. Ann Rheum Dis 2010;69:798–806.
12. Arend WP, Michel BA, Bloch DA, Hunder GG, Calabrese LH, Edworthy SM, et al. The American College of Rheumatology 1990

criteria for the classification of Takayasu arteritis. Arthritis Rheum 1990;33:1129–34.

13. Dolezalova P, Price-Kuehne FE, Ozen S, Benseler SM, Cabral DA, Anton J, et al. Disease activity assessment in childhood vasculitis: development and preliminary validation of the Paediatric Vasculitis Activity Score (PVAS). Ann Rheum Dis 2013;72:1628–33.

14. Luqmani RA, Bacon PA, Moots RJ, Janssen BA, Pall A, Emery P, et al. Birmingham Vasculitis Activity Score (BVAS) in systemic necrotizing vasculitis. QJM 1994;87:671–8.

15. Misra R, Danda D, Rajappa SM, Ghosh A, Gupta R, Mahendranath KM, et al. Development and initial validation of the Indian Takayasu Clinical Activity Score (ITAS2010). Rheumatology (Oxford) 2013;52:1795–801.

16. Exley AR, Bacon PA, Luqmani RA, Kitas GD, Gordon C, Savage CO, et al. Development and initial validation of the Vasculitis Damage Index for the standardized clinical assessment of damage in the systemic vasculitides. Arthritis Rheum 1997;40:371–80.

17. Mwipatayi BP, Jeffery PC, Beningfield SJ, Matley PJ, Naidoo NG, Kalla AA, et al. Takayasu arteritis: clinical features and management: report of 272 cases. ANZ J Surg 2005;75:110–7.

18. Subramanyan R, Joy J, Balakrishnan KG. Natural history of aortoarteritis (Takayasu's disease). Circulation 1989;80:429–37.

19. Mina R, Brunner HI. Pediatric lupus—are there differences in presentation, genetics, response to therapy, and damage accrual compared with adult lupus? Rheum Dis Clin North Am 2010;36:53–80.

20. Haliloglu G, Anlar B, Aysun S, Topcu M, Topaloglu H, Turanli G, et al. Gender prevalence in childhood multiple sclerosis and myasthenia gravis. J Child Neurol 2002;17:390–2.

21. Mont'Alverne AR, Paula LE, Shinjo SK. Features of the onset of Takayasu's arteritis according to gender. Arq Bras Cardiol 2013;101:359–63.

22. Szugye HS, Zeft AS, Spalding SJ. Takayasu arteritis in the pediatric population: a contemporary United States-based single center cohort. Pediatr Rheumatol Online J 2014;12:21.

23. Hoffman GS. Takayasu arteritis: lessons from the American National Institutes of Health experience. Int J Cardiol 1996;54 Suppl:S99–102.

24. Schmidt J, Kermani TA, Bacani AK, Crowson CS, Cooper LT, Matteson EL, et al. Diagnostic features, treatment, and outcomes of Takayasu arteritis in a US cohort of 126 patients. Mayo Clin Proc 2013;88:822–30.

25. Arnaud L, Haroche J, Limal N, Toledano D, Gambotti L, Costedoat Chalumeau N, et al. Takayasu arteritis in France: a single-center retrospective study of 82 cases comparing white, North African, and black patients. Medicine (Baltimore) 2010;89:1–17.

26. Ishikawa K. Diagnostic approach and proposed criteria for the clinical diagnosis of Takayasu's arteriopathy. J Am Coll Cardiol 1988;12:964–72.

27. Mina R, Brunner HI. Update on differences between childhood-onset and adult-onset systemic lupus erythematosus. Arthritis Res Ther 2013;15:218.

28. Lopez De Padilla CM, Crowson CS, Hein MS, Pendegraft RS, Strausbauch MA, Niewold TB, et al. Gene expression profiling in blood and affected muscle tissues reveals differential activation pathways in patients with new-onset juvenile and adult dermatomyositis. J Rheumatol 2017;44:117–24.

29. Fukui S, Iwamoto N, Shimizu T, Umeda M, Nishino A, Koga T, et al. Fewer subsequent relapses and lower levels of IL-17 in Takayasu arteritis developed after the age of 40 years. Arthritis Res Ther 2016;18:293.

30. Saadoun D, Garrido M, Comarmond C, Desbois AC, Domont F, Savey L, et al. Th1 and Th17 cytokines drive inflammation in Takayasu arteritis. Arthritis Rheumatol 2015;67:1353–60.

31. Arnaud L, Haroche J, Mathian A, Gorochov G, Amoura Z. Pathogenesis of Takayasu's arteritis: a 2011 update. Autoimmun Rev 2011;11:61–7.

32. Origuchi T, Fukui S, Umeda M, Nishino A, Nakashima Y, Koga T, et al. The severity of Takayasu arteritis is associated with the HLA-B52 allele in Japanese patients. Tohoku J Exp Med 2016;239:67–72.

33. Renauer PA, Saruhan-Direskeneli G, Coit P, Adler A, Aksu K, Keser G, et al. Identification of susceptibility loci in IL6, RPS9/LILRB3, and an intergenic locus on chromosome 21q22 in Takayasu arteritis in a genome-wide association study. Arthritis Rheumatol 2015;67:1361–8.

LETTERS

The specificity of monoclonal anti–citrullinated protein antibodies: comment on the article by Steen et al

To the Editor:

I read with great interest the article by Steen et al (1), which reported that human plasma cell–derived monoclonal antibodies (mAb) to posttranslationally modified proteins recognize amino acid motifs rather than specific proteins. However, I believe some potentially misleading conclusions were drawn. In their study, Steen and colleagues showed the isolation of IgG-secreting synovial plasma cells from one presumably high anti–citrullinated protein/peptide antibody (ACPA) responder rheumatoid arthritis (RA) patient, followed by the generation of the corresponding recombinant antibodies for evaluating their specificities and functions. Four of 93 recombinant antibodies were shown to have citrulline reactivity. This prevalence (4% [4 of 93]) is substantially less than the figure of ~25% of IgG-secreting synovial B cells being citrulline-specific, as reported earlier by the same group (2).* In addition, those antibodies were of high affinity (equilibrium constant [K_d] values in the nM range), and all studied antibodies were highly somatically mutated (2), which also differs from the findings of the present investigation (K_d values in the μM range). Since the methodology of cloning and approaches to analyzing the clones (i.e., enzyme-linked immunosorbent assay [ELISA], surface plasmon resonance) are similar, these discrepancies need further explanation, and additional evidence of the epitope specificity of the 4 new antibodies is required. For instance, the high-throughput screen, using some 170,000 synthesized peptides, in fact provides limited information regarding epitope specificity, as peptides bound to the solid phase do not often yield proper binding information.

An even more serious issue is that the 2 mAb from the authors' earlier study (2) (B02 [also referred to as B2] and D10), claimed to be ACPAs, have now been analyzed in more depth and crystallized, demonstrating that these 2 antibodies do not have any citrulline-specific reactivity (3). Antibodies B02 and D10 were consistently used in studies by the same group to show that ACPAs induce osteoclast activation, bone erosions in vivo, and induction of behavior reflecting pain (4,5). In fact, these 2 were the only antibodies that consistently showed those effects. Surprisingly, in the report by Steen et al (1), they maintain that ACPAs have in vitro and in vivo models shown to induce phenotypes consistent with symptoms associated with RA, such as bone loss and joint pain (citing refs. 4–6 below).

---

*Correction added 28 January 2019 after online publication: Reference 2 has been retracted since the time of initial publication of this letter.

Steen and colleagues mention that previous studies utilizing human monoclonal ACPAs, including those from their own laboratory, used a single, more limited detection system and often high concentrations of the antibodies, which potentially yielded false-positive responses (1). The authors also note that false-positive signals may stem from a type of polyreactive antibody, common in systemic lupus erythematosus. The statement regarding assay discrepancies is surprising, as the same type of assays were used previously. In addition, it implies that these polyreactive autoantibodies frequently found in lupus patients induce pain, bone erosion, and osteoclast activation. This would be a novel and interesting possibility, although we have not observed any obvious lupus-type reactivity of antibodies B02 or D10. As these 2 antibodies have consistently been shown to activate osteoclasts, and to induce bone erosions and a behavior reflecting pain, it can be concluded that these effects must have been caused by unknown mechanisms, and not through binding of citrullinated targets.

It can be argued that in some of the reported experiments, purified polyclonal ACPAs and other monoclonal ACPAs were used. However, only antibodies B02 and D10 have shown consistent results, while few of the other monoclonal ACPAs used have shown effects and when effects were observed, they were not consistent. The observation that purified polyclonal ACPAs induce pain could be explained by the possibility that the sample preparation contains antibodies cross-reactive with joints, as cartilage-reactive antibodies have been shown to induce pain-like behavior predating the induction of arthritis (7).

Steen et al also claimed that the 4 newly described antibodies induced bone erosions (1). This is, however, a matter of discussion since only 1 of the 4 antibodies had a significant effect on osteoclasts in vitro whereas another, in fact, showed an opposite effect. The variable effects could, of course, be due to a unique specific targeting of some unknown epitopes on the osteoclast. An alternative explanation could be that the effect is due to the in vitro preparations of these recombinant antibodies. Factors like partial denaturation, aggregation, and glycosylation could affect the preparations and explain the results. Importantly, these modifications strongly affect binding to low-affinity Fc receptor (FcR) expressed on osteoclasts. This explanation could also help in understanding the discrepancy between reports by Harre et al (6,8): in the first report, they claimed that osteoclasts are stimulated through interaction with citrullinated antigens, whereas in the later report they claimed that stimulation was through interaction with FcR modified by the antibody Fc glycosylation.

In the field of rheumatology, it is indeed surprising that testing for ACPAs, used in the classification of RA, is widely based on an assay that contains nonspecified peptide sequences (the CCP2 kit) without controls. In addition, as of now the reported ACPAs have not been molecularly characterized. Add the sentence: It would be fair to clearly point out the need to discuss and revise some of the earlier statements made about the pathogenesis of RA.

To avoid any misunderstanding, I would like to emphasize that it is still possible that ACPAs induce bone erosions and arthralgia. However, convincing new evidence for such phenomena is required.

Rikard Holmdahl, MD, PhD
Karolinska Institutet
Stockholm, Sweden

1. Steen J, Forsström B, Sahlström P, Odowd V, Israelsson L, Krishnamurthy A, et al. Recognition of amino acid motifs, rather than specific proteins, by human plasma cell-derived monoclonal antibodies to posttranslationally modified proteins in rheumatoid arthritis. Arthritis Rheumatol 2018;71:196–209.

2. Amara K, Steen J, Murray F, Morbach H, Fernandez-Rodriguez BM, Joshua V, et al. Monoclonal IgG antibodies generated from joint-derived B cells of RA patients have a strong bias toward citrullinated autoantigen recognition. J Exp Med 2013;210:445–55.

3. Ge C, Xu B, Liang B, Lonnblom E, Lundstrom SL, Zubarev RA, et al. Structural basis of cross-reactivity of anti-citrullinated protein antibodies. Arthritis Rheumatol 2018. E-pub ahead of print.

4. Krishnamurthy A, Joshua V, Haj Hensvold A, Jin T, Sun M, Vivar N, et al. Identification of a novel chemokine-dependent molecular mechanism underlying rheumatoid arthritis-associated autoantibody-mediated bone loss. Ann Rheum Dis 2016;75:721–9.

5. Wigerblad G, Bas DB, Fernades-Cerqueira C, Krishnamurthy A, Nandakumar KS, Rogoz K, et al. Autoantibodies to citrullinated proteins induce joint pain independent of inflammation via a chemokine-dependent mechanism. Ann Rheum Dis 2016;75:730–8.

6. Harre U, Georgess D, Bang H, Bozec A, Axmann R, Ossipova E, et al. Induction of osteoclastogenesis and bone loss by human autoantibodies against citrullinated vimentin. J Clin Invest 2012;122:1791–802.

7. Bas DB, Su J, Sandor K, Agalave NM, Lundberg J, Codeluppi S, et al. Collagen antibody–induced arthritis evokes persistent pain with spinal glial involvement and transient prostaglandin dependency. Arthritis Rheum 2012;64:3886–96.

8. Harre U, Lang SC, Pfeifle R, Rombouts Y, Frühbeiber S, Amara K, et al. Glycosylation of immunoglobulin G determines osteoclast differentiation and bone loss. Nat Commun 2015;6:6651.

Reply

To the Editor:

We thank Dr. Holmdahl for his interest in our recent study on the specificity and function of human mAb generated from synovial plasma cells which react with citrullinated proteins and peptides. He also commented on our previous study from 2013 (1) that was based on mAb generated from synovial memory B cells. Dr. Holmdahl's letter provides us with an opportunity to

discuss and clarify some methodologic issues concerning RA mAb expression, specificity, and functionality. We believe cloning and characterization of human mAb from patients represents an important approach to the understanding of origins and functions of autoantibodies in the pathogenesis of immune-mediated diseases. In fact, the RA field has been especially active in making use of mAb derived from the immunoglobulin sequences from patient-derived B cells and plasma cells. Thus, several recently published studies (2–4), including our own, extend the first generation of RA patient B cell–derived mAb (1,5–8).

One of the concerns Dr. Holmdahl expressed is the specificity of the mAb that we described in our report and the assays utilized. To clarify: we first characterized the reactivity of the mAb against several citrullinated peptides and their arginine counterparts using extensive titration in ELISAs. Then we performed validation experiments using whole proteins in both Western blot and binding assays. We are confident with the data we presented, which demonstrate distinct multireactivity patterns with different citrullinated antigens, without concomitant reactivity with the corresponding native (arginine-containing) proteins and peptides in a variety of experimental settings. Therefore, the relatively weak K_d values we reported for these ACPAs should not be interpreted as a lack of citrulline reactivity. This is rather a reflection of the broad citrulline cross-reactivity that we and others have reported.

We do, however, acknowledge the discrepancy when comparing our current study with our first published study of mAb generated from synovial memory B cells (1). The strong K_d values shown in the first study were not correct and have recently been retracted.* Moreover, although the ELISAs used at the time repeatedly demonstrated citrulline in the absence of arginine reactivity, this widely used assay was not technically optimized for use in detailed studies of fine specificity differences of autoantibodies. We have communicated both of these issues with the journal. In our current, more stringent pipeline of quality control of the expressed antibodies and validated downstream assays, these previously described mAb (1) are no longer citrulline reactive. Interestingly, however, several of the reported mAb demonstrated a certain polyreactivity, which could have contributed to the binding to citrullinated peptides that we observed at the time. Importantly, and as further discussed below, such polyreactivity, and other autoantibody specificities of mAb generated from B cells from RA joints, may also contribute to disease processes in RA.

Another concern raised in Dr. Holmdahl's letter relates to the frequencies of citrulline-reactive cells reported in different studies. Obviously, both the assays and the total number of analyzed mAb are important in establishing such information. Although our study delved deeply into the characteristics of plasma cell–derived ACPAs from synovial fluid, the sample studied was from a single individual, and our investigation was therefore not powered

In the field of rheumatology, it is indeed surprising that testing for ACPAs, used in the classification of RA, is widely based on an assay that contains nonspecified peptide sequences (the CCP2 kit) without controls. In addition, as of now the reported ACPAs have not been molecularly characterized. Add the sentence: It would be fair to clearly point out the need to discuss and revise some of the earlier statements made about the pathogenesis of RA.

To avoid any misunderstanding, I would like to emphasize that it is still possible that ACPAs induce bone erosions and arthralgia. However, convincing new evidence for such phenomena is required.

Rikard Holmdahl, MD, PhD
Karolinska Institutet
Stockholm, Sweden

1. Steen J, Forsström B, Sahlström P, Odowd V, Israelsson L, Krishnamurthy A, et al. Recognition of amino acid motifs, rather than specific proteins, by human plasma cell-derived monoclonal antibodies to posttranslationally modified proteins in rheumatoid arthritis. Arthritis Rheumatol 2018;71:196–209.

2. Amara K, Steen J, Murray F, Morbach H, Fernandez-Rodriguez BM, Joshua V, et al. Monoclonal IgG antibodies generated from joint-derived B cells of RA patients have a strong bias toward citrullinated autoantigen recognition. J Exp Med 2013;210:445–55.

3. Ge C, Xu B, Liang B, Lonnblom E, Lundstrom SL, Zubarev RA, et al. Structural basis of cross-reactivity of anti-citrullinated protein antibodies. Arthritis Rheumatol 2018. E-pub ahead of print.

4. Krishnamurthy A, Joshua V, Haj Hensvold A, Jin T, Sun M, Vivar N, et al. Identification of a novel chemokine-dependent molecular mechanism underlying rheumatoid arthritis-associated autoantibody-mediated bone loss. Ann Rheum Dis 2016;75:721–9.

5. Wigerblad G, Bas DB, Fernades-Cerqueira C, Krishnamurthy A, Nandakumar KS, Rogoz K, et al. Autoantibodies to citrullinated proteins induce joint pain independent of inflammation via a chemokine-dependent mechanism. Ann Rheum Dis 2016;75:730–8.

6. Harre U, Georgess D, Bang H, Bozec A, Axmann R, Ossipova E, et al. Induction of osteoclastogenesis and bone loss by human autoantibodies against citrullinated vimentin. J Clin Invest 2012;122:1791–802.

7. Bas DB, Su J, Sandor K, Agalave NM, Lundberg J, Codeluppi S, et al. Collagen antibody–induced arthritis evokes persistent pain with spinal glial involvement and transient prostaglandin dependency. Arthritis Rheum 2012;64:3886–96.

8. Harre U, Lang SC, Pfeifle R, Rombouts Y, Frühbeiber S, Amara K, et al. Glycosylation of immunoglobulin G determines osteoclast differentiation and bone loss. Nat Commun 2015;6:6651.

Reply

To the Editor:

We thank Dr. Holmdahl for his interest in our recent study on the specificity and function of human mAb generated from synovial plasma cells which react with citrullinated proteins and peptides. He also commented on our previous study from 2013 (1) that was based on mAb generated from synovial memory B cells. Dr. Holmdahl's letter provides us with an opportunity to discuss and clarify some methodologic issues concerning RA mAb expression, specificity, and functionality. We believe cloning and characterization of human mAb from patients represents an important approach to the understanding of origins and functions of autoantibodies in the pathogenesis of immune-mediated diseases. In fact, the RA field has been especially active in making use of mAb derived from the immunoglobulin sequences from patient-derived B cells and plasma cells. Thus, several recently published studies (2–4), including our own, extend the first generation of RA patient B cell–derived mAb (1,5–8).

One of the concerns Dr. Holmdahl expressed is the specificity of the mAb that we described in our report and the assays utilized. To clarify: we first characterized the reactivity of the mAb against several citrullinated peptides and their arginine counterparts using extensive titration in ELISAs. Then we performed validation experiments using whole proteins in both Western blot and binding assays. We are confident with the data we presented, which demonstrate distinct multireactivity patterns with different citrullinated antigens, without concomitant reactivity with the corresponding native (arginine-containing) proteins and peptides in a variety of experimental settings. Therefore, the relatively weak K_d values we reported for these ACPAs should not be interpreted as a lack of citrulline reactivity. This is rather a reflection of the broad citrulline cross-reactivity that we and others have reported.

We do, however, acknowledge the discrepancy when comparing our current study with our first published study of mAb generated from synovial memory B cells (1). The strong K_d values shown in the first study were not correct and have recently been retracted.* Moreover, although the ELISAs used at the time repeatedly demonstrated citrulline in the absence of arginine reactivity, this widely used assay was not technically optimized for use in detailed studies of fine specificity differences of autoantibodies. We have communicated both of these issues with the journal. In our current, more stringent pipeline of quality control of the expressed antibodies and validated downstream assays, these previously described mAb (1) are no longer citrulline reactive. Interestingly, however, several of the reported mAb demonstrated a certain polyreactivity, which could have contributed to the binding to citrullinated peptides that we observed at the time. Importantly, and as further discussed below, such polyreactivity, and other autoantibody specificities of mAb generated from B cells from RA joints, may also contribute to disease processes in RA.

Another concern raised in Dr. Holmdahl's letter relates to the frequencies of citrulline-reactive cells reported in different studies. Obviously, both the assays and the total number of analyzed mAb are important in establishing such information. Although our study delved deeply into the characteristics of plasma cell–derived ACPAs from synovial fluid, the sample studied was from a single individual, and our investigation was therefore not powered

---

*Correction added 25 January 2019 after online publication: Reference 1 has been retracted since the time of initial publication of this letter.

to address the matter of frequencies. We instead acknowledge that valid enumeration and phenotyping of antigen-specific B cells between patients, time points, and anatomic sites represent an interesting area for future investigation, especially given the use of tetramers (2–4) and high-throughput approaches.

Our results are in accordance with recently published independent data from Elliott et al at Stanford (3), which show similar citrullinated peptide cross-reactivity, and from our own collaboration with researchers at the University of Minnesota (2). Interestingly, one emerging unifying feature of ACPAs, which was first demonstrated in polyclonal ACPAs purified from RA serum, is the extensive *N*-glycosylation sites in the Fab region (9). This was verified, in mAb studies, to be a result of the pronounced accumulation of somatic hypermutations (10); these results were based on mAb sequences from our recent study that Dr. Holmdahl comments on, as well as the study by Titcombe et al (2). This feature is also true for the mAb from van de Stadt et al (5) that Dr. Holmdahl used. The reason for these Fab glycosylations remains to be understood, but it represents another validation of features enriched in ACPAs.

Finally, Dr. Holmdahl addresses the functional properties of different ACPAs. Our starting point in the two studies he commented on (11,12) has been the observation that polyclonal ACPAs purified on CCP2 columns, which trap antibodies reacting with several citrullinated peptides and proteins and not with the arginine counterparts (13), are able to activate osteoclasts in vitro and cause bone loss and pain behavior in vivo. Several mechanisms may work in parallel, including direct antibody recognition of targets on the respective cell surfaces and additional contributions from FcγR engagement, for example. In our view, patient-derived mAb can contribute significantly in dissecting these two scenarios. Indeed some of the mAb described in the report commented on by Dr. Holmdahl and also in the recent report by Titcombe et al (2) were shown to cause osteoclast activation, bone loss, and pain. Importantly, none of the mAb expressed in our laboratory have demonstrated identical citrulline-binding patterns, unless they are genetically related. We therefore conclude from these studies that the diversity in reactivity and function between different monoclonal ACPAs, rather than reflecting a problem, offers us opportunities to investigate how different ACPAs may have various functions in the pathogenesis of RA.

Obviously, other antibodies besides ACPAs may also contribute to these processes, and in this context, antibody B02 from our first study (1) is an interesting mAb that activates osteoclasts and causes pain. We continue to investigate targets and functions of this and other antibodies, being aware that the weak citrulline reactivity reported in the study by Amara et al (1) is presumably not responsible for the functional effects of these antibodies. Notably, RA-relevant pathogenic functionalities have been demonstrated also with RA patient–derived mAb that target proteins with modifications other than citrullination, including malondialdehyde modifications (14).

In summary, we wish to emphasize that there is an accumulating body of data on the specificity and functions of human monoclonal ACPAs and other RA-derived autoantibodies emerging from our and several other laboratories. Together, these data illustrate the overall potential of research using human mAb from patients with autoimmune disease. We will be happy to share our mAb for further analyses of the origins and functions of autoantibodies in RA, as there is undoubtedly still much to be discovered.

Vivianne Malmström, PhD
Johanna Steen, PhD
Lars Klareskog, MD, PhD
Karolinska Institutet
Stockholm, Sweden

1. Amara K, Steen J, Murray F, Morbach H, Fernandez-Rodriguez BM, Joshua V, et al. Monoclonal IgG antibodies generated from joint-derived B cells of RA patients have a strong bias toward citrullinated autoantigen recognition. J Exp Med 2013;210:445–55.
2. Titcombe P, Wigerblad G, Sippl N, Zhang N, Shmagel A, Sahlström P, et al. Pathogenic citrulline-multispecific B cell receptor clades in rheumatoid arthritis. Arthritis Rheumatol 2018;70:1933–45.
3. Elliott SE, Kongpachith S, Lingampalli N, Adamska JZ, Cannon BJ, Mao R, et al. Affinity maturation drives epitope spreading and generation of proinflammatory anti–citrullinated protein antibodies in rheumatoid arthritis. Arthritis Rheumatol 2018;70:1946–58.
4. Lu DR, McDavid AN, Kongpachith S, Lingampalli N, Glanville J, Ju CH, et al. T cell–dependent affinity maturation and innate immune pathways differentially drive autoreactive B cell responses in rheumatoid arthritis. Arthritis Rheumatol 2018;70:1732–44.
5. Van de Stadt LA, van Schouwenburg PA, Bryde S, Kruithof S, van Schaardenburg D, Hamann D, et al. Monoclonal anti-citrullinated protein antibodies selected on citrullinated fibrinogen have distinct targets with different cross-reactivity patterns. Rheumatology (Oxford) 2013;52:631–5.
6. Li S, Yu Y, Yue Y, Liao H, Xie W, Thai J, et al. Autoantibodies from single circulating plasmablasts react with citrullinated antigens and porphyromonas gingivalis in rheumatoid arthritis. Arthritis Rheumatol 2016;68:614–26.
7. Corsiero E, Bombardieri M, Carlotti E, Pratesi F, Robinson W, Migliorini P, et al. Single cell cloning and recombinant monoclonal antibodies generation from RA synovial B cells reveal frequent targeting of citrullinated histones of NETs. Ann Rheum Dis 2016;75:1866–75.
8. Amara K, Clay E, Yeo L, Ramskold D, Spengler J, Sippl N, et al. B cells expressing the IgA receptor FcRL4 participate in the autoimmune response in patients with rheumatoid arthritis. J Autoimmun 2017;81:34–43.
9. Rombouts Y, Willemze A, van Beers JJ, Shi J, Kerkman PF, van Toorn L, et al. Extensive glycosylation of ACPA-IgG variable domains modulates binding to citrullinated antigens in rheumatoid arthritis. Ann Rheum Dis 2016;75:578–85.
10. Lloyd KA, Steen J, Amara K, Titcombe PJ, Israelsson L, Lundström SL, et al. Variable domain N-linked glycosylation and negative surface charge are key features of monoclonal ACPA: implications for B-cell selection. Eur J Immunol 2018;48:1030–45.
11. Krishnamurthy A, Joshua V, Haj Hensvold A, Jin T, Sun M, Vivar N, et al. Identification of a novel chemokine-dependent molecular mechanism underlying rheumatoid arthritis-associated autoantibody-mediated bone loss. Ann Rheum Dis 2016;75:721–9.
12. Wigerblad G, Bas DB, Fernades-Cerqueira C, Krishnamurthy A, Nandakumar KS, Rogoz K, et al. Autoantibodies to citrullinated pro-

teins induce joint pain independent of inflammation via a chemokine-dependent mechanism. Ann Rheum Dis 2016;75:730–8.

13. Ossipova E, Cerqueira CF, Reed E, Kharlamova N, Israelsson L, Holmdahl R, et al. Affinity purified anti-citrullinated protein/peptide antibodies target antigens expressed in the rheumatoid joint. Arthritis Res Ther 2014;16:R167.
14. Grönwall C, Amara K, Hardt U, Krishnamurthy A, Steen J, Engström M, et al. Autoreactivity to malondialdehyde-modifications in rheumatoid arthritis is linked to disease activity and synovial pathogenesis. J Autoimmun 2017;84:29–45.

Using high-resolution computed tomography to detect interstitial lung disease in patients with systemic sclerosis: comment on the concise communication by Bernstein et al

To the Editor:

We read with interest the concise communication by Bernstein et al (1) regarding practice patterns among rheumatologists when screening for interstitial lung disease (ILD) in patients with systemic sclerosis (SSc). Referencing the study by Suliman et al (2), the authors state that pulmonary function tests (PFTs) are not sensitive or specific for detecting ILD in this population. The primary message in that study (2) is that PFTs yield a false-negative rate of 62.5% for early detection of ILD in SSc when high-resolution computed tomography (HRCT) is used as the gold standard. It is important to note, however, that the primary measurement used to define baseline abnormality in the study by Suliman and colleagues was forced vital capacity (FVC) <80% of predicted. As already pointed out by Degano et al (3), the incorporation of other measures, including diffusing capacity for carbon monoxide (DLco) and possibly functional residual capacity, improves sensitivity. This was documented by Suliman and colleagues, who found that incorporating other measures of pulmonary function, including DLco <70% of predicted, increased sensitivity for detecting ILD to 72%.

Although the presence and extent of baseline fibrosis on HRCT has been shown to be prognostically valuable in SSc (4), a 1992 study by Steen and colleagues also showed that among patients with SSc who had normal DLco (defined as ≥80% of predicted, rather than ≥70% of predicted per the study by Suliman et al) at baseline, only 2 of 218 (<0.01%) developed clinically significant pulmonary disease after 7.2 years of follow-up (5). This suggests that baseline DLco may be a sensitive indicator of pulmonary disease requiring treatment in SSc, although lacking in specificity.

Based on these considerations, we believe it may be premature to dismiss PFTs as a screening tool for clinically significant scleroderma lung disease. The significance of HRCT abnormalities suggestive of ILD in the absence of alterations in lung volumes or gas exchange remains unclear, as is reflected in the inconsistent use of this tool by rheumatologists, as described by Bernstein and colleagues.

Ann E. Warner, MD
Kent K. Huston, MD
Center for Rheumatic Disease
Kansas City, MO

1. Bernstein EJ, Khanna D, Lederer DJ. Screening high-resolution computed tomography of the chest to detect interstitial lung disease in systemic sclerosis: a global survey of rheumatologists. Arthritis Rheumatol 2018;70:971–2.
2. Suliman YA, Dobrota R, Huscher D, Nguyen-Kim TD, Maurer B, Jordan S, et al. Pulmonary function tests: high rate of false-negative results in the early detection and screening of scleroderma-related interstitial lung disease. Arthritis Rheumatol 2015;67:3256–61.
3. Degano B, Soumagne T, Eberst G, Méaux-Ruault N, Gil H, Magy-Bertrand N. Pulmonary function parameters other than vital capacity should be considered in screening for interstitial lung disease in patients with systemic sclerosis: comment on the article by Suliman et al [letter]. Arthritis Rheumatol 2016;68:2346–7.
4. Hoffmann-Vold AM, Aaløkken TM, Lund MB, Garen T, Midtvedt Ø, Brunborg C, et al. Predictive value of serial high-resolution computed tomography analyses and concurrent lung function tests in systemic sclerosis. Arthritis Rheumatol 2015;67:2205–12.
5. Steen VD, Graham G, Conte C, Owens G, Medsger TA Jr. Isolated diffusing capacity reduction in systemic sclerosis. Arthritis Rheum 1992;35:765–70.

Reply

To the Editor:

We thank Drs. Warner and Huston for their interest in our concise communication. We agree that PFTs should be considered as a screening tool for clinically significant ILD in SSc. However, we disagree that the importance of HRCT abnormalities suggestive of ILD is unclear when alterations in lung volumes or gas exchange are absent. Patients with SSc and normal PFT parameters can still experience a clinically significant decline in their lung function over time. In a retrospective cohort study of 98 patients with SSc who had mild ILD on baseline HRCT and a mean baseline FVC of 102% of predicted, 26% experienced a clinically significant decline in lung function at 1-year follow-up (1). In the phase II trial of tocilizumab for the treatment of diffuse cutaneous SSc, the mean FVC at baseline was 82% of predicted in the control arm, yet 23% of the patients in the control arm experienced a 10% decline in FVC over 48 weeks (2). Similar findings were reported in the phase III trial by Khanna et al (3).

Moreover, there are data from population-based cohorts demonstrating that early, subclinical ILD on HRCT has both biologic and clinical relevance for predicting clinical ILD (4,5). In community-dwelling adults, subclinical ILD on HRCT is associated with lower FVC, reduced exercise capacity, elevated serum levels of interleukin-6, and an increased risk of developing clinically evident ILD and ILD-specific mortality at 12-year follow-up (4–6).

PFTs have a critical role in the initial assessment of lung function in patients with SSc, and in monitoring lung function trajectory. Yet, with its 100% sensitivity (it is the gold standard for ILD detection) and the availability of modern technology that can deliver radiation doses as low as 0.15 mGy (7), HRCT has substantial advantages. Further research into the clinical impact of HRCT screening for ILD in patients with SSc will allow for the development of clear, data-driven recommendations to inform practicing rheumatologists.

Elana J. Bernstein, MD, MSc (iD)
Columbia University Medical Center
New York, NY
Dinesh Khanna, MD, MS
University of Michigan
Ann Arbor, MI
David J. Lederer, MD, MS (iD)
Columbia University Medical Center
New York, NY

1. Wu W, Jordan S, Becker MO, Dobrota R, Maurer B, Fretheim H, et al. Prediction of progression of interstitial lung disease in patients with systemic sclerosis: the SPAR model. Ann Rheum Dis 2018;77:1326–32.

2. Khanna D, Denton CP, Jahreis A, van Laar JM, Frech TM, Anderson ME, et al. Safety and efficacy of subcutaneous tocilizumab in adults with systemic sclerosis (faSScinate): a phase 2, randomised, controlled trial. Lancet 2016;387:2630–40.

3. Khanna D, Lin CJ, Kuwana M, Allanore Y, Batalov A, Butrimiene I, et al. Efficacy and safety of tocilizumab for the treatment of systemic sclerosis: results from a phase 3 randomized controlled trial [abstract]. Arthritis Rheumatol 2018;70 Suppl 10. URL: https://acrabstracts.org/abstract/efficacy-and-safety-of-tocilizumab-for-the-treatment-of-systemic-sclerosis-results-from-a-phase-3-randomized-controlled-trial/.

4. Podolanczuk AJ, Oelsner EC, Barr RG, Hoffman EA, Armstrong HF, Austin JH, et al. High attenuation areas on chest computed tomography in community-dwelling adults: the MESA study. Eur Respir J 2016;48:1442–52.

5. Podolanczuk AJ, Oelsner EC, Barr RG, Bernstein EJ, Hoffman EA, Easthausen IJ, et al. High attenuation areas on chest CT and clinical respiratory outcomes in community-dwelling adults. Am J Respir Crit Care Med 2017;196:1434–42.

6. Putman RK, Hatabu H, Araki T, Gudmundsson G, Gao W, Nishino M, et al. Association between interstitial lung abnormalities and all-cause mortality. JAMA 2016;315:672–81.

7. Newell JD Jr, Fuld MK, Allmendinger T, Sieren JP, Chan KS, Guo J, et al. Very low-dose (0.15 mGy) chest CT protocols using the COPDGene 2 test object and a third-generation dual-source CT scanner with corresponding third-generation iterative reconstruction software. Invest Radiol 2015;50:40–5.

ACR Announcements

ACR Meetings

Annual Meetings
 November 8–13, 2019, Atlanta
 November 6–11, 2020, Washington, DC

Winter Rheumatology Symposium
 January 26–February 1, 2019, Snowmass

State-of-the-Art Clinical Symposium
 April 5–7, 2019, Chicago

For additional information, contact the ACR office.

ACR Open Rheumatology Accepting Submissions and Publishing Soon

The American College of Rheumatology will be publishing the first issue of its third official journal, *ACR Open Rheumatology* (*ACROR*), in early 2019. Editors-in-Chief Drs. Patricia P. Katz and Edward H. Yelin, and Clinical and Basic Science Deputy Editors Drs. David I. Daikh and Bruce N. Cronstein, will be heading *ACROR*'s editorial team.

ACROR will publish manuscripts describing potentially important findings of rigorously conducted studies in all aspects of rheumatology. As an open access journal, immediate access to full content of *ACROR* will be available to all readers. The electronic-only format of the journal, as well as other aspects of the review and production processes, will allow for faster review and publication, and liberal sharing of articles. The projected article publication fee (APC) for *ACROR* will be $2,500 with a discounted rate of $2,000 for articles in which the first or corresponding author is an ACR/ARP member. In addition, there will be waivers of the APC for all articles submitted through March 31, 2019.

For additional information, visit www.acropenrheum.org.

New Division Name

Rheumatology is truly a people specialty: We often develop lifelong relationships with our patients as well as our colleagues. We increasingly recognize that providing the best rheumatologic care requires a team effort. The collegial nature of our specialty is reflected in the ACR's mission statement: To empower rheumatology professionals to excel in their specialty.

In keeping with this mission, we are pleased to announce that our health professionals' membership division is changing its name to Association of Rheumatology Professionals (ARP). This name change highlights the dedication of the ACR to serve the entire rheumatology community. It also reflects our broadened base of interprofessional members (administrators, advanced practice nurses, health educators, nurses, occupational therapists, pharmacists, physical therapists, physician assistants, research teams, and more).

The name is new, but our commitment and promise remain the same: We are here for you, so you can be there for your patients.

ACR State-of-the-Art Clinical Symposium

The 2019 State-of-the-Art Clinical Symposium (SOTA), to be held April 5–7 in Chicago, Illinois, offers high-impact rheumatology education over the course of a single weekend. The symposium will provide more than 10 hours of nonconcurrent sessions with an emphasis on clinical application to rheumatology practice. Attendees will hear key opinion leaders speak on a range of content in areas such as therapeutic developments, recent research findings, and scientific advances. The program will include breakfast and lunch roundtable discussions to allow for personal interactions with experts.

The Fellows-in-Training (FIT) Educational Session at SOTA will be offered as a presymposium session encouraging FITs to explore career opportunities and participate in hands-on workshops designed to further their understanding of essential rheumatologic areas. (FIT travel scholarship recipients are required to attend this session.)

In addition, the presymposium program Rheumatology Documentation and Coding will provide guidance from expert coders on the changes to the 2019 payment policies and insight into difficult E&M coding situations. Be sure to register by the early-bird deadline of February 6 and book your hotel room by March 15. For additional information and to register, visit www.rheumatology.org/Learning-Center/Educational-Activities.